



HAL
open science

Modèle de marge, analyse de sensibilité avec des marges et quantification d'incertitudes dans des graphes de fonctions pour des systèmes industriels complexes

Adrien Touboul

► To cite this version:

Adrien Touboul. Modèle de marge, analyse de sensibilité avec des marges et quantification d'incertitudes dans des graphes de fonctions pour des systèmes industriels complexes. Variables complexes [math.CV]. École des Ponts ParisTech, 2021. Français. NNT : 2021ENPC0017 . tel-03435011

HAL Id: tel-03435011

<https://pastel.hal.science/tel-03435011>

Submitted on 18 Nov 2021

HAL is a multi-disciplinary open access archive for the deposit and dissemination of scientific research documents, whether they are published or not. The documents may come from teaching and research institutions in France or abroad, or from public or private research centers.

L'archive ouverte pluridisciplinaire **HAL**, est destinée au dépôt et à la diffusion de documents scientifiques de niveau recherche, publiés ou non, émanant des établissements d'enseignement et de recherche français ou étrangers, des laboratoires publics ou privés.



École des Ponts
ParisTech



THÈSE DE DOCTORAT
de l'École des Ponts ParisTech

Model of margin, margin sensitivity analysis and uncertainty quantification in graphs of functions in complex industrial systems

École doctorale MSTIC

Mathématiques appliquées et probabilités

Thèse préparée au sein du laboratoire CERMICS et financée par l'IRT SystemX

Thèse soutenue le 21/07/2021 par
Adrien TOUBOUL

Composition du jury:

Thierry Klein
Professeur, Université Toulouse 3 - ENAC

Rapporteur

Bertrand Iooss
Directeur de recherche, EDF R&D

Rapporteur

Bernard Lapeyre
Professeur, CERMICS, ENPC

Directeur

Julien Reygner
Chargé de recherche, CERMICS, ENPC

Encadrant

Anthony Nouy
Professeur, École Centrale de Nantes

Examineur, Président du jury

Guillaume Obozinski
Chargé de recherche, Swiss Data Science Center

Examineur

Claudia Eckert
Professeure, Open University

Examineur

Mouadh Yagoubi
Docteur, IRT SystemX

Invité

Abstract

This thesis focuses on two problems motivated by simulations during the design phase of industrial complex systems. The first part is dedicated to model and to identify costly design margins during the design process. We investigate the fundamental basis of the margin concept and provide a mathematical object to model it. With this model, we exhibit how margins are taken, independently of the field. Various margin practices from different fields are modeled within this framework. Some tools, inspired from the sensitivity analysis domain, are developed to identify which margins contribute the most to a cost or to a loss of performance. These works thus propose a non ambiguous approach to a quantitative analysis of margins. The second part focuses on uncertainty quantification (U.Q) in a multidisciplinary context. The design process of a complex system is modeled by the composition of computer codes, that is represented by a directed acyclic graph. Each node is associated to a computer code whose inputs are random variables. These variables can either come from the outputs of other disciplines (external variable) or be modeled within the discipline (internal variable). We investigate a U.Q method that is based on sample reweighting and allows for disciplinary autonomy. First, at each node and for each external variable, some synthetic samples that do not follow the true law are generated and the respective outputs are computed. Second, a method is chosen to weight to outputs with respect to the inputs, and these weights are propagated in the graph. The final result is a weighted sample whose law approximates the theoretical joint law of the graph. In the first chapter, we study a particular weighting method based on a Wasserstein distance criterion. An explicit expression of the weights is derived, for which we prove the consistency and give some theoretical rates of convergence in terms of expected Wasserstein distance. Then, we generalize the approach by defining the WLAMs (Weighted Linear Approximation Methods), for which we define a local consistency criterion. Under the assumption of local consistency at each node, we prove the convergence towards the true joint law. We show that a discrete Bayesian network can be used to simplify the numerical computations in the propagation phase.

Résumé court

Cette thèse s'intéresse à deux problèmes, initialement motivés par la simulation dans les systèmes industriels complexes. La première partie est dédiée à la modélisation et l'identification des marges de conception coûteuses. Nous étudions les composantes fondamentales de la notion de de marge de conception et proposons un objet mathématiques pour la modéliser. Grâce à ce modèle, nous décrivons la façon dont les marges sont prises, indépendamment du champs d'application. Diverses pratiques d'ingénieurs sont ainsi modélisées avec ce modèle et des outils sont développés pour faire de l'analyse de sensibilité et trouver les marges les plus coûteuses. La seconde partie se focalise sur la quantification d'incertitude (U.Q) dans un contexte multidisciplinaire. Le processus de conception des systèmes complexes est modélisé par un graphe orienté acyclique. Chaque noeud est associé à un code de calcul dont les entrées sont des variables aléatoires. Ces variables peuvent provenir d'autres disciplines (variables externes) ou être modélisées par la discipline elle-même (variables internes). Nous étudions une méthode basée sur la repondération d'échantillons, qui a l'avantage de permettre une autonomie entre discipline. Dans un premier temps, un calcul basé sur un échantillon synthétique est effectué pour chaque noeud et chaque variable externe. Cet échantillon ne suit pas la vraie loi de la variable aléatoire. Ensuite, dans un second temps, les sorties synthétiques sont repondérées en fonction des entrées et les poids sont propagés dans le graphe. La méthode retourne un échantillon pondéré dont la loi empirique approche la loi théorique. Nous étudions tout d'abord une méthode spécifique, basée sur la minimisation d'une distance de Wasserstein. Nous calculons les poids sous forme explicite

et nous en démontrons la consistance ainsi que des taux de convergence asymptotiques. Nous généralisons ensuite l'approche, en définissant des WLAMs (Méthode de pondérations linéaire en la loi), pour lesquels nous définissons un critère de consistance locale. Sous l'hypothèse que chaque noeud est consistant, nous démontrons que la méthode converge globalement. Un réseau bayésien discret peut être utilisé pour faciliter les calculs numériques.

Acknowledgement

Pursuing a Ph.D. was an long and inspiring journey through an uneven path. At certain times, finalizing some ideas involved intensity and rush. At other times, weeks and months would fly by in a second while digging for new concepts. What remained important, nonetheless, was the influence of surrounding people, relatives, friends, and others. This work could not have been completed without them and I hope these few words show my everlasting appreciation of their support during the past few years.

First and foremost, I would like to thank those who had a direct impact on this project. My thesis director, Bernard Lapeyre was the first to show me that research in mathematics could be an interesting path to follow. The two-months internship I did with you on stochastic calculus was eye-opening; mathematics is not a monolithic bloc that is shaped only by a few top-level researchers. It is instead an always expanding tree with neverending ramifications. There are not enough researchers to explore this tree and there will probably never be, as its rate of expansion increases with their number. Your skills in probability, your extreme kindness, and your teaching culture made me realize that it was possible to grasp my own branch and to contribute to research in this field.

Another very important person in this journey is my thesis supervisor Julien Reygner. Not only has he bore me the great honor to entrust me with carrying out this work on his side, but he also has consistently fulfilled his “supervision contract” for more than three years. You taught me a lot, in probability, in mathematical modeling, but also in scientific writing (the unforeseen skill a Ph.D. student must acquire). Your kindness and empathy were of great help during the less bright moments and I am sure you will have plenty of successful experiences as a thesis director in the future.

I deeply acknowledge the rapporteurs of the manuscript Thierry Klein and Bertrand Iooss for their insightful reports, as well as the other members of the jury, Claudia Eckert, Anthony Nouy, Guillaume Obozinski that took the time to study my work and give very interesting feedback.

This thesis could not have been carried out without industrial partners who believed in the topic and chose to fund this project. I would like to thank especially Mouadh Yagoubi who believed in the topic of margins and followed it from its birth to its final form. I acknowledge Fabien Mangeant, Pierre Benjamin and Éric Duceau for having identified the problems that initiated this thesis from the industrial point of view. Other partners, among whom are Jean-Michel Edaliti, Pascal Lamothe, Pascal Menegazzi, and IRT SystemX research engineers Romain Barbedienne, Henri Sohier, and Jean-Patrick Brunet have provided deeply relevant insights that nurtured the vision in terms of application. I am really glad that I had my first professional experience with you.

I remain obliged to Isabelle Simunic, the general secretary of the CERMICS, for her kindness, her constant positive attitude, and her dedication to her job. Without you, I could not have finished my thesis since I would have surely forgotten to renew my university enrolment (or something similar).

As aforementioned, the support of my social environment was of utmost importance in completing this work. I would like to dedicate a special thanks to my family; my parents, my sister,

my two grandmothers, my aunts, uncles, and cousins who gave me the energy to overcome obstacles I had faced even when they knew but a glimpse of what I was working on. My girlfriend's presence was of great help and an infinite source of motivation during the last moments of this thesis. I am immensely thankful for her kindness, her patience, and the balance that she has brought into my life.

One of the great advantages of being an IRT SystemX's Ph.D. student is to be mixed with two "families" of Ph.D. students, researchers, and engineers, one from the institute itself and another ones from the supervising laboratory. I am very grateful for the opportunity to have spent time and to create lasting friendships with people from both sides. Many thanks to ¹Ali, Kevin, Maria, Sofiane, Antoine, Sylvain, Étienne, Clarisse, Rafaël, Ludovic, Cyrille, Simo, Gabriel, Sami, Julien, William, Pierre, Adrien, Clément, Jeet, Éleu, Robert, Benoît, Laurent, Antoine, Inass, Guillaume, Shangwei, Grégoire, Dylan, Alexandre, Mei, Olivia, Thomas, Wenzhuo, Sébastien, Chetra, Yves and Jean-Luc Lechien, Chiara, Adel, Laura, Mouad, Ming, Victor, Stephen, Pascal, Gaspard, Thibault, Yinyin, Régis, Jules, Oumaïma, David, Natkamon, Jakob, Pierre-Alain, Clément, Mathieu and Élyse. I really enjoyed the journey with you, made up of interesting scientific discussion and other numerous fond memories.

In the unfortunate event in which my memory is failing and your name is not in this list but only in my heart, please do not be upset; I now owe you a drink of your choice either at the Hall of Beer (Orsay) or at the Descartes (Champs-sur-Marne), whichever suits you better².

Lastly, I would like to thank my friends from outside of the professional environment. You helped me keep a healthy balance, far from the abstract world.

¹As any ranking between you would be irrelevant, the order of has been chosen pseudo-randomly (seed = 2021).

²For the sake of scientific integrity, this idea is a slight adaptation of Remerciements section in Lingling CAO's thesis (2019).

Contents

1	Résumé	11
1.1	Contexte et motivation industrielle	11
1.2	Modélisation des marges de conception	12
1.2.1	De l'utilisation des marges au problème de surdimensionnement	12
1.2.2	Marge : les fondamentaux	13
1.2.3	Lien entre marge et risque	14
1.2.4	L'identification des marges importantes	15
1.2.5	La réduction des marges demandées importantes	16
1.2.6	Organisation de la partie I	17
1.3	Propagation d'incertitude dans des graphes de modèles	17
1.3.1	Le cadre classique de l'analyse d'incertitudes	17
1.3.2	Interactions multidisciplinaires : échange de variables	19
1.3.3	Graphes de fonctions	19
1.3.4	Propagation sur un noeud	21
1.3.5	Propagation sur le graphe et méthode d'approximation par pondération linéaire en la loi (WLAMs)	24
1.3.6	Organisation de la partie II	25
1.4	Un objectif commun : la réduction des marges importantes	26
I	Model of margin and margin sensitivity analysis	29
2	Introduction and motivation	31
2.1	Why model margins?	31
2.2	Frequently asked questions about margins	32
3	State of the art	35
3.1	Margins in engineering fields	35
3.1.1	Confidence intervals	35
3.1.2	Uncertainty sets in robust optimization (Operations Research)	36
3.1.3	Control and robust control	37
3.1.4	Partial safety factors	38
3.1.5	Safety factors	40
3.1.6	Coherent risk measures	40
3.2	Margin frameworks	41
3.2.1	Probabilistic margins in nuclear safety	41
3.2.2	Quantification of Margins and Uncertainty	43
3.2.3	Performance margins and safety performance margins in Space engineering	44

3.2.4	Margin allocation in industrial complex systems	45
3.2.5	Margins as the cause of over-capacity/overdesign	48
3.3	Our contributions regarding the existing literature	50
4	Model of margin	51
4.1	Problem description	52
4.2	Basis of the model	52
4.2.1	Effective margin	53
4.2.2	Demanded margin	57
4.3	Construction of a model of margin	59
4.3.1	Unidirectional model of margin	60
4.3.2	Bidirectional model of margin	60
4.3.3	Fixed and free variables in probing sets	61
4.3.4	A simple description of models of margin	61
4.4	Margin quantification	61
4.4.1	The four steps of uncertainty mitigation with margins	61
4.4.2	Margin quantification with level of risk	64
4.5	The existing literature	66
4.5.1	Statistics	66
4.5.2	Robust optimization	66
4.5.3	Control and robust control	68
4.5.4	Partial safety factor	69
4.5.5	Coherent risk measure	70
4.5.6	Nuclear safety	70
4.5.7	Performance margin and safety performance margin	71
4.5.8	Margin allocation in industrial complex systems	72
4.5.9	Margin as the cause of over-capacity	73
5	Margin sensitivity analysis and margin reduction	75
5.1	Induced cost and induced margin	75
5.1.1	Composition of demanded margin operators	75
5.1.2	Induced margin	76
5.1.3	Induced cost	78
5.2	Margin sensitivity analysis	80
5.2.1	Induced function	80
5.2.2	Local sensitivity analysis	80
5.2.3	Global sensitivity analysis along a margin reduction path	81
5.3	Mechanisms of margin reduction	87
5.3.1	Improve the maturity of margin quantification	87
5.3.2	Update the reducible uncertainties	88
5.3.3	Perform a mutual quantification of margins	88
6	Model of margin: an operational implementation	93
6.1	Introduction	93
6.2	Industrial case: an automotive battery sizing	94
6.2.1	Initial problem	94
6.2.2	Modeled phenomena	94
6.2.3	Aim of the analysis	95
6.3	Taking a margin	96

6.3.1	Taking a margin on a set of points	96
6.3.2	Taking a margin on a point	97
6.4	Application to the industrial case	97
6.4.1	Three design approaches	97
6.4.2	Detail of the design with explicit margins	99
6.4.3	Generalization of the industrial case	99
6.4.4	Conclusion of the section	102
6.5	Structure of an implementation of a model of margin	102
6.5.1	Metamodel definition	103
6.6	Conclusion of the chapter	107
7	Conclusion and perspectives	109
7.1	Conclusion	109
7.2	Perspectives	110
7.2.1	Industrial applications	110
7.2.2	Applied mathematics	111
8	More on models of margins	115
8.1	Models of margin on one coordinate	115
8.2	Commutation	118
II	Uncertainty propagation in graphs of models	121
9	Introduction and motivation	123
9.1	Industrial motivation	123
9.2	Sample reweighting	126
9.3	Outline of the part	126
10	Reweighting samples	129
10.1	Introduction	129
10.1.1	Covariate shift in U.Q	129
10.1.2	Density ratio estimation	130
10.1.3	Organization of the chapter	132
10.1.4	Notation	132
10.2	Wasserstein distance minimization and Nearest Neighbor Regression	132
10.2.1	Optimal weights for Wasserstein distances	132
10.2.2	NNR reformulation	135
10.3	Convergence analysis	135
10.3.1	Consistency	136
10.3.2	Rates of convergence	137
10.3.3	Proofs	139
10.4	Discussion	145
10.4.1	Convergence to μ_X	145
10.4.2	Rate of convergence of $\widehat{QI}_{n_{\text{off}}, n_{\text{on}}}^{(k_{n_{\text{off}}})}$ in the noiseless case	146
10.4.3	Noisy case	147
10.4.4	Reformulation of our results in terms of Nearest Neighbors	152
10.5	Numerical illustration	154
10.5.1	Influence of $\mu_{X'}$ on the convergence of $\widehat{\mu}_X^{(1)}$	154

10.5.2	Influence of $\mu_{X'}$ on the convergence of $\widehat{\text{QI}}_{n_{\text{off}}, n_{\text{on}}}^{(k_{n_{\text{off}}})}$	156
11	Uncertainty quantification in graphs of functions	157
11.1	Introduction	157
11.1.1	Graph of computer codes	158
11.1.2	Reweighting methods	159
11.1.3	Outline and main results	160
11.2	Reweighting procedure	161
11.2.1	Weighted Linear Approximation Method	161
11.2.2	Computing weights on the graph	164
11.3	Algorithms for the numerical computation of the weights	166
11.3.1	Line graphs	166
11.3.2	General DAG with an intermediate Bayesian network	167
11.4	Industrial application	169
11.4.1	Description of the case	170
11.4.2	Results	171
11.5	Conclusion and perspectives	172
*		

Chapitre 1

Résumé

1.1 Contexte et motivation industrielle

L'éventail toujours plus grand des possibilités technologiques, soutenu par les innovations industrielles, a permis de concevoir de grands systèmes répondant à de multiples exigences et combinant un grande variété de composants de natures différentes. Nous pouvons citer comme exemple les avions, les voitures, les engins spatiaux ou même les centrales nucléaires, que nous regroupons sous l'appellation *systèmes industriels complexes*¹. Une de leur premières évocations dans la littérature [102] précise que ce sont des systèmes pour lesquels "*des composants satisfaisants ne se combinent pas toujours en un système satisfaisant*" [Notre traduction]. En d'autres termes, la complexité liée à l'agrégation de plusieurs composants fait apparaître des phénomènes dits "émergents" issus des interactions entre composants. Le comportement de l'ensemble est donc extrêmement difficile à prévoir en étudiant seulement chaque composant séparément. Une autre façon de voir les systèmes industriels complexes est de les présenter comme des systèmes dont les comportements, les évolutions et les enjeux principaux ne peuvent pas être compris complètement par un seul esprit humain. Pour parvenir à les concevoir, il est donc nécessaire de faire appel des ingénieurs de disciplines différentes, dont le nombre peut varier de la centaine (*e.g.* pour une nouvelle série de voiture) à la dizaine de milliers (*e.g.* la conception d'un avion).

Le processus de conception de ces systèmes complexes est complexe lui aussi et l'on y observe de nombreuses sources d'incertitudes à presque toutes les échelles. Du point de vue de la conduite de projet et de la définition des exigences du système, le domaine de l'*ingénierie système* [58, 63, 72] propose de formaliser les pratiques pour en maîtriser le pilotage. Un des outils proposés par exemple, est de multiplier les différentes représentations du système (fonctionnelle, physique,...) pour guider les choix de conception. Des questions vont être formulées sur le système, portant sur l'optimisation, la validation d'exigences, ou la certification par exemple, mais ces pratiques ne permettent pas à elles seules de les résoudre.

Face à ces requêtes, des ingénieurs spécialisés vont interagir entre eux et mettre en place des techniques pour y répondre, basées sur la modélisation mathématique et physique, puis sur l'expérimentation ou la *simulation*. Sur ce dernier point, il est admis que, dans certaines industries, la modélisation et la simulation numérique sont arrivées à un niveau de maturité plus que convenable [29]. Les entreprises produisant des systèmes industriels complexes ont à leur disposition des experts qui peuvent répondre quantitativement à des questions spécifiques sur des sous-systèmes. Cependant, en raison du grand nombre d'acteurs en jeu, la coordination et la

¹Nous rajoutons le mot "industriels" pour les différencier des systèmes complexes en physique, qui ont une définition différente.

compilation de ces résultats restent un exercice assez difficile. La modélisation et la gestion des incertitudes de façon quantitative, à l'échelle globale du système, est un enjeu important pour la conception et est source de grands défis industriels et de questions scientifiques ouvertes.

Les travaux de cette thèse ont été conduits à l'Institut de Recherche Technologique SystemX, au sein du projet AMC (Agilité et Marge de Conception), qui regroupe des partenaires industriels des domaines de l'aéronautique (Airbus) et de l'automobile (Groupe PSA, Valeo, Sherpa, Siemens, Renault, DPS) autour de la thématique des techniques de conception de systèmes complexes. Ils ont été encadrés par le CERMICS, le laboratoire de mathématiques appliquées de l'École Nationale des Ponts et Chaussées.

Cette thèse en mathématiques appliquées se propose d'approcher la question des incertitudes dans les processus de conception de systèmes industriels complexes via deux angles différents. La première partie se concentre sur la modélisation de la notion de *marge de conception*, qui est une pratique de gestion de l'incertitude communément utilisée par les ingénieurs. La deuxième partie étudie une méthode de propagation d'incertitude dans le cadre d'un graphe de fonctions, représentant les interactions entre les différentes disciplines d'ingénierie.

1.2 Partie I : modélisation et analyse de sensibilité des marges de conception pour les systèmes industriels complexes

L'utilisation de *marges de conception* est peut-être le moyen le plus ancien pour gérer les incertitudes ; il est sans doute l'un des plus intuitifs. Il consiste à faire des choix plus robustes ou plus sûrs que le strict nécessaire prescrit par un modèle.

Supposons, par exemple, que vous deviez arriver à 9 h à un rendez-vous très important (une soutenance de thèse, pour prendre un exemple au hasard). Vous avez calculé que le trajet de votre maison à l'amphithéâtre était de 30 min porte à porte, en prenant les transports en commun. Au vu de l'extrême importance de l'enjeu, vous n'allez sans doute pas partir à 8 h30 min, mais bien avant, disons 7 h45 min, pour être sûr d'arriver à l'heure. Ces 45 min en plus (différence entre 8 h30 min et 7 h45 min), sont utilisées pour couvrir des risques qui peuvent être identifiés (retard d'un train, grève des transports, tombée de neige dans la nuit...) ou même des risques auxquels vous n'avez pas pensé (perte de vos clés...). Elles sont un exemple parfait de *marge de conception*.

1.2.1 De l'utilisation des marges au problème de surdimensionnement

De nos jours, des méthodes avancées ont été développées pour modéliser l'incertitude et gérer les risques en ingénierie, comme celles basées sur la théorie des probabilités [37]. Elles ont vocation à gérer l'incertitude de façon plus précise que les méthodes basées sur des marges. Toutefois, nos partenaires industriels ont constaté que dans un environnement multidisciplinaire avec une grande diversité d'acteurs et d'objectifs, les marges de conception restent un des mécanismes principaux pour gérer les multiples risques. L'hypothèse industrielle qui motive les travaux sur les marges est que l'incertitude dans la conception de systèmes complexes est gérée en grande partie à *l'échelle locale* de chaque acteur, qui *prennent chacun des marges de conception*. Comme cette gestion n'est pas faite à l'échelle globale, chaque acteur choisit la valeur des marges en fonction de l'information à sa disposition et des marges non pertinentes apparaissent. Un exemple typique est qu'un même risque peut être couvert par les marges de plusieurs acteurs, sans que chacun ne soit au courant des marges prises par les autres. Un autre exemple arrive quand deux acteurs prennent des marges pour couvrir des événements qui ne peuvent pas arriver au même moment, conduisant à des conceptions en pire cas irréalistes (cet aspect est développé en Section 6).

L'accumulation de marges non pertinentes peut entraîner un phénomène appelé *surconception* ou *surdimensionnement*, car certaines marges impactent négativement les performances et le coût, sans améliorer significativement les objectifs en termes de sûreté de fonctionnement du système [46]. Pour résoudre ce problème, plusieurs stratégies ont été envisagées dans la littérature scientifique. En sciences de la conception, des travaux basés sur des entretiens dans des bureaux d'études ou des analyses de systèmes industriels complexes en opération [46, 67, 68] permettent d'identifier et de classer les marges, ainsi que de préciser la façon dont elles interagissent [44] (voir la Section 3.2.5). Dans certains domaines spécifiques (*e.g.* le génie nucléaire ou spatial), une définition de marge est proposée, comme référence pour les pratiques du domaine [38, 39, 42, 83] (voir les Sections 3.2.3 et 3.2.1) et le lien entre risque et marges est clairement identifié via des modèles probabilistes. Ces définitions de référence facilitent la communication des marges entre tous les acteurs. En conception des systèmes industriels complexes, une définition simple de marge est proposée, et des méthodes d'*allocation* et d'*analyse de sensibilité* permettent de choisir les valeurs des marges et de quantifier leur impact en modélisant le système à une échelle plus globale [23, 24, 27, 111–113] (voir les Sections 3.2.4 et 3.2.5).

Notre démarche est complémentaire à la littérature et se rapproche dans l'esprit de celle des mathématiques appliquées à la physique. Nous partons du concept intuitif de marge de conception en ingénierie pour nous intéresser à ce qu'il y a de fondamental en celui-ci. Ensuite, nous en proposons une définition mathématique, puis regardons comment modéliser les pratiques existantes à partir de cette définition. Enfin nous proposons des outils pour identifier les marges importantes, en nous inspirant du domaine de l'*analyse de sensibilité*. Cela nous a permis de poser des bases non ambiguës à une approche quantitative des marges et a ouvert un certain nombre de perspectives pour la modélisation de problèmes de conception.

Pour comprendre cette approche, retournons aux bases et intéressons-nous à ce qu'est une *marge* en terme d'ingénieur.

1.2.2 Marge : les fondamentaux

Le vocable “marge” ou “margin” en anglais est issu du latin “margo” qui signifie frontière ou bordure. Si ce mot est toujours utilisé sous cette acception, son sens a été élargi par métonymie. De nos jours, il peut aussi désigner la distance à une frontière, une frontière incluse à l'intérieur d'une autre frontière ou même le domaine entre les deux frontières. La marge d'une feuille de papier est ainsi l'espace blanc dans lequel rien ne doit être écrit et est contenu entre deux frontières : le bord de la feuille et le bord de la zone d'impression.

Cette zone entre deux frontières est un sens qui semble être d'usage commun en ingénierie, souvent avec l'hypothèse implicite que cette zone couvre un risque lié à une incertitude ; on peut voir la marge d'une feuille de papier comme une zone où les caractères peuvent déborder si il y a un problème d'alignement lors de l'impression. En ingénierie, un des plus vieux exemples documentés [47, pp 44], [1, 34] est le “coefficient de sûreté” ou “safety factor” en anglais. Il mesure, en un certain sens, la charge supplémentaire qu'une structure peut supporter, comparée à une charge nominale. De façon plus générale, la notion que nous voulons formaliser mathématiquement peut être décrite informellement de la façon suivante.

Definition 1.2.1. *Marge, (informel, 1) Une marge est une quantité en plus qui permet de s'assurer du succès ou de la sûreté de fonctionnement.*

Nous retrouvons bien dans cette quantité en plus, le domaine entre un point de fonctionnement du système et un point de défaillance. Si le succès ou la sûreté étaient certains, l'ajout d'une quantité en plus ne serait pas nécessaire ; le besoin de s'en “assurer” dénote la présence d'incertitudes. Comme nous le verrons dans la revue de la littérature du Chapitre 3, cette définition se

décline de façon variée dans différents domaines d'ingénierie.

Un premier concept important est la distinction entre la marge en tant que quantité requise par les ingénieurs pour se couvrir d'un risque, et la marge en tant que quantité réelle qu'un système possède pour éviter la défaillance ou le dysfonctionnement. C'est le sens de la dichotomie entre la *marge effective*, qui est la mesure de la quantité en plus pour un système donné, et la *marge demandée*, qui traduit l'exigence d'avoir au moins une certaine valeur de marge effective (voir Section 2.1). Cette distinction est rarement explicite dans la littérature, mais nous a permis de comprendre plus facilement les différents concepts utilisés en pratique. Le lien entre les deux est qu'une marge demandée m se traduit comme l'exigence qu'un système ait au moins une marge effective supérieure à m .

Pour calculer une *marge effective*, la mesure de la quantité en plus se fait naturellement en mathématiques par une métrique/distance. Toutefois, cette distance ne se calcule pas sur l'ensemble des variables descriptives et tous les états du système, mais seulement dans un sous-ensemble de ceux-ci et dans une unité précise. Nous proposons en Section 4.2 un modèle de marge, noté \mathbf{M} , qui décrit mathématiquement tous ces paramètres. La définition mathématique de la marge effective (Définition 4.2.1) est donc la mesure de cette "distance", au sens large, entre un design u (*i.e.* un choix de conception) et un ensemble interdit \mathbf{F} . Elle s'écrit $\text{em}_{\mathbf{M}}(u, \mathbf{F}) \in \mathbb{R}$. La définition de la marge demandée m (Définition 4.2.2) découle directement de celle de la marge effective, en interdisant les designs avec une marge effective inférieure à m . Elle agit en réduisant l'ensemble des designs acceptables \mathbf{A} , ou bien, de façon équivalente, en étendant les designs interdits \mathbf{F} . Mathématiquement, c'est une application qui transforme un ensemble de designs interdits \mathbf{F} en un ensemble encore plus grand $\mathbf{F}' = \mathbf{d}\mathbf{m}_{\mathbf{M},m}(\mathbf{F})$, pour une valeur de marge demandée m donnée.

1.2.3 Lien entre marge et risque

Comme nous l'avons vu précédemment, la notion de marge est intrinsèquement liée au risque qu'elle essaye de prévenir. Pour étudier cette relation, nous devons d'abord préciser ce qu'est le risque. Si plusieurs définitions existent dans la littérature [9, 10], nous utilisons une conceptualisation du risque comme combinaison d'incertitudes et de conséquences [11]

$$\text{Risque} = (\text{Incertainitudes}, \text{Conséquences}),$$

la *mesure* du risque prenant en compte ces deux composantes. En pratique, il existe différentes façons de modéliser l'incertitude, allant d'une vague idée de la variation d'un paramètre incertain à la représentation précise de sa loi de probabilité. La mesure des conséquences dépend aussi beaucoup de la problématique considérée; est-ce que l'on raisonne sur un système critique ou bien sur des équipements de confort? Peut-on le coût en cas d'évènement redouté? Finalement, la *mesure* du risque, qui combine les incertitudes et les conséquences en une indice (quantitatif ou qualitatif) peut aussi varier, comme les différentes mesures de risque introduites dans [98] en témoignent. Pour que notre propos reste général, nous n'imposons ni de modélisation particulière du risque, ni d'estimation spécifique des conséquences.

Du point de vue de l'application, nous distinguons cependant les incertitudes réductibles (ou épistémiques) des incertitudes irréductibles (ou aléatoires) [37, Section 14.1], [60, Section 2]. Les incertitudes réductibles sont, par définition, les incertitudes qui peuvent être réduites *pendant le processus de conception* (par exemple en effectuant de nouvelles expérimentations, ou par l'apport de nouvelles informations). Les incertitudes irréductibles sont les autres incertitudes. Les marges issues des incertitudes réductibles sont ainsi appelées *marges réductibles* (Figure 1.1). Cette caractéristique nous permettra de les cibler lorsque nous voudrions réduire l'impact des marges sur un coût.

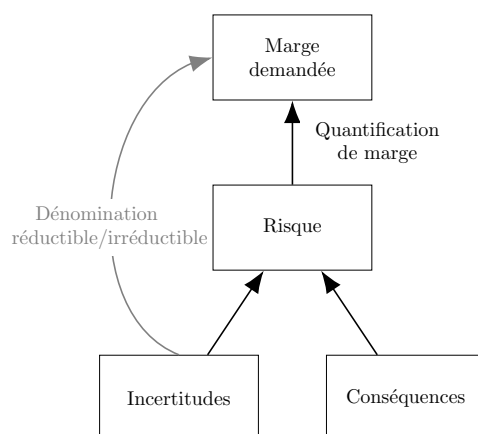


FIGURE 1.1 : Dans le processus de conception, des marges demandées sont prises pour couvrir des risques. On appelle marge réductibles (resp. irréductibles) les marges demandées qui couvrent des incertitudes réductibles (resp. irréductibles).

Nous modélisons ensuite les étapes méthodologiques qui amènent un ingénieur à choisir la valeur d'une marge. Nous détaillons cette approche en Section 4.4.1, que nous appelons *quantification de marge*. En substance, elle consiste à choisir un ou plusieurs modèles de marge et des marges demandées pour couvrir le risque. Dans le cas d'une seule marge, l'analyste choisit un modèle \mathbf{M} et une valeur de marge demandée $m > 0$ tels que le nouvel ensemble interdit $\mathbf{F}' = \mathbf{dm}_{\mathbf{M},m}(\mathbf{F})$ couvre des risques qui ne sont pas modélisés par \mathbf{F} . Dans le cas de plusieurs marges, un ensemble de paires modèle de marge et marge demandée $(\mathbf{M}_1, m_1), \dots, (\mathbf{M}_n, m_n)$ est choisi, tel que le nouvel espace interdit, résultant de la *composition des opérateurs*

$$\mathbf{F}' = \mathbf{dm}_{\mathbf{M}_n, m_n} \circ \dots \circ \mathbf{dm}_{\mathbf{M}_1, m_1}(\mathbf{F})$$

couvre les risques.

1.2.4 L'identification des marges importantes

L'accumulation des marges demandées dans le processus de conception Une fois que nous avons identifié le mécanisme de quantification de marge, nous vérifions en Section 4.5 que les principales pratiques de la littérature peuvent être décrites par des modèles de marge. Fort de ce constat, nous interprétons le processus de conception d'un système industriel complexe comme la composition successive d'opérateurs de marge demandée, modélisant la prise de marges par divers acteurs. Cette description mathématique permet de proposer une réponse quantitative aux questions suivantes.

- Comment le coût du système évolue avec les marges demandées ?
- Comment une marge effective évolue avec les marges demandées ?

Le *coût induit* et la *marge induite* calculent respectivement le coût supplémentaire et la marge effective perdue, en fonction des valeurs des différentes marges demandées. En notant les marges demandées, $(m_1, \dots, m_n) \in \mathbb{R}^n$, ces deux notions ont la forme générale d'une fonction

$$\begin{aligned} \mathbb{R}_+^{*n} &\mapsto \mathbb{R}_+ \\ (m_1, \dots, m_n) &\rightarrow \text{indF}(m_1, \dots, m_n) \end{aligned}$$

qui est croissante en fonction de chaque marge demandée.

Analyse de sensibilité des marges Maintenant que nous avons défini la relation entre les marges demandées et un coût, il nous reste à trouver des indicateurs pertinents pour classer les marges demandées en fonction de leur impact sur le coût. Nous nous inspirons des pratiques d'*analyse de sensibilité* [66, 100] pour définir deux familles d'indicateurs. Notons $(\bar{m}_1, \dots, \bar{m}_n)$ les marges demandées réelles. La première famille d'indicateurs $(\mathcal{D}_i)_{i \in \llbracket 1, n \rrbracket}$ est calculée de façon locale, en fonction des dérivées partielles. L'indice \mathcal{D}_i quantifie l'impact de la marge demandée \bar{m}_i sur le coût induit, sous hypothèse qu'il est presque linéaire. Ce coût se décompose de façon approximative

$$\text{indF}(\bar{m}_1, \dots, \bar{m}_n) \simeq \sum_{i=1}^n \mathcal{D}_i$$

comme la somme des impacts liés à chaque marge i . La deuxième famille d'indicateurs $(S_i^s)_{i \in \llbracket 1, n \rrbracket}$ est calculée en intégrant les dérivées partielles de $(\bar{m}_1, \dots, \bar{m}_n)$ à $(0, \dots, 0)$ le long d'un chemin noté s . L'indice S_i^s quantifie un impact global de la marge demandée \bar{m}_i sur le coût induit et la décomposition

$$\text{indF}(\bar{m}_1, \dots, \bar{m}_n) = \sum_{i=1}^n S_i^s$$

est exacte. Le calcul de ces indices nécessite cependant plus d'évaluations du modèle et demande de fixer un chemin de réduction de marge s de façon arbitraire.

1.2.5 La réduction des marges demandées importantes

Une fois que les marges demandées importantes sont identifiées, une étape naturelle est d'essayer de les réduire. L'étude des mécanismes de diminution des marges demandées se situe encore à la lisière de nos réflexions et requiert sans doute plus de maturité pour arriver à une modélisation mathématique complète. Nous avons toutefois identifié, en Section 5.3, trois façons différentes de réduire les marges demandées, tout en gardant les mêmes critères de sûreté de fonctionnement.

1. Monter en maturité dans la phase de quantification de marge.

Des marges demandées élevées peuvent être causées par un déficit de confiance dans les calculs ou la modélisation. Arriver à relier plus précisément le risque et la valeur de la marge demandée permet en général de réduire les valeurs de marge.

2. Mettre à jour les marges réductibles.

Les marges réductibles (Figure 1.1) sont dues à des incertitudes qui peuvent se réduire au fur et à mesure que le processus de conception avance dans le temps. Elles peuvent se réduire d'elles-mêmes (*e.g.* un choix de conception a été fait par un acteur, qui fixe une valeur pour les autres) ou bien lorsqu'on les cible activement (*e.g.* on demande plus de tests pour réduire une erreur statistique). Mettre à jour et réduire ces incertitudes conduit mécaniquement à réduire les marges associées.

3. Faire de la quantification mutuelle.

Lorsque les marges sont quantifiées par des acteurs qui ne partagent pas d'informations, elles ne permettent pas de prendre en compte les corrélations ou indépendances entre les incertitudes qu'elles couvrent. Cela peut mener à de la conception en "pires cas irréalistes" où le système est conçu pour faire face à des situations qui n'arrivent jamais dans la réalité. Quantifier plusieurs marges demandées en même temps permet de toutes les réduire, en satisfaisant le même critère de sûreté de fonctionnement.

1.2.6 Organisation de la partie I

Après un bref rappel du contexte au chapitre 1, nous effectuons une revue de la littérature existante sur les marges dans le chapitre 3. Les définitions du *modèle de marge* et des concepts associés (marge effective, marge demandée, quantification de marge) sont exposées au chapitre 4 (Section 4.2). Nous y réinterprétons aussi la littérature dans le cadre du modèle de marge. L'analyse de sensibilité par rapport à des marges demandées est développée dans le chapitre 5, ainsi que des pistes pour réduire les marges influentes, une fois qu'elles ont été identifiées. Un mécanisme de réduction de marge, la quantification mutuelle, est illustré sur un cas d'usage dans le chapitre 6. Nous concluons la partie et décrivons les perspectives qui nous semblent les plus prometteuses dans le chapitre 7. Le chapitre 8 est consacré à des développements annexes.

1.3 Partie II : Quantification d'incertitude et analyse de sensibilité dans des graphes de modèles

Dans cette partie, nous nous intéressons à un contexte industriel légèrement différent de la partie précédente. Nous voulons effectuer de *l'analyse d'incertitude* probabiliste (quantification d'incertitude et analyse de sensibilité) dans une portion d'un système industriel complexe qui met en jeu plusieurs disciplines. Cette problématique a motivé des travaux de recherche récents dans la communauté de quantification d'incertitude [4, 6, 57, 82, 84, 101]. La spécificité de notre contexte industriel impose que les calculs ne peuvent pas s'effectuer dans l'ordre nécessaire pour les méthodes classiques (*e.g.* approches par Monte-Carlo). Nous allons donc étudier des méthodes qui sont compatibles avec une certaine *autonomie des disciplines*.

Nous représentons la partie du système complexe à simuler par un graphe $\mathcal{G} = (\mathcal{V}, \mathcal{E})$. Les noeuds \mathcal{V} représentent les disciplines et les arêtes \mathcal{E} représentent des interactions entre les disciplines, dont la nature sera précisée plus bas (voir Figure 1.2).

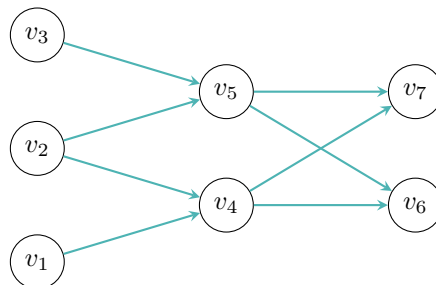


FIGURE 1.2 : Graphe d'interactions entre les disciplines. Un sommet v_i représente une discipline et une arête représente une interaction.

Avant de développer le cas multi-acteurs, nous décrivons brièvement en quoi consiste l'analyse d'incertitudes dans la modélisation probabiliste en ingénierie.

1.3.1 Le cadre classique de l'analyse d'incertitudes

L'analyse d'incertitudes consiste en un ensemble de méthodes numériques et de pratiques appliquées pour extraire de l'information d'un phénomène modélisé par

$$Y = f(X) \tag{1.1}$$

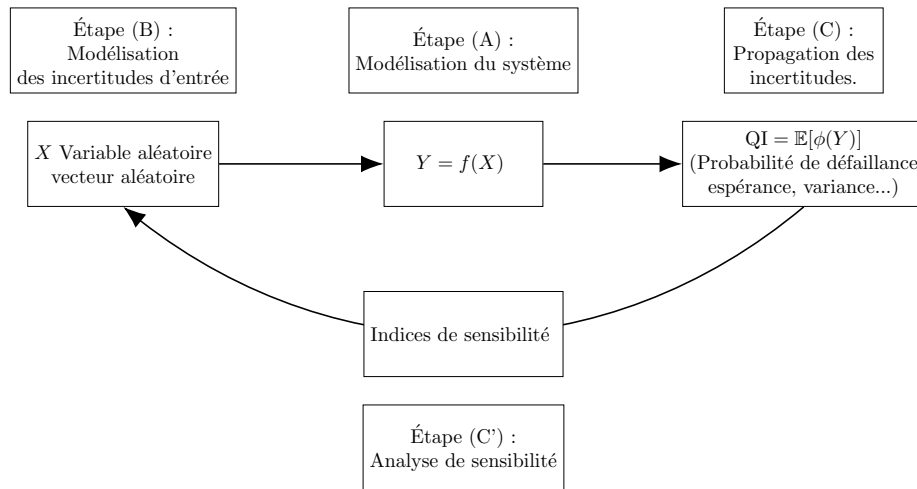


FIGURE 1.3 : Méthodologie ABCC' (figure adaptée de [36]).

où $X = (X_1, \dots, X_n)$ est un vecteur aléatoire, f est un code de calcul déterministe et Y est la sortie de ce code. Dans un contexte industriel, des études peuvent être décrites dans le cadre développé dans [36, 37, 107], composé de quatre étapes A-B-C-C' (Figure 1.3).

- (A) La modélisation mathématique du phénomène, via la relation fonctionnelle $Y = f(X)$.
- (B) La modélisation probabiliste de l'incertitude en entrée X . Elle peut se faire, par exemple, par l'estimation de paramètres de la loi de probabilité de l'entrée.
- (C) La propagation d'incertitude/quantification d'incertitude (U.Q) consiste à calculer la loi de sortie (ou une quantité d'intérêt qui lui est liée), en fonction de l'entrée.
- (C') L'analyse de sensibilité (S.A), permet de quantifier quelles sont les entrées parmi les (X_1, \dots, X_n) qui contribuent le plus à la variabilité de Y .

Le "prime" de C' signifie que l'étude se concentre parfois seulement sur l'analyse de sensibilité, sans faire de propagation d'incertitude. Bien que les étapes de modélisation (A) et (B) dépendent beaucoup du champ d'ingénierie considéré, les étapes (C) et (C') ont pu être étudiées de façon transverse à tous les domaines. Elles ont été la source de multiples investigations académiques ces dernières décennies [54] et c'est sur ces deux points que se consacrera notre étude.

En U.Q, les défis portent par exemple sur la construction de métamodèles, surfaces de réponse ou approximations (approcher f à partir d'un petit nombre de points, puis propager l'incertitude) avec des techniques du type Krigeage [75], polynôme de chaos [88, 108], approximation par tenseur de rangs faibles [28], etc. En S.A [66, 100], la recherche s'est portée, entre autres, sur la définition et les calculs d'indices qui permettent de classer l'impact de chaque entrée. Les méthodes populaires sont par exemple le screening et la décomposition de variance (*e.g.* Indices de Sobol [65]).

Notons que la construction de métamodèles en U.Q a de fortes ressemblances avec la régression en apprentissage statistique supervisé (tel que défini dans [59]), puisqu'il s'agit, étant donné des couples $(X_i, Y_i)_{i \in [1, n]}$, d'estimer f . Une des différences principales est qu'en quantification d'incertitude, la loi de l'entrée X est très souvent supposée connue et simulable informatiquement et f est calculable mais chère. En apprentissage statistique, le paradigme est différent car l'on a seulement accès à des observations $(X_i, Y_i)_{i \in [1, n]}$.

1.3.2 Interactions multidisciplinaires : échange de variables

Revenons maintenant au cas multi-acteur. Nous supposons que chaque discipline v possède un modèle f_v qui représente le phénomène considéré. Ce modèle permet de calculer la sortie Y_v qui est un vecteur aléatoire, via l'équation

$$Y_v = f_v(X_v, \Theta_v). \quad (1.2)$$

Contrairement au cas classique de l'analyse d'incertitude en Section 1.3.1, nous distinguons maintenant les entrées qui

- proviennent d'autres disciplines. Elles sont représentées par le vecteur X_v et sont appelées *variables externes* ;
- ne requièrent pas d'information provenant d'autres disciplines. Elles sont représentées par le vecteur Θ_v et sont appelées *variables internes*. Elles peuvent modéliser à la fois
 - (a) des variables aléatoires de lois connues et simulables sur demande par l'acteur v (approche du type quantification d'incertitude "classique") ;
 - (b) des variables aléatoires simulées à chaque évaluation de f_v par v mais non simulables en dehors de cette évaluation (approche du type simulateur stochastique [127]) ;
 - (c) des variables aléatoires observées (*e.g.* un bruit dans une approche Statistiques/Machine learning [18, 59]).

Nous supposons que les variables externes X_v et internes Θ_v sont indépendantes l'une de l'autre, de lois respectives μ_{X_v} et μ_{Θ_v} . En notant les parents directs du sommet v dans le graphe \mathcal{G} par $\mathcal{P}(v) = \{u \in \mathcal{V} \mid (u, v) \in \mathcal{E}\}$, le vecteur des variables externes s'écrit comme la réunion des sorties des parents

$$X_v = (X_{u,v})_{u \in \mathcal{P}(v)}$$

et la variable transmise du noeud u au noeud v est une transformation de la sortie de u

$$X_{u,v} = g_{u,v}(Y_u),$$

où $g_{u,v}$ est une fonction facile à calculer (typiquement le choix de ne garder qu'un sous-ensemble de composants du vecteur Y_u), contrairement à f_v qui est coûteuse. Dans le graphe de la Figure 1.2, les interactions sont maintenant des échanges de variables, qui sont représentées en Figure 1.4.

1.3.3 Graphes de fonctions et non simultanément : la besoin de méthodes basées sur la décomposition

Non-simultanément des calculs Pour effectuer de la propagation d'incertitude dans un tel graphe, une méthode naturelle serait d'utiliser de l'échantillonnage de Monte-Carlo. Dans le cas de la Figure 1.4, les acteurs v_5, v_6, v_7 généreraient tous un nombre $n \in \mathbb{N}$ d'observations de leur sorties respectives, qui seraient ensuite transmises comme entrées à v_4, v_3 . Ces derniers calculeraient l'image de ces entrées, en générant en plus n observations de Θ_4 et Θ_3 , et transmettraient leurs échantillons à v_2 et v_1 .

Toutefois, du fait de l'organisation complexe du processus de conception, les acteurs n'ont souvent pas la même temporalité, ni la même localisation spatiale. Faire un échange d'échantillon "en ligne", en suivant l'ordre donné par le graphe est difficile en pratique. L'acteur v_3 pourrait par exemple faire une série de calculs en début de projet puis s'arrêter, avant même que v_6 et

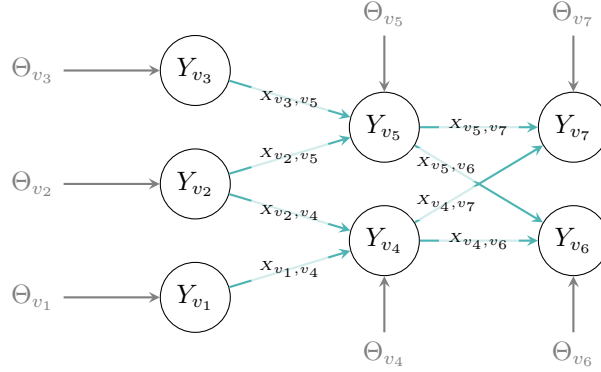


FIGURE 1.4 : Exemple d'un graphe de modèle numérique, orienté et acyclique, avec 7 acteurs. Par exemple, pour l'acteur v_5 , nous avons $Y_{v_5} = f_{v_5}(X_{v_3,v_5}, X_{v_2,v_5}, \Theta_{v_5})$. La variable Y_{v_5} est transformée en $X_{v_5,v_7} = g_{v_5,v_7}(Y_{v_5})$ puis transmise à v_7 . Elle est aussi transformée en $X_{v_5,v_6} = g_{v_5,v_6}(Y_{v_5})$ puis transmise à v_6 .

v_7 aient commencé à faire les leurs. La technique de Monte-Carlo n'est donc pas adaptée pour ce cas ; nous cherchons donc une technique qui permettrait de faire les calculs de façon non séquentielle. Cette problématique se rencontre dans la littérature d'optimisation multidisciplinaire, sous le terme "d'autonomie des disciplines" et d'approches dites de décomposition [3, Sec. 2.4]. En quantification d'incertitude multidisciplinaire, un algorithme de propagation basé sur la décomposition a été proposé pour la première fois en 2012 [5, 6] par S. Amaral, D. Allaire et K. Willcox.

Algorithme de propagation par repondération Notre but est d'approcher la loi jointe du vecteur de variables aléatoires $(Y_v)_{v \in \mathcal{V}}$. L'algorithme se décompose en deux étapes.

- *Phase offline* : Chaque acteur fait appel localement à sa fonction de calcul f_v . Il donne comme entrée un échantillon *synthétique* de X_v tiré selon une loi choisie par v et un échantillon de Θ_v tiré selon sa vraie loi μ_{Θ_v} ². Des échantillons

$$(X'_{j,v}, Y'_{j,v})_{j \in [1, n_v]} = (X'_{j,v}, f(X'_{j,v}))_{j \in [1, n_v]}$$

sont générés à chaque noeud.

- *Phase online* : Les échantillons sont réunis par un acteur externe, l'*architecte de simulation*. Il va repondérer successivement les échantillons pour approcher la vraie loi.

Tout l'enjeu ici est de trouver comment pondérer les échantillons pour avoir une approximation consistante. Dans le chapitre 10, nous allons étudier une méthode de pondération différente de celle proposée initialement en [5, 6]. Elle sera basée sur la minimisation des distances de Wasserstein entre deux mesures empiriques, ce qui résulte dans l'utilisation de méthodes de plus proches voisins. Ensuite, dans le chapitre 11, nous proposerons un cadre général pour la propagation de poids dans le graphe, dans lequel une large famille de pondérations peuvent s'inscrire. Nous les nommons méthodes de pondérations linéaires en loi ou WLAMs, pour *Weighted Linear*

²Comme dit précédemment, le vecteur Θ_v peut aussi représenter un bruit d'observation ou une quantité stochastique d'un simulateur stochastique sans changer le raisonnement, du moment où il reste indépendant de X_v .

Approximation Methods. Nous étudierons quelles sont les caractéristiques de ces méthodes qui garantissent la convergence de cet algorithme. Nous verrons aussi que la propagation de poids peut se voir comme un problème d'inférence dans un réseau bayésien.

Le reste de cette section est dédiée à une explication plus détaillée de nos résultats.

1.3.4 Propagation sur un noeud : repondération par minimisation de la distance de Wasserstein et plus proches voisins (k -NN)

1.3.4.a Pondération par un acteur

Nous allons tout d'abord nous intéresser à la pondération effectuée pour un seul acteur v dans une approche de décomposition. L'ensemble des variables d'entrée externes sont réunies dans le vecteur $X_v = (X_{u,v})_{u \in \mathcal{J}(v)}$ et les variables d'entrée internes sont réunies dans le vecteur Θ_v (voir schéma Figure 1.5).

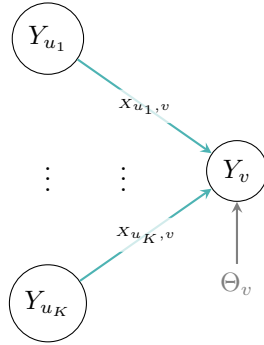


FIGURE 1.5 : Représentation des entrées d'un noeud.

Dans un but de simplification des notations, nous abandonnons temporairement le symbole v en indice et notons $X = X_v$, $Y = Y_v$, etc. Au niveau de v , la pondération s'effectue de la façon suivante.

Phase offline : calcul de f sur un échantillon synthétique Durant la phase *offline*, l'acteur v effectue des calculs de f sans avoir accès à la loi de X . Il utilise donc un échantillon *synthétique* de variables $(X'_j)_{j \in \llbracket 1, n_{\text{off}} \rrbracket}$ indépendantes identiquement distribuées, de loi commune $\mu_{X'}$, ainsi qu'un échantillon $(\Theta_j)_{j \in \llbracket 1, n_{\text{off}} \rrbracket}$ tiré selon la vraie loi μ_{Θ} . Ces échantillons servent au calcul de

$$(\mathbf{X}'_{n_{\text{off}}}, \mathbf{Y}'_{n_{\text{off}}}) = \left(X'_j, Y'_j \right)_{j \in \llbracket 1, n_{\text{off}} \rrbracket},$$

avec $Y'_j = f(X'_j, \Theta_j)$, $j \in \llbracket 1, n_{\text{off}} \rrbracket$. Insistons sur le fait que la loi $\mu_{X'}$ est choisie par v avec peu d'informations sur X . Elle a donc très peu de chance d'être la vraie loi de X .

Phase online : repondération de l'échantillon Durant la phase *online*, l'architecte de simulation a accès à des échantillons $(X_i)_{i \in \llbracket 1, n_{\text{on}} \rrbracket}$, tirés selon la vraie loi de X . Cependant, il ne peut pas faire d'évaluation de la fonction f .

Le coeur de notre approche consiste à *repondérer* l'échantillon des sorties synthétiques $(Y'_j)_{j \in \llbracket 1, n_{\text{off}} \rrbracket}$ avec des poids $\mathbf{w}_{n_{\text{off}}} = (w_j)_{j \in \llbracket 1, n_{\text{off}} \rrbracket}$, qui dépendent de $(X_i)_{i \in \llbracket 1, n_{\text{on}} \rrbracket}$, de telle sorte que l'échantillon

$$(Y'_j, w_j)_{j \in \llbracket 1, n_{\text{off}} \rrbracket}$$

approche la loi de Y . Cela signifie que pour tout ϕ continue bornée, nous souhaitons avoir

$$\frac{1}{n_{\text{off}}} \sum_{j=1}^{n_{\text{off}}} w_j \phi(f(X'_j, \Theta_j)) \xrightarrow[n_{\text{off}, n_{\text{on}} \rightarrow +\infty}{} \mathbb{E}[\phi(f(X, \Theta))], \quad (1.3)$$

ou en termes de loi empirique, la mesure

$$\widehat{\mu}_{Y'_j}^{\mathbf{w}_{n_{\text{off}}}} = \frac{1}{n_{\text{off}}} \sum_{j=1}^{n_{\text{off}}} w_j \delta_{Y'_j} \quad (1.4)$$

doit converger étroitement vers μ_Y quand n_{off} et n_{on} tendent vers l'infini. Pour parvenir à ce résultat, le vecteur de poids $\mathbf{w}_{n_{\text{off}}}$ doit dépendre à la fois de l'échantillon synthétique $(X'_i)_{i \in \llbracket 1, n_{\text{off}} \rrbracket}$ et de celui tiré selon la vraie loi $(X_j)_{j \in \llbracket 1, n_{\text{on}} \rrbracket}$.

1.3.4.b Une première méthode de pondération : estimation des ratios d'importances

Dans l'algorithme original de 2012 [5], les poids sont construits pour approcher le *ratio d'importance*

$$w_j = \frac{\widetilde{\mu}_X}{\widetilde{\mu}_{X'}}(X'_j) \simeq \frac{\mu_X}{\mu_{X'}}(X'_j) = w(X'_j)$$

en prenant pour $\widetilde{\mu}_X$ et $\widetilde{\mu}_{X'}$ des estimations de densité à noyaux construits à partir des échantillons. L'observation à la base de l'échantillonnage d'importance, qui est que

$$\begin{aligned} \frac{1}{n_{\text{off}}} \sum_{j=1}^{n_{\text{off}}} w(X'_j) \phi(f(X'_j, \Theta_j)) &\xrightarrow[n_{\text{off}} \rightarrow +\infty}{} \int \phi(f(x, \theta)) \frac{\mu_X}{\mu_{X'}}(x) \mu_{X'}(x) dx d\mu_{\Theta}(\theta) \\ &= \int \phi(f(x, \theta)) \mu_X(x) dx d\mu_{\Theta}(\theta) \\ &= \mathbb{E}[\phi(f(X, \Theta))] \end{aligned}$$

permet de conclure à la convergence en loi. Plus généralement, différentes techniques d'estimation de ratio d'importance ont été développées dans la littérature [109] pour estimer $w(X'_j)$. Toutefois, ces techniques supposent l'existence d'un w vérifiant $\mu_X(dx) = w(x)\mu_{X'}(dx)$, ce qui revient à dire que μ_X est *absolument continue par rapport à $\mu_{X'}$* .

Dans notre contexte cependant, $\mu_{X'}$ doit être choisi par l'acteur v sans avoir une information précise sur μ_X . Par expérience, v peut connaître l'étendue de son support, mais comme X peut être la sortie d'une fonction, son support exact peut être une sous-variété de l'espace. Imaginons que le code de calcul du parent u soit

$$Y_u = f_u(X_u) = (X_u^2, \sin(2\pi X_u)), \quad X_u \sim \mathcal{U}([-1, 1]).$$

L'acteur v peut savoir que son entrée $X = Y_u$ prend ses valeurs dans le rectangle $[-0.5, 1.5] \times [-1.5, 1.5]$, mais ne sait pas qu'elles sont exactement dans la courbe $(t^2, \sin(2\pi t))$. Nous pouvons donc nous retrouver dans une situation semblable à celle de la Figure 1.6, où le support de μ_X est inclus dans celui de $\mu_{X'}$, mais l'absolue continuité n'est pas vérifiée. Nous cherchons une méthode consistante dans ces cas-là.

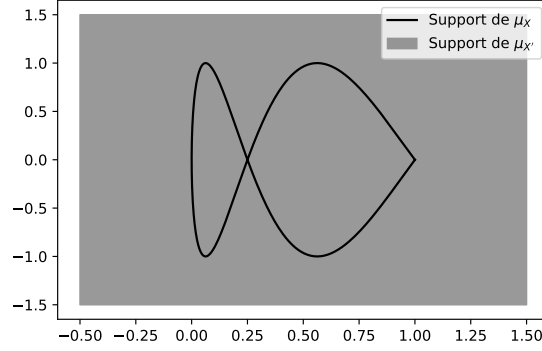


FIGURE 1.6 : La mesure μ_X n'est pas absolument continue par rapport à $\mu_{X'}$, mais le support de μ_X est inclus dans celui de $\mu_{X'}$.

1.3.4.c Surmonter la non absolue continuité : méthode de pondération par minimisation d'une distance de Wasserstein

Cette nécessité d'abandonner l'hypothèse d'absolue continuité nous amène à considérer naturellement la famille de distances de Kantorovich–Rubinstein, plus connues sous le nom de distances de Wasserstein W_q , dont nous rappelons la définition.

Definition (Distance de Wasserstein). Soit $\mathcal{P}_q(\mathbb{R}^d)$ l'ensemble des mesures de probabilité sur \mathbb{R}^d de moment d'ordre $q \in [1, +\infty)$ fini. La distance de Wasserstein d'ordre q entre deux mesures μ et ν de $\mathcal{P}_q(\mathbb{R}^d)$ est définie par

$$W_q(\mu, \nu) = \inf \left\{ \int_{\mathbb{R}^d \times \mathbb{R}^d} |x - x'|^q d\gamma(x, x') : \gamma \in \Pi(\mu, \nu) \right\}^{1/q},$$

où $\Pi(\mu, \nu)$ est l'ensemble des mesures de probabilité sur $\mathbb{R}^d \times \mathbb{R}^d$ de lois marginales μ et ν .

Contrairement à certaines mesures de dissimilarité, comme la divergence de Kullback-Leibler, la distance de Wasserstein est bien définie même lorsque aucune des deux mesures n'est absolument continue par rapport à l'autre. Nous nous référons à [90] pour une revue des résultats existants sur cette distance.

Au lieu de nous intéresser directement à la convergence de $\hat{\mu}_{\mathbf{Y}'_{n_{\text{off}}}}^{\mathbf{w}_{n_{\text{off}}}}$ vers μ_Y de l'Équation (1.4), nous regardons d'abord l'approximation de μ_X par $\hat{\mu}_{\mathbf{X}'_{n_{\text{off}}}}^{\mathbf{w}_{n_{\text{off}}}}$, en notant

$$\hat{\mu}_{\mathbf{X}'_{n_{\text{off}}}}^{\mathbf{w}_{n_{\text{off}}}} = \frac{1}{n_{\text{off}}} \sum_{j=1}^{n_{\text{off}}} w_j \delta_{X'_j}, \quad (1.5)$$

un argument utilisant l'expression duale de la distance de Wasserstein W_1 nous permettant de remonter à l'approximation de μ_{Y_v} par $\hat{\mu}_{\mathbf{Y}'_{n_{\text{off}}}}^{\mathbf{w}_{n_{\text{off}}}}$. Nous découpons classiquement l'erreur via l'inégalité triangulaire

$$W_q(\mu_X, \hat{\mu}_{\mathbf{X}'_{n_{\text{off}}}}^{\mathbf{w}_{n_{\text{off}}}}) \leq W_q(\mu_X, \hat{\mu}_{\mathbf{X}_{n_{\text{on}}}}) + W_q(\hat{\mu}_{\mathbf{X}_{n_{\text{on}}}}, \hat{\mu}_{\mathbf{X}'_{n_{\text{off}}}}^{\mathbf{w}_{n_{\text{off}}}}),$$

avec $\widehat{\mu}_{\mathbf{X}_{n_{\text{on}}}}$ la mesure empirique de l'échantillon $(X_i)_{i \in \llbracket 1, n_{\text{on}} \rrbracket}$. La convergence de la mesure empirique vers la mesure théorique est étudiée dans la littérature [50], et nous donne les taux de convergence de l'espérance de $W_q(\mu_{X_v}, \widehat{\mu}_{\mathbf{X}_{n_{\text{on}}}})$ vers 0. Nos travaux se concentrent donc sur l'étude du deuxième terme $W_q(\widehat{\mu}_{\mathbf{X}_{n_{\text{on}}}}, \widehat{\mu}_{\mathbf{X}'_{n_{\text{off}}}}^{\mathbf{w}})$. Nous commençons par montrer que les poids optimaux minimisant la distance

$$\mathbf{w}_{n_{\text{off}}}^* = \underset{\mathbf{w}}{\operatorname{arginf}} W_q(\widehat{\mu}_{\mathbf{X}_{n_{\text{on}}}}, \widehat{\mu}_{\mathbf{X}'_{n_{\text{off}}}}^{\mathbf{w}}),$$

ont une expression simple en terme de plus proches voisins. La composante w_j^* du vecteur optimal, est proportionnelle au nombre de points dans $(X_i)_{i \in \llbracket 1, n_{\text{on}} \rrbracket}$ dont X_j' est le 1-plus proche voisin, parmi tous les points de $(X_j')_{i \in \llbracket 1, n_{\text{off}} \rrbracket}$.

Résultats Nous démontrons la consistance dans la section 10.3.1 : sous des hypothèses faibles de moment et d'inclusion du support de μ_X dans le support de $\mu_{X'}$, la quantité $W_q(\widehat{\mu}_{\mathbf{X}_{n_{\text{on}}}}, \widehat{\mu}_{\mathbf{X}'_{n_{\text{off}}}}^{\mathbf{w}^*})$ converge bien vers 0 en espérance. Dans la section 10.3.2, nous nous intéressons aux taux de convergence. Sous des hypothèses plus fortes, notamment que $\mu_{X'}$ ait une densité $p_{X'}$ avec un certain poids et que l'on ait

$$\mathbb{E} \left[\frac{1 + |X|^q}{p_{X'}(X)^{q/d}} \right] < +\infty,$$

nous démontrons le taux de convergence suivant

$$\mathbb{E} \left[W_q^q(\widehat{\mu}_{\mathbf{X}_{n_{\text{on}}}}, \widehat{\mu}_{\mathbf{X}'_{n_{\text{off}}}}^{\mathbf{w}^*}) \right] \propto n^{-q/d} \left(\mathbb{E} \left[\frac{1}{p_{X'}(X)^{q/d}} \right] + o(1) \right).$$

Remarquons ici que $\widehat{\mu}_X$ ne doit pas nécessairement être à densité. Nous nous sommes donc affranchis de l'hypothèse d'absolue continuité. Ces résultats nous permettent de calculer des taux de convergence pour l'estimation de la quantité d'intérêt de l'équation (1.3) dans un cas sans variable aléatoire Θ . Si l'on veut inclure Θ , un estimateur basé sur le 1-plus proche voisin n'est plus forcément consistant. Nous le remplaçons par des poids basés sur des $k_{n_{\text{off}}}$ -plus proches voisins avec $k_{n_{\text{off}}}$ qui doit tendre vers l'infini avec n_{off} . Une adaptation simple du cas pour 1-plus proche voisin permet de retrouver de la consistance et de calculer des taux de convergence.

Le Chapitre 10 nous permet de voir quantitativement comment se comporte une méthode de pondération au niveau d'un noeud. Dans la prochaine section, nous revenons au cas général du graphe.

1.3.5 Propagation sur le graphe et méthode d'approximation par pondération linéaire en la loi (WLAMs)

Revenons au cas général du graphe; nous pouvons maintenant décrire le fonctionnement de l'algorithme un peu plus précisément.

Phase offline Si un noeud v n'a pas de parents (*i.e.* c'est une racine du graphe), il génère des observations

$$\mathbf{S}_{v, n_v} = (Y'_{v,j})_{j \in \llbracket 1, n_v \rrbracket}$$

avec $Y'_{v,j} = f_v(\Theta_{v,j})$. Si un noeud v a des parents, il génère des échantillons synthétiques

$$\mathbf{S}_{v, n_v} = (X'_{v,j}, Y'_{v,j})_{j \in \llbracket 1, n_v \rrbracket}$$

avec $Y'_{v,j} = f_v(X'_{v,j}, \Theta_{v,j})$.

Phase online Nous découpons la phase online en deux étapes.

Approximation des loi conditionnelles Pour chaque noeud v qui n'est pas une racine, des échantillons $(X'_{u,v,j})_{j \in \llbracket 1, n_u \rrbracket}$ issus des parents $u \in \mathcal{J}(v)$ sont calculés. Ces échantillons vérifient, pour $j \in \llbracket 1, n_u \rrbracket$

$$\begin{aligned} X'_{u,v,j} &= g_{u,v}(Y'_{u,j}) \\ &= g_{u,v}(f_u(X'_{u,j}, \Theta_{u,j})), \end{aligned}$$

c'est à dire qu'ils sont issus des sorties de l'échantillons synthétique des parents. En utilisant ces derniers et \mathbf{S}_{v,n_v} , une *méthode de pondération* calcule un tableau à $|\mathcal{J}(v)| + 1$ dimensions, qui pour chaque multi-indice $(j_u)_{u \in \mathcal{J}(v)}$, contient des poids $(W_{v,j_v}(\mathbf{S}_{v,n_v}, (X'_{u,v,j_u})_{u \in \mathcal{J}(v)}))$. Ces poids doivent approcher la probabilité conditionnelle que Y_v prenne la valeur Y'_{v,j_v} sachant que $X_v = (X'_{u,v,j_u})_{u \in \mathcal{J}(v)}$.

Propagation des poids Une fois que ce tableau de poids est construit pour chaque noeud, il reste à combiner ces poids pour retrouver la loi jointe. Un *algorithme de propagation des poids* doit permettre de calculer une approximation de la loi des $(Y_v)_{v \in \mathcal{V}}$.

Nos travaux se concentrent sur deux questions portant sur deux aspects importants de l'algorithme.

- Que fait une *méthode de pondération* et quelles propriétés doit-elle vérifier pour que notre algorithme approche effectivement la loi jointe des $(Y_v)_{v \in \mathcal{V}}$?

L'article séminal [5] propose une pondération par estimation des ratios d'importance. Nous proposons une pondération par minimisation de distance de Wasserstein dans le Chapitre 10. Ces deux méthodes peuvent se voir comme des cas particuliers de méthodes d'approximation par pondération linéaire en lois (WLAMs), que nous définissons dans un cadre abstrait et qui généralisent les deux techniques. Nous proposons une définition de consistance au niveau d'un noeud, qui permettra d'avoir un résultat de convergence dans un sens approprié vers la loi au niveau du graphe.

- Une fois que les poids sont calculés à chaque noeud du graphe, comment reconstruire les lois jointes $(Y_v)_{v \in \mathcal{V}}$?

La pondération à chaque noeud peut se voir comme une table de probabilité conditionnelle (CPT) des sorties par rapport aux entrées. Sous cette interprétation, la propagation de poids est équivalente au problème dit d'*inférence dans réseau bayésien discret*. Nous explicitons cette formulation et montrons comment construire ce réseau bayésien. En utilisant les algorithmes classiques de ce domaine, nous pouvons donc effectuer la propagation des poids pour approcher la loi jointe de n'importe quel sous-ensemble de variables dans le graphe.

1.3.6 Organisation de la partie II

Le chapitre 10 est dédié à l'étude théorique de la méthode de pondération par distance de Wasserstein. Nous y dérivons les résultats de consistance en Section 10.3.1 et les taux de convergence en Section 10.3.2. Dans la Section 10.4 nous appliquons ces résultats aux calculs de quantités d'intérêt. Dans le chapitre 11, nous décrivons l'approche de propagation de poids généralisée. En Section 11.2.1.a, nous définissons tout d'abord la famille des WLAMs, qui sont des méthodes

de pondération particulières et nous établissons un critère de consistance local. Sous l’hypothèse de consistance locale à chaque noeud, nous démontrons la convergence faible de la loi dans l’ensemble du graphe en Section 11.2.2.b. Enfin, nous explicitons un réseau bayésien discret pour les calculs numériques dans la section 11.3 et nous appliquons cette méthode sur un cas industriel dans la section 11.4.

1.4 Un objectif commun : la réduction des marges importantes

Nous avons vu que les résultats des Parties I et II répondent à des questions différentes et peuvent se comprendre de façon indépendante. Ils se rejoignent cependant sur une application commune : la réduction des marges de conception qui contribuent le plus à un coût dans un système industriel complexe.

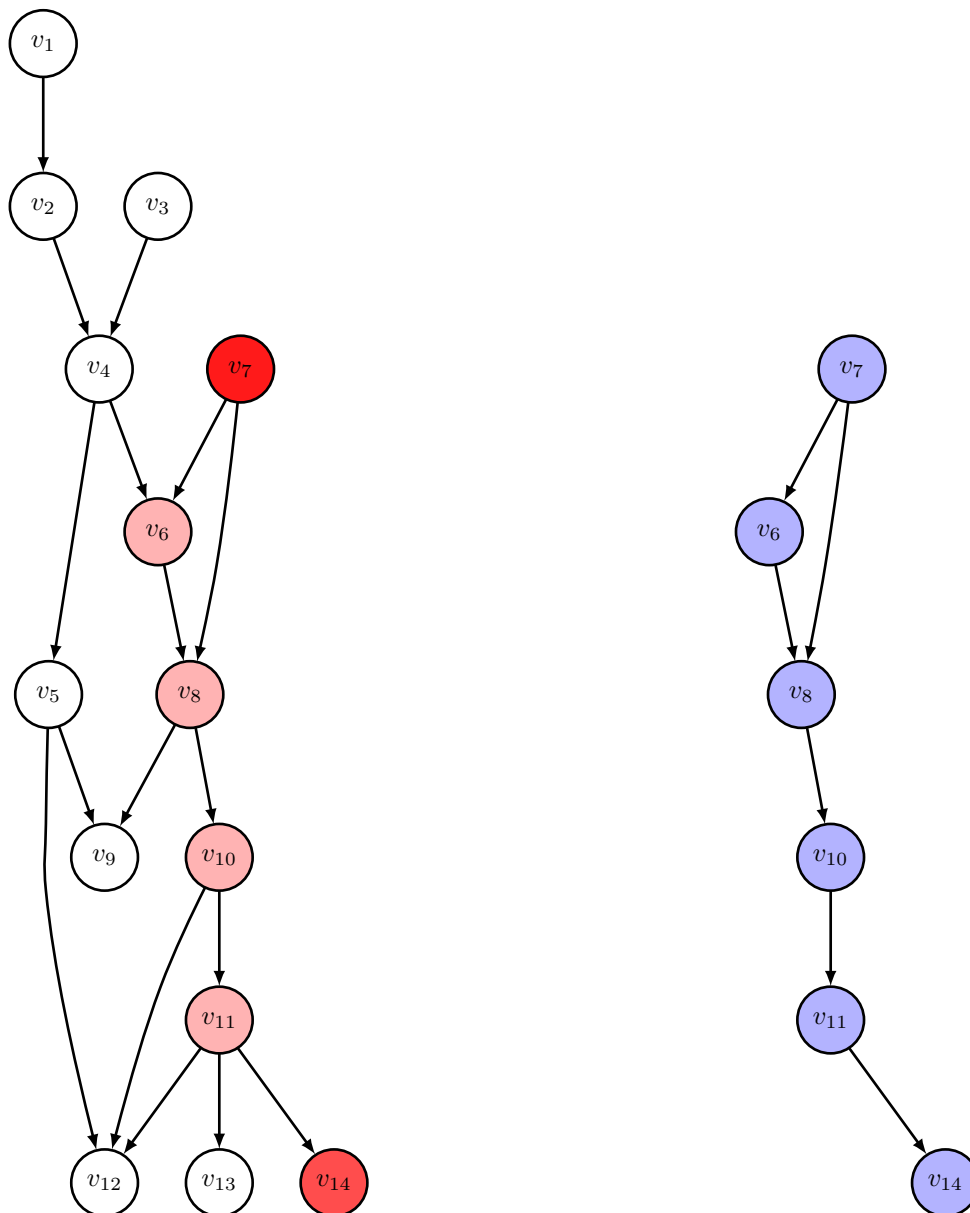
Le constat industriel est qu’une modélisation probabiliste précise de l’ensemble des incertitudes dans tout le processus de conception serait très coûteuse. Dans certains contextes, elle serait même impossible à mettre en place. Nous voulons donc surtout nous concentrer sur les parties où les incertitudes peuvent avoir un grand impact négatif sur un coût ou sur une performance finale. Nous quantifions tout d’abord l’impact des différentes marges pour un coût donné, dans un graphe d’interactions entre disciplines (Figure 1.7a). Cette étape nécessite seulement l’estimation de l’ordre de grandeur des marges demandées à chaque niveau et ne requiert pas d’approche probabiliste. Le but est d’identifier les principaux contributeurs à un coût (*e.g.* la masse du système, la résistance, etc.) via l’analyse de sensibilité du chapitre 5. Ensuite, une fois que le sous-ensemble des contributeurs est identifié, un effort de modélisation probabiliste et de quantification d’incertitude est effectué à chaque niveau, en utilisant des WLAMs (Figure 1.7b). Cette étape peut se faire de façon asynchrone, sans que les disciplines aient à effectuer la modélisation et les calculs au même moment. La reconstruction se fait par la technique de propagation du chapitre 11.

Pour le moment, cette approche reste toutefois à l’état de perspective. Même si ces travaux nous ont permis de décrire rigoureusement une grande partie du problème, il reste encore au moins deux verrous de modélisation.

Le premier verrou est celui de la propagation des marges et de leur décomposition dans un système multidisciplinaire, pendant la phase de la Figure 1.7a. Comme nous l’évoquons dans les perspectives du Chapitre 7, propager les marges dans un système multidisciplinaire revient à interpréter la marge induite d’un parent comme la marge demandée d’un enfant. Il reste à préciser cette relation, pour que la décomposition de la marge induite d’un acteur “parent” se transmette à la décomposition de la marge induite d’un acteur “enfant”. Des premières expériences sur des cas jouets ont été concluantes et nous sommes donc confiants sur la possibilité d’effectuer une propagation des indicateurs de sensibilité de marge sur un graphe.

Le deuxième verrou est celui des critères probabilistes pour la quantification mutualisée de marges. Plus précisément, en agrégeant les marges de plusieurs acteurs, il faut aussi agréger les risques et leurs niveaux d’acceptation. Une description plus complète de la quantification de marge mutualisée avec un modèle de risque probabiliste est nécessaire pour être sûr de garder le même niveau d’exigence en terme de sûreté de fonctionnement.

Des perspectives plus détaillées sont listées dans les Chapitres 7 et 11.



(a) L'analyse de sensibilité sur les marges permet d'identifier que le coût de v_{14} est dû en grande partie à la prise de marge séquentielle depuis v_7 .

(b) Une propagation d'incertitude locale est demandée à chaque acteur du sous-graphe entre v_7 et v_{14} . Une *quantification de marge mutualisée*, se basant sur des critères probabilistes permet de réduire les marges et donc le coût final. La propagation peut se faire de façon découplée, via des WLAMs.

FIGURE 1.7 : Réduction globale des marges par quantification des marges mutualisée via un modèle de risque probabiliste, en se basant sur les résultats des Parties I et II. C'est un cas fictif décrivant une application plausible.

Part I

Model of margin and margin sensitivity analysis

Chapter 2

Introduction and motivation

2.1 Why model margins?

The use of margins to cover some risks is maybe one of the oldest practices when designing a system. Broadly speaking, a margin is an extra quantity taken to cover the risk, understood as some uncertainties and their consequences. However, this definition actually covers two notions:

- **the demanded margin** is a requirement of a minimum extra quantity, to cover some risks;
- **the effective margin** is the actual extra quantity that a design has and that can be used to cover uncertainties. It is sometimes used when analyzing a design to characterize the risk.

During the design of industrial complex systems, one way to mitigate risks is to require demanded margins on multiple quantities to cover various risks. These additional requirements reduce the range of design choices and consequently decrease the performance obtainable and/or increase the cost. In this specific context, two questions are motivated by the industrial stakes:

- **Do the demanded margins have a great impact on the system performance or on its cost?**
- **On which uncertainties should the analyst focus to reduce impactful margins?**

We put the stress on the fact that, in the engineering practices, the uncertainties **are not modeled within a probabilistic framework in general**.

The works developed in this part are the continuation of [115] and are devoted to answering these very two questions, in a quantitative way. The first step is to have a mathematical model for the demanded and the effective margins, that can be used to describe a wide variety of engineering practices. In our review of the literature in Chapter 3, we did not find any definition that fitted this purpose and thus, we proposed a *model of margin* in Chapter 4. The effective margin on a given quantity is defined as a distance to a forbidden set on a subspace of the designs. The demanded margin is defined as an operator that reduces the set of the possible designs.

Once these two notions are rigorously defined, we can describe what happens when an engineer “takes a margin”. In fact, they define a model of margin and choose a demanded margin to cover the risks; we call this phase *margin quantification* (Section 4.4.1).

Now, assuming that multiple demanded margins have been taken, we must compute the impact of these margins on the cost of the system or on its performance. In Chapter 5, we

identify a quantity, that is the induced cost or induced loss of performance, for which we propose some sensitivity indices with respect to the margins. The additional cost/loss of performance is decomposed as the sum of the contributions of the demanded margins, either by some locally computed indices or globally computed indices. This task has a strong resonance with the factor prioritization in sensitivity analysis (see [54, 100] for a comprehensive review of the techniques). Indeed, sensitivity analysis is defined in [99] as “*the study of how uncertainty in the output of a model (numerical or otherwise) can be apportioned to different sources of uncertainty in the model input*” and factor prioritization ranks the input variables by order of the impact they have on an output. In our case, the input variables are the demanded margins and the output variable is the cost or the performance.

Finally, when the influential margins are identified, we put in light three ways to decrease their negative impact without reducing the safety or reliability target. The first one (Section 5.3.1) is to precise how the margin quantification is done. The second one (Section 5.3.2) is to focus on the margins that are taken to cover reducible uncertainties. By definition, these uncertainties can be reduced during the design of the system; a new assessment can shrink them and thus decrease the associated margins. A third way is to model the correlation/independence between the uncertainties that cause margins (Section 5.3.3). When the margin quantification is performed separately on each variable, the margins cannot model the correlation and then lead to a worst-case design that is sometimes unrealistic (*e.g.* it might never happen almost surely). A probabilistic modeling of a few targeted variables may lead to a significant decrease in terms of margins. An application is presented in Chapter 6. The conclusion is drawn in Chapter 7 along with some perspectives both on the industrial applications and on the mathematical study of the model of margin.

We conclude this introductory chapter by a presentation of some relevant notions under the form of short questions and answers. During the author’s Ph.D. thesis, industrial partners formulated practical questions about margins and some of them are presented in the following section.

2.2 Frequently asked questions about margins

- What is a design margin?

We call design margins the margins that are used in the design phases of an industrial system. It is a real nonnegative number $m \geq 0$, it is unidimensional and is most of the time related to a physical quantity (distance, mass, current intensity...).

- Is a margin a characteristic of the system or a kind of safety factor?

In fact the word designates both concepts. To avoid any confusion we distinguish two types of margins: the *effective margin* (Def. 4.2.4), is broadly speaking the distance from a design point to the failure, and the *demand margin* (Def. 4.2.8), is a requirement on the design in terms of effective margins, to cover some uncertainties. We can remark that in both cases, they are a real unidimensional nonnegative number.

- Are margins good in design phases?

Practically speaking, one can see the use of margins as a tradeoff between the complexity of the uncertainty model and the cost of production/operation of a system. In that sense, they are neither good nor bad in essence, but sometimes some gain can be made by questioning their relevance.

- Is a margin a random quantity?

The margins we model are *deterministic quantities* that are used to cover the uncertainties and their consequences. Choosing their value is done in the *margin quantification* phase (Sec. 4.4.1). During this phase, engineers can use probabilistic computations and criterion, but it is not always the case.

- **How about the margin of error in Statistics? It depends on a random sample.**

The margin of error that is sometimes used in *margin quantification* (Section 4.4.1), may indeed be random (*i.e.* proportional to the standard deviation estimator $\hat{\sigma}_n$). However, when focusing on what happens in the design after the margin quantification, it is considered as a fixed quantity and its randomness is not taken into account.

- **Some engineers talk about margins as a range of freedom/operating range and some describe it as an additional constraint. How do you interpret it?**

This range of freedom is the “other point of view” of a *demanded* margin. Assume that an electronic device is designated to work at temperatures between $[T_{\text{nom}} - m_T; T_{\text{nom}} + m_T]$ with $T_{\text{nom}} = 40^\circ\text{C}$ and $m_T = 50^\circ\text{C}$. From the device designer point of view, the demanded margin m_T is an additional constraint - they must ensure it works properly in both high and low temperatures. However, from the user of the device point of view, it is a range of freedom, as they can use it in either in hot and cold environments.

- **What is the cost of a margin?**

The cost of the margin is intuitively the extra cost due to the presence of margins. It is calculated as the cost with margins minus the cost without margins. We define it generally in Section 5.1, as the *induced cost*.

- **Which margins can be removed from a design?**

At first, one must assume that all the margins are taken for specific purposes (safety, uncertainty about the future, etc.). Consequently, they must not be removed without extra analysis, as it could lead to unfortunate consequences. The basis of the approach is that “One can remove a margin only if they ensure the criterion for which it was taken and the decision based on it are still valid after removing it”.

- **How can we remove a margin?**

At the sources of the margins lie the uncertainties and their consequences. If these uncertainties can be reduced during the project, it is possible to remove the margins that cover them. Another way to remove margins is to take into account the correlation or independence between the uncertainty sources, as they are typically not taken into account in margins. These aspects are described in Section 5.3.

- **Does removing margins always reduce the cost of a system?**

In most cases, removing margins indeed reduces the associated cost in a design, as it permits to explore a wider range of decisions. However, in some cases, especially when a quantity is shared between multiple stakeholders, increasing the margin for a player could result in more range of freedom for another player. In that case, more margins could result in a more optimal solution (see the “allocated margin” in the perspective of Section 7.2.1).

- **Where are the important margins in a system?** For a given induced cost or induced loss of performance, one can identify the impactful margins by a sensitivity analysis. We propose some quantitative indices to measure it in Chapter 5. One can also compute the impact of a margin on other margins, by performing a sensitivity analysis on an *induced margin* (Section 5.1).

Chapter 3

State of the art

In order to propose our own model of margin, our literature review focuses on two categories of publications. The first one is those presenting engineering notions, such as confidence intervals, that can be interpreted as margins.

The second category is frameworks for margins, that were industrially motivated by the needs for a unified practice or at least, a unified definition. This need typically appears in large industrial system design, for regulatory, licensing or efficiency purposes.

Engineering field	Notion	Section
Statistics	Confidence interval	3.1.1
Robust optimization	Uncertainty set, Info-gap model	3.1.2
Control	Phase margin, Gain margin	3.1.3
Robust control	Stability radius	3.1.3
Civil engineering	Partial safety factor	3.1.4
Mechanics of materials	Safety factor	3.1.5
Finance and robust optimization	Coherent risk measure, Acceptance set	3.1.6
Engineering field	Framework name	Section
Nuclear safety	Traditional margin, Probabilistic margin	3.2.1
	Quantification of margin and uncertainties (QMU)	3.2.2
Complex system design	Performance margins, Safety performance margins	3.2.3
	Margin allocation and tradeoff	3.2.4
	Buffer, Excess, Margin value method (MVM)	3.2.5

Table 3.1: Margin notions and frameworks in the literature that we studied to construct our model. This table echoes Table 4.2 in which we reinterpret them as margins under our framework.

3.1 Margins in engineering fields

3.1.1 Confidence intervals

Confidence intervals are statistical objects that were first introduced in [86] by J. Neyman in 1937. They have become the standard way to handle uncertainty in estimation and tests [19, 32, 121] and are practically used in any engineering field using statistics such as survey design, control, finance, statistical quality [85, 96], etc.

Definition 3.1.1 (Confidence interval). Let $\theta \in \mathbb{R}$ be a parameter of the law of the random variable X and X_1, \dots, X_n be n i.i.d. copies of X . A confidence interval Λ_n of level $1 - \alpha \in [0; 1]$ is an interval that is a function of X_1, \dots, X_n , such that

$$\mathbb{P}(\theta \in \Lambda_n) = 1 - \alpha.$$

Other types of confidence interval can be found in the literature, such as asymptotic confidence intervals for which the equality holds in the limit $n \rightarrow +\infty$ or conservative confidence intervals for which the probability is required to be greater than or equal to $1 - \alpha$.

A widely known example is when X is a normal random variable of mean θ and variance σ^2 , that is assumed known. In that case, the centered confidence interval of level $1 - \alpha \geq 0.5$ for the parameter θ is

$$\Lambda_n = \left[\hat{\theta}_n - q_{1-\alpha/2} \frac{\sigma}{\sqrt{n}}; \hat{\theta}_n + q_{1-\alpha/2} \frac{\sigma}{\sqrt{n}} \right]$$

with $\hat{\theta}_n = \frac{1}{n} \sum_{i=1}^n X_i$ and $q_{1-\alpha/2}$ is the quantile of level $1 - \alpha/2$ of a standard random variable. By the Central Limit Theorem, it is also an asymptotic confidence interval of $\theta = \mathbb{E}[X]$ for any random variable X with finite variance.

The value $m = q_{1-\alpha/2} \frac{\sigma}{\sqrt{n}}$ is the extra quantity taken to prevent the statistical uncertainty involved by taking $\hat{\theta}_n$ instead of θ . It is then a demanded margin.

3.1.2 Uncertainty sets in robust optimization (Operations Research)

In Operations Research, the field of Robust Optimization is devoted to solve the following optimization problem [16]:

$$\begin{aligned} & \text{minimize } f_0(\mathbf{x}) \\ & \text{subject to } f_i(\mathbf{x}, u_i) \leq 0 \quad \forall u_i \in \mathcal{U}_i, i \in \llbracket 1, n \rrbracket \end{aligned} \quad (3.1)$$

with the u_i representing the uncertain parameters and \mathcal{U}_i the so-called *uncertainty sets*, that are used to model the uncertainty on the variables u_1, \dots, u_n . The underlying idea behind this formulation is that, in some applications, a probabilistic description of the uncertainties might not be relevant (*e.g.* observations of data are lacking but there is an expert judgment). Instead the uncertainty on u_i is modeled by a set, that is often centered at a nominal value \hat{u}_i .

One of the topics of interest of the field is to study the tractability of the problem (3.1) for some family of uncertainty sets, coupled with specific optimization problems. The uncertainty sets can take the form of an interval/cuboid, but also more complex forms, such as an ellipsoid, for which we recall the definition.

Definition 3.1.2 (Ellipsoidal uncertainty set). An ellipsoidal uncertainty set [14] [16, Section 3.1] centered on $\hat{u} \in \mathbb{R}^n$ is defined as:

$$\mathcal{U}^Q(\hat{u}, \gamma) = \{ \tilde{u} : (\tilde{u} - \hat{u})' \Sigma^{-1} (\tilde{u} - \hat{u}) \leq \gamma^2 \} \quad (3.2)$$

with $\Sigma \in \mathbb{R}^{d \times d}$ a positive definite matrix and $\gamma > 0$.

The coordinates $\hat{u}_1, \dots, \hat{u}_n$ are the nominal values of the parameters u_1, \dots, u_n and the choice of γ sets the extent of the domain. The quantity γ is then a demanded margin.

3.1.2.a Extensions of robust optimization

An extension of robust optimization is the use of data to construct the uncertainty sets [17], from some data and confidence intervals of statistical tests. The value of the demanded margin is then chosen based on data.

Let $(\mathcal{X}, \mathcal{F})$ be a measurable space and \mathbf{F} be a (measurable) failure set included in \mathcal{X} . Other approaches, known as *Optimal Uncertainty Quantification* [89] and *Distributionally robust optimization* [122], are interested in probabilistic constraints such as $\mathbb{P}_{X \sim \mu_X}(X \notin \mathbf{F}) \geq p$ that must hold for all μ_X in \mathcal{P} . The set \mathcal{P} is a family of probability distributions of random variables taking their value in \mathcal{X} . In this context, demanded margins are then taken on the probability measures of random variables.

3.1.2.b Info-gap methodology

The info-gap methodology, exposed in [12, 13] aims to be a decision theory under uncertainty, without a probabilistic modeling.

Info-gap model The methodology is based on a mathematical object called *info-gap model* that can be seen as a *parametrized uncertainty set* of Equation (3.1). If u is a point of a Banach space \mathcal{X} , an info-gap model is a family of sets $\mathcal{U}(\alpha, u)$ parametrized by $\alpha \in [0, +\infty)$ such that

$$\text{if } 0 \leq \alpha \leq \beta, \quad \text{then } \mathcal{U}(\alpha, u) \subset \mathcal{U}(\beta, u)$$

and $\mathcal{U}(0, u) = \{u\}$. It also often verifies the following linearity property, for $\alpha > 0$

$$\mathcal{U}(\alpha, u) = \alpha \mathcal{U}(1, 0) + u. \quad (3.3)$$

Robustness The robustness at a point $u \in \mathcal{X}$ is defined as the greatest α for which the requirements are satisfied for all points in the uncertainty set. For a vector of decision x , its expression is [13, Eq. 3.1]

$$\hat{\alpha}(x, u) = \max \{ \alpha \mid f(x, u) \leq 0, \quad \forall u \in \mathcal{U}(\alpha, u) \},$$

with $f(x, u)$ being positive if and only if the constraints are not met. By denoting the failure set $\mathbf{F}(x) = \{u \mid f(x, u) > 0\}$, we can rewrite the robustness as

$$\hat{\alpha}(x, u) = \max \{ \alpha \mid y \notin \mathbf{F}(x), \quad \forall y \in \mathcal{U}(\alpha, u) \}. \quad (3.4)$$

The last expression really puts in light that $\hat{\alpha}(x)$ is an effective margin: it measures the extra quantity around u that separates it from the failure states $\mathbf{F}(x)$.

Robust-satisficing optimization Robust-satisficing optimization [13, Sec. 11] consists in choosing the most robust decision x at a critical point u_c

$$x^* = \operatorname{argmax}_x \hat{\alpha}(x, u_c).$$

3.1.3 Control and robust control

In order to ensure some robustness in the design of systems, the theory of control and robust control have developed some notions of margins. The goal of the analysis is to ensure the stability of a system that is modeled by the complex transfer function

$$H_{cl}(s) = \frac{H_{fo}(s)}{1 + H_{ol}(s)}, \quad s \in \mathbb{C}, \quad (3.5)$$

with H_{fo} being the *feedforward*, H_{ol} the *open-loop* and H_{cl} the *closed-loop* transfer functions, that are rational complex functions with real coefficients. The stability is ensured as soon as the roots of the polynomial

$$1 + H_{ol}(s) = a_0 + a_1s + a_2s^2 + \dots + a_ns^n$$

have negative real parts. Such a polynomial is called *strictly Hurwitz*.

3.1.3.a Gain margin and phase margin

The gain margin and the phase margin [51, Section 6.4], [77, Section 8.4.2] came from the Strecker-Nyquist criterion, introduced in [87], that is a graphical method to verify the stability. It is based on Cauchy's argument principle that states that when H_{ol} has no poles with positive real parts, the number of roots with positive real parts of $1 + H_{ol}(s)$ is actually the number of times the graph in the complex plane of

$$H_{ol}(tj)$$

encircles the point $-1 + 0j$ when t goes from $-\infty$ to $+\infty$ (j is the complex number of imaginary part equal to 1 and null real part). The gain and the phase margins measure how far the curve $(H_{ol}(tj))_{t \in [-\infty, +\infty]}$ is from encircling -1 , either in terms of additional gain or additional phase. They are effective margins.

3.1.3.b Stability radius

Besides ensuring that $1 + H_{ol}(s)$ is strictly Hurwitz, the robust control approach verifies that polynomials around $1 + H_{ol}(s)$ are also strictly Hurwitz, to cover possible uncertainties. More precisely, they investigate the stability of polynomials with coefficients parametrized by $\mathbf{q} \in Q$

$$1 + H_{ol,\mathbf{q}}(s) := p(s, \mathbf{q}) = a_0(\mathbf{q}) + a_1(\mathbf{q})s + \dots + a_n(\mathbf{q})s^n$$

with Q being the domain of the design parameters and check the stability by ensuring that each polynomial in the set

$$P(Q) = \{p(s, \mathbf{q}) \mid \mathbf{q} \in Q\}$$

are strictly Hurwitz. The set of parameters is typically a box $Q = [q_{1,-}, q_{1,+}] \times \dots \times [q_{l,-}, q_{l,+}]$ with l the number of parameters. After centering Q on the origin, the *stability radius* ρ ([2, Chap. 7]) is the smallest dilatation $\lambda > 0$ such that $P(\lambda Q)$ has an element that is not stable. It writes

$$\rho = \inf \{ \lambda > 0 \mid \exists p \in P(\lambda Q) \text{ that is not strictly Hurwitz} \}. \quad (3.6)$$

The number ρ plays the role of a margin, measuring the "extra quantity" by which the parameters can vary from their mean value $(q_{i,-} + q_{i,+})/2$, before reaching an unstable state. It is then an effective margin.

From a computational point of view, Kharitonov's theorem [69] has permitted to handle cases when the a_i are linear in \mathbf{q} . Tsypkin-Polyak's locus method [118] dealt with other shapes of parameter sets Q .

3.1.4 Partial safety factors

The semi-probabilistic approach with partial safety factors was described in the ISO document *General principles on reliability for structures* [106, Section 9] and was applied, for instance, in

the European standards documents for structural engineering *Eurocode* [35]. It was used for the design of civil engineering structures, when the failure modes, their consequences and the representation of the uncertainties can be *categorized and standardized*. In that case, some safety coefficients, the so-called partial factors, can be calibrated with a probabilistic model so that the rules for design can be written deterministically.

More precisely, it is assumed that the structural response can be categorized either as a desirable state or a failure state, the failure being defined through the inequality

$$G(x_1, \dots, x_m, y_1, \dots, y_n) := R(x_1, \dots, x_m) - S(y_1, \dots, y_n) \leq 0. \quad (3.7)$$

Here, (x_1, \dots, x_m) are the resistance parameters, (y_1, \dots, y_n) are the action parameters, the function R models the resistance and the function S models the action effect. In order to take some uncertainties into account, a partial factor

$$\gamma \in [1, +\infty)$$

is assigned to each variable so that the value used in the computation, called design value, is different from the one that is estimated, designated under the name of characteristic value.

The design value of the resistance is $R_d = R(x_{1,d}, \dots, x_{m,d})/\gamma_R$ with γ_R accounting for the model uncertainty of the resistance model. For each resistance parameter x_i , its design value is $x_{i,d} = x_{i,k}/\gamma_{x_i}$ with $x_{i,k}$ being its characteristic value, determined through experiments for instance, and γ_{x_i} accounting for the uncertainty on the material property. The function R is assumed to be an increasing function of each resistance parameter.

The design value for the action is $S_d = S(y_{d,1}, \dots, y_{d,n})\gamma_S$ with γ_S accounting for the uncertainties in modeling the effects of the actions. For each action, the design value is $y_{j,d} = \gamma_{y_j} y_{j,k}$ with $y_{j,k}$ being the characteristic value of the action γ_{y_j} accounting for the uncertainty in its determination. The function S is assumed to be an increasing function of each action parameter.

Finally, the verification using partial factors consists in checking that the inequality

$$G_d = R_d - S_d = R(x_{1,k}/\gamma_{x_1}, \dots, x_{m,k}/\gamma_{x_m})/\gamma_R - S(\gamma_{y_1} y_{1,k}, \dots, \gamma_{y_n} y_{n,k})\gamma_S > 0 \quad (3.8)$$

holds. Under this criterion, each partial factor $\gamma - 1$ takes the role of a demanded margin, *i.e.* the “extra quantity” between the design value and the characteristic value that mitigates the risks.

Partial factors calibration The choice of the numerical values of the partial factor in the standards is called *design code calibration* - code is here a synonym of standard. According to [80], the choice of these values was done in the past by real life feedback and references to expert judgments. Modern approaches, such as those followed in [53, 80, 105, 110] [76, Section 10], consist in calibrating partial safety factors with a probabilistic model for a given domain of validity - thus providing a rule that covers a range of scenarios. The introduction of [105] shows a clear 7-step process used in the calibration:

1. Definition of the scope of the rules, by choosing which type of structures it applies to.
2. Definition of the reliability targets, in term of probability of failure.
3. Definition of how the rules would be presented.
4. Identification of typical failure modes and of stochastic models.
5. Choice of a measure of closeness between the target reliability and the one actually reached

6. Determination of the optimal partial safety factors, by minimizing the distance between the computed probability of failure and the targets.
7. Verification

The calibration finally gives numerical values for the partial factors, along with the type of structure considered and the target reliability.

3.1.5 Safety factors

In mechanics of material, failure analysis is devoted to identify when the failure occurs, for a given structure and solicitation. Some authors in this field [21, 22, 124] provide a definition of a safety factor λ_l of the form

$$\lambda_l = \max_{\substack{\mathbf{H}\boldsymbol{\Sigma} + \lambda\mathbf{F}_0 = 0 \\ (N_{i,j}^l, M_{i,j}^l) \in G, \quad l \in \llbracket 1, n \rrbracket}} \lambda$$

The symbols $N_{i,j}$ (resp. $M_{i,j}$) represent the values of the tensor of the membrane force (resp. the bending moment). The first equation $\mathbf{H}\boldsymbol{\Sigma} + \lambda\mathbf{F}_0 = 0$ is the equilibrium principle for the finite element methods with \mathbf{F}_0 being the reference load for the structure. The vector $\boldsymbol{\Sigma} = (N_{i_1, j_1}^e, \dots, N_{i_n, j_n}^e, M_{i_1, j_1}^e, \dots, M_{i_n, j_n}^e)$ is the vector of the static unknowns at different points of the mesh and \mathbf{H} is the stiffness matrix. From the finite element solution, the values of the central membrane force and bending moment $(N_{i,j}^l, M_{i,j}^l)$ are evaluated by interpolation at some given points indexed by $l \in \llbracket 1, n \rrbracket$. There is a failure if one of these points does not belong to G .

The quantity λ_l represents the maximum extent to which it is possible to increase \mathbf{F}_0 before reaching the failure. It is then an effective margin.

3.1.6 Coherent risk measures

Coherent risk measure Coherent risk measures were introduced in [8] by P. Artzner, F. Delbaen, J-M. Eber and D. Heath in the field of Mathematical finance and are widely popular in risk management for regulatory purposes.

Let X be a real random variable modeling the final net worth of a position. A *risk measure* is a function taking X as input and returning a deterministic real number

$$\rho : \begin{array}{l} L^0(\Omega, \mathbb{R}) \\ X \end{array} \begin{array}{l} \rightarrow \\ \mapsto \end{array} \begin{array}{l} \mathbb{R} \\ \rho(X) \end{array}$$

with $L^0(\Omega, \mathbb{R})$ denoting the set of the real random variables. Intuitively, $\rho(X)$ is the measure of the risk that is associated to holding the position X . If the measure is *coherent* (see below), the risk is expressed in terms of cash and $\rho(X)$ actually represent the amount of money to put aside in order to cover the risk of the position. This extra quantity is used to cover the risk; it is then a *demanded margin*.

A risk measure is *coherent* if it satisfies the following properties:

- Translation property. For each deterministic value $x \in \mathbb{R}$

$$\rho(X + x) = \rho(X) - x. \quad (3.9)$$

- Positive homogeneity. For any $\beta \geq 0$

$$\rho(\beta X) = \beta \rho(X).$$

- Convexity. For any $(X, Y) \in (L^0(\Omega, \mathbb{R}))^2$ and $t \in [0, 1]$

$$\rho(tX + (1 - t)Y) \leq t\rho(X) + (1 - t)\rho(Y).$$

- Monotonicity. If $(X, Y) \in (L^0(\Omega, \mathbb{R}))^2$ and $X \leq Y$ then

$$\rho(Y) \leq \rho(X).$$

Let us denote by F_X^{-1} the inverse CDF of X . A classic result is that the Value at Risk of level α

$$\text{VaR}_\alpha(X) = -F_X^{-1}(\alpha),$$

the that is widely used in financial risk management and represents the worst loss in the $1 - \alpha$ proportion of the best cases, is actually not coherent. It lacks convexity and thus cannot model the decrease of the risk by the diversification of the portfolio. That is why, its integrated version, the Conditional Value at Risk

$$\text{CVaR}_\alpha(X) = -\frac{1}{\alpha} \int_0^\alpha \text{VaR}_p(X) dp, \quad (3.10)$$

is proposed as an alternative. It is coherent and models the mean loss of the α worst scenarios.

Acceptance set We can associate an acceptance set to each risk measure

$$\mathcal{A}_\rho = \{X \in L^0(\Omega, \mathbb{R}) \mid \rho(X) \leq 0\},$$

the that contains the random variable with a measure of risk smaller than 0. In other terms, the position with positive risk are not allowed. Conversely, for any subset of random variables $\mathcal{A} \subset L^0(\Omega, \mathbb{R})$, it is possible to associate a risk measure

$$\rho_{\mathcal{A}} = \inf \{r \in \mathbb{R} \mid X - r \notin \mathcal{A}\}.$$

If \mathcal{A} contains all the random variables that are nonnegative, and the only nonpositive random variable in \mathcal{A} is 0, then $\rho_{\mathcal{A}}$ is coherent if and only if \mathcal{A} is convex and is a positively homogeneous cone (*i.e.* $X \in \mathcal{A}$ implies that $aX \in \mathcal{A}$ for any positive a).

3.2 Margin frameworks

3.2.1 Probabilistic margins in nuclear safety

In order to validate and license nuclear reactor designs in terms of safety, multiple methodologies were developed to take into account uncertainties. These methods have evolved with time, as practices were refined and the computing power increased and the related margins changed accordingly.

Former practices: traditional margins According to the American department of energy (DOE) report [74, Sec. 3.4], a margin is traditionally defined in nuclear engineering on a “safety-significant” parameter $y(a)$ as the difference between the load and the capacity, with a representing the event considered. The load represents the actual value of $y(a)$ in operation while the capacity is the maximum or minimum value of $y(a)$ that the system can withstand. When

the requirement of $y(a)$ is to stay below an upper threshold y_{upp} , the expression of the margin is [41, 42, 83]

$$M(y(a)) = \begin{cases} \frac{y_{\text{upp}} - y(a)}{y_{\text{upp}} - y_{\text{ref}}} & \text{if } y_{\text{ref}} \leq y(a) \leq y_{\text{upp}}, \\ 0 & \text{if } y(a) \geq y_{\text{upp}}, \\ 1 & \text{if } y(a) \leq y_{\text{ref}}, \end{cases} \quad (3.11)$$

with a being the scenario considered, $y(a)$ the value of the parameter when a occurs, y_{ref} a reference value for normalization and y_{upp} the upper threshold limit. When the requirement is a lower threshold y_{low} , the margin is

$$M(y(a)) = \begin{cases} \frac{y(a) - y_{\text{low}}}{y_{\text{ref}} - y_{\text{low}}} & \text{if } y_{\text{low}} \leq y(a) \leq y_{\text{ref}}, \\ 0 & \text{if } y(a) \leq y_{\text{low}}, \\ 1 & \text{if } y(a) \geq y_{\text{ref}}. \end{cases}$$

Notice that the unnormalized version also exists [128]

$$M(y(a)) = y_{\text{sup}} - y(a).$$

Another traditional margin is given in the Safety Margin Action Plan final report [64, Eq. 4-1] called *margin to damage*

$$\text{MD} = \frac{\bar{C} - \bar{L}}{\sqrt{\sigma_C^2 + \sigma_L^2}}$$

with \bar{C} and σ_C (resp. \bar{L} and σ_L) are the mean value and standard deviation of the capacity (resp. load). We must remark it is also of use in Civil engineering, under the name of the Cornell index [76].

Probabilistic margins A drawback of the traditional margins of the form of Equation 3.11, is that they require too conservative - *i.e.* pessimistic - computations [42, 83]. In fact, $y(a)$ being a deterministic value conditionally to a , it has to take into account the modeling, estimation and numerical simulation error, whose extent is not sharply estimated. That is why the use of *probabilistic margins* is prescribed. To construct them, one needs a random variable Y representing the uncertainty that y is facing. For a given safety criterion $1 - \alpha \in [0, 1]$ (the regulatory instance typically impose 95%), the theoretical expression of the probabilistic margin is the difference between the quantile of Y of level $1 - \alpha$, denoted by $Q_{1-\alpha}(Y)$ and the limiting safety threshold. For instance, in the case of an upper limit, its expression is

$$M_{\text{prob}}^{\text{theo}}(\alpha) = \begin{cases} \frac{y_{\text{sup}} - Q_{1-\alpha}(Y)}{y_{\text{sup}} - y_{\text{ref}}} & \text{if } y_{\text{ref}} \leq Q_{1-\alpha}(Y) \leq y_{\text{upp}}, \\ 0 & \text{if } Q_{1-\alpha}(Y) \geq y_{\text{upp}}, \\ 1 & \text{if } Q_{1-\alpha}(Y) \leq y_{\text{ref}}. \end{cases} \quad (3.12)$$

This margin has the good property that

$$\mathbb{P}_{\text{model}} \left(\frac{y_{\text{sup}} - Y}{y_{\text{sup}} - y_{\text{ref}}} \geq M_{\text{prob}}^{\text{theo}}(\alpha) \right) \geq 1 - \alpha,$$

that means that it gives the “worst margin” in the fraction α of the best cases. Here, the notation $\mathbb{P}_{\text{model}}$ means that the probability is computed on the theoretical model.

In practice, however, $Q_{1-\alpha}(Y)$ is computed from a statistical estimation $\hat{Q}_{1-\alpha}(Y)$. With a naive estimation method (empirical quantile), the probability for the estimated value $\hat{Q}_{1-\alpha}(Y)$ to be lower than the actual value of the quantile $Q_{1-\alpha}(Y)$ is 1/2. To cover the risk of this quantile

to be underestimated, a level of *confidence in the estimation* is chosen and we can construct a lower-bounded confidence interval $[\hat{Q}_{1-\alpha,\beta}(Y), +\infty)$ (Section 3.1.1) such that

$$\mathbb{P}_{\text{est}} \left(Q_\alpha(Y) \in [\hat{Q}_{1-\alpha,1-\beta}(Y), +\infty) \right) \geq 1 - \beta$$

the probability measure \mathbb{P}_{est} being defined with respect the randomness due to the statistical estimation. Finally, the probabilistic margin is defined by choosing both a safety level α , accounting for the variability of Y in the model and a confidence level β accounting for the estimation error, leading to the expression

$$M_{\text{prob}}(\alpha, \beta) = \begin{cases} \frac{y_{\text{sup}} - \hat{Q}_{1-\alpha,1-\beta}(Y)}{y_{\text{sup}} - y_{\text{ref}}} & \text{if } y_{\text{ref}} \leq \hat{Q}_{1-\alpha,1-\beta}(Y) \leq y_{\text{upp}}, \\ 0 & \text{if } \hat{Q}_{1-\alpha,1-\beta}(Y) \geq y_{\text{upp}}, \\ 1 & \text{if } \hat{Q}_{1-\alpha,1-\beta}(Y) \leq y_{\text{ref}}. \end{cases}$$

This expression permits to control separately the modeled uncertainty of Y with α and the estimation/computation uncertainty with β . In practice, the quantile $\hat{Q}_{1-\alpha,1-\beta}(Y)$ is computed with the Wilks' method [123], that often requires only a small number of observations of Y_i , thanks to the use of order statistics. This margin is computed to measure the distance between a given design to a failure; it is thus an effective margin.

3.2.2 Quantification of Margins and Uncertainty

The Quantification of Margins and Uncertainty (QMU) is a methodology that addresses risk and risk mitigation in complex systems, when some information remains unknown. It is mainly motivated by the needs for decision indicators for licensing and certifying nuclear stockpiles. They are used with other considerations (social, economic, political, etc.) to support decision in the so-called ‘‘Risk-informed Decision Making’’ methodology. Here, existing systems are scrutinized, and the effective margins are assessed to ensure that they actually cover the risk, especially as the systems age.

The margin is defined under a quite general form in [60, Sec. 6.1]: it is assumed that the system can be represented by a performance vector $\mathbf{P} \in \mathbb{R}^n$ and a requirement vector $\mathbf{R} \in \mathbb{R}^n$. The margin of a system is a function

$$\begin{aligned} M : \mathbb{R}^n \times \mathbb{R}^n &\rightarrow \mathbb{R} \\ (\mathbf{P}, \mathbf{R}) &\mapsto M(\mathbf{P}, \mathbf{R}) \end{aligned}$$

such that

$$M(\mathbf{P}, \mathbf{R}) \geq 0 \Rightarrow \text{compliance of the performance } \mathbf{P} \text{ with the requirement } \mathbf{R},$$

and

$$M(\mathbf{P}, \mathbf{R}) < 0 \Rightarrow \text{noncompliance of the performance } \mathbf{P} \text{ with the requirement } \mathbf{R}.$$

The most common example being the case when \mathbf{P} and \mathbf{R} are unidimensional and \mathbf{R} expresses an upper (resp. lower) requirement, in which case the margin is expressed as $M(\mathbf{P}, \mathbf{R}) = \mathbf{R} - \mathbf{P}$ (resp. $M(\mathbf{P}, \mathbf{R}) = \mathbf{P} - \mathbf{R}$). The performance and requirement can be some physical quantity (see [60, Sec. 3.1]) but can also represent some probability of failure.

The goal is ultimately to quantify the amplitude of the margins versus the amplitude of the uncertainty they cover, in the sense that margins must be high enough to cover uncertainties with a reasonable risk level. The first approach that we can identify in the earliest publications

[103, 104], is to compute a ratio margin over uncertainty, under the form of an inverse coefficient of variation

$$C = \frac{\mathbb{E}[M(\mathbf{P}, \mathbf{R})]}{\sqrt{\text{Var}(M(\mathbf{P}, \mathbf{R}))}}.$$

We can remark that, by Chebyshev's inequality, the probability of $M(\mathbf{P}, \mathbf{R})$ to be lower than zero is bounded by $1/C^2$, as soon as the variance is finite and $\mathbb{E}[M(\mathbf{P}, \mathbf{R})] > 0$.

More recent contributions [60, 61, 92] stress the fact that this representation is not enough to communicate on uncertainty and there is a need to separate the epistemic/reducible uncertainty, that is the uncertainty arising from a lack of knowledge, and the aleatory uncertainty, modeling the "true" randomness of the phenomenon analysed. This separation must be clear in the presentation of the results by, for instance, representing them under different forms. The main motivation is that the decision might not be the same if a quantity is subject to large uncertainty due to the randomness of the phenomenon or if it is due to a lack of knowledge. For instance, in [62] the margin is expressed on a probability of failure, taking into account the aleatory uncertainty, but keeping the epistemic randomness. The margin is then a random variable due to the epistemic uncertainty; as it is unidimensional, its cumulative distribution function can be plotted [62, Fig. 2.2], permitting to visualize the impact of the epistemic uncertainty on the estimation.

3.2.3 Performance margins and safety performance margins in Space engineering

Space engineering is a field in which the complexity and inherent uncertainties of the designed systems has required harmonized risk management practices and consequently harmonized margin practices. A proficient literature on the topic is constituted from the NASA publications such as the Risk Management Handbook [39], the Risk-Informed Decision Making Handbook [40], the System Safety Handbook [38] and Systems Engineering Handbook [63].

Performance margin A *performance margin* is defined in [39, Sec. 4.1.3.1] as "the distance from the achieved value of a performance measure at any point in time to a decision boundary for that measure.[...] Sometimes, however, the maximum allowed value is taken to be the performance requirement minus a contingency percentage of that value (*e.g.* 10%). [...] In that case the decision boundary is 90% of the performance requirement."

If we denote by p the performance measure and p_{req} an upper performance requirement, the performance margin is the classic expression

$$m_{\text{perf}} = p_{\text{req}} - p.$$

in which we recognize the "extra quantity" to ensure the performance. There may be a further contingency ν (equal to 90% in the previous example) such that the performance margin is in fact

$$m_{\text{perf}} = \nu p_{\text{req}} - p,$$

Notice the similarity between ν and the inverse of partial safety factors of Section 3.1.4 $1/\gamma$. In fact it is also a margin as it is a quantity included to cover uncertainty, that is used, for instance, "[...] to allow for mass growth that is expected to occur, based on prior experience [...]" [39, Sec. 4.1.3.1].

In this framework, p_{req} and ν are deterministic but p may be a random variable and consequently m_{perf} is also a random variable. A safety requirement in that case is typically that the random margin m_{perf} must be greater than m_{req} with a probability greater than $1 - \alpha \in [0, 1]$.

Safety performance margin A *safety performance margin* is a margin on a safety performance. A safety performance is defined in [38, Sec. 2.1] as the the probability of the complementary of an harmful event *i.e.* one minus the probability of an adverse event. If we denote by F the harmful event, the safety performance is just a performance expressed in terms of probability

$$p = 1 - \mathbb{P}(F) = \mathbb{P}(F^c).$$

A safety requirement p_{req} is then the minimum acceptable level of safety performance and the safety performance margin is

$$m_{\text{sfty perf}} = \mathbb{P}(F^c) - p_{\text{req}}$$

or in the normalized form

$$\tilde{m}_{\text{sfty perf}} = \frac{\mathbb{P}(F^c) - p_{\text{req}}}{p_{\text{req}}}.$$

The motivation for these safety performance margin is that, although a part of the risk is modeled in F , another part, linked to the unknown unknowns, is not modeled [38, Sec. 3.1.1]. The unknown unknowns are the uncertainties that the analyst is not even aware of and the analysis of previous projects show they can have a substantial impact.

Margin value In order to choose their value, [15] observed that a real-life mission failure in space launches (Soyuz, Space shuttle, Ariane; etc.) puts in light some unknown unknowns/underappreciated risks. These risks are taken into account after the accident and incorporated by practitioners in the simulation models.

The authors performed a retrospective analysis, *i.e.* they estimated the ratio of the probability computed by the models with the new risks and the models without these risk incorporated. As a result, they knew the order of magnitude of the error of the models that did not take the unknown unknowns into account. They give the margin values for $\tilde{m}_{\text{sfty perf}}$, for different maturity of the projects taken in Table 3.2 given in terms of multiplicative margin

$$\tilde{m}_{\text{sfty perf}} \geq m_{\text{req}} \Leftrightarrow \mathbb{P}(F^c) = (1 + m_{\text{req}})p_{\text{req}}.$$

3.2.4 Margin allocation in industrial complex systems

Still motivated by aeronautics and astronautics use cases, but from a slightly different point of view, some authors concentrated on the allocation/determination of margins in complex systems design. The margins are integrated in a decision-oriented framework and are chosen thanks to an underlying probabilistic model.

Margin determination The first publications of this kind come from D.P Thunissen's PhD Thesis (2005) [111–113], that proposes a five-step method to *determine* - *i.e.* choose the value of - the margins in a project management context. The goal is to choose the reserves that must be kept on *tradable parameters* and cover the uncertainties; in practice this choice is guided by an underlying probabilistic model. Tradable parameters are defined as important variables that include for instance the cost of a project, the mass of the system, the schedule, and other important performance variables.

Let y be a tradable quantity, the method assumes that two models are created: a deterministic model that yields a reference value y_{det} and a probabilistic model Y that accounts for the uncertainties of the project. The margin of level $\alpha \in [0, 1]$ is defined as [112, Eq. 8.1]

$$M(\alpha) = 100 \frac{Q_{1-\alpha}(Y) - y_{\text{det}}}{y_{\text{det}}},$$

Context of the design	Prescribed value for $\hat{m}_{\text{sfty perf}}$
The system had at least 125 actual cycles of operation.	~ 0
New system, developed with low time pressure and high reliability and safety having a higher priority than cost and schedule.	~ 1
New system, developed with moderate time pressure with cost and schedule having an equal priority than reliability and safety.	~ 2
New system, developed with significant time pressure but with reliability and safety having a higher priority than cost and schedule.	~ 4
New system, developed with significant time pressure, with cost and schedule having a higher priority than reliability and safety.	~ 9 and larger

Table 3.2: Safety performance margin requirement as a function of the design context and maturity, for space programs, summarized from [15, Table 3]. The context descriptions and values are given **for illustration only**, please refer to the original article for a comprehensive understanding of these values.

with $Q_\alpha(Y)$ being the quantile of Y of level α . Typically, the margins are computed for three levels of confidence, 0.05, 0.01 and 0.001 and the margin allocated depends on the decision maker needs by the formula

$$y_{\text{marg}} = y_{\text{det}}(1 + M(\alpha)/100) = Q_{1-\alpha}(Y) \quad (3.13)$$

i.e. the quantile of the level $1 - \alpha$ of the random model Y , similarly to a classic probabilistic approach. One advantage of monitoring this margin is the ability to see the evolution of the margins as the design gains in maturity and compare its value between designs. This margin is used as a requirement to choose the reserves to keep; it is thus a demanded margin.

Margin allocation and tradeoff More recently, X. Chen’s PhD thesis (2017) [27, 56] developed a framework to choose margin values by considering the interactions between margins, performance and risk.

Methodology Two stakeholders take part in the design: the *designer* and the *expert in uncertainties and probabilistic modeling*. This distinction finds its origins in industrial organizations, where there is often a difference between engineers/architects who have knowledge and experience on the system and handle uncertainties with deterministic margins and experts in statistics and probability, who do not have an extensive knowledge of the system but can more easily model uncertainties within a probabilistic framework (*e.g.* with probabilities of failure, random variables, quantiles, etc.). The goal is to choose relevant margins while keeping the two activities separated.

It is decomposed in two phases: the margin allocation and the tradeoff analysis, summarized in Figure 3.1.

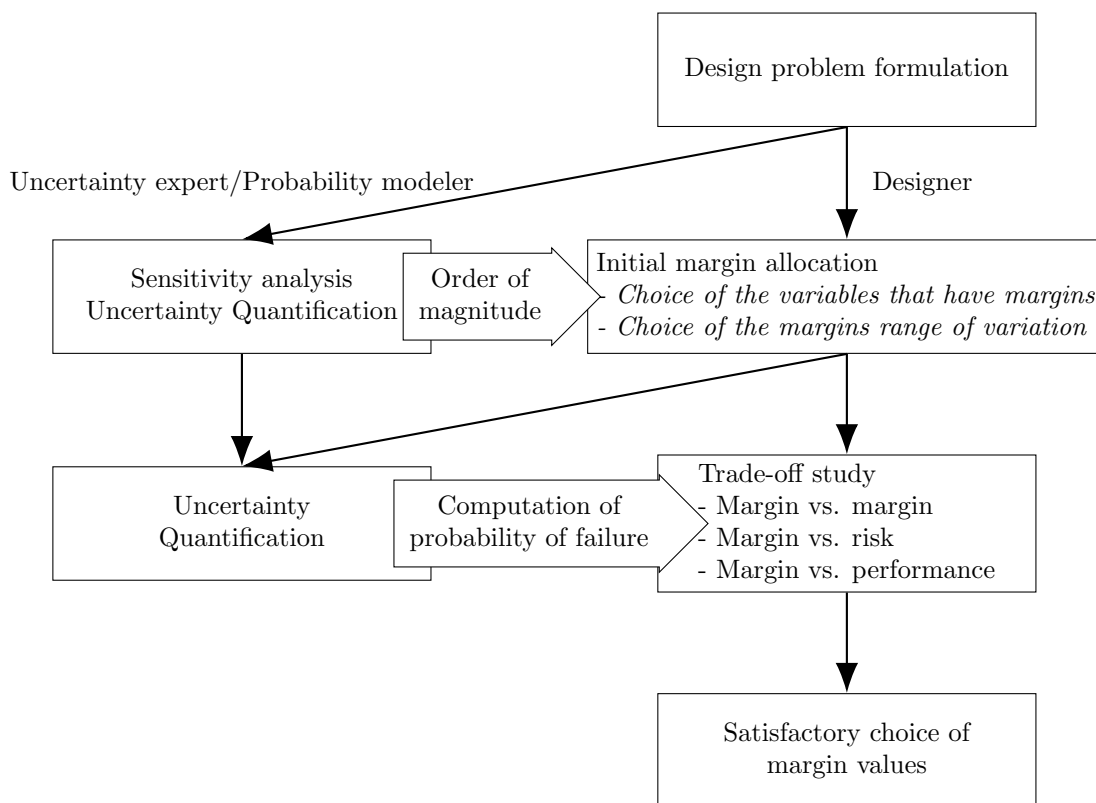


Figure 3.1: Summary of the methodology proposed in [27], closely adapted from [27, Fig. 4-3]

The margins m_i presented in these publications are defined only for unidimensional components $y_i \in \mathbb{R}$ and can only be of the form “the lower the better”

$$y_{i,\text{marg}} = y_i + m_i \text{ (absolute)} \quad / \quad y_{i,\text{marg}} = y_i(1 + m_i/100) \text{ (percentage)}$$

or “the greater the better”

$$y_{i,\text{marg}} = y_i - m_i \text{ (absolute)} \quad / \quad y_{i,\text{marg}} = y_i(1 - m_i/100) \text{ (percentage)} .$$

Margin allocation The initial margin allocation consists in finding the variables on which margins must be modeled, to choose their initial value and their possible range of variation. They can account for two types of uncertainty:

- The requirement uncertainty, due to the vagueness of the constraints formulation;
- The modeling uncertainty, due to a lack of knowledge.

If the number of variables with margins is too large, probabilistic sensitivity analysis and screenings can be used to identify the real contributors. The initial allocation (*i.e.* the choice of their values) is done either using a quantile of a probabilistic model (similarly to the aforementioned Thunissen approach), or by designer’s expert judgement if the probabilistic model is not available.

Tradeoff analysis This phase consists in choosing a satisfactory allocation of margin. This choice is based on the visualization of the impact of a margin on other margins, on the performance and on the risk.

- *Impact of margins on other margins*

If the value of a margin on a variable is too high, it could forbid to take margins on other parameters as the design would not satisfy the constraints. The authors propose a graphical solution to study this tradeoff, by some interactive plot of the feasible/infeasible regions with respect to the margins in [56, Fig. 4.13] as well as some parallel coordinate plot in [56, Fig. 4.14]

- *Impact of margins on the risk*

Let \mathcal{D} be the space of the designs. For a given design point $u \in \mathcal{D}$, an underlying probabilistic model permits to define some infeasible design space, based on a risk level $1 - \alpha \in [0, 1]$

$$\mathbf{F}(\alpha) = \{u \in \mathcal{D} \mid \mathbb{P}(\text{Constraints satisfied for } u) \leq \alpha\}.$$

Similarly, it is possible to define a failure set with margin only with a deterministic model

$$\mathbf{F}'(m_{i_1}, \dots, m_{i_n}) = \{u \in \mathcal{D} \mid \text{Constraints satisfied for } u_{\text{margin}}(m_{i_1}, \dots, m_{i_n})\},$$

where $u_{\text{margin}}(m_{i_1}, \dots, m_{i_n})$ is the design choice u with margins m_{i_1}, \dots, m_{i_n} on the components i_1, \dots, i_n .

By comparing graphically the probabilistic failure set $\mathbf{F}(\alpha_0)$ for a given level α_0 with the failure set with margins \mathbf{F}' , it is possible to see if the margins are well allocated [56, 4.3.4.2]. A first criterion is to check that the set with margins actually contains the probabilistic failure set, *i.e.* $\mathbf{F}(\alpha_0) \subset \mathbf{F}'$. This permits to know that the risks are actually mitigated by the margins. The second criterion proposed is to verify that the set with margin \mathbf{F}' has a similar shape to $\mathbf{F}(\alpha_0)$. This ensures that the margins are allocated on “the good variables”.

3.2.5 Margins as the cause of over-capacity/overdesign

In contrast with the margin allocation of Section 3.2.4, some authors in engineering design and design science focused on the multidisciplinary aspect of margins exchange and the identification of margins in design processes.

As early as 2004 [43], C. Eckert, P.J. Clarkson, W. Zanker described the tolerance margins as an important factor in system change management. In 2012, C. Eckert, O. Isaksson and C. Earl identified the margins as an important factor for over-capacity [45]. This observation was confirmed with the study of an in-operation complex system - an hospital - in [68] and a set of interviews of engineers in trucks design processes in [46, 67]. In [44], they propose a formal definition for margins, encompassing the various practices in design. Informally the margin is described as *the extent to which a parameter value exceeds what it needs to meet its functional requirements regardless of the motivation for which the margin was included*. For a given design choice $y \in \mathcal{D}$, the capability of the parameter i , denoted $C_i(y)$, is the value the parameter can reach. For a requirement/constraint R_i on this parameter, the margin is defined by

$$M_i(y) = R_i - C_i(y)$$

if the requirement is of the type “must not exceed” or

$$M_i(y) = C_i(y) - R_i$$

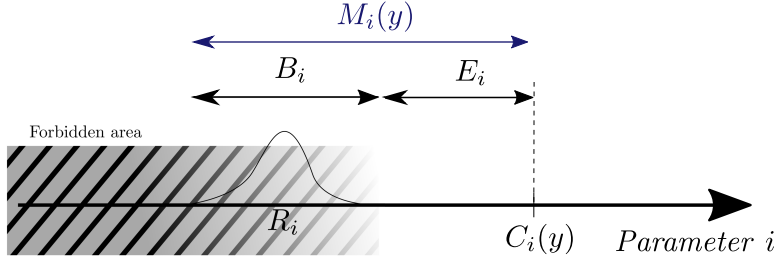


Figure 3.2: Distinction between the buffer B_i and the excess E_i in [44], closely adapted from [44, Fig. 3]. The buffer B_i covers the uncertainty due to the vagueness of the requirement R_i .

if the requirement is of the type “must exceed”. When R_i depends on the chosen solution, it is called a constraint, and when it is stated independently it is called a requirement. This margin is divided in $M_i(y) = B_i + E_i$, the buffer B_i being the part covering the uncertainties and the excess E_i being the remaining part. An illustration is given in Figure 3.2, for a “must exceed” requirement, the uncertainty being on the requirement value R_i .

The quantity B_i is a requirement used to cover the uncertainty and it is thus a demanded margin. The excess is what remains, once the requirements have been made; it is the effective margin of the system, taking into account the demanded margin requirements.

Margin-value method Based on these conceptual distinctions, the recent works of A. Brahma and D.C. Wynn [23, 24] (2020) focused on the identification of the excess part of the margins in the design process. The ultimate goal is to have a quantitative estimate of the over-design parts in complex systems. In order to evaluate the impact of the margins on the design, they define three metrics:

1. Excess margin

The first metric is the classic excess margin, in the “must exceed” normalized form

$$\text{Excess}_i(y) = \frac{y_i - y_{i,\text{thresh}}}{y_{i,\text{thresh}}}.$$

It quantifies by how much the parameter y_i oversatisfies its requirement/constraint $y_{i,\text{thresh}}$;

2. The adverse impact on performance

The second metric quantifies the impact of the Excess on y_i on a given performance parameter P_k . We denote by P_k its value computed with y_i and $P_{k,\text{thresh}}$ its value computed by taking $y_{i,\text{thresh}}$ instead of y_i . In other terms, the margin on y_i is removed and the other margins remain the same. The impact

$$\text{Impact}_{i,k} = \frac{P_k - P_{k,\text{thresh}}}{P_{k,\text{thresh}}}$$

computes by how much the performance P_k is impacted by the margin on y_i .

3. The absorption benefit

This metric quantifies the positive impact of the excess margins, in the sense that they permit to satisfy more cumbersome requirements. For an input requirement R_l , the maximum

value possible before a design change, denoted by R_{\max} , is computed. The deterioration is defined as

$$\text{Deterioration}_l = \frac{R_{\max} - R_l}{R_l}$$

that quantifies by how much the requirement R_l can be tougher. This new requirement R_{\max} has imposed new values of threshold for the variables $y_{i,\text{newthresh}}$. The part of deterioration of R_l that was absorbed by the variable $y_{i,\text{newthresh}}$ is measured by

$$\text{Absorption}_{il} = \frac{y_{i,\text{newthresh}} - y_{i,\text{thresh}}}{y_{i,\text{thresh}} \text{Deterioration}_l}.$$

These three metrics altogether help spotting where it can be interesting to investigate the excess margins and to remove them.

3.3 Our contributions regarding the existing literature

In order to perform a sensitivity analysis of the cost/loss of performance with respect to the margins, one needs to rigorously define how the margins impact it. The notion of demanded margin is crucial in this step, because it is this type of margin that induces a cost. Although it is often easily possible to distinguish *a posteriori* the notions of demanded and effective margins in the literature (introduced in Section 2.1), we did not find an explicit separation of the two concepts. The margin definition is often implicit, or designated as a difference between the value a unidimensional design variable and a limiting threshold. However, such a definition may be ambiguous, for instance when the limiting threshold is a function of another variable, and the evolution of this second variable is not precised.

For these reasons, we propose a mathematical model of margin (Section 4.2), that is the basis of the definition of the effective (Section 4.2.1) and demanded margin (Section 4.2.2). Using these rigorous notions, we are able to quantify precisely how the cost/loss of performance is impacted through the induced function in Section 5.1. This function is analyzed through a Sensitivity Analysis approach in Chapter 5, developed specifically for this context. The final goal of our approach is close to the Margin value method of Section 3.2.5 and the tradeoff study of the margin allocation described in Section 3.2.4, but we developed different tools.

On a more methodological side, we use this framework to provide a general description of the process of uncertainty mitigation with margins in Section 4.4.1. It includes a margin quantification phase, that permits to interpret a lot of practices from the literature in Section 4.5. Some ways to reduce margins are also described in Section 5.3.

We refer to the conclusion of this part, in Chapter 7, for a comprehensive summary of our works on margins.

Chapter 4

Model of margin

As stated in Section 2.1, the vocable engineering margin actually covers two notions, the effective margin and the demanded margin. In Sections 4.1 and 4.2, we propose the mathematical foundation to rigorously define them. Then, based on these tools, we model in Section 4.4.1 a general approach to risk mitigation with margins, the *margin quantification*, that is commonly followed by engineers. Finally, in Section 4.5, the margins from the literature review of Chapter 3 are reinterpreted within our framework.

Use case, part 1 (Description). A simple industrial use case with a toy model is developed in these framed boxes. Its aim is to illustrate the theoretical concepts by practical examples.

Initial setup The action takes place in an aeronautics department, in charge of the design of an aircraft wing. The global aircraft architect asks them a value W_{\max} for the maximum weight of the wing. They identified two main variables that contribute to the mass: the radius of a specific composite property κ and the loads F the wing is facing, that give the weight with the relationship

$$W = f(\kappa, F),$$

for a known function f , that is increasing both in κ and F . The true value of (κ, F) , denoted by

$$(\kappa_0, F_0)$$

is not known by the engineers. A nominal value F_{nom} is assessed for F and a safety factor $\beta_F > 1$ is taken to cover the uncertainties. For κ they know that the true value is the expectation of a normal random variable $\kappa_0 = \mathbb{E}[\mathbf{K}]$ of known standard deviation $\sigma_{\mathbf{K}}$ for which they have n i.i.d observations $(\mathbf{K}_i)_{i \in \llbracket 1, n \rrbracket}$. They estimate its value with

$$\hat{\kappa} = \frac{1}{n} \sum_{i=1}^n \mathbf{K}_i$$

and take into account the margin of statistical error m_{κ} . The maximum weight is now expressed as $W_{\max} = \max W(\kappa', F')$ with (κ', F') ranging over $[\hat{\kappa}, \hat{\kappa} + m_{\kappa}] \times [F_{\text{nom}}, \beta_F F_{\text{nom}}]$. The architect asks them the smallest possible value of W_{\max} which avoids underestimating the true value with a certain level of confidence. They now ask themselves

- What is the impact of the margins on the mass transmitted?
- What margins should they reduce to provide the lowest estimation of W_{\max} possible, with the same level of confidence?

4.1 Problem description

We assume that the phenomenon or system studied is described by variables in a *state space* E . The physical equations or logical relationships that link these variables is given by the set of the *problem constraints* \mathcal{C} .

Definition 4.1.1 (State space). *The state space, denoted by E , is a set.*

An element of the state space will generically be called a *design*, denoted by the symbol u .

Definition 4.1.2 (Problem constraints). *The set of the problem constraints is $\mathcal{C} \subset E$.*

We call (E, \mathcal{C}) the *problem description*. We denote a *forbidden set* or *failure set* by

$$\mathbf{F} \subset \mathcal{C},$$

to which a design u belongs if and only if the system/phenomenon is in an adverse situation that the analyst needs to prevent. The *acceptance set* is simply its complementary in the set of the physically acceptable designs

$$\mathbf{A} = \mathcal{C} \setminus \mathbf{F}.$$

In the model of the phenomenon, it is possible but not desirable for a design u to be outside the acceptance set \mathbf{A} , but it is impossible to be outside the set of the problem constraints \mathcal{C} .

Use case, part 2. The state space is composed of the four variables from Use case 1

$$E = \{(W_{\max}, W, \kappa, F) \in \mathbb{R}_+^4\}.$$

The problem constraints are given by the equation

$$\mathcal{C} = \{(W_{\max}, W, \kappa, F) \in E \mid W = f(\kappa, F)\}.$$

The failure set is composed by the designs for which the mass transmitted W_{\max} is lower than the actual mass

$$\mathbf{F} = \{(W_{\max}, W, \kappa, F) \in \mathcal{C} \mid W_{\max} < W\},$$

which encodes the requirement “not to underestimate W_{\max} ”.

4.2 Basis of the model

The core concept of the margin is the existence of an extra quantity in the distance from a design u to a failure set \mathbf{F} . This distance will be measured in a metric space \mathbb{S} , through a projection map ϕ_u , which indicates on which scalar quantity, related to u , the margin is taken. However, this distance *a priori* depends on which paths connecting u to \mathbf{F} are taken into consideration. The notion of probing set introduced below specifies these paths.

Definition 4.2.1 (Probing set). *Let $u \in \mathcal{C}$, the probing set at the point u is a set*

$$\mathcal{G}_u \subset \mathbf{E}$$

such that $u \in \mathcal{G}_u$.

Definition 4.2.2 (Margin space and projection map). *The margin space is a space \mathbb{S} endowed with a distance $d_{\mathbb{S}}$. A projection map is a function from the probing set to the margin space*

$$\phi_u : \mathcal{G}_u \rightarrow \mathbb{S}. \quad (4.1)$$

In the margin space, *the distance* between two designs is expressed in the units of the margin.

Definition 4.2.3 (Model of margin). *A model of margin on the set \mathcal{C} is composed of a margin space and a family of projection maps along with their probing sets*

$$\mathbf{M} = (\mathbb{S}, (\mathcal{G}_u)_{u \in \mathcal{C}}, (\phi_u)_{u \in \mathcal{C}}). \quad (4.2)$$

In practice, ϕ_u is often a projection onto the coordinate on which one wants to compute a margin and the distance $d_{\mathbb{S}}$ of \mathbb{S} gives the reference unit for the measure of the margin.

Use case, part 3. We now describe two models of margin corresponding to the notion of “taking a margin” on κ and F .

Model of margin on κ For a design $u = (W_{\max}, W, \kappa, F) \in \mathbf{A}$, the probing set for the model of margin \mathbf{M}_{κ} on κ is

$$\mathcal{G}_{\kappa, u} = \{v = (W'_{\max}, W', \kappa', F') \in \mathbf{E} \mid W_{\max} = W'_{\max}, \kappa \leq \kappa', F = F'\}.$$

The margin space is $\mathbb{S}_{\kappa} = \mathbb{R}_+$, and for any design $u \in \mathcal{C}$, the projection map is

$$\phi_{\kappa, u}(v) = \kappa' - \kappa.$$

Model of margin on F Likewise, the probing set of the model of margin \mathbf{M}_F on F is

$$\mathcal{G}_{F, u} = \{v = (W'_{\max}, W', \kappa', F') \in \mathbf{E} \mid W_{\max} = W'_{\max}, \kappa = \kappa', F \leq F'\}.$$

In order to represent the fact that the margin β_F is expressed as a ratio, we take $\mathbb{S}_F = [1, +\infty)$ and

$$\phi_{F, u}(v) = \frac{F'}{F}.$$

4.2.1 Effective margin

The *effective margin* is a margin $m \in \mathbb{R} \cup \{-\infty, +\infty\}$ that a design u has with respect to a forbidden set \mathbf{F} . As various choices are possible to compute such a margin, one needs first to define a model of margin \mathbf{M} . Then, the associated effective margin function $\text{em}_{\mathbf{M}}$ computes the effective margin.

Definition 4.2.4 (Effective margin function). *Let $(\mathbf{E}, \mathcal{C})$ be a problem description, \mathbf{F} be a forbidden set and $\mathbf{M} = (\mathbb{S}, (\mathcal{G}_u)_{u \in \mathcal{C}}, (\phi_u)_{u \in \mathcal{C}})$ be a model of margin. For any $u \in \mathcal{C}$, we set $u_{\mathbb{S}} = \phi_u(u)$,*

$\mathbf{F}_S(u) = \phi_u(\mathbf{F} \cap \mathcal{G}_u)$ and $\mathbf{A}_S(u) = \phi_u(\mathbf{A} \cap \mathcal{G}_u)$, where we recall that $\mathbf{A} = \mathcal{C} \setminus \mathbf{F}$. The effective margin at the design u for the margin model \mathbf{M} and the forbidden set \mathbf{F} is defined by

$$\text{em}_{\mathbf{M}}(u, \mathbf{F}) = \begin{cases} d_S(u_S, \mathbf{F}_S(u)) & \text{if } u \in \mathbf{A}, \\ -d_S(u_S, \mathbf{A}_S(u)) & \text{if } u \in \mathbf{F}, \end{cases} \quad (4.3)$$

with the convention $d_S(u, \emptyset) = +\infty$.

Use case, part 4. When a design u is in \mathbf{A} , its effective margin on κ is

$$\text{em}_{\mathbf{M}_\kappa}(u, \mathbf{F}) = \max \{m \geq 0 \mid f(\kappa + m, F) \leq W_{\max}\}$$

and the effective margin on F is

$$\text{em}_{\mathbf{M}_F}(u, \mathbf{F}) = \max \{\beta \in [1, +\infty) \mid f(\kappa, \beta F) \leq W_{\max}\} - 1,$$

for which an illustration is given in Figure 4.1.

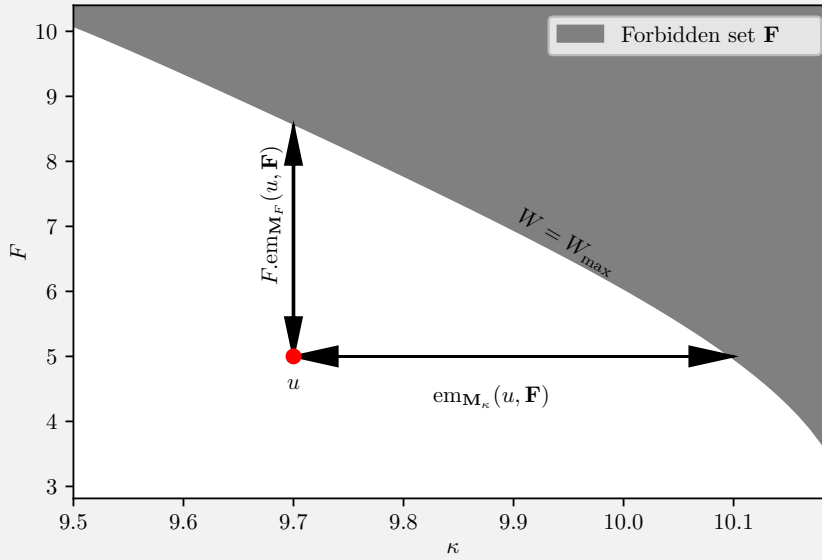


Figure 4.1: Visualization of the effective margin for the models of margin \mathbf{M}_κ and \mathbf{M}_F , in the plane (κ, F) , at the design $u : W_{\max} = 490, \kappa = 9.7$ and $F = 5$.

The effective margin on κ is in the unit of κ and measures the distance from u to \mathbf{F} , the value of F being fixed. The effective margin on F is dimensionless and measures by how much it is possible to multiply F before reaching \mathbf{F} , the value of κ being fixed.

The failure and acceptance property stated below follows from Definition 4.2.4. In substance, given a design u in \mathbf{A} , any point in the probing set \mathcal{G}_u that is at a distance lower than the effective margin of u is also in \mathbf{A} . Thus, the effective margin is the actual extra quantity separating u from \mathbf{F} .

Proposition 4.2.5 (Acceptability and failure property). *With the notation of Definition 4.2.4, let $u \in \mathcal{C}$.*

- (i) *If $u \in \mathbf{A}$, then for all $v \in \mathcal{C} \cap \mathcal{G}_u$, if $d_{\mathbb{S}}(\phi_u(u), \phi_u(v)) < \text{em}_{\mathbf{M}}(u, \mathbf{F})$, then $v \in \mathbf{A}$.*
- (ii) *If $u \in \mathbf{F}$, then for all $v \in \mathcal{C} \cap \mathcal{G}_u$, if $d_{\mathbb{S}}(\phi_u(u), \phi_u(v)) < |\text{em}_{\mathbf{M}}(u, \mathbf{F})|$, then $v \in \mathbf{F}$.*

An immediate consequence of this definition is that if a design u has a strictly positive margin, then it is in \mathbf{A} and if it has a strictly negative margin, then it is in \mathbf{F} . A point with exactly zero margin may be either in \mathbf{F} or \mathbf{A} .

Example 4.2.6 (Unidimensional model). *The effective margin for a phenomenon described by one real number $u \in \mathbb{R}$ is the most intuitive. In that case $\mathbf{E} = \mathcal{C} = \mathbb{R}$ and we compute the margin for two natural failure sets, an upper bound $\mathbf{F}_{\text{upp}} = (u_{\text{upp}}, +\infty)$ and a lower bound $\mathbf{F}_{\text{low}} = (-\infty, u_{\text{low}})$.*

To construct our model of margin, the projection map is the identity and the distance is the standard distance in \mathbb{R}

$$\begin{aligned} \forall (u, v) \in \mathbb{R}^2, \quad \phi_u(v) &= v, \\ \mathbb{S} &= \mathbb{R}, \quad d_{\mathbb{S}}(v_1, v_2) = |v_1 - v_2|, \end{aligned}$$

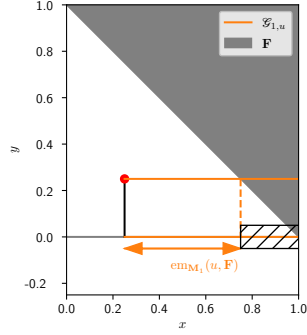
and we define three probing sets $\mathcal{G}_{\rightarrow, u} = [u, +\infty)$, $\mathcal{G}_{\leftarrow, u} = (-\infty, u]$, $\mathcal{G}_{\leftrightarrow, u} = \mathbb{R}$, that we associate respectively to the models of margin \mathbf{M}_{\rightarrow} , \mathbf{M}_{\leftarrow} , $\mathbf{M}_{\leftrightarrow}$.

		$\mathbf{F} = (-\infty, u_{\text{low}})$	$\mathbf{F} = (u_{\text{upp}}, +\infty)$
\mathbf{M}_{\rightarrow}	$u \notin \mathbf{F}$	$\text{em}_{\mathbf{M}}(u, \mathbf{F}) = +\infty$	$\text{em}_{\mathbf{M}}(u, \mathbf{F}) = u_{\text{upp}} - u > 0$
	$u \in \mathbf{F}$	$\text{em}_{\mathbf{M}}(u, \mathbf{F}) = u - u_{\text{low}} \leq 0$	$\text{em}_{\mathbf{M}}(u, \mathbf{F}) = -\infty$
\mathbf{M}_{\leftarrow}	$u \notin \mathbf{F}$	$\text{em}_{\mathbf{M}}(u, \mathbf{F}) = u - u_{\text{low}} > 0$	$\text{em}_{\mathbf{M}}(u, \mathbf{F}) = +\infty$
	$u \in \mathbf{F}$	$\text{em}_{\mathbf{M}}(u, \mathbf{F}) = -\infty$	$\text{em}_{\mathbf{M}}(u, \mathbf{F}) = u_{\text{upp}} - u \leq 0$
$\mathbf{M}_{\leftrightarrow}$	$u \notin \mathbf{F}$	$\text{em}_{\mathbf{M}}(u, \mathbf{F}) = u - u_{\text{low}} > 0$	$\text{em}_{\mathbf{M}}(u, \mathbf{F}) = u_{\text{upp}} - u > 0$
	$u \in \mathbf{F}$	$\text{em}_{\mathbf{M}}(u, \mathbf{F}) = u - u_{\text{low}} \leq 0$	$\text{em}_{\mathbf{M}}(u, \mathbf{F}) = u_{\text{upp}} - u \leq 0$

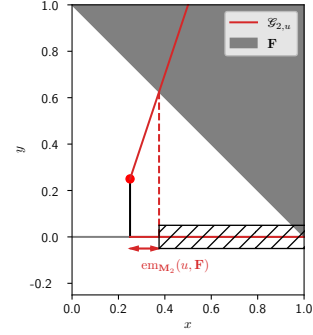
Table 4.1: Value of the effective margin for various models of margin and failure sets, in the unidimensional case.

The values of the effective margins for the different combinations are summarized in Table 4.1. We can remark that we retrieve the classic expression of the margin, except for the increasing model of margin \mathbf{M}_{\rightarrow} and the decreasing model of margin \mathbf{M}_{\leftarrow} for which there are some infinite values. For \mathbf{M}_{\rightarrow} , the positive infinite value means that when u is greater than u_{low} , it can increase by any amount without reaching the failure set $(-\infty, u_{\text{low}})$. The value $-\infty$ means that, when u is in $(u_{\text{upp}}, +\infty)$, there are no amount of increase in the positive direction that will make it leave the forbidden set $(u_{\text{upp}}, +\infty)$. For \mathbf{M}_{\leftarrow} , the negative infinite value means that when u is in $(-\infty, u_{\text{low}})$ there are no amount decrease that can make it leave the forbidden set. The positive infinite value means that when u is lower than u_{upp} , it can decrease by any amount without reaching the forbidden set.

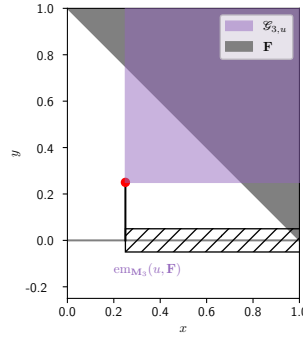
Remark 4.2.7 (Influence of the probing set). *The value of a margin on one coordinate is often ambiguous because the “boundary” from which one computes the margin depends on other coordinates. The probing set defines what are the values to take into account. In Figure 4.2, for $\mathbf{E} = \mathcal{C} = \mathbb{R}^2$ and various probing sets, we can see that the value of the effective margin on x greatly varies with respect to the values of (x', y') that are allowed in the computation. In practice, a lot of situations can be modeled by deciding which variables to fix, which variables can only increase or only decrease and which variables are free (see Section 4.3.4).*



(a) With a probing set defined by $\mathcal{E}_{1,u} = \{(x', y') \in \mathbb{R}^2 | x' \geq x, y' = y\}$, the effective margin on x is $\text{em}_{\mathbf{M}_1}(u, \mathbf{F}) = 0.5$.



(b) With a probing set defined by $\mathcal{E}_{2,u} = \{(x', y') \in \mathbb{R}^2 | (x', y') = (x, y) + \lambda(1, 3), \lambda \geq 0\}$, the effective margin on x is $\text{em}_{\mathbf{M}_2}(u, \mathbf{F}) = 0.125$.



(c) With a probing set defined by $\mathcal{E}_{3,u} = \{(x', y') \in \mathbb{R}^2 | x' \geq x, y' \geq y\}$, the effective margin on x is $\text{em}_{\mathbf{M}_3}(u, \mathbf{F}) = 0$.

Figure 4.2: Computation of the effective margin on x , at the point $u = (x, y) = (0.25, 0.25)$, for various probing sets. The three models of margin $\mathbf{M}_1, \mathbf{M}_2, \mathbf{M}_3$ have different probing sets but share the same projection map $\phi_u(x', y') = x' - x \in \mathbb{S} = \mathbb{R}^+$, problem description $\mathbf{E} = \mathcal{E} = \mathbb{R}^2$ and failure set $\mathbf{F} = \{(x, y) | y > 1 - x\}$.

4.2.2 Demanded margin

The *demanded margin* is a real number $m \geq 0$ that means that someone has required a margin of at least m in the analysis of the phenomenon. It requires a model of margin \mathbf{M} to tell precisely which margin must be greater than m . The *demanded margin operator* shows the impact of the failure set on which a demanded margin has been taken.

Definition 4.2.8 (Demanded margin operator). *Let $m \geq 0$ and \mathbf{M} be a model of margin for the problem description $(\mathbf{E}, \mathcal{C})$. The demanded margin operator $\mathbf{dm}_{\mathbf{M},m}$ is the function that takes a forbidden set \mathbf{F} as input and returns another forbidden set \mathbf{F}'*

$$\mathbf{F}' = \mathbf{dm}_{\mathbf{M},m}(\mathbf{F})$$

with, if $m > 0$

$$\mathbf{F}' = \{u \in \mathcal{C} \mid \text{em}_{\mathbf{M}}(u, \mathbf{F}) < m\}.$$

When $m = 0$, we define

$$\mathbf{F}' = \mathbf{F} \cup \{u \in \mathcal{C} \mid \text{em}_{\mathbf{M}}(u, \mathbf{F}) = 0\} = \{u \in \mathcal{C} \mid \text{em}_{\mathbf{M}}(u, \mathbf{F}) \leq 0\}.$$

The nonnegative real number m is called the *demanded margin*.

Taking a demanded margin m is equivalent to declaring forbidden all the points with less than m effective margin. When $m > 0$, the inequality is strict to keep the points with an effective margin equal to m in the new acceptance set $\mathbf{A}' = \mathcal{C} \setminus \mathbf{F}'$. When $m = 0$, a design with zero effective margin - that can be either in \mathbf{F} or \mathbf{A} - is included in the new forbidden set \mathbf{F}' .

Example 4.2.9. *Using the variable problem description of Example 4.2.6, we can compute the impact of a demanded margin $m > 0$ with model of margin $\mathbf{M}_{\leftrightarrow}$ on the upper bound failure set*

$$\mathbf{dm}_{\mathbf{M}_{\leftrightarrow},m}((u_{\text{upp}}, +\infty)) = (u_{\text{upp}} - m, +\infty),$$

and on the lower bound failure set

$$\mathbf{dm}_{\mathbf{M}_{\leftrightarrow},m}((-\infty, u_{\text{low}})) = (-\infty, u_{\text{low}} + m).$$

As one can intuitively guess in that case, a demanded margin of $m > 0$ is equivalent to choosing a requirement of $u_{\text{low}} + m$ in the case of a lower bound and $u_{\text{upp}} - m$ in the case of an upper bound.

A fundamental property of the demanded margin operator is that it always reduces the set of acceptable designs \mathbf{A} , or equivalently it extends the forbidden set \mathbf{F} .

Proposition 4.2.10 (Inclusion). *For any demanded margin $m \geq 0$, we have*

$$\mathbf{F} \subset \mathbf{F}',$$

which rewrites equivalently

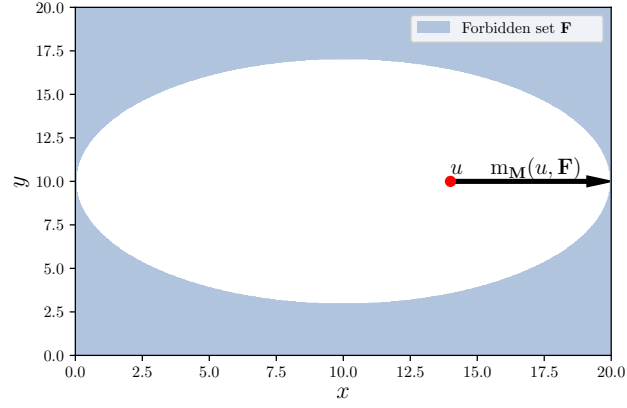
$$\mathbf{A}' \subset \mathbf{A}.$$

Proof. By definition of the effective margin, if $u \in \mathbf{F}$ then $\text{em}_{\mathbf{M}}(u, \mathbf{F}) \leq 0 \leq m$ for any $m \geq 0$. As $u \in \mathcal{C}$, we have $u \in \mathbf{F}'$. \square

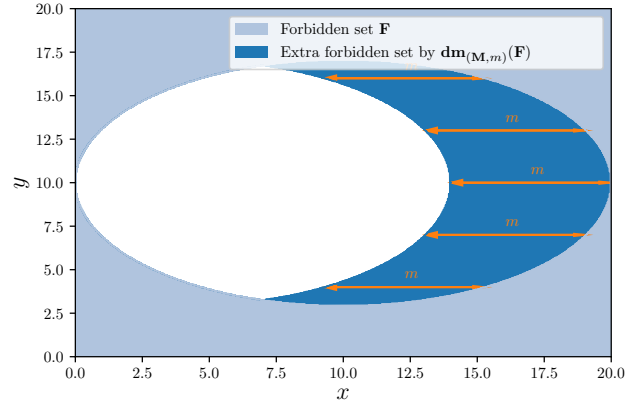
A way to see the demanded margin as an extra requirement is the following relationship, for $m > 0$

$$\forall u \in \mathcal{C}, \quad u \notin \mathbf{dm}_{\mathbf{M},m}(\mathbf{F}) \Leftrightarrow \text{em}_{\mathbf{M}}(u, \mathbf{F}) \geq m, \quad (4.4)$$

which means that belonging to a set with demanded margin $\mathbf{dm}_{\mathbf{M},m}(\mathbf{F})$ is equivalent to having an effective margin larger than m .



(a) The effective margin is computed for a specific design $u \in \mathbf{A}$. For the point $u = (14, 10)$, its effective margin is $\text{em}_{\mathbf{M}}(u, \mathbf{F}) = 6$.



(b) The demanded margin operator expands the forbidden set \mathbf{F} and reduces the acceptance set \mathbf{A} . The darker area shows the expanded forbidden set for a demanded margin $m = 6$.

Figure 4.3: Illustration of the difference between the effective and the demanded margin. The problem description is $\mathbf{E} = \mathcal{C} = \mathbb{R}^2$ and the model of margin \mathbf{M} consists in an increasing probing set on x : $\mathcal{S}_{(x,y)} = \{(x', y') \in \mathbf{E} \mid x' \geq x, y' = y\}$ and a projection map $\phi_{(x,y)}(x', y') = x' \in \mathbb{R}$. The forbidden set is $\mathbf{F} = \{(x, y) \in \mathbb{R}^2 \mid (x - 10)^2 / 2 + (y - 10)^2 > 10^2\}$.

Use case, part 5. Engineers have chosen the values of $m_\kappa > 0$ on κ and a safety coefficient $\beta_F > 1$ on F , based on the uncertainties they are facing. These values are, in fact, some *demanded margins*. We can compute the image of $\mathbf{F} = \{u \in \mathcal{E} | f(\kappa, F) > W_{\max}\}$, by the margin operator

$$\begin{aligned} \mathbf{F}'_\kappa &= \mathbf{dm}_{\mathbf{M}_\kappa, m_\kappa}(\mathbf{F}) \\ &= \{u \in \mathcal{E} \mid \text{em}_{\mathbf{M}_\kappa}(u, \mathbf{F}) < m_\kappa\} \\ &= \{u \in \mathcal{E} \mid f(\kappa + m_\kappa, F) > W_{\max}\}. \end{aligned}$$

In this computation, we used the fact f is increasing in κ , thus $\text{em}_{\mathbf{M}_\kappa}(u, \mathbf{F}) \geq m_\kappa$ is equivalent to $(W_{\max}, f(\kappa + m_\kappa, F), \kappa + m_\kappa, F) \notin \mathbf{F}$. This is not true for a general failure set \mathbf{F} .

The same reasoning can be done with $\mathbf{dm}_{\mathbf{M}_\kappa, m_\kappa}(\mathbf{F})$ and the variable F , leading to the acceptance set with both margins

$$\begin{aligned} \mathbf{F}'_{\kappa, F} &= \mathbf{dm}_{\mathbf{M}_F, \beta_F - 1}(\mathbf{F}'_\kappa) \\ &= \{u \in \mathcal{E} \mid f(\kappa + m_\kappa, \beta F) > W_{\max}\}. \end{aligned}$$

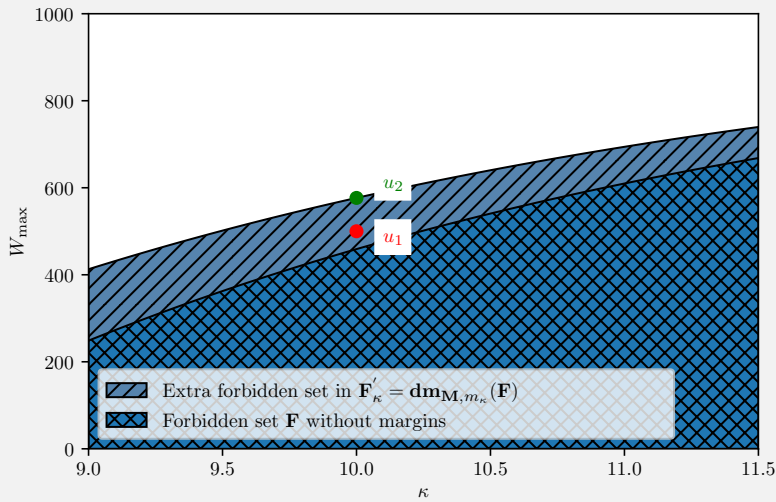


Figure 4.4: Action of the demanded margin operator for a demanded margin $m_\kappa = 0.5$, plotted in the plane (W_{\max}, κ) , the variable F being fixed. The design u_1 is initially acceptable but is forbidden after the demanded margin has been taken. In order to find another acceptable design for the same value of κ , the value of the mass transmitted W_{\max} must increase, leading for instance to the point u_2 .

4.3 Construction of a model of margin

Definition 4.2.3 provides models of margin for general problem descriptions (E, \mathcal{E}) . In engineering practices however, margins can often be represented in a more compact form, either as a directional model of margin (Sections 4.3.1 and 4.3.2) or as a slightly more complex one (Section 4.3.4). An illustration of these concepts, based on an use case is provided in Chapter 8.

4.3.1 Unidirectional model of margin

The directional model of margin is the natural model for calculating a margin on one variable, *all other variables being fixed*. When it is unidirectional it computes either a positive change or a negative change, but not both at the same time.

Definition 4.3.1 (Unidirectional model of margin). *Let (E, \mathcal{C}) be a problem description such that $E = \prod_{k=1}^n E_k$ and E_i is metric and totally ordered for a given $i \in \llbracket 1, n \rrbracket$. Let $u = (u_1, \dots, u_n)$ be a point in \mathcal{C} . The increasing directional model of margin in the component i is denoted by $\mathbf{M}_{i, \rightarrow}$ and is defined by*

$$\begin{aligned} \mathcal{G}_u &= \{v \in \mathcal{C} \mid v_i \geq u_i \text{ and } v_j = u_j \text{ for } i \neq j\} \\ \phi_u(v) &= v_i, \end{aligned}$$

with $v = (v_1, \dots, v_n)$. The decreasing directional model of margin in the component v is denoted by $\mathbf{M}_{i, \leftarrow}$ and has the same definition with $v_i \leq u_i$.

When E is a vector space, a natural extension of this definition is an increasing directional model of margin in an arbitrary direction $e \in E$. For a design u , the probing set \mathcal{G}_u is the semi-line starting at u of direction vector e , *i.e.*

$$\mathcal{G}_u = \{u + \lambda e, \lambda \geq 0\}.$$

The decreasing directional model of margin follows the same definition with $\lambda \leq 0$. For a given failure set $\mathbf{F} \subset E$ and point $u \in \mathbf{A}$, the effective margin is expressed

$$\text{em}_{\mathbf{M}_{i, \rightarrow}}(u, \mathbf{F}) = \inf \{\lambda \geq 0 \mid u + \lambda e_i \in \mathbf{F}\}$$

by Definition 4.2.4. It is the smallest λ such that it is possible to reach a point in the failure set and verifies the equations of the problem at the same time. When e is a direction vector on the canonical coordinate i , we retrieve the definition of a model of margin in the component i .

4.3.2 Bidirectional model of margin

The bidirectional model of margin consider both increasing and decreasing changes on the variable, *all other variables being fixed*.

Definition 4.3.2 (Bidirectional model of margin). *Let (E, \mathcal{C}) be a problem description such that $E = \prod_{k=1}^n E_k$ and E_i is metric for a $i \in \llbracket 1, n \rrbracket$. Let $u = (u_1, \dots, u_n)$ be a point in \mathcal{C} . The bidirectional model of margin in the component i is denoted by $\mathbf{M}_{i, \leftrightarrow}$ and is defined by, for all $u \in \mathcal{C}$*

$$\begin{aligned} \mathcal{G}_u &= \{v \in \mathcal{C} \mid v_j = u_j \text{ for } j \neq i\} \\ \phi_u(v) &= v_i. \end{aligned}$$

with $v = (v_1, \dots, v_n)$.

A consequence of the definition is that for all $u \in \mathbf{A}$

$$\text{em}_{\mathbf{M}_{i, \leftrightarrow}}(u) = \min(\text{em}_{\mathbf{M}_{i, \rightarrow}}(u), \text{em}_{\mathbf{M}_{i, \leftarrow}}(u)).$$

4.3.3 Fixed and free variables in probing sets

A more general way to describe probing sets is in term of free and fixed variables. We assume that $E = \prod_{i=1}^n E_i$, and each E_i is totally ordered. A design u is composed of n variables (u_1, \dots, u_n) and we can construct a probing set by assigning to each variable $i \in \llbracket 1, n \rrbracket$ one of the four labels

- \rightarrow can vary in the increasing direction. The constraint $v_i \geq u_i$ is added to the probing set;
- \leftarrow can vary in the decreasing direction. The constraint $v_i \leq u_i$ is added to the probing set;
- \leftrightarrow free to change (any direction). No constraints are added;
- \times fixed variable. The constraint $v_i = u_i$ is added in the probing set,

so that the probing set at the design u is composed of the designs v that verify the constraints.

For instance, the probing sets from Use Case part 3 can be described by

$$(\mathcal{G}_{\kappa, u})_{u \in \mathcal{E}} : \quad W_{\max} : \times, \quad W : \leftrightarrow, \quad \kappa : \rightarrow, \quad F : \times$$

and

$$(\mathcal{G}_{F, u})_{u \in \mathcal{E}} : \quad W_{\max} : \times, \quad W : \leftrightarrow, \quad \kappa : \times, \quad F : \rightarrow.$$

The probing sets of an increasing directional model of margin assigns the status \rightarrow to the main variable and the status \times to all the other variables. For a decreasing directional model of margin, the main variable has the status \leftarrow and for a bidirectional one it has the status \leftrightarrow .

4.3.4 A simple description of models of margin

To conclude this part, we introduce a way to describe simply a lot of models of margin. Let (E, \mathcal{E}) be a problem description and let a design be $u = (u_1, \dots, u_n) \in E = \prod_{i=1}^n E_i$. Only two aspects must be specified.

1. The variable or the set of variables on which the margin is measured, that define the *margin space*.

For one variable it consists in an index $i \in \llbracket 1, n \rrbracket$ with a distance d_{E_i} . The projection map is then $\phi_u(v) = v_i$ and $\mathbb{S} = E_i$ (e.g. $E_i = \mathbb{R}$ and d_{E_i} is the absolute value). For a set of variables, it can be a set of indices i_1, \dots, i_K and a distance d on the product space $\prod_{k=1}^K E_{i_k}$. The projection map is $\phi_u(v) = (v_1, \dots, v_K)$ and $\mathbb{S} = \prod_{k=1}^K E_{i_k}$.

2. Which variables are fixed, free or may vary in a given direction, defining the *probing sets*.
As described in the previous section, one only has to assign the status $\leftarrow, \rightarrow, \leftrightarrow$ or \times to each component.

4.4 Margin quantification: one of the four steps of uncertainty mitigation with margins

4.4.1 The four steps of uncertainty mitigation with margins

When engineers use margins to cover uncertainties, it is possible to identify some recurring practices, occurring independently of the field considered. We call them the four steps of uncertainty mitigation with margins, that are the following.

1. Model the phenomenon considered, with equations or numerical simulations. *Definition of the problem description* $(\mathbf{E}, \mathcal{E})$.
2. (Can be done in later phases) Exhibit how the system can fail. *Definition of \mathbf{F}* .
3. Identify the risks, *i.e.* the uncertainties and their impacts on the analysis. *An extremely wide range of methods can be used to identify, model and quantify the uncertainty of a system.*
4. Margin quantification.
 - (a) Choose on which variables take the demanded margins. *Definition of $\mathbf{M}_1, \dots, \mathbf{M}_n$* .
 - (b) Assess the demanded margins values required to mitigate the uncertainties. *Choice of the value of the demanded margin m_1, \dots, m_n* .
 - (c) (If there are more than one model of margin) Choice of the order in which to compose the demanded margin operators $\mathbf{dm}_{\mathbf{M}_1, m_1}, \dots, \mathbf{dm}_{\mathbf{M}_n, m_n}$.

After these steps, the analyst proceeds to the initial task assigned such as margin allocation or design analysis shown in Figure 4.5. These steps are often implicit and not shared among all the stakeholders; the fact that the margins are not shown in the design may lead to the problem of *hidden margins*. The model of margin makes the steps 1,2 and 4a explicit and this information is available for a subsequent analysis of the system, such as sensitivity analysis.

Similarly to the uncertainty quantification in probabilistic modeling, we call *margin quantification* to the step 4.

Definition 4.4.1 (Margin quantification). *Given a problem description $(\mathbf{E}, \mathcal{E})$, a failure set \mathbf{F} , an assessment of the uncertainties and some models of margin $\mathbf{M}_1, \dots, \mathbf{M}_n$, the act of choosing the demanded margins m_1, \dots, m_n such that*

$$\mathbf{F}' = \mathbf{dm}_{\mathbf{M}_n, m_n} \circ \dots \circ \mathbf{dm}_{\mathbf{M}_1, m_1}(\mathbf{F})$$

covers the uncertainties is called margin quantification.

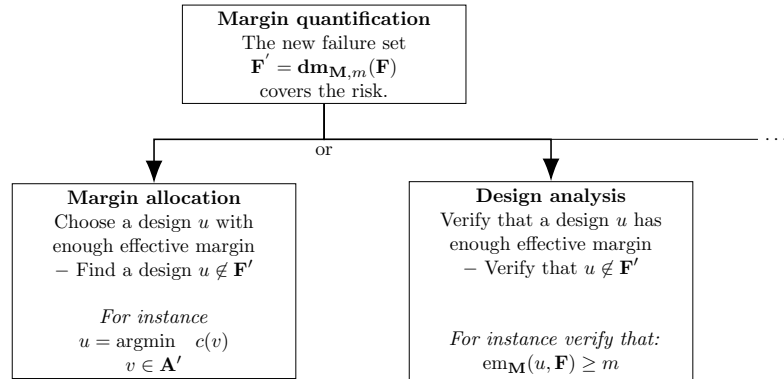


Figure 4.5: After the margin quantification, various steps can be done, such as allocating the margins by choosing a design outside the new failure set (by optimizing a cost function c for instance) or verifying that a design has enough effective margin.

Remark 4.4.2 (Taking multiple margins). *Let \mathbf{M}_1 and \mathbf{M}_2 be two models of margin on the same problem description. Let \mathbf{F} be a failure set, for which a margin m_1 is taken in \mathbf{M}_1 and then, a margin m_2 is taking in \mathbf{M}_2 . The resulting failure set \mathbf{F}'' is the image of \mathbf{F} by the composition of the margin operators*

$$\mathbf{F}'' = \mathbf{dm}_{\mathbf{M}_2, m_2}(\mathbf{dm}_{\mathbf{M}_1, m_1}(\mathbf{F})).$$

In terms of models, this means that the risks that \mathbf{M}_1 and \mathbf{M}_2 must cover can happen at the same time. This aspect is discussed more deeply in Chapter 5 and in the use case of Chapter 6.

Use case, part 6. Here are how engineers follows the four steps in the use case

Step 1 They identified the variables E , the equations \mathcal{C} .

Step 2 They constructed the forbidden set \mathbf{F} .

Step 3 They identified two sources of uncertainty: the statistical uncertainty due to the estimation of κ_0 by $\hat{\kappa}$ and the uncertainty due to the replacement of F_0 by the nominal value F_{nom} .

Step 4 They decided to take a margin (*i.e.* impose a demanded margin) on κ with \mathbf{M}_κ and F with \mathbf{M}_F (step 4a). In order to quantify the value of the demanded margin m_κ (step 4b), they now choose a level of confidence $1 - \alpha = 0.99$ and use the statistical theory to set

$$m_\kappa = \frac{q_{0.99}\sigma_\kappa}{\sqrt{n}},$$

with $q_{0.99}$ being the quantile of level 0.99 of a standard normal random variable. In that case, they can verify that if W_{max} is chosen as a function of $\hat{\kappa}$ and F_0 , such that

$$(W_{\text{max}}, f(\hat{\kappa}, F_0), \hat{\kappa}, F_0) \notin \mathbf{dm}_{\mathbf{M}_\kappa, m_\kappa}(\mathbf{F}) \text{ almost surely,}$$

then

$$\mathbb{P}((W_{\text{max}}, f(\kappa_0, F_0), \kappa_0, F_0) \notin \mathbf{F}) \geq 1 - \alpha.$$

In other terms, the uncertainty due to the statistical estimation is covered by replacing \mathbf{F} with $\mathbf{dm}_{\mathbf{M}_\kappa, m_\kappa}(\mathbf{F})$. The value $m_\kappa = \frac{q_{0.99}\sigma_\kappa}{\sqrt{n}}$ ensures a level of confidence of $1 - \alpha$.

For the value of β_F (step 4b), they use an internal document of reference, based on previous experimental results. It states that in early design phase, when the shape of the wing is not known, the value of the coefficient must be $\beta_F = 3$. In their uncertainty model, it means that they consider that $F_0 \leq \beta_F F_{\text{nom}}$ is certain.

The resulting failure set is given by applying the composition of the demanded operators

$$\mathbf{F}'_{\kappa, F} = \mathbf{dm}_{\mathbf{M}_\kappa, m_\kappa}(\mathbf{dm}_{\mathbf{M}_F, \beta_F - 1}(\mathbf{F})) = \left\{ u \in \mathcal{C} \mid \left(W_{\text{max}}, W, \kappa + \frac{q_{0.99}\sigma_\kappa}{\sqrt{n}}, 3F \right) \in \mathbf{F} \right\},$$

for which they conclude that if W_{max} is chosen as a function of $\hat{\kappa}$ and F_{nom} such that

$$(W_{\text{max}}, f(\hat{\kappa}, F_{\text{nom}}), \hat{\kappa}, F_{\text{nom}}) \notin \mathbf{F}'_{\kappa, F} \text{ almost surely,}$$

then

$$(W_{\max}, f(\kappa_0, F_0), \kappa_0, F_0) \notin \mathbf{F}$$

with probability at least $1 - \alpha$. In other terms, if the "nominal design" is not in the forbidden set with margins, the true design, which is uncertain, will not be in the forbidden set, with a certain level of confidence.

Engineers can now provide a value of W_{\max} among all the acceptable values $\mathbf{A}'_{\kappa, F} = \mathcal{E} \setminus \mathbf{F}'_{\kappa, F}$. As they were asked to provide the smallest value, their choice is given by the minimization problem

$$\begin{aligned} W_{\max}^* &= \inf\{W_{\max} \in \mathbb{R}_+ \mid \exists (W, \kappa, F) \in \mathbb{R}_+^3 \text{ s.t. } (W_{\max}, W, \kappa, F) \in \mathbf{A}'_{\kappa, F}\} \\ &= f(\hat{\kappa} + m_{\kappa}, \beta_F F_{\text{nom}}). \end{aligned}$$

It is important to notice that in Definition 4.4.1, we do not propose a mathematical model for the assessment of the uncertainties.

The first reason is because it is still possible to make some reasoning and study the system using only already quantified margin as a proxy for the system uncertainty. Even an imprecise map of the margin in the system can still be useful in a sensitivity analysis to identify the most important contributors. If the model for uncertainty is known, it is still possible to use it to reduce the non relevant margins, as it is done in Section 6.

The second reason is that the uncertainty model depends on the practices of the engineering field and the experience of the analyst doing them. The review of the literature on the civil engineering field of Section 3.1.4 is particularly revealing; at the beginning, the partial safety factors - that are demanded margins - were chosen purely based on the experience/expert judgment. Then, they were calibrated to handle a large variety of situations, using a higher level probabilistic modeling. Finally, in some specific cases, an explicit probabilistic modeling can be performed, ensuring the "best tailored" factors. Margins can be defined in these three types of situation and the existence of similar approaches in other fields makes no doubt. In our approach, we want to model the practices of most of the engineers working on an industrial systems; we then need to remain agnostic of the uncertainty representation.

4.4.2 Margin quantification with level of risk

The margin quantification of Definition 4.4.1 is quite general as it aims is to describe engineering approaches. In the case where one is interested in developing a methodology for margin quantification, we can outline some good properties that the model of risk in Steps 3 and 4 could satisfy.

Step 3, identification of the risks

- (a) Identify the sources of the uncertainties and if they are reducible¹;
- (b) Identify a measure of the risk ρ and an admissible risk level α , based on the consequences of the uncertainties;
- (c) Assess the range of the uncertainties s .

Then, Step 4b is modified to choose demanded margins $m_1(s, \alpha), \dots, m_n(s, \alpha)$, that are functions of the admissible level of risk and s . When such a form is achieved, we say that there is an *explicit model of risk* for the margin quantification. This approach gives more information that can then

¹Reducible uncertainties are uncertainties can be practically reduced during the design process, as introduced in Chapter 1.

be used to eliminate the costly margins. Knowing that some uncertainties that cause margins are reducible allows for *margin reduction* (Section 5.3) for instance.

Example 4.4.3 (The statistical approach). *In Use case, part 6, there is an explicit model of risk for κ , that makes Step 3 explicit.*

- (a) *The source of the uncertainty is the statistical uncertainty due to the estimation of κ_0 by $\hat{\kappa}$. It is reducible under the condition that more observations of \mathbf{K} are available.*
- (b) *The measure of the risk is the probability that the condition $W_{\max} \geq W = f(\kappa_0, F_0)$ does not hold when $\hat{\kappa}$ replace κ_0 . The chosen level is $\alpha = 0.01$.*
- (c) *The range of the uncertainty is σ_R/\sqrt{n} , with n the size of the sample $(\mathbf{K}_i)_{i \in [1, n]}$.*

The demanded margin value is set as $m_\kappa = q_{0.99}\sigma_R/\sqrt{n}$ to ensure a level of confidence of $1 - \alpha$.

Example 4.4.4 (A probabilistic model). *Another probabilistic approach is used in the literature, in the margin allocation approach for instance (Section 3.2.4). Let $(\mathbf{E}, \mathcal{E})$ be a problem description such that $\mathbf{E} = \{(x, y) \in \mathbf{E}_x \times \mathbf{E}_y\}$. The first step is the construction of a failure set by a deterministic model \mathbf{F} . The variable y models the uncertainty with respect to a reference value y_{ref} , so that $y = y_{\text{ref}}$ means that no uncertainty is included in the model. The variable x is deterministic and chosen by the analyst. Steps 3 and Steps 4 are the following.*

- 3 (a) *The uncertainty on y can come from various sources, that are listed and modeled in a random variable Y .*
- (b) *The risk is measured by the probability of (x, Y) to belong in the failure set \mathbf{F} , to be bounded by α*

$$\mathbb{P}((x, Y) \in \mathbf{F}) < \alpha.$$
- (c) *A nominal deterministic value y_{ref} is computed and the range of uncertainty is given in $Y - y_{\text{ref}}$.*
- 4 (a) *A margin is taken on y , through the model \mathbf{M}_y .*
- (b) *Some probabilistic computation gives the value of demanded margins m_y such that if a nominal design $u_{\text{ref}} = (x, y_{\text{ref}})$ is not in the failure set with margins*

$$\mathbf{F}' = \mathbf{dm}_{\mathbf{M}_y, m_y}(\mathbf{F})$$

then the probabilistic criterion holds

$$\mathbb{P}((x, Y) \in \mathbf{F}') < \alpha. \quad (4.5)$$

This means that if the nominal design is not in the forbidden set with margins, the true design (that is uncertain in general) is acceptable with the required confidence level. It is interesting to notice that, if \mathbf{F} contains all the design with zero effective margins, Equation (4.5) can be rewritten as the probability

$$\mathbb{P}(\mathbf{em}_{\mathbf{M}_y}((x, Y), \mathbf{F}) \leq 0) < \alpha,$$

or, in terms of quantile,

$$Q_\alpha(\mathbf{em}_{\mathbf{M}_y}((x, Y), \mathbf{F})) > 0.$$

with $Q_\alpha(Z)$ being the quantile of level α of the random variable Z . This form is used in design analysis to check that margins are high enough.

4.5 The existing literature under the prism of the model of margin

Having the model of margin and the four steps of uncertainty mitigation in mind, we are now armed to interpret the industrial practices of Section 3.1 in our framework. We will see that they often relate to a specific part of the process, either by defining a model of margin, computing an effective margin or performing a margin quantification either to allocate margins or to verify that the risk mitigation criteria are met. In Table 4.2, we summarize the methods of the literature under the prism of the model of margin framework and we develop each point in the rest of the section.

4.5.1 Statistics

This section refers to notions reviewed in Section 3.1.1.

Depending on the goal, three classic shapes can be chosen for a confidence interval in the estimation of θ by $\hat{\theta}$:

- An upper-bounded confidence interval $(-\infty, \hat{\theta} + m]$;
- A centered confidence interval $[\hat{\theta} - m, \hat{\theta} + m]$;
- A lower-bounded confidence interval $[\hat{\theta} - m, +\infty)$.

Choosing one of these three shapes is actually equivalent to choosing either an *increasing directional* model of margin (upper-bounded), a *bidirectional* model of margin (centered) or a *decreasing directional* model of margin (lower-bounded), introduced in Sections 4.3.1 and 4.3.2.

Let us denote by \mathbf{M}_θ the model of margin on θ and assume that a design can be written $u = (x, \theta) \in \mathbf{E}$. The choice of the margin m_α for a given level $1 - \alpha$, e.g. $m_\alpha = q_{1-\alpha/2}\sigma/\sqrt{n}$, is a *margin quantification*. It is based on the observation that if a nominal design $(x, \hat{\theta})$ satisfies

$$(x, \hat{\theta}) \notin \mathbf{dm}_{\mathbf{M}_\theta, m_\alpha}(\mathbf{F}) \text{ almost surely,}$$

with x a random variable that is a function of the estimated parameter $\hat{\theta}$, then the probability that the true design (x, θ) is acceptable is greater than or equal to $1 - \alpha$, i.e.

$$\mathbb{P}((x, \theta) \in \mathbf{F}) \geq 1 - \alpha.$$

Notice that here the randomness comes from the fact that x is a random variable.

4.5.2 Robust optimization

This section refers to notions reviewed in Section 3.1.2.

Choosing the shape of the uncertainty sets is actually choosing a model of margin. For instance, the ellipsoidal uncertainty set can be modeled by a projection on the uncertain parameter \tilde{u} with the following distance on the margin space

$$d_{\mathcal{S}}(u, v)^2 = (u - v)' \Sigma^{-1} (u - v). \quad (4.6)$$

Engineering field	Concept	Interpretation in the model of margin framework
Statistics	Choice of an upper/centered/lower interval Length of the confidence interval	Defines a model of margin Margin quantification
Robust optimization	Shape of the uncertainty set Performing the optimization Data driven robust optimization	Defines a model of margin Optimization under demanded margin constraints Margin quantification
Info-gap theory	Info-gap model Stability radius Robust-satisficing optimization	Defines a model of margin Effective margin Optimization of the margin
Civil engineering	Partial factor Partial factor calibration	Defines a model of margin Margin quantification
Control	Phase margin, Gain margin	Defines a model of margin
Robust Control	Stability radius	Effective margin
Finance	Monetary risk measure Requirement that the risk is negative Acceptance set	Effective margin Margin quantification Acceptance set $\mathbf{A} = \mathbf{F}^c$
Nuclear safety	Quantification of margins and uncertainty Traditional margins Probabilistic margin	Margin quantification and design analysis Defines a model of margin Wilks' quantile of an effective margin Margin quantification and design analysis
Space engineering	Performance margin/Safety performance margins Margin value	Defines a model of margin Margin quantification
Complex system design	Margin allocation and tradeoff in complex systems Tradeoff analysis	Margin quantification Study of the impact of margins
Design science	Buffer Excess Margin value method	Demanded margin/Margin quantification Effective margin Margin sensitivity analysis

Table 4.2: Reinterpretation of the literature on the margins in the model of margin framework.

In the framework of the model of margin, a robust optimization problem with constraint of the form $\mathbf{F} = \{(\mathbf{x}, \mathbf{u}) \mid f_1(\mathbf{x}, u_1) \leq 0, \dots, f_n(\mathbf{x}, u_n) \leq 0\}$ can be rewritten

$$\begin{aligned} & \text{minimize } f_0(\mathbf{x}) \\ & \text{subject to } (\mathbf{x}, \hat{\mathbf{u}}) \notin \mathbf{dm}_{\mathbf{M}_{\mathbf{u}}, m}(\mathbf{F}) \end{aligned}$$

with $\mathbf{u} = (u_1, \dots, u_n)$ being the vector of the uncertain parameters and $\hat{\mathbf{u}}$ being a nominal value of this vector. The object $\mathbf{M}_{\mathbf{u}}$ is a model of margin on the whole vector \mathbf{u} , the projection map being the identity and the probing set being the whole space of the parameters. The distance depends on the shape of the uncertainty set. In the case of an ellipsoidal uncertainty set (given in Definition 3.1.2), γ plays the role of m .

The data-driven robust optimization consists in calibrating the shape of the uncertainty set with data and then choose the value of the demanded margin m to use in $\mathbf{dm}_{\mathbf{M}_{\mathbf{u}}, m}$. It is then a *margin quantification*.

Info-gap theory Let \mathcal{U} be an info-gap model verifying the linearity property given in Equation (3.3). The real function $p_{\mathcal{U}(0,1)}(u) = \inf \{\alpha \in \mathbb{R}_+ \mid u \in \alpha \mathcal{U}(0,1)\}$ is called the gauge or Minkovski functional of the set $\mathcal{U}(0,1)$ in the functional analysis literature [30, Proposition 1.4]. Under the assumption that $\mathcal{U}(0,1)$ is an absorbing set, the gauge is actually a mathematical seminorm so we can rewrite

$$\mathcal{U}(\alpha, u) = \{v \in \mathcal{C} \mid \|u - v\|_{\mathcal{U}(0,1)} \leq \alpha\}$$

with $\|\cdot\|_{\mathcal{U}(0,1)} = p_{\mathcal{U}(0,1)}(\cdot)$. The robustness of Equation (3.4) can then be rewritten as a pseudometric

$$\begin{aligned} \hat{\alpha}(x, u) &= \sup \{\alpha > 0 \mid \forall v, \|u - v\|_{\mathcal{U}(0,1)} \leq \alpha, v \notin \mathbf{F}(x)\} \\ &= d_{\mathcal{U}(0,1)}(u, \mathbf{F}(x)), \end{aligned}$$

$d_{\mathcal{U}(0,1)}$ being the pseudometric induced by the seminorm $\|\cdot\|_{\mathcal{U}(0,1)}$. If we define the state space by $(x, u) \in \mathbb{E}$, the robustness of an info-gap model is the *effective margin*

$$\hat{\alpha}(x, u) = \text{em}_{\mathbf{M}_x}((x, u), \mathbf{F}_{\text{IG}})$$

with a probing set $\mathcal{G}_{(x,u)} = \{(y, v) \in \mathbb{E} \mid y = x\}$, and a projection map $\phi_{x,u}(y, v) = v$. The distance on the margin space \mathbb{S} is $d_{\mathbb{S}} = d_{\mathcal{U}(0,1)}$. The failure set is $\mathbf{F}_{\text{IG}} = \{(x, u) \in \mathbb{E} \mid u \in \mathbf{F}(x)\}$.

4.5.3 Control and robust control

This section refers to notions reviewed in Section 3.1.3.

Phase margin and gain margin The phase margin and the gain margin provide a way to compute a margin for a given design; they define then a model of margin.

Stability radius The stability radius ρ is the effective margin for the model of margin $\mathbf{M}_{\mathbf{q}}$ that we now define. The state space and the problem constraints are the space where the vector of the parameters can take its value $\mathbf{q} \in \mathbb{E} = \mathcal{C} \subset \mathbb{R}^l$, $l \in \mathbb{N}$. There is a failure whenever the polynomial associated to \mathbf{q} is not strictly Hurwitz, *i.e.*

$$\mathbf{F} = \{\mathbf{q} \in \mathcal{C} \mid p(s, \mathbf{q}) \text{ is not strictly Hurwitz}\}.$$

The projection map is the identity $\phi_{\mathbf{q}}(\mathbf{q}') = \mathbf{q}'$. The margin space is $\mathbb{S} = \mathbb{R}^l$ with a normalized supremum norm such that $Q = \prod_{i \in [1, l]} [-q_i, q_i]$ is the unit ball (assuming the parameters are centered), *i.e.*

$$d_{\mathbb{S}}(\mathbf{r}, \mathbf{s}) = \sup_{i \in [1, l]} \frac{|r_i - s_i|}{q_i} = \inf \{ \lambda \geq 0 \mid (\mathbf{r}, \mathbf{s}) \in \lambda Q \}.$$

with $\mathbf{r} = (r_1, \dots, r_l)$ and $\mathbf{s} = (s_1, \dots, s_l)$. The parameter space being centered, the effective margin is computed at the nominal point $0_{\mathbb{R}^l}$

$$\begin{aligned} \text{em}_{\mathbf{M}}(0_{\mathbb{R}^l}, \mathbf{F}) &= d_{\mathbb{S}}(0_{\mathbb{R}^l}, \mathbf{F}) \\ &= \inf_{w \in \mathbf{F}} d_{\mathbb{S}}(0_{\mathbb{R}^l}, w) \\ &= \inf \{ \lambda \geq 0 \mid w \in \lambda Q \text{ and } w \in \mathbf{F} \} \\ &= \rho \end{aligned}$$

by definition of the Stability radius in Equation (3.6).

4.5.4 Partial safety factor

This section refers to notions reviewed in Section 3.1.4.

Let us consider the case of one resistance parameter x and one action parameter y with one resistance variable R_d and one action effect variable S_d . The state space contains the values $(x, y, R_d, S_d) \in \mathbf{E}$ and the set of problem constraints

$$\mathcal{C} = \{(x, y, R_d, S_d) \in \mathbf{E} \mid R_d = R(x), S_d = S(y), x > 0, y > 0\}$$

is constructed from the phenomenon equations, so that

$$\mathbf{F} = \{(x, y, R_d, S_d) \in \mathcal{C} \mid R_d < S_d\}.$$

Provided that R is increasing and continuous in x , a partial safety factor $\gamma > 1$ on a stress variable x corresponds to a *demanded margin* $m_x = 1 - 1/\gamma$ associated to the model of margin \mathbf{M} , that has a decreasing probing set

$$(\mathcal{G}_u)_{u \in \mathcal{C}} : \quad x : \leftarrow, \quad y : \times, \quad R_d : \leftrightarrow, \quad S_d : \leftrightarrow$$

with the family of projection maps

$$\phi_u(v) = \frac{x'}{x}.$$

The following equivalences hold

$$\begin{aligned} u \notin \mathbf{dm}_{\mathbf{M}, 1 - \frac{1}{\gamma}}(\mathbf{F}) &\Leftrightarrow \inf_{v \in \mathbf{F}} \left| 1 - \frac{x'}{x} \right| \geq 1 - \frac{1}{\gamma} \\ &\Leftrightarrow \inf_{v \in \mathbf{F}} x - x' \geq \left(1 - \frac{1}{\gamma} \right) x \\ &\Leftrightarrow \inf_{v \in \mathbf{F}} -x' \geq -\frac{x}{\gamma} \\ &\Leftrightarrow \inf_{v \in \mathbf{F}} -R(x') \geq -R\left(\frac{x}{\gamma}\right) \end{aligned}$$

because R is increasing and continuous in x . We can remark that

$$\inf_{v \in \mathbf{F}} -R(x') = \sup_{(x', y, R_d, S_d) | R(x') < S(y)} R(x') = S(y),$$

so that the condition finally rewrites

$$u \notin \mathbf{dm}_{\mathbf{M}, 1 - \frac{1}{\gamma}}(\mathbf{F}) \Leftrightarrow S(y) \leq R(x/\gamma),$$

in which we retrieve the partial safety factor of Equation 3.8. This proof can be adapted to multiple resistance variable by defining the same kind of models of margin and composing them. The same kind of equivalence also holds with y , with the probing set

$$(\mathcal{G}_u)_{u \in \mathcal{E}} : \quad x : \times, \quad y : \rightarrow, \quad R_d : \leftrightarrow, \quad S_d : \leftrightarrow$$

and a demanded margin $m_y = \gamma - 1$.

The act of calibrating the value of the partial factor, either by expert judgment or using a high level probabilistic model consists in choosing the value m_x and m_y taking into account the uncertainties; it is then a *margin quantification*.

4.5.5 Coherent risk measure

This section refers to notions reviewed in Section 3.1.6.

A coherent risk measure is the opposite of an effective margin on a space of random variables. The state space is the set of real-valued random variables $\mathbf{E} = L^0(\Omega, \mathbb{R})$ and a design X is a random variable modeling the final net worth of a given portfolio allocation.

For a given risk measure ρ , the failure set contains the positions that have a positive risk

$$\mathbf{F} = \{X \in \mathbf{E} \mid \rho(X) > 0\}.$$

We can define a model of margin \mathbf{M}_X on X , that have a probing set describing the translations of X

$$\mathcal{G}_X = \{X' \in \mathbf{E} \mid X' = X + \lambda, \lambda \in \mathbb{R}\}$$

and a projection map

$$\phi_X(X + \lambda) = \lambda.$$

When $X \in \mathbf{A}$, this model of margin measures by how much X can decrease before being in the failure set

$$\begin{aligned} \text{em}_{\mathbf{M}_X}(X, \mathbf{F}) &= \sup \{\lambda \geq 0 \mid \rho(X - \lambda) \leq 0\} \\ &= \sup \{\lambda \geq 0 \mid \lambda \leq -\rho(X)\} \quad (\text{translation property}) \\ &= -\rho(X). \end{aligned}$$

In other terms, the measure of the risk $\rho(X)$ is the opposite of a margin on X for an acceptance set $\mathbf{A} = \mathbf{F}^c$ defined by $\rho(X) \leq 0$.

4.5.6 Nuclear safety

This section refers to notions reviewed in Sections 3.2.1 and 3.2.2.

Both traditional and probabilistic margins are effective margins that are used in design analysis to evaluate the safety of a design or compare two designs. In our framework, a design is

defined as $u = (y, a) \in E$ where y denotes the physical quantities and a the vector of the environment variables. The equations are given by $\mathcal{E} = \{(y, a) \in E | f(y, a) = 0\}$, with f including the physical and logical relationships. We treat the case of a requirement on y in terms of upper threshold, for which the failure set is expressed as

$$\mathbf{F} = \{(y, a) \in \mathcal{E} | y \leq y_{\text{upp}}\}.$$

For a given reference value y_{ref} , we can define an increasing model of margin \mathbf{M} with a mapping function

$$\phi_u(v) = \begin{cases} y' & \text{if } y' \geq y_{\text{ref}}, \\ y_{\text{ref}} & \text{if } y' < y_{\text{ref}}, \end{cases}$$

and a probing set

$$\mathcal{G}_u = \{v \in E | y' \geq y\}$$

with $u = (y, a)$ and $v = (y', a')$. With this model of margin, the value of the effective margin for the design u is

$$\text{em}_{\mathbf{M},m}(u, \mathbf{F}) = \begin{cases} y_{\text{sup}} - y & \text{if } y_{\text{sup}} \geq y_{\text{ref}}, \\ y_{\text{sup}} - y_{\text{ref}} & \text{if } y_{\text{sup}} < y_{\text{ref}}. \end{cases}$$

We retrieve the expression of the traditional margin

$$M(y, a) = \frac{\max(\text{em}_{\mathbf{M}}(y, a), 0)}{y_{\text{sup}} - y_{\text{ref}}}$$

by normalizing it by a reference value and capping it at 0.

In order to construct the probabilistic margin, y is replaced with a random variable Y . A safety level is chosen $\alpha \in [0, 1]$ for the probabilistic criterion

$$\mathbb{P}((Y, a) \notin \mathbf{F}) < \alpha.$$

As illustrated in Example 4.4.4, this condition can be rewritten

$$Q_\alpha(\text{em}_{\mathbf{M},m}((Y, a), \mathbf{F})) > 0,$$

or in the normalized form

$$Q_\alpha(M(Y, a)) > 0.$$

This effective margin is used to analyze the design; if it is positive, then the the probabilistic criterion is satisfied. In order to compute it numerically, a probabilistic method is used with a level of confidence $1 - \beta$ on the error, parametrizing this margin by α and β .

4.5.7 Performance margin and safety performance margin

This section refers to notions reviewed in Section 3.2.3.

Performance margin Let $u = (p, p_{\text{req}}) \in E = \mathcal{E} = \mathbb{R}_+^{*2}$ be a performance parameter and a requirement. Given a forbidden set of the form $\mathbf{F} = \{(p, p_{\text{req}}) \in E | p > p_{\text{req}}\}$, the performance margin on p , is

$$m_{\text{perf}} = p_{\text{req}} - p.$$

This quantity is an effective margin with a model of margin \mathbf{M}_p with projection map $\phi_u(p', p'_{\text{req}}) = p'$ and probing set $\mathcal{G}_u = \{(p', p'_{\text{req}}) | p'_{\text{req}} = p_{\text{req}}\}$, such that

$$\text{em}_{\mathbf{M}_p}(p, \mathbf{F}) = p_{\text{req}} - p, \tag{4.7}$$

(see Example 4.2.6). The performance margin with contingency writes

$$m_{\text{perf}} = \nu p_{\text{req}} - p \quad (4.8)$$

with a coefficient $\nu \in (0, 1)$. Similarly to the safety coefficient, $1 - \nu$ can be seen as a demanded margin on the requirement p_{req} . Its model of margin $\mathbf{M}_{p_{\text{req}}}$ has a projection map

$$\phi_u(p'_{\text{req}}, p') = \frac{p'_{\text{req}}}{p_{\text{req}}},$$

for which the effective margin at the point $u \notin \mathbf{F}$ writes

$$\begin{aligned} \text{em}_{\mathbf{M}_{p_{\text{req}}}}((p, p_{\text{req}}), \mathbf{F}) &= \inf_{p'_{\text{req}} < p} \frac{|p_{\text{req}} - p'_{\text{req}}|}{p_{\text{req}}} \\ &= 1 - \frac{p}{p_{\text{req}}}. \end{aligned}$$

It follows from this observation that

$$\mathbf{dm}_{\mathbf{M}_{p_{\text{req}}}, 1-\gamma}(\mathbf{F}) = \{(p, p_{\text{req}}) \mid \gamma p_{\text{req}} > p\}$$

and then the margin of Equation (4.8) writes

$$m_{\text{perf}} = \text{em}_p((p, p_{\text{req}}), \mathbf{dm}_{\mathbf{M}_{p_{\text{req}}}, 1-\gamma}(\mathbf{F})) = \gamma p_{\text{req}} - p,$$

i.e. it is an effective margin on p , once a demanded margin on p_{req} has been taken.

Safety performance margin Let Y be a random vector modeling the (uncertain) state of the phenomenon/design and let the adverse event be $Y \in G$ of probability $p \in [0, 1]$. We can model the problem with the variables $(Y, p) \in \mathbf{E}$, such that the equations are given by

$$\mathcal{E} = \{(Y, p) \in \mathbf{E} \mid p = \mathbb{P}(Y \in G)\}.$$

The rest of the model is identical to the aforementioned performance margin leading to the expression

$$m_{\text{sfty perf}} = p_{\text{req}} - p.$$

Margin value The prescribed values for the safety performance margins, in Table 3.2, are demanded margins that are chosen to cover the unknown unknowns and depends on the maturity of the design. This is a case of *margin quantification*.

4.5.8 Margin allocation in industrial complex systems

This section refers to notions reviewed in Section 3.2.4.

In margin allocation, a trading parameter (cost, mass...) is associated (sometimes implicitly) to two variables: the allocated budget y_{budget} and the value that will be actually consumed y . They are both in the state space $(y_{\text{budget}}, y) \in \mathbf{E}$ and the problem constraints \mathcal{E} depend on the system considered. When the variable is of the type “the smaller the better” (for instance a monetary cost), there is a failure whenever the budgeted variable is smaller than the actual value

$$\mathbf{F} = \{(y_{\text{budget}}, y) \in \mathcal{E} \mid y_{\text{budget}} < y\}.$$

If we define a model of margin \mathbf{M}_y on y , with a probing set

$$(\mathcal{G}_u)_{u \in \mathcal{E}} : y : \leftrightarrow, y_{\text{budget}} : \times$$

and projection map

$$\phi_u(v) = \frac{y'}{y}$$

with $u = (y_{\text{budget}}, y)$ and $v = (y'_{\text{budget}}, y')$, we get the following expression for the effective margin

$$\text{em}_{\mathbf{M}_y}((y_{\text{budget}}, y), \mathbf{F}) = \frac{y_{\text{budget}} - y}{y}.$$

However, as the value of y is unknown, it is replaced by an estimated value y_{det} and a demanded margin is included in the failure set. Similarly to Example 4.4.4, a random variable Y is constructed to model the uncertainty that is generated when replacing y with y_{det} . For a given level of risk $\alpha \in [0, 1]$, the demanded margin is chosen as a function of α

$$m(\alpha) = \frac{Q_{1-\alpha}(Y) - y_{\text{det}}}{y_{\text{det}}}$$

such that if $(y_{\text{budget}}, y_{\text{det}}) \in \mathbf{dm}_{\mathbf{M}, m(\alpha)}(\mathbf{F})$, then the probability of having a positive margin with the random model is greater than $1 - \alpha$

$$\mathbb{P}(\text{em}_{\mathbf{M}}((y_{\text{budget}}, Y), \mathbf{F}) > 0) \geq 1 - \alpha.$$

In this context of margin allocation, a probabilistic model with a level of confidence is used to choose the demanded margin value. It is then a margin quantification with an explicit model of risk.

The *impact of margins on other margins* tradeoff analysis consists in imposing some directional demanded margins on some variables and then studying what are the effective margins (i.e the remaining margins that could be taken) on other variables.

The *impact of margins on the risk* consists in comparing graphically the failure set with a probabilistic model and confidence level with a failure set with a deterministic model and demanded margins. It permits to check the quality of the margin quantification. When the quantification is well done, the two models should have a very similar shape.

4.5.9 Margin as the cause of over-capacity

This section refers to notions reviewed in Section 3.2.5.

The distinction buffer/excess can be interpreted as a distinction demanded margin/remaining effective margin in our framework. Indeed, the description of the buffer margin is that it “caters for uncertainties”, and thus follows the definition of a demanded margin that has been quantified. The excess margin is the remaining part, and is then the effective once the demanded margin has been taken.

In order to illustrate this point, let us consider a problem description of the type $(y, y_{\text{req}}) \in E = \mathcal{E} = \mathbb{R}^2$ and a forbidden set of the form

$$\mathbf{F} = \{(y, y_{\text{req}}) \in \mathcal{E} \mid y < y_{\text{req}}\}.$$

When there are some uncertainties, let us say on the value of y_{req} , the margin quantification consists in choosing a *demanded margin* $m > 0$ to cover these uncertainties. It is usually done with a bidirectional model of margin $\mathbf{M}_{y_{\text{req}}}$ on y_{req} , i.e. the probing sets are

$$(\mathcal{G}_u)_{u \in \mathcal{E}} : y : \times, y_{\text{budget}} : \leftrightarrow$$

and the projection maps

$$\phi_u(y', y'_{\text{req}}) = y'_{\text{req}}.$$

After taking a demanded margin, the resulting forbidden set is

$$\mathbf{F}' = \mathbf{dm}_{\mathbf{M}_{y_{\text{req}}}, m}(\mathbf{F}) = \{(y, y_{\text{req}}) \in \mathcal{C} \mid y < y_{\text{req}} + m\}.$$

For a given design u , the remaining margin is measured in terms of *effective margin*

$$\text{em}_{\mathbf{M}_{y_{\text{req}}}}(u, \mathbf{F}') = y - (y_{\text{req}} + m),$$

so that we can rewrite the initial margin

$$y - y_{\text{req}} = m + \text{em}_{\mathbf{M}_{y_{\text{req}}}}(y, \mathbf{dm}_{\mathbf{M}_{y_{\text{req}}}, m}(\mathbf{F}')).$$

The buffer margin m is in fact a demanded margin to cover some uncertainties. The excess margin $\text{em}_{\mathbf{M}}(y, \mathbf{F}')$ is the remaining effective margin on the point y , with respect to a forbidden set on which the demanded margin has been taken.

We remark that a benefit of the model of margin is that the demanded and effective margins can be defined on different variables: various buffers can be taken on a set variables and the excess can be measured on another variable.

Margin value method A part of the objective of the margin value method is close to the margin sensitivity analysis of Chapter 5.

The *excess* metric is an effective margin, as exposed above.

The *impact* metric measures by how much a performance is increased when one margin on a variable i is set to its limit value. In its spirit, it is close to the *induced loss of performance* we defined in Section 5.1. Indeed, the idea is to put the margin to 0 and see by how much the performance is increased. Let us remark that the global sensitivity analysis of Section 5.2.3 permits to analyze the impact on the design when removing *multiple* demanded margins at the same time.

The *absorption benefits* are not considered in our framework for the moment as we concentrated only on the negative impacts of the margins. Reinterpreting the absorption under the prism of the effective/demanded margin is a very interesting perspective.

Chapter 5

Margin sensitivity analysis and margin reduction

So far, Chapter 4 has shown the *descriptive* ability of the model of margin to encompass engineering margin practices. This chapter develops a set of tools and methods to address the motivating industrial question of the *design margin reduction*.

5.1 Induced cost and induced margin

In the design margin literature, authors often refer to the impact of margins on other margins and the cost of the margins (see Sections 3.2.4 and 3.2.5 for instance). To compute the cost of the margin, we define the *induced cost* as the difference between the cost of a design with demanded margin and the cost of a design without margin. In our context it has the property of being an increasing function of the demanded margins.

When one computes the impact of some margins on another margin, they actually compute the impact of some *demanded margins* on an *effective margin*. We define the *induced margin*, in a similar way to the cost, that is the difference between the effective margin without demanded margin and the effective margin with demanded margins. Throughout this section, we fix a problem description (E, \mathcal{E}) .

5.1.1 Composition of demanded margin operators

As stated in Remark 4.4.2, when multiple margins are taken to cover some risks, the demanded margin operators are functionally composed. For a given problem description and failure set \mathbf{F} , the resulting failure set after taking a demanded margin m_1 in \mathbf{M}_1 , m_2 in \mathbf{M}_2, \dots and m_n in \mathbf{M}_n is denoted by

$$\mathbf{F}'(m_1, \dots, m_n) = \mathbf{dm}_{\mathbf{M}_n, m_n} \circ \dots \circ \mathbf{dm}_{\mathbf{M}_1, m_1}(\mathbf{F}). \quad (5.1)$$

We can remark that the greater the demanded margins are, the stronger the constraints are, and thus the larger the forbidden set is. This is the meaning of Proposition 5.1.1.

Proposition 5.1.1 (Monotonicity of the inclusion). *Let $(m_1, \dots, m_n) \in \mathbb{R}_+^n$ and $(m'_1, \dots, m'_n) \in \mathbb{R}_+^n$ such that $m_i \leq m'_i$ for all i in $\llbracket 1, n \rrbracket$. Then*

$$\mathbf{F}'(m_1, \dots, m_n) \subset \mathbf{F}'(m'_1, \dots, m'_n).$$

Proof. Let us remark that if a failure set \mathbf{F}_1 is included in another failure set \mathbf{F}_2 , then, for any design $u \in \mathcal{C}$ and any model of margin \mathbf{M} , the effective margin with respect to \mathbf{F}_1 will always be greater than or equal to the effective margin with respect to \mathbf{F}_2 (the distance to the set included in the other is the greatest). Thus,

$$\text{if } \mathbf{F}_1 \subset \mathbf{F}_2, \quad \text{then } \mathbf{dm}_{\mathbf{M},m}(\mathbf{F}_1) \subset \mathbf{dm}_{\mathbf{M},m}(\mathbf{F}_2) \quad (5.2)$$

for any \mathbf{M} and $m \geq 0$. A second property is that greater margin always expands the failure set, for $m' \geq m \geq 0$

$$\mathbf{dm}_{\mathbf{M},m}(\mathbf{F}) = \{u \in \mathcal{C} \mid \text{em}_{\mathbf{M}}(u, \mathbf{F}) < m\} \subset \{u \in \mathcal{C} \mid \text{em}_{\mathbf{M}}(u, \mathbf{F}) < m'\} = \mathbf{dm}_{\mathbf{M},m'}(\mathbf{F}). \quad (5.3)$$

We can conclude by induction over n that

$$\mathbf{F}'(m_1, \dots, m_n) \subset \mathbf{F}'(m'_1, \dots, m'_n). \quad \square$$

5.1.2 Induced margin

The *induced margin* measures the impact of multiple demanded margins on an effective margin.

Definition 5.1.2 (Induced margin). *Let m_1, \dots, m_n be n positive nonnegative margins associated to the models of margins $\mathbf{M}_1, \dots, \mathbf{M}_n$, let \mathbf{F} be a failure set. The induced margin on the model of margin \mathbf{M} is the difference between the effective margin in \mathbf{M} with the n demanded margins and without the n demanded margins*

$$\text{indM}_{\mathbf{M}}(u, m_1, \dots, m_n) = \text{em}_{\mathbf{M}}(u, \mathbf{F}'(0, \dots, 0)) - \text{em}_{\mathbf{M}}(u, \mathbf{F}'(m_1, \dots, m_n))$$

and is defined for each design u verifying $|\text{em}_{\mathbf{M}}(u, \mathbf{F}'(0, \dots, 0))| < +\infty$.

The induced margin is nonnegative and is an increasing function of the demanded margins, as shown in Proposition 5.1.3.

Proposition 5.1.3 (Monotonicity of the induced margin). *Let $u \in \mathcal{C}$, (m_1, \dots, m_n) and (m'_1, \dots, m'_n) be two vectors of \mathbb{R}_+^n such that $m_i \leq m'_i$ for all $i \in \llbracket 1, n \rrbracket$. Then*

$$0 \leq \text{indM}(u, m_1, \dots, m_n) \leq \text{indM}(u, m'_1, \dots, m'_n).$$

Proof. As stated previously, if $u \in \mathcal{C}$ and $\mathbf{F} \subset \mathbf{F}'$ then $\text{em}_{\mathbf{M}}(u, \mathbf{F}) \geq \text{em}_{\mathbf{M}}(u, \mathbf{F}')$. Proposition 5.1.1 ensures that

$$\mathbf{F}'(0, \dots, 0) \subset \mathbf{F}'(m_1, \dots, m_n) \subset \mathbf{F}'(m'_1, \dots, m'_n).$$

Thus

$$\text{em}_{\mathbf{M}}(u, \mathbf{F}'(0, \dots, 0)) \geq \text{em}_{\mathbf{M}}(u, \mathbf{F}'(m_1, \dots, m_n)) \geq \text{em}_{\mathbf{M}}(u, \mathbf{F}'(m'_1, \dots, m'_n))$$

and then

$$0 \leq \text{indM}_{\mathbf{M}}(u, m_1, \dots, m_n) \leq \text{indM}_{\mathbf{M}}(u, m'_1, \dots, m'_n). \quad \square$$

Let us consider the unidimensional case $u \in \mathbb{R}$, with an upper bound $\mathbf{F} = [u_{\text{req}}, +\infty)$ and an increasing model of margin \mathbf{M} . The induced margin on u measured by \mathbf{M} due to a demanded margin $m > 0$ with model of margin \mathbf{M} is m

$$\begin{aligned} \text{indM}_{\mathbf{M}}(u, m) &= \text{em}_{\mathbf{M}}(u, [u_{\text{req}}, +\infty)) - \text{em}_{\mathbf{M}}(u, \mathbf{dm}_{\mathbf{M},m}([u_{\text{req}}, +\infty))) \\ &= \text{em}_{\mathbf{M}}(u, [u_{\text{req}}, +\infty)) - \text{em}_{\mathbf{M}}(u, [u_{\text{req}} - m, +\infty)) \\ &= u_{\text{req}} - u - (u_{\text{req}} - m - u) \\ &= m. \end{aligned}$$

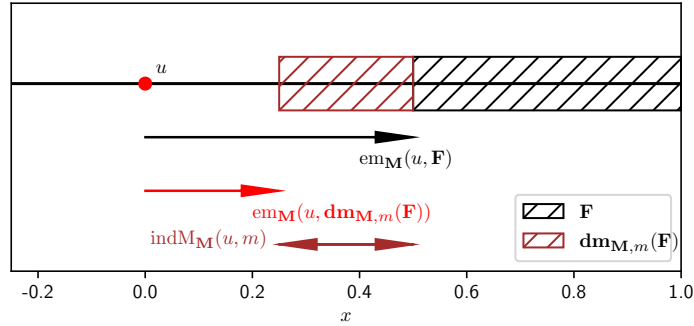


Figure 5.1: Induced margin in the one dimensional case, where $indM_M(u, m) = m = 0.25$.

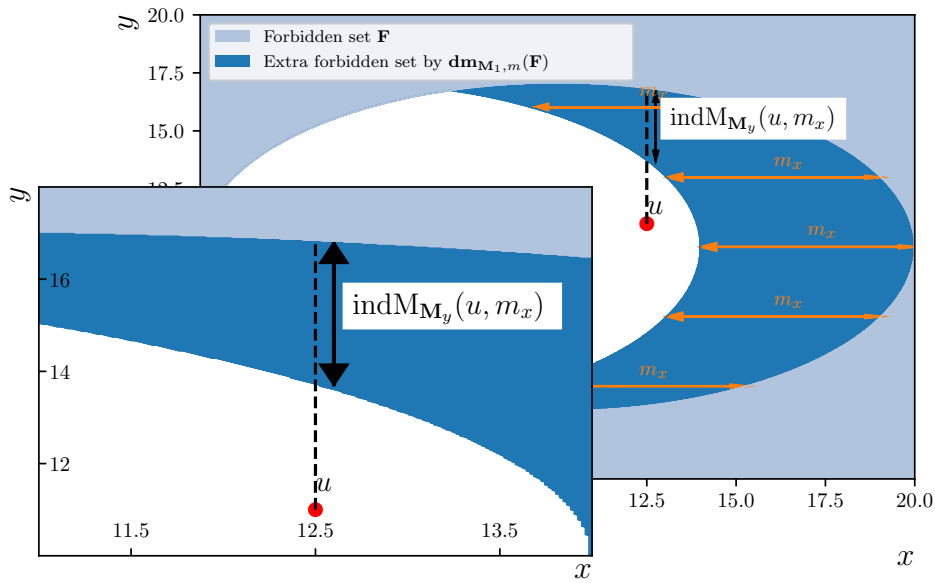


Figure 5.2: When $u = (x, y)$, we can compute the induced margin on y due to taking a margin on x . The effective margin is computed with an increasing model of margin M_y in y and the demanded margin is a increasing model of margin M_x in x .

The induced margin is illustrated for a one-dimensional case in Figure 5.1 and for a two-dimensional case in Figure 5.2.

We can interpret the induced margin in two ways:

- It measures a kind of demanded margins in \mathbf{M} to cover an uncertainty.
If the demanded margins m_1, \dots, m_n are taken to cover the uncertainty A , then the induced margin $\text{indM}_{\mathbf{M}}$ is the expression of the margin in \mathbf{M} that is used to mitigate A .
- It measures the effective margin in \mathbf{M} that is consumed by the demanded margins m_1, \dots, m_n .
If two kinds of uncertainty A (e.g statistical uncertainty) and B (e.g modeling uncertainty) are identified and the demanded margins m_1, \dots, m_n cover the uncertainty A , then the induced margin measure the loss of effective margin in \mathbf{M} that could possibly be used to cover B .

5.1.3 Induced cost

In this section, we define some settings in which the *induced cost*, *i.e.* the cost of the demanded margins, can be defined.

We assume that the design can be described by some variables that are fixed during the analysis $x = (x_1, \dots, x_n)$ and some variables that can be chosen to optimize the design $y = (y_1, \dots, y_m)$. The state space writes $\mathbf{E} = \prod_{i=1}^n E_{x_i} \times \prod_{j=1}^m E_{y_j}$ with possibly $n = 0$ or $m = 0$. As usual, we denote by \mathcal{C} the set of the problem constraints and $\mathbf{F} \subset \mathcal{C}$ the forbidden set. For $x \in \prod_{i=1}^n E_{x_i}$, we assume that the cost of a design can be computed as

$$\begin{aligned} \text{cost}(x, \mathbf{F}) &= \inf c(x, y) \\ & y \in \mathcal{H}_x \\ & (x, y) \in \mathcal{C} \setminus \mathbf{F} \end{aligned}$$

with \mathcal{H}_x being the optimization space, that depends possibly on x . The cost is not necessarily a monetary cost but can model other parameters such as the mass of the system, the power consumed, the number of days of work, etc. An immediate property is that a wider forbidden set restricts the optimization space and thus increases the cost, *i.e.* if $\mathbf{F} \subset \mathbf{F}'$ then

$$\text{cost}(x, \mathbf{F}') \geq \text{cost}(x, \mathbf{F}).$$

The *induced cost* monitors this inflation with respect to the demanded margins.

Definition 5.1.4 (Induced cost). *Let m_1, \dots, m_n be n nonnegative demanded margins associated to the models of margin $\mathbf{M}_1, \dots, \mathbf{M}_n$ and let \mathbf{F} be a forbidden set. The induced cost is the difference between the cost with margins and the cost without margins*

$$\text{indC}(x, m_1, \dots, m_n) = \text{cost}(x, \mathbf{F}'(m_1, \dots, m_n)) - \text{cost}(x, \mathbf{F}'(0, \dots, 0)).$$

Similarly to the induced margin, the induced cost also verifies a nonnegativity and monotonicity property.

Proposition 5.1.5 (Monotonicity of the induced cost). *Let (m_1, \dots, m_n) and (m'_1, \dots, m'_n) be two vectors of \mathbb{R}_+^n such that $m_i \leq m'_i$ for all $i \in \llbracket 1, n \rrbracket$. Then*

$$0 \leq \text{indC}(x, m_1, \dots, m_n) \leq \text{indC}(x, m'_1, \dots, m'_n).$$

Proof. Proposition 5.1.1 us that $\mathbf{F}'(m_1, \dots, m_n) \subset \mathbf{F}'(m'_1, \dots, m'_n)$. We conclude using the fact that a wider forbidden set increases the cost. \square

The induced cost function matches our intuition in the sense that greater margins increase the cost.

Induced loss of performance It is possible to model an induced loss of performance, by replacing the cost c by the opposite of a performance measure $-p$. In that case, the induced function is nonpositive and represents the loss of performance due to demanded margins.

Use case, part 7. In the use case, the state space is decomposed as $W_{\max} \in E_{y_1} = \mathbb{R}_+$ and $(W, \kappa, F) \in E_{x_1} \times E_{x_2} \times E_{x_3} = \mathbb{R}_+^3$ and the cost is W_{\max} . Engineers must provide the smallest value of W_{\max} that has a certain confidence level and consequently, they transmit W_{\max}^* , that is the minimum value under constraints with margins

$$\begin{aligned} W_{\max}^* = \text{cost}((\hat{\kappa}, F_{\text{nom}}), \mathbf{F}'(m_\kappa, m_F)) &= \inf W_{\max} \\ W &= f(\hat{\kappa}, F_{\text{nom}}) \\ (W_{\max}, W, \hat{\kappa}, F_{\text{nom}}) &\notin \mathbf{F}'(m_\kappa, m_F) \end{aligned}$$

with $m_F = \beta_F - 1$, $\mathbf{F}'(m_\kappa, m_F) = \mathbf{dm}_{\mathbf{M}_\kappa, m_\kappa}(\mathbf{dm}_{\mathbf{M}_F, m_F}(\mathbf{F}))$ being the failure set with margins and \mathbf{F} is defined in Use case, part 2. We have . The induced cost

$$\text{indC}((\hat{\kappa}, F_{\text{nom}}), m_\kappa, m_F) = \text{cost}((\hat{\kappa}, F_{\text{nom}}), \mathbf{F}'(m_\kappa, m_F)) - \text{cost}((\hat{\kappa}, F_{\text{nom}}), \mathbf{F}'(0, 0)).$$

is plotted in Figure 5.3.

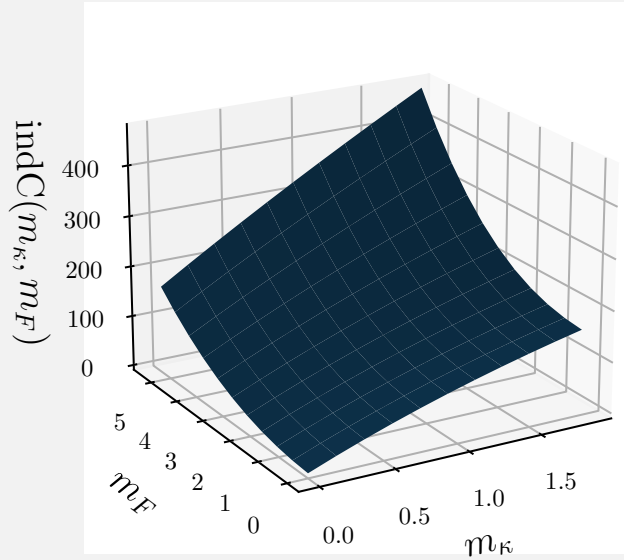


Figure 5.3: Graph of the induced cost $m_\kappa, m_F \mapsto \text{indC}(m_\kappa, m_F)$.

5.2 Margin sensitivity analysis

5.2.1 Induced function

In this section, we are considering an induced cost for a fixed point $x \in E_x$ or an induced margin for a fixed design $u \in \mathcal{E}$. The goal is to identify where the demanded margins should be decreased. We start with some initial values of demanded margins, denoted by

$$(\bar{m}_1, \dots, \bar{m}_n) \in \mathbb{R}_+^n$$

and for some lower values of demanded margins $(m_1, \dots, m_n) \in [0, \bar{m}_1] \times \dots \times [0, \bar{m}_n]$, we study the *induced function*

$$\text{indF}(m_1, \dots, m_n) = \begin{cases} \text{indC}(x, m_1, \dots, m_n) & \text{for an induced cost,} \\ \text{indM}_{\mathbf{M}}(u, m_1, \dots, m_n) & \text{for an induced margin,} \end{cases}$$

that is *nonnegative* and *nondecreasing*. We seek to characterize the gain in cost or in effective margin when each m_i goes from \bar{m}_i to 0.

5.2.2 Local sensitivity analysis

If indF is differentiable at the point $(\bar{m}_1, \dots, \bar{m}_n)$, the Taylor expansion provides the approximation

$$\text{indF}(m_1, \dots, m_n) \simeq \text{indF}(\bar{m}_1, \dots, \bar{m}_n) - \sum_{i=1}^n (\bar{m}_i - m_i) \frac{\partial \text{indF}}{\partial m_i}(\bar{m}_1, \dots, \bar{m}_n),$$

so that the induced value is approximated by

$$\text{indF}(\bar{m}_1, \dots, \bar{m}_n) \simeq \sum_{i=1}^n \bar{m}_i \frac{\partial \text{indF}}{\partial m_i}(\bar{m}_1, \dots, \bar{m}_n).$$

By the monotonicity of indF , the quantity $\bar{m}_i \frac{\partial \text{indF}}{\partial m_i}(\bar{m}_1, \dots, \bar{m}_n)$ is nonnegative. When indF has variations that are almost linear, it quantifies the contribution of the margin \bar{m}_i to the induced cost/margin under a first-order approximation.

Definition 5.2.1. Let $(\mathbf{M}_1, \bar{m}_1), \dots, (\mathbf{M}_n, \bar{m}_n)$ be n pairs of model of margin/demanded margin and indF an induced cost parametrized by m_1, \dots, m_n . The local sensitivity index with respect to the variable $i \in \llbracket 1, n \rrbracket$ is

$$\mathcal{D}_i = \bar{m}_i \frac{\partial \text{indF}}{\partial m_i}(\bar{m}_1, \dots, \bar{m}_n)$$

and the relative local sensitivity index is

$$\tilde{\mathcal{D}}_i = \frac{\mathcal{D}_i}{\sum_{j=1}^n \mathcal{D}_j} \in [0, 1].$$

Use case, part 8. In order to quantify the impact of the margins on κ and F , the engineers compute the local sensitivity indices. Their expression are

$$\mathcal{D}_\kappa = m_\kappa \frac{\partial \text{indC}}{\partial \kappa}(\hat{\kappa} + m_\kappa, \beta_F F_{\text{nom}})$$

and

$$\mathcal{D}_F = (\beta_F - 1) \frac{\partial \text{indC}}{\partial F}(\hat{\kappa} + m_\kappa, \beta_F F_{\text{nom}}).$$

The normalized values are plotted in Figure 5.4.

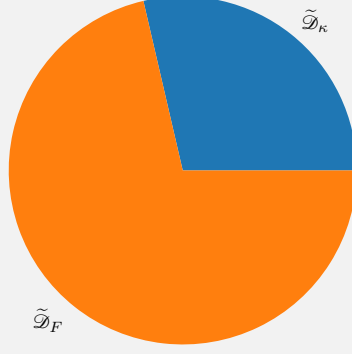


Figure 5.4: Local decomposition of the induced cost on W_{\max}

If the cost function is actually linear, the induced function can be decomposed as

$$\text{indF}(\bar{m}_1, \dots, \bar{m}_n) = \sum_{i=1}^n \mathcal{D}_i, \quad (5.4)$$

motivating the expression of the indices.

Remark 5.2.2. *The local sensitivity indices that we propose are close from the Sigma-Normalized derivatives from the Sensitivity Analysis literature [100]*

$$S_i = \sigma_i \frac{\partial \text{indF}}{\partial m_i}(\bar{m}_1, \dots, \bar{m}_n),$$

but the demanded margin \bar{m}_i takes the role of the standard deviation σ_i of the variable i . This similarity is due to the fact that a demanded margin \bar{m}_i is chosen to cover the extent of the uncertainty in a model with margins and σ_i actually measures the extent of the uncertainty in a probabilistic model. They then play a similar role in two different models. When the margin quantification is done with a statistical model and the variable i is Gaussian, the demanded margin m_i is actually proportional to σ_i , up to a factor depending on the level of confidence.

5.2.3 Global sensitivity analysis along a margin reduction path

The local sensitivity analysis provides a good approximation when the induced function has quasi linear variations. When it is not the case, we propose a global sensitivity analysis that take into account the variations in all the domain. We now assume that indF is continuously differentiable

on $[0, \bar{m}_1] \times \dots \times [0, \bar{m}_n]$ and we want to quantify each impact through a decomposition of the form

$$\text{indF}(\bar{m}_1, \dots, \bar{m}_n) = \sum_{i=1}^n S_i$$

with each S_i measuring the impact of the margin \bar{m}_i on indF .

Global sensitivity decomposition on a linear path For each variable $i \in \llbracket 1, n \rrbracket$, we define a linear path function

$$\mathcal{L}_i(t) = (1-t)\bar{m}_i, \quad t \in [0, 1],$$

with t being called the path parameter. Using the chain rule, we can differentiate the function

$$\frac{d}{dt} \text{indF}(\mathcal{L}_1(t), \dots, \mathcal{L}_n(t)) = - \sum_{i=1}^n \bar{m}_i \frac{\partial \text{indF}}{\partial m_i}((1-t)\bar{m}_1, \dots, (1-t)\bar{m}_n)$$

and remark that, similarly to the local decomposition, the infinitesimal decrease of indF can be decomposed in n infinitesimal decreases $-\bar{m}_i \frac{\partial \text{indF}}{\partial m_i}(t\bar{m}_1, \dots, t\bar{m}_n)dt$, each measuring the impact of the margin i . By integrating from $t = 0$ to $t = 1$, we get

$$\begin{aligned} \int_0^1 -\frac{d}{dt} \text{indF}(\mathcal{L}_1(t), \dots, \mathcal{L}_n(t)) dt &= \text{indF}(\bar{m}_1, \dots, \bar{m}_n) \\ &= \sum_{i=1}^n \int_0^1 \bar{m}_i \frac{\partial \text{indF}}{\partial m_i}((1-t)\bar{m}_1, \dots, (1-t)\bar{m}_n) dt. \end{aligned}$$

The global sensitivity index on a linear path of the variable i is defined as

$$S_i^{\mathcal{L}} = \int_0^1 \bar{m}_i \frac{\partial \text{indF}}{\partial m_i}((1-t)\bar{m}_1, \dots, (1-t)\bar{m}_n) dt,$$

and $\text{indF}(\bar{m}_1, \dots, \bar{m}_n)$ can be decomposed as the sum of each individual impact

$$\text{indF}(\bar{m}_1, \dots, \bar{m}_n) = \sum_{i=1}^n S_i^{\mathcal{L}}. \quad (5.5)$$

These indices can be seen as the generalization of the local sensitivity indices for nonlinear induced functions. Proposition 5.2.3 shows the relevance of this expression, by stating that in the case where all demanded margins m_i have a separate impact on the induced function, the sensitivity indices capture exactly each of these impacts.

Proposition 5.2.3. *If the induced function is the sum of n separate univariate functions*

$$\text{indF}(m_1, \dots, m_n) = \sum_{i=1}^n f_i(m_i)$$

then the sensitivity index for the margin m_i is

$$S_i^{\mathcal{L}} = f_i(\bar{m}_i).$$

In particular, if f_i is linear, then $S_i^{\mathcal{L}} = \mathcal{D}_i$.

Proof. It is a direct consequence of the linearity of the differentiation/integration. □

Use case, part 9. Engineers now compute the global decomposition on the linear path

$$S_{\kappa}^{\mathcal{L}} = m_{\kappa} \int_0^1 \frac{\partial \text{indC}(tm_{\kappa}, t(\beta_F - 1))}{\partial m_{\kappa}} dt$$

and

$$S_F^{\mathcal{L}} = (\beta_F - 1) \int_0^1 \frac{\partial \text{indC}(tm_{\kappa}, t(\beta_F - 1))}{\partial m_F} dt,$$

the result is drawn in Figure 5.5. They remark that the variable κ has a greater importance in the global decomposition than in the local decomposition of Figure 5.4. As a conclusion, if they want to reduce the induced cost on W_{\max} they should focus on reducing margin on F_{nom} first.

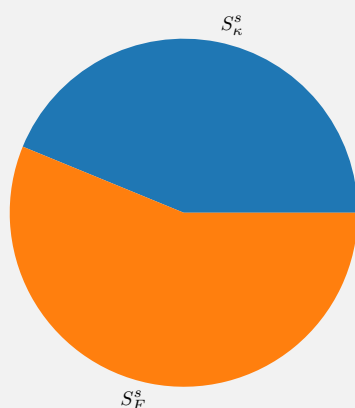


Figure 5.5: Global decomposition on a linear path of the induced cost on W_{\max}

Global decomposition on a general margin reduction path So far, the global sensitivity indices were computed by imposing that each demanded margin is an affine function of $t : (1 - t)\bar{m}_i$. This linear decrease contains the implicit assumption that, if the demanded margin were reduced, each margin would decrease at the same rate (in proportion).

It is however possible to choose other paths, that take the value \bar{m}_i at $t = 0$ and 0 at $t = 1$, so that the decomposition of Equation 5.5 still holds. For instance, one might want to compute the decomposition when the first margin m_1 vanishes and the others remain the same, then the margin m_2 vanishes and the others remain the same, etc... In general, these paths are called *margin reduction paths*.

Definition 5.2.4 (Margin reduction path). Let $(\bar{m}_1, \dots, \bar{m}_n) \in \mathbb{R}_+^n$ be n positive real numbers, representing demanded margins. A margin reduction path is a function

$$s : [0, 1] \rightarrow \mathbb{R}_+^n \\ t \mapsto (s_1(t), \dots, s_n(t))$$

such that

- (i) s is absolutely continuous;
- (ii) $s(0) = (\bar{m}_1, \dots, \bar{m}_n)$;
- (iii) $s(1) = (0, \dots, 0)$;
- (iv) For all $i \in \llbracket 1, n \rrbracket$, $s_i(t)$ is nonincreasing.

We can now provide the general definition of a global sensitivity index.

Definition 5.2.5 (Global sensitivity index). *Let s be a margin reduction path, the global sensitivity index of the demanded margin m_i along the path s is*

$$S_i^s = \int_0^1 -s'_i(t) \frac{\partial \text{indF}}{\partial m_i}(s_1(t), \dots, s_n(t)) dt \quad (5.6)$$

and the relative global sensitivity index is

$$\tilde{S}_i^s = \frac{S_i^s}{\sum_{j=1}^n S_j^s}.$$

For any margin reduction path, the induced function can be decomposed

$$\text{indF}(\bar{m}_1, \dots, \bar{m}_n) = \sum_{i=1}^n S_i^s$$

and the indices are always nonnegative. However, for two different paths s and s' , the equality of the indices is not guaranteed in general:

$$S_i^s \neq S_i^{s'},$$

except in two noticeable cases. The first one is when indF is the sum of univariate functions, in which case the global sensitivity index does not depend on the choice of the path.

Proposition 5.2.6. *Proposition 5.2.3 holds for any reduction path s .*

Proof. It is a consequence of the linearity of the differentiation and integration. \square

The second case is when s' is a reparametrization of s by a continuously differentiable function.

Proposition 5.2.7. *Let $r : [0, 1] \mapsto [0, 1]$ be a nondecreasing C^1 function such that $r(0) = 0$ and $r(1) = 1$. Then, for $i \in \llbracket 1, n \rrbracket$, we have*

$$S_i^s = S_i^{s \circ r},$$

Proof. Differentiating the i -th component of $s \circ r$ gives the expression $(s \circ r)'_i = r'(s'_i \circ r)$. The i -th sensitivity index along the path $s \circ r$ is then

$$\begin{aligned} S_i^{s \circ r} &= \int_0^1 r'(t) s'_i(r(t)) \frac{\partial \text{indF}}{\partial m_i}(s_1(r(t)), \dots, s_n(r(t))) dt \\ &= \int_0^1 s'_i(t^*) \frac{\partial \text{indF}}{\partial m_i}(s_1(t^*), \dots, s_n(t^*)) dt^* \\ &= S_i^s, \end{aligned}$$

with the change of variable $t^* = r(t)$. \square

This proposition shows that the sensitivity indices depend only on the 1-dimensional curve $\{(s_1(t), \dots, s_n(t)), t \in \llbracket 0, 1 \rrbracket\}$, that is embedded in an \mathbb{R}^n -dimensional space. Thus, the variable t plays only the role of a convenient parametrization.

Remark 5.2.8. *The global sensitivity indices that we propose are similar to the derivative-based sensitivity measure, introduced in [73]*

$$w_{(i)} = \int_{[0, m_1] \times \dots \times [0, m_n]} \frac{\partial f}{\partial x_i}(x_1, \dots, x_n) dx_1 \dots dx_n. \quad (5.7)$$

In our context, we exploit the particular form of the cost function f and integrate only on a sub path of $[0, m_1] \times \dots \times [0, m_n]$ so that we can achieve an exact decomposition of the cost that is not possible with those from Equation (5.7).

Representation of the decomposition Let s be a margin reduction path, and $0 < t_a < t_b < 1$ be two values of the path parameter. Let us remark that we can define the sensitivity indices between t_a and t_b such that

$$\begin{aligned} \text{indF}(m_{1,b}, \dots, m_{n,b}) - \text{indF}(m_{1,a}, \dots, m_{n,a}) &= \sum_{i=1}^n \int_a^b -s'(t) \frac{\partial \text{indM}}{\partial m_i}(s_1(t), \dots, s_n(t)) dt \\ &= \sum_{i=1}^n S_i^{t_a, t_b, s}, \end{aligned}$$

with $m_{i,a} = s_i(t_a)$ and $m_{i,b} = s_i(t_b)$. In other terms, each difference of the form $\text{indF}(m_{1,b}, \dots, m_{n,b}) - \text{indF}(m_{1,a}, \dots, m_{n,a})$ can be decomposed in terms of sensitivity indices, and not only the difference $\text{indF}(\bar{m}_1, \dots, \bar{m}_n) - \text{indF}(0, \dots, 0)$, that was studied above. By rewriting

$$\text{indF}(m_{1,b}, \dots, m_{n,b}) - \text{indF}(m_{1,a}, \dots, m_{n,a}) = 1 \cdot (\text{indF}(m_{1,b}, \dots, m_{n,b}) - \text{indF}(m_{1,a}, \dots, m_{n,a}))$$

one can grasp the intuition that the surface of the rectangle of length

$$(\text{indF}(m_{1,b}, \dots, m_{n,b}) - \text{indF}(m_{1,a}, \dots, m_{n,a}))$$

and width 1 can be partitioned into n surfaces of area $S_i^{t_a, t_b, s}$, $i \in \llbracket 1, n \rrbracket$ and can thus be naturally represented graphically in a similar way as Figure 5.6.

In order to draw this decomposition, one must choose a discretization step $0 < \delta t < 1$ and, for each $N \in \llbracket 0, \lfloor 1/\delta t \rfloor \rrbracket$, compute the decomposition of the induced function between $N\delta t$ and $(N+1)\delta t$.

$$\text{indF}(m_{1, (N+1)\delta t}, \dots, m_{n, (N+1)\delta t}) - \text{indF}(m_{1, N\delta t}, \dots, m_{n, N\delta t}) = \sum_{i=1}^n S_i^{N\delta t, (N+1)\delta t, s}$$

Then, the rectangle between the abscissa $\text{indF}(m_{1, N\delta t}, \dots, m_{n, N\delta t})$ and $\text{indF}(m_{1, (N+1)\delta t}, \dots, m_{n, (N+1)\delta t})$ and the ordinate 0 and 1 is partitioned into n surfaces by giving a area $S_i^{N\delta t, (N+1)\delta t, s}$ to the variable $i \in \llbracket 1, n \rrbracket$.

Use case, part 10. The engineers follow this visualization method to decompose the induced cost as a partition of a rectangle and obtain Figure 5.6. The total area of the orange surface is equal to the global sensitivity index $S_{\kappa}^{\mathcal{L}}$ and the area of the blue surface is equal to $S_F^{\mathcal{L}}$. They can see that when they want to reduce the induced cost, the variable F will be the main contributor to the decrease from 500 to 150 and then κ will contribute the most.

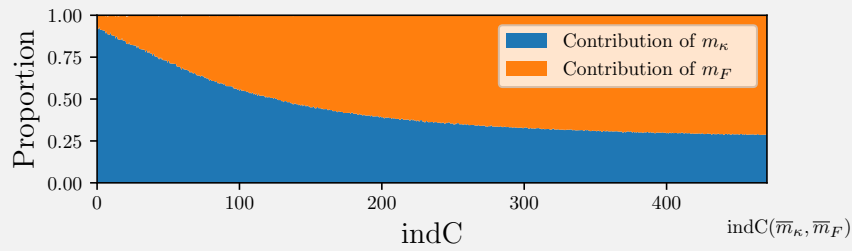


Figure 5.6: Decomposition of the induced cost on W_{\max} with respect to the demanded margins m_{κ} and m_F . The induced cost is in abscissa and the proportion in the ordinate.

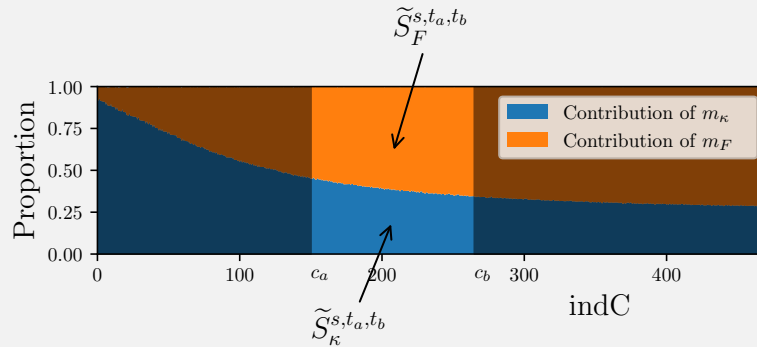


Figure 5.7: The value of the sensitivity index between two induced cost c_a and c_b is the area of each surface between the two costs.

5.3 Mechanisms of margin reduction

Modeling the margins and performing a sensitivity analysis on the induced costs permits to highlight where the impactful demanded margins are. Once this step is done, there remains to know how to remove the margins. We propose three approaches.

5.3.1 Improve the maturity of margin quantification

The margin quantification, in engineering practices, takes a variety of forms, leading to more or less precise results. For instance, sometimes the forbidden set is not known, or only the order of magnitude of the demanded margin is known. By precisising the link between the uncertainty and the demanded margin in the margin quantification phase, the demanded margins could possibly greatly decrease and approach more sharply the safety or reliability goal.

Let us take the example of Civil engineering as an illustration. In *De architectura* [93], the earliest known treatise of civil engineering, Vitruvius declares about building a wall that “in the course of time, the mortar has lost its strength [...] and so the monuments are tumbling down and going to pieces [...]. He who wishes to avoid such a disaster should leave a cavity behind the facings, and on the inside build walls **two feet** thick [...]”. This value of two feet includes a demanded margin, taken to cover the risk of failure over time. However, the choice is not based on a model, but purely on experience; one has no clue *a priori* of how far the chosen two feet are from the forbidden set, and even the very definition of the forbidden set is quite nebulous in this context. There *is* a demanded margin in those two feet, but it is not possible to know how much.

In modern approaches, models from continuum mechanics provide a quantitative approximation of where the failure happens. Some safety factors β_1, \dots, β_n , that increase the constraint or decrease the resistance (Section 3.1.4), are taken to cover the uncertainty. In that case, the thickness of a wall is chosen using an approximated mechanical model, knowing that the margin to the real failure set is of order of magnitude β_1, \dots, β_n .

Last, when the failure of multiple walls has been observed, along with the external conditions, probabilistic models coupled with continuum mechanics models can be constructed. One can then link the demanded margin to the probability of failure. The demanded margins are chosen in order to satisfy an acceptable probability of failure.

The margin quantifications of the three examples above show a different degree of maturity (illustrated in Figure 5.8). As a rule of thumb, if one assumes that the design already satisfies a safety goal, the more precise the margin quantification is, the smaller the margin can be. It is explained by the fact that a part of the uncertainty *in the modeling* is reduced and thus the margins can be decreased. Some measures that can be made in terms of model to improve the margin maturity are:

- Constructing a failure set that better represents the safety goals;
- Have a more precise simulation of the behaviour;
- Identify the level of risk that would be considered as acceptable;
- Model more precisely the uncertainties, in a quantitative way.

Even if these measures may read as an engineering triviality in the sense that “a better model would lead to a better fitted design”, one must keep in mind that in a margin sensitivity context, they need to be applied only where the impactful margins are identified. Thus, this effort shall not be made on the whole system, but only where substantial potential gains are identified.

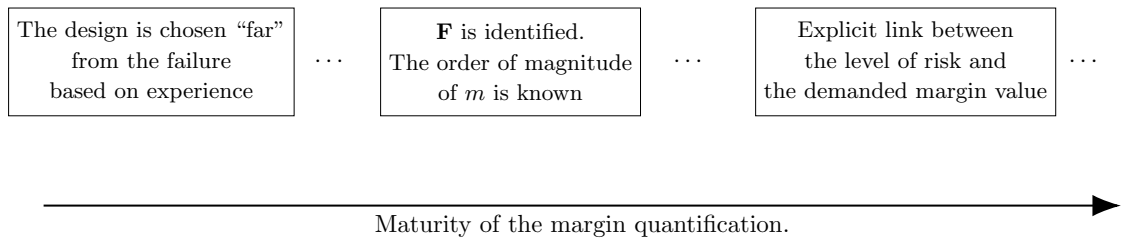


Figure 5.8: The variety of engineering approaches leads to different maturity in terms of margin quantification.

5.3.2 Update the reducible uncertainties

As margins are used to cover some uncertainties, if the uncertainties are *reducible*, the associated margins can be lowered when uncertainties are actually reduced. Sometimes, the uncertainties can be reduced by an active action; it can be done for instance by

- Providing a better model for the uncertainties.
One could think of the civil engineering example, in which the earliest partial factor were demanded margins quantified by the experience and had an high value. Then, engineers proposed a probabilistic modeling that permitted to reduce the margin for a vast range of cases;
- Reducing the statistical uncertainties, by drawing more observations of the quantity of interest;
- Reducing the numerical errors with more trusted model and simulation for the phenomenon.

In other cases, uncertainties just vanish by themselves, as the design gains in maturity. It happens for instance when the demanded margins are some room for manoeuvre because a quantity was not yet fixed. When it is actually chosen - for instance when the supplier gives of a component with known characteristics - these margins have no more reason to exists. They can just be removed.

5.3.3 Perform a mutual quantification of margins

Another way to reduce margins is to take into account the correlation between the underlying uncertainties. In substance, two demanded margins that were quantified separately cannot model the correlation between the uncertainty they cover. As a consequence, it may result in an unrealistic worst-case design. The application of Chapter 6 illustrates one specific aspect of such a worst case and the core idea can be understood from Example 5.3.1.

Example 5.3.1. *The goal of the design problem is to choose the minimum value of the resistance $R^* \in \mathbb{R}$ such that R^* is greater than the stress $S(Y_1, Y_2)$ for all the possible values of the random variables Y_1 and Y_2 . The margin quantification phase would consist in identifying the range of variation for each variable Y_1 and Y_2 . In practice, two nominal values would be chosen $(y_1^*, y_2^*) \in \mathbb{R}^2$ along with four directional increasing and decreasing margins $(m_{1,-}, m_{1,+}, m_{2,-}, m_{2,+}) \in \mathbb{R}^4$ so that*

$$Y_1 \in [y_1^* - m_{1,-}, y_1^* + m_{1,+}] \text{ and } Y_2 \in [y_2^* - m_{2,-}, y_2^* + m_{2,+}]$$

almost surely. Finally, the resistance is calculated as

$$\begin{aligned} R_{\text{marg}}^* &= \max S(y_1, y_2) \\ y_1 &\in [y_1^* - m_{1,-}, y_1^* + m_{1,+}] \\ y_2 &\in [y_2^* - m_{2,-}, y_2^* + m_{2,+}]. \end{aligned}$$

Now, let us assume that the randomness of Y_1 and Y_2 come from the same source, $Y_1 = g_1(X)$ and $Y_2 = g_2(X)$ with X a uniform random variable $\mathcal{U}([x_-, x_+])$.

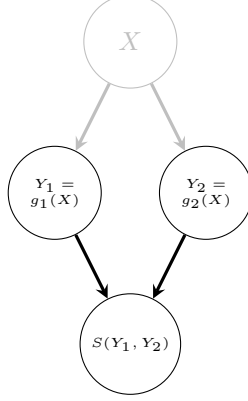


Figure 5.9: Diamond workflow leading to the worst-case approach in design with margins, when the dependency of Y_1 and Y_2 on X are forgotten.

In that case, the maximum required resistance can be refined as

$$\begin{aligned} R_{\text{des}}^* &= \max S(g_1(x), g_2(x)) \\ x &\in [x_-, x_+]. \end{aligned}$$

As the margin quantification implies $g_1([x_-, x_+]) \subset [y_1^* - m_{1,-}, y_1^* + m_{1,+}]$ and $g_2([x_-, x_+]) \subset [y_2^* - m_{2,-}, y_2^* + m_{2,+}]$, the choice with margins taken separately is always greater than the choice with the correlations,

$$R_{\text{des}}^* \leq R_{\text{marg}}^*,$$

the inequality being strict most of the time. In other terms, the choice taking the correlations into account permits to have a more precise estimate than sole margin approach.

For instance, if we take

$$\begin{aligned} R(y_1, y_2) &= y_1 + y_2 \\ y_1 = g_1(x) &= 2x \\ y_2 = g_2(x) &= -x \end{aligned}$$

the values are $R_{\text{marg}}^* = 2x_+ - x_-$ and $R_{\text{des}}^* = x_+$. The overdesign, in terms of resistance R is equal to $R_{\text{marg}}^* - R_{\text{des}}^* = x_+ - x_- > 0$.

In order to formalize this example, let us consider a problem description (E, \mathcal{C}) and a forbidden set \mathbf{F} . We assume that n risks R_1, \dots, R_n must be covered by n models of margin $\mathbf{M}_1, \dots, \mathbf{M}_n$, such that \mathbf{M}_i is defined to cover R_i at a level α_i . We can identify two ways to quantify margins.

Sequential quantification

- The demanded margin m_1 is chosen to cover R_1 at the level α_1 for \mathbf{F} , resulting in the forbidden set $\mathbf{F}'_1 = \mathbf{dm}_{M_1, m_1}(\mathbf{F})$.
- The demanded margin m_2 is chosen to cover R_2 at the level α_2 for \mathbf{F}'_1 , resulting in the forbidden set $\mathbf{F}'_2 = \mathbf{dm}_{M_2, m_2}(\mathbf{F}'_1)$.
- ⋮
- The demanded margin m_n is chosen to cover R_n at the level α_n for \mathbf{F}'_{n-1} , resulting in the forbidden set $\mathbf{F}'_n = \mathbf{dm}_{M_n, m_n}(\mathbf{F}'_{n-1})$.

We rename $\mathbf{F}'_{\text{seq}} = \mathbf{F}'_n$. This sequential quantification represents a multidisciplinary context. When multiple engineering disciplines must interact together, each one often takes its margins to cover its own risks and communicates their possible designs (*i.e.* failure sets) with no information on the risks covered.

Mutual quantification The risks R_1, \dots, R_n are assessed together and a new forbidden set \mathbf{F}'_{mut} is chosen to cover them at the levels $\alpha_1, \dots, \alpha_n$ (see Example 5.3.3, for instance).

From a modeling point of view, the mutual quantification represents a complete communication of the uncertainties between all stakeholders in a multidisciplinary context.

Principle 5.3.2 (Sequential versus mutual quantification). *If \mathbf{F}'_{mut} and \mathbf{F}'_{seq} are chosen to cover the same risks R_1, \dots, R_n at the levels $\alpha_1, \dots, \alpha_n$, we have, in general*

$$\mathbf{A}'_{\text{seq}} \subset \mathbf{A}'_{\text{mut}}.$$

In other terms, for the same reliability/safety target, the sequential quantification is more conservative than the mutual quantification and the sequential quantification has a tendency to forbid designs based on unrealistic constraints.

The non optimality of the sequential quantification is due to two characteristics.

- The correlation are not taken into account.
- The demanded region is often a rectangular box.

The demanded region is the area around a design that must be included in the acceptance set in order for the design to be acceptable, due to the demanded margins. The mutual quantification must focus on these two aspects to find a better \mathbf{F}'_{mut} . Chapter 6 establishes that, when two risks are mutually exclusive, it is sufficient to take the intersection of the failure set with demanded margin, instead of composing the demanded margin operators. The safe region around the design point is not a box anymore but permits to choose a more efficient design. In Example 5.3.1, an efficient forbidden set cannot result from demanded margins on y_1 and y_2 taken separately; the shape must take their correlation into account. In Example 5.3.3, only focusing on the correlation and not on the shape of reduction still permits to reduce the impact of the margins.

Last, we must acknowledge that this principle is based on an intuition built upon particular cases. Finding a rigorous and precise definition of the mutual margin quantification and proving its optimality is one of the main perspectives of development for this framework.

Example 5.3.3 (Sum of two Gaussian variables). *In this stress-resistance problem, the state space \mathbf{E} is composed by two stress variables $(s_1, s_2) \in \mathbb{R}_+$ and a resistance variable $r \in \mathbb{R}_+$ and there are no problem constraints $\mathcal{C} = \mathbb{R}_+^3$. The failure happens when the resistance is lower than the sum of the two stresses*

$$\mathbf{F} = \{r < s_1 + s_2\}.$$

Two design values for the stress \hat{s}_1 and \hat{s}_2 are estimated, but are uncertain. The differences between the estimated and the true values $s_{1,0}$ and $s_{2,0}$ are centered independent normal random variables G_1 and G_2 of variance σ_1^2 and σ_2^2 . The goal is to choose the lowest r that does not fail, with a probability of $1 - \alpha$.

Sequential quantification *Let us consider the case where the discipline v_1 is in charge of s_1 and the discipline v_2 is in charge of s_2 . In order to obtain a global confidence level α , each discipline needs to cover the risk at the level $1 - \alpha_1 = 1 - \alpha_2 = \sqrt{1 - \alpha}$*

Margin quantification of v_1 *The discipline v_1 does not know the true value $s_{1,0}$ and thus replace it by its estimated value \hat{s}_1 . In order to cover the related uncertainties, they want to take a demanded margin m_1 on $\mathbf{M}_{s_1, \rightarrow}$ so that if*

$$(r_1, \hat{s}_1, s_2) \notin \mathbf{dm}_{m_1, \mathbf{M}_{s_1, \rightarrow}}(\mathbf{F}) \Leftrightarrow r_1 \geq \hat{s}_{1,0} + m_1 + s_2$$

almost surely, then

$$\mathbb{P}(r < s_{1,0} + s_{2,0}) \leq \alpha_1.$$

Using the fact that $\hat{s}_{1,0} - s_{1,0} = G_1$, they conclude that they can take $m_1 = q_{1-\alpha_1}\sigma_1$. The new forbidden set $\mathbf{F}'_1 = \mathbf{dm}_{m_1, \mathbf{M}_{s_1, \rightarrow}}(\mathbf{F})$ is transmitted to v_2 .

Margin quantification of v_2 *The discipline v_2 follows the same approach as v_1 , but replacing \mathbf{F} with \mathbf{F}'_1 . They conclude that if they replace $s_{2,0}$ by $\hat{s}_{2,0}$, they have to take a margin $m_2 = q_{1-\alpha_2}\sigma_2$ with the model of margin $\mathbf{M}_{2, \rightarrow}$. The final forbidden set is*

$$\mathbf{F}'_2 = \mathbf{dm}_{m_2, \mathbf{M}_{2, \rightarrow}}(\mathbf{F}'_1) = \{r < \hat{s}_{1,0} + q_{1-\alpha_1}\sigma_1 + \hat{s}_{2,0} + q_{1-\alpha_2}\sigma_2\}$$

and the choice is $r_{\text{seq}} = \hat{s}_{1,0} + \hat{s}_{2,0} + q_{\sqrt{1-\alpha}}(\sigma_1 + \sigma_2)$.

Mutual quantification *As the information is shared, the designer knows that the difference between the true and the estimated value $\hat{s}_{1,0} + \hat{s}_{2,0} - s_{1,0} - s_{2,0}$ is a normal random variable of variance $\sigma_1^2 + \sigma_2^2$. The designer can thus take a margin either on s_1 or s_2 of value $m = q_{1-\alpha}\sqrt{\sigma_1^2 + \sigma_2^2}$ to cover the risk. The choice is then*

$$r_{\text{mut}} = \hat{s}_{1,0} + \hat{s}_{2,0} + q_{1-\alpha}\sqrt{\sigma_1^2 + \sigma_2^2}.$$

Conclusion of the example *As both $q_{1-\alpha} < q_{\sqrt{1-\alpha}}$ and $\sqrt{\sigma_1^2 + \sigma_2^2} < \sigma_1 + \sigma_2$, the value of r_{mut} is lower than r_{seq} , whereas they were chosen to meet the same confidence level. The design with mutual margin quantification leads to a more efficient design than a design with sequential margin quantification, that pays the price of not sharing the information on the risks.*

Chapter 6

Model of margin: from the mathematical formulation to an operational implementation

This chapter describes joint works with Romain Barbedienne¹ and Jean-Michel Edaliti² in the context of the AMC project at IRT SystemX. They were presented at the “5th International Conference on System Reliability and Safety” and subsequently published in [114]. We present this version with minor updates to standardize the notations.

6.1 Introduction

Uncertainties are generated all along the life cycle of large industrial systems, in their design, manufacturing, operation and even their end-of-life. Some quantitative methods, designated under the name of Uncertainty Quantification (UQ), have been developed to provide meaningful indicators for decision. A probabilistic modeling of these uncertainties is often used [37]. However it appears that, in some industrial collaborative contexts, UQ methods are not widely shared across the variety of engineering stakeholders who must interact together, thus limiting the opportunity to go beyond purely deterministic simulations. In these contexts, engineers keep using margins to ensure the reliability of the models, the simulations and the system in general. Margins are informally understood here as *an amount of something included so as to be sure of success or safety* (Oxford dictionary). However, the margins are often implicit or *hidden*, as they are not monitored [44]. Thus, they cannot be used as indicators to characterize the system.

To address this problem, some recent works, such as [44], focused on laying the theoretical foundation of the concept of margin in design science. In order to rigorously formulate problems on margins, independently from the engineering field or modeling practice, we proposed a formal mathematical framework to define margins in Chapter 4. More precisely, the concept of *model of margin* was proposed, describing the sufficient information to uniquely define a margin. This approach is pursued in this paper, based on a use case. A practical link between the model of margin and the risks prevented is presented hereafter. Section 6.4 shows how models of margin can be used in an industrial context to formalize and generalize the margin practices. Section

¹IRT SystemX

²Sherpa Engineering

6.5 presents a design pattern used to guide the numerical implementation of the margin presets for the use case.

6.2 Industrial case: an automotive battery sizing

6.2.1 Initial problem

The use case presented in this section is typically part of a pre-design sizing study. To this end, simple models are used in order to get a first idea of the characteristics of the system. The numerical values used in this paper are provided for the purpose of the demonstration only and are not actual values used by our industrial partners.

The system of interest for this use case is a battery used to power the starting engine of an automotive combustion engine. The battery also supplies the vehicle components with power when the engine is not running. When the engine is running, the alternator provides enough power to charge the battery and to operate the car devices.

We concentrate hereafter on satisfying the requirement: *the battery should store and supply enough energy to crank the engine running in tough conditions*. It is refined as follows:

- The battery must handle at least 6 months of storage in warm, temperate and cold countries;
- To ensure that the engine actually start, there must be enough power to perform three crankings.

6.2.2 Modeled phenomena

The variables used in this section are classified and explained in Table 6.1 and Table 6.2. Due to the specific needs of our analysis, we chose to only model the following phenomena:

Self-discharge Because of their internal electric conductivity, batteries cannot keep their state of charge, even when unused. The conductivity is temperature-dependent and thus affects the self-discharge rate. We assume furthermore that the discharge rate is independent from the battery state of charge at a given time. The energy consumed during a period of inactivity of t_{in} is approximated by:

$$E_{\text{discharge}} = C_{\text{batt}} V_{\text{batt}} t_{in} k_0 (\theta_{\text{dis}} - \theta_{\text{ref}_1})^\alpha \quad (6.1)$$

Post-cooling After the engine stops, some additional energy is required to cool the engine and avoid hot spots. The post-cooling energy is expressed as:

$$E_{\text{cool}} = \begin{cases} 0, & \text{if } \theta < \theta_s \\ P_{\text{cool}}(t_m + (t_c - t_m) \frac{\theta_{\text{cool}} - \theta_s}{\theta_c - \theta_s}), & \text{if } \theta \in [\theta_s; \theta_c] \\ P_{\text{cool}} t_c, & \text{if } \theta > \theta_c. \end{cases} \quad (6.2)$$

Electronic Control Unit standby mode Most of the car embedded electronics components (ECU) - like the battery management system - keep operating periodically after the engine is stopped. This is modeled as a linear cost with respect to the parking duration:

$$E_{\text{standby}} = E_0 + P_{\text{standby}} t_{in}. \quad (6.3)$$

Variable	Description	Unit
Design parameters		
C_{req}	Minimum battery capacity needed	A h
Environment constraints		
θ_{cool}^+	Maximum cooling temperature required	K
θ_{start}^-	Minimum starting temperature required	K
θ_{dis}^+	Maximum mean temperature required	K
Non-controllable variables		
C_{batt}	Capacity consumed	A h
E_{start}	Energy required to start the vehicle	J
$E_{\text{discharge}}$	Battery self-discharge energy	J
E_{cool}	Energy used to cooling engine	J
E_{standby}	Energy consumed by standby equipments	J
θ_{dis}	Mean battery temperature	K
θ_{cool}	Engine temperature (cooling)	K
θ_{start}	Engine temperature (start)	K

Table 6.1: Description of model variables

Starting energy The energy required to start the engine is dependent on the temperature. This has an impact on the duration of the starting phase, which is modeled by a dependency of the time on the temperature:

$$E_{\text{start}} = P_{\text{start}} \left(t_{\text{start}} + K_1 (\theta_{\text{start}} - \theta_{\text{ref}_2})_+^\beta \right) \quad (6.4)$$

Total energy consumed The starting energy is counted three times to match the requirements. The expression of the total energy consumed is:

$$E_{\text{batt}} = E_{\text{discharge}} + E_{\text{cool}} + E_{\text{standby}} + 3 E_{\text{start}} \quad (6.5)$$

from which we deduce the expression of the total consumed capacity:

$$C_{\text{batt}} = \frac{E_{\text{batt}}}{V_{\text{batt}}}. \quad (6.6)$$

6.2.3 Aim of the analysis

The goal of the analysis is to determine the minimum battery capacity C_{req} that fulfills the requirements stated in Section 6.2.1. The designer must choose the design parameter C_{req} such that for all $\theta_{\text{cool}} \leq \theta_{\text{cool}}^+$, $\theta_{\text{dis}} \leq \theta_{\text{dis}}^+$ and $\theta_{\text{start}} \geq \theta_{\text{start}}^-$ the inequation:

$$C_{\text{req}} \geq C_{\text{batt}}(\theta_{\text{cool}}, \theta_{\text{start}}, \theta_{\text{dis}}). \quad (6.7)$$

Variable	Description	Unit
Constants		
t_{in}	Vehicle parking duration	s
θ_s	Engine temperature that requires cooling	K
K_0	self-discharge coefficient	$K^{-\alpha}/s$
θ_{ref_1}	Temperature with zero self-discharge	K
α	Exponent of the temperature dependency	No unit
θ_c	Critical engine temperature that requires a long time cooling	K
t_c	Critical cooling time	s
t_m	Minimal cooling time	s
P_{cool}	Power of the engine cooling system	W
$P_{standby}$	Power consumed by standby equipments	W
P_{start}	Power of the starter	W
t_{start}	Time required to start engine at the temperature θ_{ref_2}	s
K_1	Additional cooling time coefficient	s/K^β
θ_{ref_2}	Reference temperature	K
β	Exponent of the temperature and time dependency	No unit
V_{batt}	Battery nominal voltage	V

Table 6.2: Description of model constants.

is true. The temperature constraints $\theta_{cool}^+, \theta_{dis}^+, \theta_{start}^-$ represent the range of temperature for which the requirements must hold. The other limits, $\theta_{cool}^-, \theta_{dis}^-$ and θ_{start}^+ are not considered here, as they have no influence on our modeling.

6.3 Taking a margin

6.3.1 Taking a margin on a set of points

When one speaks of *taking a margin* m , most of the times they implicitly think of defining a model of margin \mathbf{M} and imposing a minimum margin $m > 0$ for this model of margin. In that case, the requirement value m is called the *demanded margin*, by opposition to an *effective margin*, which is the margin actually measured for a point u . In this chapter, instead of writing that the acceptance set \mathbf{A} is reduced by imposing a margin $em_{\mathbf{M}}(u, \mathbf{F}) > m$, we write that *m margin is taken in \mathbf{M}* , \mathbf{M} being a model of margin.

6.3.2 Taking a margin on a point

Sometimes, it is easy to choose the “best” point u^* as a unique solution of:

$$u^* = \arg \min_{u \in \mathbf{A}} c(u). \quad (6.8)$$

c is a cost function, that can be trivial to compute. It can be the value of one coordinate of u for instance. It might be easy as well to choose the best point v^* from the “marged” acceptance set $\mathcal{E} \setminus \mathbf{dm}_{M,m}(\mathbf{F})$ for the same cost function. It seems common that, in that case, one says that “ v^* is the point u^* with m margin”.

6.4 Application to the industrial case

In this section, we compare two classic design methods to choose the battery capacity to an approach enabled by the model of margin, namely the *design with explicit margins*. Each of the three methods have in common a formulation of an optimization problem under constraints:

$$C_{\text{req}}^* = \arg \min_{C_{\text{req}} \in \mathcal{D}} C_{\text{req}}. \quad (6.9)$$

The difference lies in the construction of the optimization space \mathcal{D} .

6.4.1 Three design approaches

6.4.1.a Worst-case design

The worst-case approach consists in taking each environment variable at its worst value for all the considered environments. Looking at the given reference values in Table 6.3, and considering the monotony of the capacity with respect to the environment variables, the worst case happens when $\theta_{\text{cool}}^+ = 80^\circ\text{C}$, $\theta_{\text{dis}}^+ = 35^\circ\text{C}$ and $\theta_{\text{start}}^- = -18^\circ\text{C}$. The optimization space \mathcal{D} is then constructed by applying the condition of Equation (6.7) with the aforementioned values. Thanks to the monotonicity of the model, we compute the optimal design as $C_{\text{batt}}(80, -18, 35)$, which leads to a numerical value of:

$$C_{\text{req}}^* = 92 \text{ A h.}$$

This approach is interpreted as a sequential margin accumulation in Section 6.4.2.

Environment	θ_{cool}^+	θ_{dis}^+	θ_{start}^-	probability
Temperate	65°C	20°C	0°C	p_{temp}
Cold	65°C	20°C	-18°C	p_{cold}
Warm	80°C	35°C	0°C	p_{warm}

Table 6.3: Reference environment constraints depending on the environment.

6.4.1.b Probabilistic design

In the probabilistic approach, each environment of Table 6.3 is assigned to an event. The universe is then composed of three exclusive events $\Omega = \{\omega_{\text{temp}}, \omega_{\text{cold}}, \omega_{\text{warm}}\}$, modeling the event “being in a temperate (resp. cold and warm) country”. A probability measure is constructed from data on the consumer profiles and assigns the probabilities p_{temp} , p_{cold} and p_{warm} to each event.

θ_{cool}^+ , θ_{dis}^+ and θ_{start}^- are now random variables whose laws are given by the values associated to the probability of each scenario (see Table 6.3).

C_{batt} is then also a random variable. The criteria is reformulated in “satisfying Equation (6.7) with a probability of $\gamma \in [0, 1]$ ”. The optimization space \mathcal{D} is then given by the values C_{req} for which:

$$\mathbb{P}(C_{\text{batt}}(\theta_{\text{cool}}^+, \theta_{\text{start}}^+, \theta_{\text{dis}}^-) \leq C_{\text{req}}) \geq \gamma. \quad (6.10)$$

As illustrated in Figure 6.1, different choices of C_{req}^* are possible (43 A h, 63 A h or 69 A h), depending on the γ chosen.

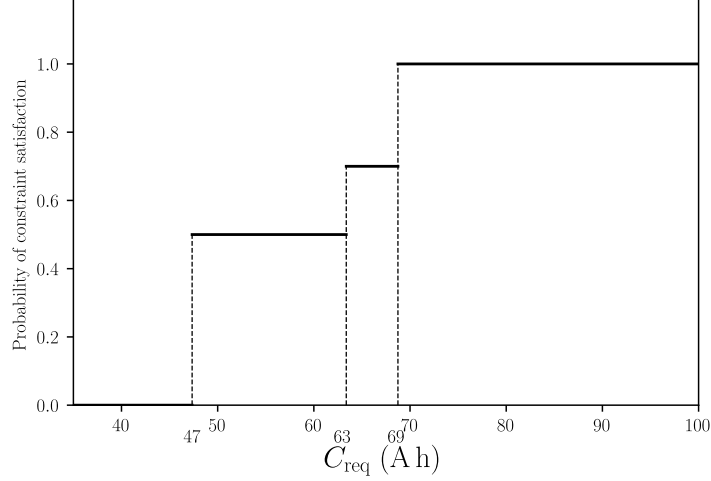


Figure 6.1: Probability γ to satisfy the constraint with respect to the value of C_{req} . This is also the cumulative distribution function of C_{batt} .

One can remark that even for $\gamma = 1$, *i.e.* when Equation (6.7) is always satisfied, the optimal value C_{req} is 69 A h, which is smaller than the worst-case value 92 A h. This characteristic is captured in margin framework, by performing a mutual accumulation on the margins instead of a sequential one, as explained in Section 6.4.2.

6.4.1.c Design with explicit margins

The global motivation of the proposed approach is to ensure that all the margins considered in the analysis are relevant. Margins can be explicitly identified and described thanks to their models of margin.

In Table 6.3, one can see that a margin of -18°C has been taken for θ_{start}^- in the cold environment, with respect to the temperate one. A margin of 15°C for θ_{cool}^+ and θ_{dis}^+ has been taken in the warm environment.

As a car cannot be in a cold country and in a warm country at the same time, a simple rule is to consider that these margins must not be taken “at the same time”, but instead separately. By applying this rule, one computes C_{req}^* as the maximum of $C_{\text{batt}}(65, 20, -18)$ and $C_{\text{batt}}(80, 35, 0)$. The numerical value is the same as the probabilistic modeling with $\gamma = 1$:

$$C_{\text{req}}^* = 69 \text{ A h.}$$

The rigorous interpretation of this use case in terms of models of margin is presented in Section 6.4.2. The rule is generalized in Section 6.4.3. Section 6.5 gives some insights to implement it globally as a numerical tool.

6.4.2 Detail of the design with explicit margins

We reformulate the industrial case within our margin framework. To do so, we first construct a deterministic problem description of the models of margin. The state space \mathbf{E} is chosen to be the set of the design variables and the environment constraints given in Table 6.1. The set of the problem constraints \mathcal{C} is given by the equations of Section 6.2.2. The acceptance set \mathbf{A} is composed of the states satisfying the criterion of Equation (6.7) and we define the failure set by $\mathbf{F} = \mathcal{C} \setminus \mathbf{A}$. The point u represents a battery designed for temperate countries. We want to prevent two risks that are not modeled in the problem description:

- (R_1) : being parked in a cold country and running out of battery;
- (R_2) : being parked in a hot country and running out of battery.

We define \mathbf{M}_1 , a directional model of margin in the direction of a decrease in θ_{start}^- . To prevent (R_1) , we take a margin of 18°C in \mathbf{M}_1 , *i.e.* we impose a smaller minimum starting temperature.

We define \mathbf{M}_2 , a directional model of margin in the direction of an increase in $\theta_{\text{cool}}^+, \theta_{\text{dis}}^+$ (*i.e.* for the direction vector that has the coordinate 1 on both θ_{cool}^+ and θ_{dis}^+). To prevent (R_2) , we take a margin of 15°C in \mathbf{M}_2 , *i.e.* we impose a greater maximum cooling and mean temperature.

These two margins lead to the conditions of Table 6.3 for warm and cold countries. In order to choose our best design, we use an informal design rule:

When two risks are mutually exclusive, there is no need to add up the margins taken for each event. Instead, one could consider the possible designs with margins for each event separately and choose the best among their intersections.

This rule actually describes an implicit consideration modeled in the probabilistic design. As a car cannot be parked in a cold country and in a warm country at the same time, the values of the constraints $\theta_{\text{dis}}^+ = 35^\circ\text{C}$ and $\theta_{\text{start}}^- = -18^\circ\text{C}$ should not be imposed at the same time. If they were, the composition of the demanded margin operators would give the resulting optimization space. Instead, the optimization space \mathcal{D} is the intersection of the designs with a margin of 18°C in \mathbf{M}_1 and of the designs with a margin of 15°C in \mathbf{M}_2 :

$$\begin{aligned} \mathcal{D} &= \{u \in \mathbb{L}^0(\Omega, \mathbf{E}) \mid \text{em}_{\mathbf{M}_1}(u, \mathbf{F}) \geq 18^\circ\text{C}\} \\ &\cap \{u \in \mathbb{L}^0(\Omega, \mathbf{E}) \mid \text{em}_{\mathbf{M}_2}(u, \mathbf{F}) \geq 15^\circ\text{C}\} \end{aligned} \quad (6.11)$$

The impact of different strategies of margin accumulation is illustrated in Figure 6.2. With this method, our optimal value is:

$$C_{\text{req}}^* = 69 \text{ A h.} \quad (6.12)$$

This result is the same as the probabilistic design with $\gamma = 1$.

6.4.3 Generalization of the industrial case

The example given in the previous section will help generalizing it. During the design process, multiple margins are taken to cover various risks. This process can be described as:

1. Starting with some failure criteria that define a set of acceptable designs \mathbf{A} .

In the previous case, \mathbf{A} is given by Equation (6.7).

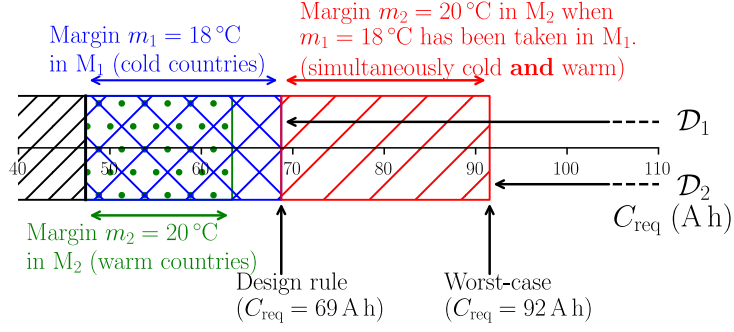


Figure 6.2: Reduction of the optimization space depending on the accumulation strategy. \mathcal{D}_1 is the optimization space in the design with explicit margins and \mathcal{D}_2 is the optimization space in the worst case.

2. Considering a first risk (R_1), that is not prevented by the failure criteria.

In the previous case (R_1) is “being parked in a cold country and running out of battery”.

3. Taking some margins on some quantities to cover the risk (R_1).

$m_1 = 18^\circ\text{C}$ margin in \mathbf{M}_1 has been taken in the previous case.

4. For each other risk (R_i) repeating Step 3.

Only (R_2) “being parked in a warm country and running out of battery” has been considered previously.

5. Getting a “marged” acceptance set $\mathcal{A}_{\text{marg}}$ covering all the risks considered.

This set was denoted by \mathcal{D} in the previous case.

6. Choosing an optimal design among $\mathcal{A}_{\text{marg}}$.

The optimal design was $C_{\text{req}} = 69 \text{ A h}$ in the previous case.

6.4.3.a Margin accumulation strategies

An interesting remark that can be made from the previous case is that there are (at least) two different ways to take two margins simultaneously, namely the *sequential accumulation* and the *mutual accumulation*.

Sequential accumulation Considering a margin m_1 has been taken in \mathbf{M}_1 , take an additional margin m_2 in \mathbf{M}_2 . This is modeled by the composition of the margin operators

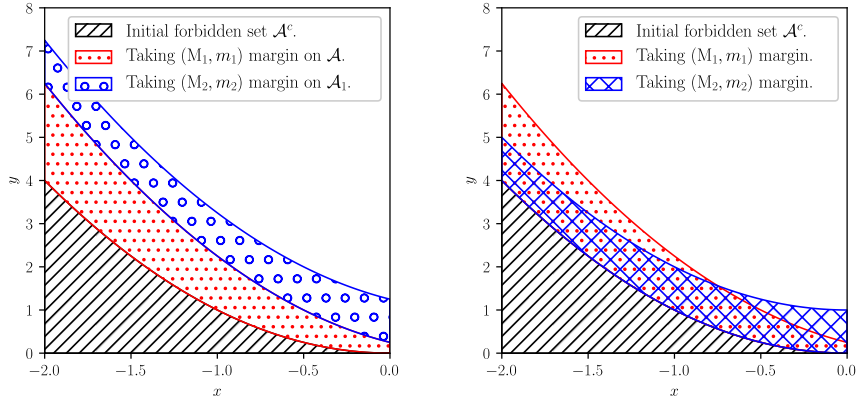
$$\mathbf{F}_{\text{seq}} = \mathbf{dm}_{\mathbf{M}_2, m_2}(\mathbf{dm}_{\mathbf{M}_1, m_1}(\mathbf{F})). \quad (6.13)$$

An illustration of sequential margins accumulation is shown in Figure 6.3a. This leads to the worst-case design in the industrial case.

Mutual accumulation The points u are required to have m_1 margin in \mathbf{M}_1 and m_2 margin in \mathbf{M}_2 . In that case, the resulting failure set is the union of

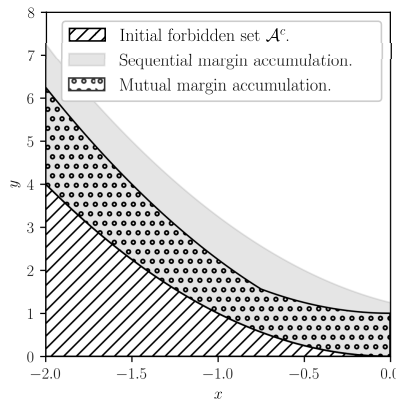
$$\mathbf{F}_{\text{mut}} = \mathbf{dm}_{\mathbf{M}_1, m_1}(\mathbf{F}) \cup \mathbf{dm}_{\mathbf{M}_2, m_2}(\mathbf{F}) \quad (6.14)$$

An illustration of mutual margins accumulation is shown in Figure 6.3b. This leads to the design with explicit margins in the industrial case.



(a) Sequential margins accumulation of a margin of 1 taken in \mathbf{M}_1 then of margin of 0.5 taken in \mathbf{M}_2 .

(b) Mutual margin accumulation of 1 margin taken in \mathbf{M}_1 and 0.5 margin taken in \mathbf{M}_2 .



(c) Comparison of both strategies (sequential is in plain grey and mutual is dotted).

Figure 6.3: Two strategies of margins accumulation for the acceptance set $\mathbf{A} = \{(x, y) | y \geq x^2\}$. \mathbf{M}_1 is a directional model of margin on a decrease in x and \mathbf{M}_2 is a directional model of margin on a decrease in y . A margin of 1 is taken in \mathbf{M}_1 and a margin of 0.5 is taken in \mathbf{M}_2 .

It is possible to prove that sequential forbidden set \mathbf{F}_{seq} is always bigger than the mutual forbidden set \mathbf{F}_{mut} . The argument is that,

$$\mathbf{dm}_{\mathbf{M}_1, m_1}(\mathbf{F}) \subset \mathbf{dm}_{\mathbf{M}_2, m_2}(\mathbf{dm}_{\mathbf{M}_1, m_1}(\mathbf{F}))$$

and

$$\mathbf{dm}_{\mathbf{M}_2, m_2}(\mathbf{F}) \subset \mathbf{dm}_{\mathbf{M}_2, m_2}(\mathbf{dm}_{\mathbf{M}_1, m_1}(\mathbf{F})),$$

leading to

$$\mathbf{dm}_{\mathbf{M}_1, m_1}(\mathbf{F}) \cup \mathbf{dm}_{\mathbf{M}_2, m_2}(\mathbf{F}) \subset \mathbf{dm}_{\mathbf{M}_2, m_2}(\mathbf{dm}_{\mathbf{M}_1, m_1}(\mathbf{F})).$$

This is illustrated in the comparison of Figure 6.3c.

Nonetheless, the sequential accumulation should not be forbidden. In fact, both strategies are relevant depending on the purpose of the accumulation.

The purpose of the sequential accumulation is first to prevent the risk (R_1) by taking a margin of m_1 in \mathbf{M}_1 . Then, assuming this risk occurs, one prevents a second risk (R_2) (potentially the same) by taking a margin of m_2 in \mathbf{M}_2 .

The mutual accumulation can be seen as preventing a risk (R_1) by taking a margin of m_1 in \mathbf{M}_1 and a second risk (R_2) by taking a margin of m_2 in \mathbf{M}_2 . The case in which (R_1) and (R_2) happen at the same time is not considered, though.

It is now possible to rewrite the informal design rule as follows:

Assuming that (R_1) and (R_2) are two risks that cannot happen at the same time and a margin of m_1 (resp. m_2) has been taken in \mathbf{M}_1 (resp. \mathbf{M}_2) to cover (R_1) (resp. (R_2)), the final acceptance set covering (R_1) and (R_2) can be constructed by the mutual accumulation of m_1 taken in \mathbf{M}_1 and m_2 taken in \mathbf{M}_2 .

It is assumed that the models of margin \mathbf{M}_1 and \mathbf{M}_2 share the same problem description and, in particular, the same acceptance set.

6.4.3.b On the construction of the acceptance set A

From a modeling point of view, in an optimization context of the type:

$$u^* = \arg \min_{u \in \mathbf{dm}_{\mathbf{M}, m}(\mathbf{F})} c(u) \quad (6.15)$$

it seems easier to express the mutual accumulation when the margins are taken on the variable threshold - θ_{cool}^+ for instance - rather than on the actual values - θ_{cool} for instance.

Taking a margin on a constraint only imposes a stronger constraint, *e.g.* a greater θ_{cool}^+ . However, margins on actual values exclude relevant designs. Let us assume that θ_{cool} is included in the point u instead of θ_{cool}^+ . In that case, a temperate constraint $\theta_{\text{cool}} > 65^\circ\text{C}$ would likely be included in the acceptance set, to make sure that the design would fulfill the temperate country requirements. A margin for the warm countries in an increase θ_{cool} would forbid any θ_{cool} value between 65°C and 80°C . Then, even a *mutual accumulation* would impose $\theta_{\text{cool}} \geq 80^\circ\text{C}$. With a similar reasoning on the two other environment variables, the optimal design would be the worst-case, instead of the one with explicit margins.

6.4.4 Conclusion of the section

The margin that were taken during the design are now rigorously defined, thanks to the models of margin. This rigorous formulation helped us expressing a particular design margin rule for general cases. This illustrates the aim and the potential of the model of margin: to formulate problems on margins and their solutions in a rigorous, general way.

6.5 Structure of an implementation of a model of margin

The previous formulation of the model of margin allows an exhaustiveness to manage each model of margin. However, it may not be simple enough to be used by a specialist simulation designer.

Method	C_{req}
Worst-case + The simplest. – Very conservative.	92 A h
Explicit margins + No more additional phenomena modeling than in the worst-case, performs better, interpretation in terms of margins. – Needs a modeling of the margins and of the risks.	69 A h
Probabilistic model + Takes into account the correlations. – Requires a probabilistic framework.	Depends on γ , ≤ 69 A h

Table 6.4: Comparison of the three design methods

In this section, a software design pattern for the model of margin is built. This pattern enables the definition of presets that could be plugged to each concept of model of margin. A focus on the preset for the use case is presented. The pattern will be described thanks to a metamodel, that defines the concepts and the relationships between these concepts.

6.5.1 Metamodel definition

The *metamodel* of the model of margin describes its components, for the purpose of their software implementations. The Unified Modeling Language (UML) is used to describe the metamodel, although one does not need to be familiar with it to understand the patterns we expose. When some UML concepts are used in a figure, their meaning is given in a table below the figure.

A UML class, represented as a box, has the same meaning as classes described in programming language as C++, Java, or Modelica. It is a collection of properties and operations. Classes can be seen as a mold, where instances can be seen as items generated from a class.

Each mathematical object is modeled with an abstract class, which is a class that cannot be instantiated as is. The classes that are actually instantiated all *inherit* from the abstract classes. The process of inheritance consists in imposing the feature (attributes and methods/operations) interfaces of the parent abstract class to the classes that inherit from it. To differentiate abstract classes from other classes, the name of abstract classes is written in *italic*. For instance, in Figure 6.4, each model of margin must have a class inheriting from *ProblemConstraints*. Each of these classes must have an operation `getState`, which represents the computation of the state (inputs and outputs) with respect to the inputs. However, the operation `getState` can be different for two models of margin, as they can refer to different phenomena.

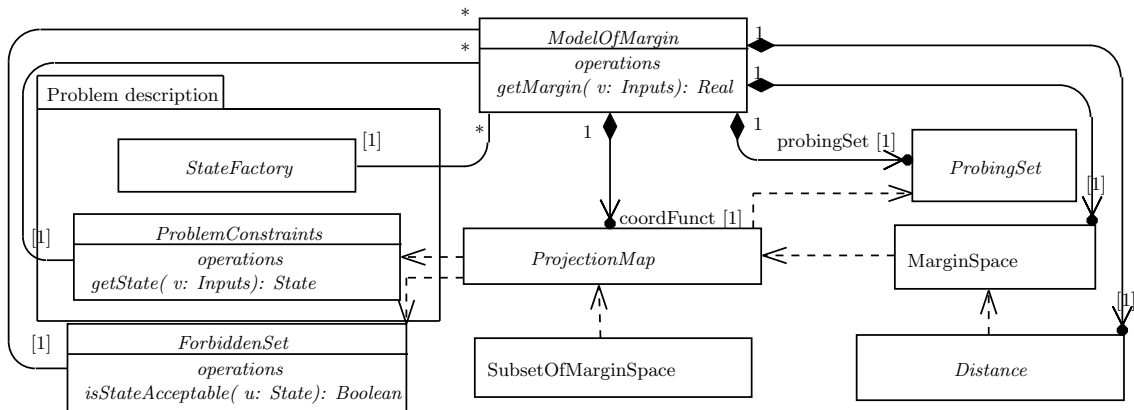
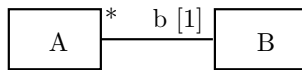
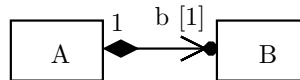


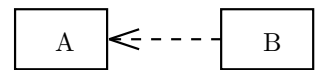
Figure 6.4: Description of Margin metamodel using UML Class Diagram

Association

A class A has an association with another class B if an object of class A needs to maintain a reference to an object of class B. [33]

Composition

A composition is a unidirectional association, it means that A is composed of B.

Dependency

A Dependency is a Relationship that signifies that a single model Element or a set of model Elements requires other model Elements for their specification or implementation. [95]

6.5.1.a Problem description

The abstract class *ModelOfMargin* is associated with the *ProblemConstraints*, *StateFactory* and *AcceptanceSet* abstract classes. The three latter classes come from a prior modeling, without any margin consideration *a priori*. They can then exist without the model of margin, and consequently, an association link is used.

State space The role of the state space E in the mathematical model of margin is to declare what are the variables that would be of interest in the model. The variables can either be input, intermediary or output variables. The numerical counterpart is the *StateFactory*, which defines how to instantiate the state.

The *BatteryState* of the use case (Figure 6.5) is implemented to be used in an optimization context. The distinction between the design parameters, the battery outputs and the environment variables allows to identify the variables on which an optimization algorithm can operate. These variables are taken from Tables 6.1 and 6.2. The *BatteryStateSpace* has a method *BuildBatteryState(...)* to construct a state instance.

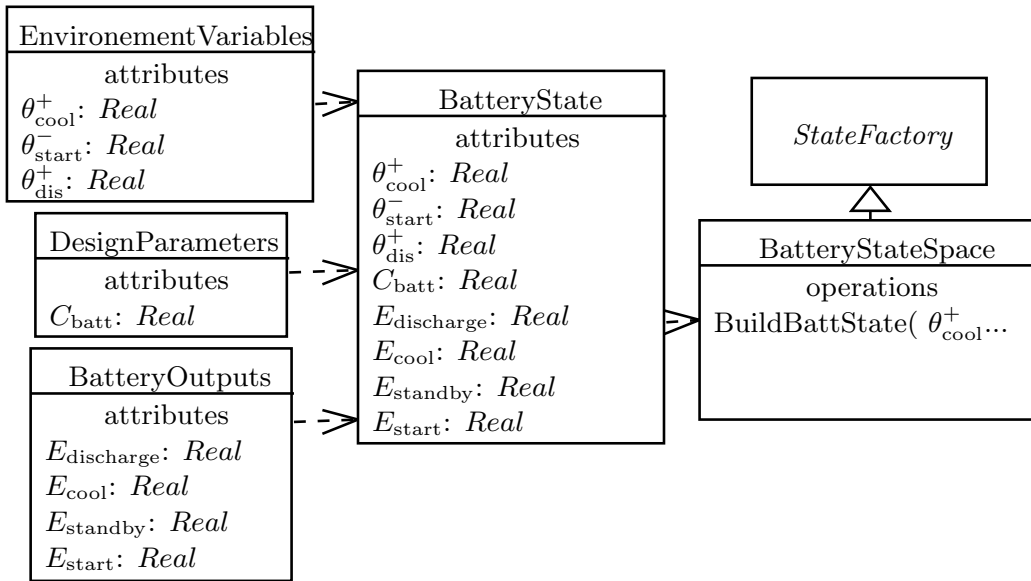


Figure 6.5: State of case study

Generalization

B class inherits from A class means that all characteristics of A class are included in B class

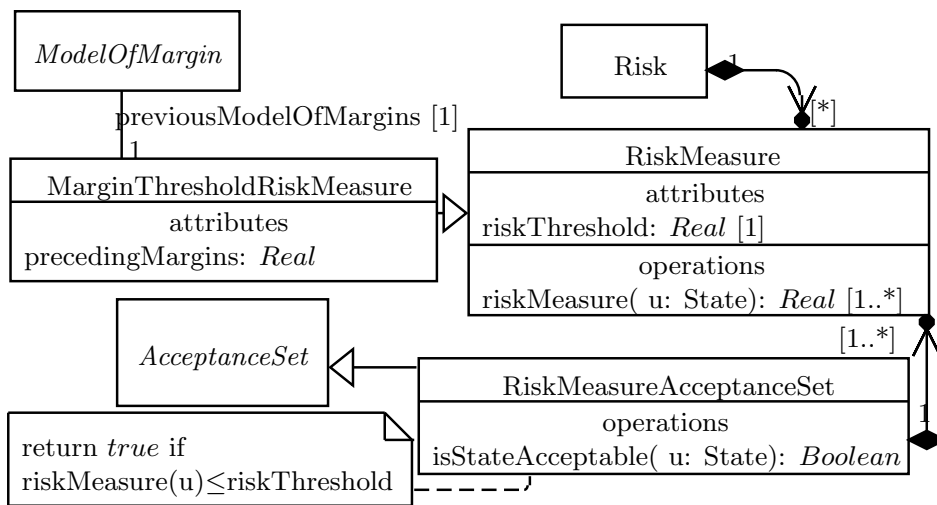


Figure 6.6: *AcceptanceSet* implementation for the case study .

Problem constraints As written in the introduction, an implementation of the *ProblemConstraints* must have a method *getState*. This method is given by the models simulating the phenomenon.

Acceptance set For the numerical representation of \mathbf{A} , we only impose that any representation inheriting from *AcceptanceSet* has an “oracle function” *isStateAcceptable*. This function returns “True” if the state given in argument is in acceptance set and “False” otherwise. The construction of this acceptance criterion may come from various sources. For instance it can be some requirements specifications documents, the simulation itself, or a demanded margin condition.

The initial acceptance set of the use case has come from the criterion of Equation (6.7) and was deduced from the high level requirements. The quantity $\rho = C_{\text{batt}} - C_{\text{req}}$ can be identified as a measure of the risk, that must be smaller than the threshold $\rho_{\text{req}} = 0$. It can thus be modeled with a *RiskMeasureAcceptanceSet*, as shown in Figure 6.6. In this specialization of *AcceptanceSet*, *isStateAcceptable* is True if and only if $\rho(\text{State}) \leq \rho_{\text{req}}$.

It has been stated that taking a margin consists in reducing the acceptance set by imposing $\text{em}_{\mathbf{M}}(u, \mathbf{F}) \geq m$ (see Section 6.3.1). The implementation of this operation is illustrated in Figure 6.6 in the *MarginThresholdRiskMeasure* class. The condition can be expressed with risk measure, by defining $\rho(u) = -\text{em}_{\mathbf{M}}(u, \mathbf{F})$ and $\rho_{\text{req}} = -m$.

6.5.1.b Specific objects of the model of margin

The problem description comes from the modeling of the phenomenon. The other objects, such as the probing set or the coordinate functions are specific to the model of margin.

Each model of margin specific object is defined as an abstract class. These classes could not exist without a model of margin and thus, they have a composition link with the *ModelOfMargin* abstract class.

Probing set For each state u , the classes inheriting from *ProbingSet* must describe the value of the states that would be explored in the computation of the margin. In a directional model of margin, it is implemented as a vector. This direction vector represents the semi-line starting at the state u and going in the direction of the vector.

In the use case, the two models of margin defined in Section 6.4.2 are directional margins. The probing direction of \mathbf{M}_1 is $-e_{\theta_{\text{start}}^-}$, the unit vector in θ_{start}^- and the probing direction of \mathbf{M}_2 is $e_{\theta_{\text{cool}}^+} + e_{\theta_{\text{dis}}^+}$, the sum of the two unit vectors in θ_{cool}^+ and in θ_{dis}^+ .

Coordinates functions and coordinates of interest The specialization of *CoordinateFunctions* must carry the information to project any state in the *ProbingSet* to an element of *CoordinatesOfInterest*.

In a directional model of margin, the coordinate of interest is formed by the abscissa of points on the semi-line. It can thus be deduced from the direction vector. In this case, the information of the *CoordinateFunctions* and *CoordinateOfInterest* can be factorized with the information used to construct the probing set.

Distance The implementation of *Distance* must describe how to compute a distance between two elements of *CoordinatesOfInterest*.

By convention, in a directional model of margin, the direction vector defining the *ProbingSet* (Section 6.5.1.b) is also the “unit vector” defining the *Distance*. However, the (mathematical) probing set and the distance remain two different conceptual objects.

6.6 Conclusion of the chapter

The application of the theoretical model of margin presented in Chapter 4 to the automotive case of Section 6.2 helped:

- Formulating a margin problem and formulating its solution in a rigorous way, in Section 6.4.2.
- Generalizing the solution so it can be applied in an approach of design with explicit margin, in Section 6.4.3. This approach consists in identifying the relevant margins.
- Deducing some software design patterns for a numerical use of the model of margin, in Section 6.5.

This is an encouraging sign for the ability of the model of margin to formalize practical margin approaches to handle risk.

Chapter 7

Conclusion and perspectives

7.1 Conclusion

In order to answer the initial problem of the modeling and the identification of the most impactful demanded margins, we proposed a framework containing the following elements.

1. A mathematical definition for the notions of effective margin and demanded margin in Section 1. The model of margin (Section 4.2) defines on which variable and for which evolution of design the margin is computed/taken. The effective margin (Section 4.2.1) is a function of a design point and a failure set, computing a specific distance between them. The demanded margin is an application reducing the set of acceptable designs by removing all the points that do not have enough effective margin.
2. A generic description of the way engineers mitigate uncertainty with margins. The margin quantification (Section 4.4.1) consists in choosing the value of a demanded margin, taking some risks into account.
3. The description of the margins from the literature within this framework, in Table 4.2. The majority of the concepts from the literature can be interpreted either as an effective margin, that monitors how far the system is from the failure point, or as a margin quantification, prescribing the value of the demanded margin in a specific context. The models of margin were explicated in Section 4.5.
4. A rigorous definition of the impact of the demanded margins on the cost, on the performance loss and on another effective margin. It is computed by the induced function with respect to demanded margins, defined in Section 5.1.
5. Some sensitivity analysis indices of the induced cost or induced margin with respect to the demanded margins. The local sensitivity indices (Section 5.2.2) and the global sensitivity indices (Section 5.2.3) permit to decompose an induced function with respect to the demanded margins. They do not require a probabilistic model.

We also present some methodological considerations to reduce influential margins. Three recommendations are stated in Section 5.3; the first one is to better formalise the margin quantification, the second one is to update the reducible margins and the last one is to take the correlation/independence into account.

An industrial application is proposed in Chapter 6, illustrating the gain that can be made when margins are computed taking into account the correlation between the risks they cover. It focuses on the way to accumulate two margins when the risks covered are mutually exclusive.

7.2 Perspectives

These works have opened up some new perspectives, both in the industrial applications and in the applied mathematics field. Here are some of the most promising ones.

7.2.1 Industrial applications

A methodology based on the model of margin In some industrial contexts, an important stake is to have a unified practice on the management of uncertainty. Identifying first, for each stakeholder, what is their model of margin, their way to quantify margin and the uncertainty they cover would help to have a picture of the current practices. A lot of margin quantification are surely implicit and an interviewing phase would be required to identify them.

Then, prescribing some ways to quantify margins, by telling which uncertainty to cover by which mean would provide some guidance. A particular attention should be taken on quantifying margins together (Section 5.3.3), in order to avoid unrealistic worst-cases.

An industrial application of margin sensitivity analysis This framework is ready for real-life industrial application at a larger scale. This would be done by choosing some reference cost/performance, computing their related induced function (Section 5.1), and decomposing them with respect to the demanded margins (Section 5.2.1). The real values of the demanded margins do not need to be actually known precisely; even an order of magnitude of where the margins have been taken and for which reason can be useful to identify the greatest contributors.

The “allocated” margin, the other side of the demanded margin In our works, we focused on the stakeholders for which the margin is a constraint. In practice, it is represented by the demanded margin operator, that expands the forbidden set

$$\mathbf{dm}_{\mathbf{M},m}(\mathbf{F}) = \{u \in \mathcal{C} \mid \text{em}_{\mathbf{M}}(u, \mathbf{F}) < m\} \quad (7.1)$$

and thus reduces the set of possible designs \mathbf{A} . Even if demanded margins are often only a constraint on the global design (*e.g.* when they cover uncertainty that are external to the design process) they may have a positive impact, when they are taken to cover an uncertainty on a possible choice in the future. In that case, a demanded margin taken on a variable, can be seen as a room for manoeuvre, a freedom of choice, that can be “consumed” by the same or another stakeholder. We can extend the model of margin by distinguishing the two notions:

- The “demanded” margin, that imposes additional constraint on the design for a given stakeholder.
- The “allocated” margin, that extends the set of possible designs and that consumes some specific demanded margins.

The allocated margin would typically be built with a symmetric definition to Equation 7.1, that reduces the forbidden set instead of increasing it. The sensitivity indices could be similarly defined on the induced cost/gain in performance, to measure the positive impact of this allocation.

This would permit to model more design scenarios, with stakeholders having demanded margins on some variables, and allocated margins on other. This model could possibly formalize the problem of “margin negotiation”, for which each stakeholder needs an allocated margin on a demanded margin shared with the others (for instance, when two engineering disciplines need to share a common budget).

7.2.2 Applied mathematics

We formulate here theoretical questions on the model of margin as a mathematical tool. We are confident on the fact that some of them could be answered by linking them to the relevant result from the literature. However, answering others might lead to original results.

The commutation of the margin operators To ensure that, for two or more models of margin, the order in which the demanded margins are taken is not important, one must ensure that the margin operators commute. Let \mathbf{M}_1 and \mathbf{M}_2 be two model of margin on the same problem description, one must ensure that

$$\forall \mathbf{F} \subset \mathcal{F}, \forall (m_1, m_2) \in \mathbb{R}_+^{*2}, \quad \mathbf{dm}_{\mathbf{M}_1, m_1}(\mathbf{dm}_{\mathbf{M}_2, m_2}(\mathbf{F})) = \mathbf{dm}_{\mathbf{M}_2, m_2}(\mathbf{dm}_{\mathbf{M}_1, m_1}(\mathbf{F})),$$

for a family of failure set $\mathcal{F} \subset \mathcal{P}(\mathcal{E})$. In Section 8.2, we show some cases under which the equality does not hold and we precise a sufficient condition in which they actually commute. Finding more relevant sufficient conditions for the commutations would permit to simplify the computations.

Optimal global decomposition In order to define the sensitivity indices of an induced function indF with respect to the demanded margins $\bar{m}_1, \dots, \bar{m}_n$ (Section 5.2.3), one needs first to choose a margin reduction path $s = (s_1(t), \dots, s_n(t))$ (Definition 5.2.4), that is somewhat arbitrary. Now, let us assume that, for each demanded margin m_i , one knows the cost of reducing \bar{m}_i to $\bar{m}_i - \Delta_i$, denoted by

$$d_i(\bar{m}_i - \Delta_i), \quad \bar{m}_i - \Delta_i \in [0, \bar{m}_i].$$

For instance, in the case of a demanded margin due to statistical uncertainty, the margin is $m_i = q_{1-\alpha} \sigma_i / \sqrt{n_i}$ with n_i the number of observations. If one needs to reduce the margin from m_i to $\bar{m}_i - \Delta_i$, then the number of sample n_i should be greater than $(q_{1-\alpha} \sigma_i / (\bar{m}_i - \Delta_i))^2$. By denoting η_i the cost of obtaining one more sample, the reduction cost is

$$d_i(\bar{m}_i - \Delta_i) = \eta_i [q_{1-\alpha}^2 \sigma_i^2 (1/(\bar{m}_i - \Delta_i)^2 - 1/\bar{m}_i^2)].$$

When such a cost can be defined for all the demanded margin, a natural choice of path would be *the path that reduces the most the induced function, under constraints of budget*. Let us denote s^* such a path, it would verify

$$\begin{aligned} \text{indF}(s_1^*(t), \dots, s_n^*(t)) &= \inf_{s \in \mathcal{S}} \text{indF}(s_1(t), \dots, s_n(t)) \\ d_1(s_1(t)) + \dots + d_n(s_n(t)) &\leq d_1(s_1^*(t)) + \dots + d_n(s_n^*(t)) \end{aligned}$$

with \mathcal{S} the set of the margin reduction paths. Under suitable assumption, this path should be unique up to a reparametrization. Thus, there would be an unique global decomposition, along the most efficient path to reducing the margin. Computing such an index would surely be of interest to show which margin should be reduced in priority.

Worst and best global sensitivity indices Another way to get rid of the arbitrariness of the choice of the path of s in the definition of the sensitivity indices

$$S_i^s = \int_0^1 s'_i(t) \frac{\partial \text{indF}}{\partial m_i}(s_1(t), \dots, s_n(t)) dt$$

would be to compute them, for the greatest and smallest bound

$$S_i^+ = \sup_{s \in \mathcal{S}} \int_0^1 s'_i(t) \frac{\partial \text{indF}}{\partial m_i}(s_1(t), \dots, s_n(t)) dt \text{ and } S_i^- = \inf_{s \in \mathcal{S}} \int_0^1 s'_i(t) \frac{\partial \text{indF}}{\partial m_i}(s_1(t), \dots, s_n(t)) dt$$

for any margin reduction path. If they are close, m_i would contribute by the same amount for any reduction path. For instance, if $\text{indF}(m_1, \dots, m_n)$ writes under the form $f(m_i) + g(m_1, \dots, m_{i-1}, m_{i+1}, \dots, m_n)$, then $S_i^+ = S_i^- = f(\bar{m}_i) - f(0)$. If they are far from each other, it would mean that the impact of m_i would greatly vary with respect to the reduction of the other demanded margins. Developing some numerical methods to compute them would provide more tools for margin sensitivity analysis.

Margin propagation and propagation of the decomposition One of the purposes of the definition of the induced margin in Section 5.1, is the ability to model the fact that demanded margins $\bar{m}_1, \dots, \bar{m}_n$ on some variables can lead to an induced margin indM on another variable. In a multidisciplinary context, the latter variable can be transmitted to other disciplines. In that case, one could morally interpret the value of the induced margin indM as a demanded margin on another problem description; the margin is *propagated*.

A design process could then be described as a succession of stakeholders that have some input demanded margins and provide some output variables with induced margins, that are themselves some input demanded margins for other stakeholders. The decomposition of the variables could also be transmitted in that case. Defining mathematically the propagation of the margin and the propagation of the decomposition would have some application in a multidisciplinary context.

Numerical ways to compute effective margins and forbidden sets with margins This thesis did not focus on the algorithms to compute effective margins (Definition 4.2.4) and to numerically represent forbidden sets with demanded margins (Section 4.2.8). Linking their theoretical formulation to some classic algorithms from the numerical literature (Newton's zero method, convex optimization...) would be a path of improvement for the effectiveness of the framework. It would permit for instance to efficiently compute induced costs and induced margins.

A rigorous principle for sequential quantification vs mutual quantification So far, the benefits of the mutual quantification with respect to a sequential quantification is stated as a principle in Section 5.3.3, based on an intuition and some observations. An interesting question to investigate is the possibility to add more rigor into it and to find the right set of assumptions that both models engineering practices and permits to demonstrate such a result.

Estimating the gain in mutual quantification The margin decompositions that we proposed use a sensitivity index for each margin. In the spirit they are crafted to identify which reducible margin should be decreased first.

However, in Section 5.3.3 we have put in light the fact that substantial gains might be obtained by performing a mutual quantification instead of a sequential one. In order to guide this practice,

some indices could provide an estimation of gain if two margins were to be mutually quantified instead of sequentially quantified, in the spirit of the higher-order Sobol indices. It would help to reduce the costs even when there are only irreducible margins.

Chapter 8

More on models of margins

8.1 Models of margin on one coordinate

Defining a model of margin on one coordinate leave quite a broad range of freedom. Let us denote by x this coordinate, the analyst must ask themselves:

- Does the margin have to be calculated only for increasing/decreasing values of x or does it have to consider the evolution in both directions?
- Does the margin have to hold when the coordinates different from x remain the same or does it need to hold for *any change*?

The answers to these questions depend on the aim of the modeling and by answering them, the analyst chooses a particular shape for the *probing set* \mathcal{G}_u . This section develops an example to highlight the different modeling possibilities.

Example 8.1.1 (Electrical switch case).

Problem description *The goal is to design the electrical circuit of Figure 8.1, for which two variables $\mathbf{E} = \{(R_d, I_d) \in \mathbb{R}^+ \times \mathbb{R}\}$ must be chosen, namely the resistance R_d and the intensity of the current I_d . The resistance $R_0 = 15 \Omega$ is fixed. The resistors at our disposal have resistances R_d that range between 5Ω and $20 \text{ k}\Omega$ and the generators can provide an intensity I_d between 0 A and 25 A . The set of the problem constraints is then $\mathcal{C} = [5, 20 \cdot 10^3] \times [0, 25]$.*

Failure set *There is a failure in the system whenever the power dissipated by Joule heating P_J is greater than a limit $P_{\max} = 33 \text{ kW}$. In order to minimize the dissipation, the switch chooses automatically the branch with the lowest resistance; the final resistance is then $\min(R_0, R_d)$. Using the Ohm's law, we can deduce that the power actually dissipated is*

$$P_J = \min(R_0, R_d) I_d^2.$$

Another mode of failure happens when the intensity is lower than $I_{\min} = 10 \text{ A}$; the generator cannot provide enough power to some critical devices (that are not represented here). The failure set is then given by the expression

$$\mathbf{F} = \left\{ I_d \geq \sqrt{P_{\max} / \min(R_0, R_d)} \right\} \cup \{ I_d \leq I_{\min} \}.$$

The acceptance set is shown by the white area in Figure 8.2.

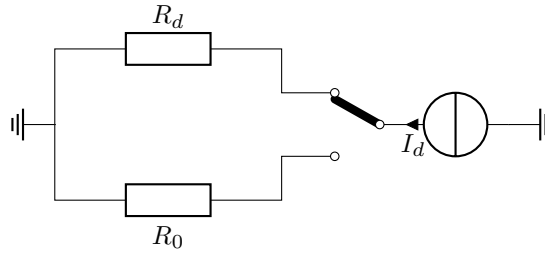


Figure 8.1: Diagram of the electrical switch model for which a margin on I_d must be defined.

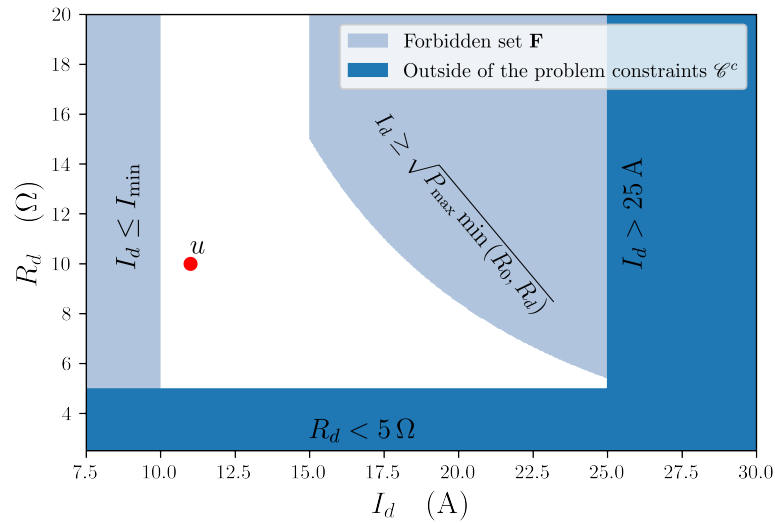


Figure 8.2: Acceptance set of the electrical switch model.

Computing a margin on I_d The analyst chooses a design $u = (R_d : 10 \Omega, I_d : 11 \text{ A})$, plotted in red in Figure 8.2 and would like to compute a margin on I_d .

- If they know that R_d is chosen once for all and will never change and that the generator may have some surges that only increase the current, they would compute by how much I_d could increase before reaching \mathbf{F} . This type of margin is modeled by a unidirectional model of margin in the positive direction (Figure 8.3), that is defined in Section 4.3.1. The effective margin is equal to 8 A in that case.
- If instead, the generator has no surge but may provide less current than specified, they would only investigate the possible decrease. This margin is also modeled with a unidirectional model of margin, but in the negative direction. Its effective margin is equal to 1 A.
- When the analyst needs to consider the variation of I_d , irrespective of an increase or decrease, they compute the minimum variation in both directions. This margin is modeled with a bidirectional model of margin, defined in Section 4.3.2. The value of the effective margin is 1 A.

- Now, they assume that the value of R_d is 10Ω for now, but it could change in the future. They see that, if they consider every possible change of R_d , the intensity can increase only by 4 A before reaching \mathbf{F} and decrease by -1 A. If they consider both directions at the time, it can only change by 1 A before reaching \mathbf{F} . These margins are modeled with Whole space projected and Half-space projected models of margin (Figure 8.4), defined in Table 8.1.

The probing sets are summarized in Table 8.1.

With Example 8.1.1, we can see that even in a simple model with two variables, there are various ways to compute a margin that lead to different values of effective margins. There is no general criterion to determine which margin is better than the other; as they measure different things and consider different scenarios, they have different uses.

The model of margin measures \rightarrow when \downarrow	only increasing (resp. decreasing) changes in I_d	both increasing and decreasing changes in I_d
R_d keeps the same value.	Directional model of margin $\mathcal{G}_{(R_d, I_d)} : R_d : \times, I_d : \rightarrow$ (resp. $\mathcal{G}_{(R_d, I_d)} : R_d : \times, I_d : \leftarrow$)	Bidirectional model of margin $\mathcal{G}_{(R_d, I_d)} : R_d : \times, I_d : \leftrightarrow$
R_d can take any value.	Half-space model of margin $\mathcal{G}_{(R_d, I_d)} : R_d : \leftrightarrow, I_d : \rightarrow$ (resp. $\mathcal{G}_{(R_d, I_d)} : R_d : \leftrightarrow, I_d : \leftarrow$)	Whole space model of margin $\mathcal{G}_{(R_d, I_d)} : R_d : \leftrightarrow, I_d : \leftrightarrow$

Table 8.1: Four possible probing sets in Example 8.1.1, for a model of margin on R_d .

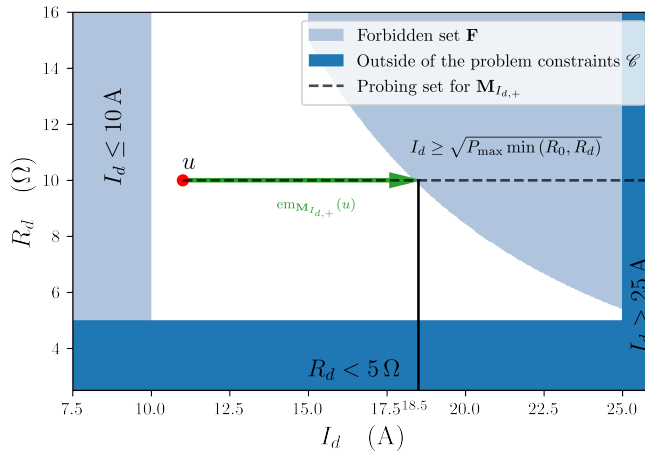


Figure 8.3: Unidirectional models of margin in Example 8.1.1. The effective margin in the increasing direction is $em_{\mathbf{M}_{I_d, \rightarrow}}(u) = 7.5$ A.

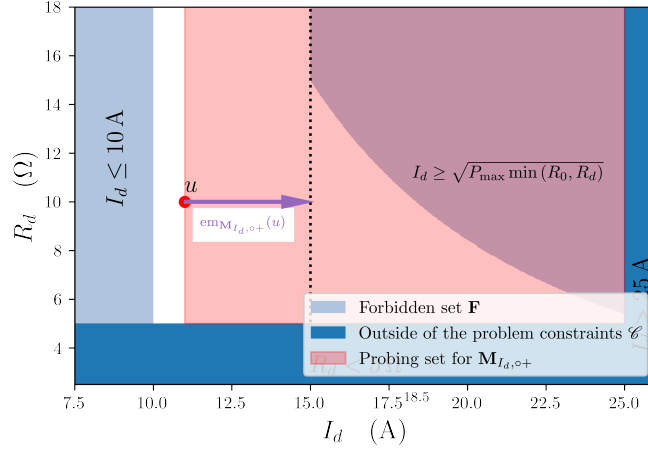


Figure 8.4: Increasing half-space model of margin $\mathbf{M}_{I_d, \circ+}$ in the Example 8.1.1. The effective margin for the design u is $\text{em}_{\mathbf{M}_{I_d, \circ+}}(u, \mathbf{F}) = 15 - 11 = 4$.

8.2 Commutation and non commutation of the demanded margins operators

Let \mathbf{M}_1 and \mathbf{M}_2 be two models of margin defined on the same problem description. One can wonder if taking first a margin m_1 on \mathbf{M}_1 and then a margin m_2 on \mathbf{M}_2 is equivalent to taking *first* a margin m_2 on \mathbf{M}_2 and *then* a margin m_1 on \mathbf{M}_1 . In general the answer is no and this property can be formulated as the commutation of the demanded margin operators.

Definition 8.2.1 (Commutation of the demanded margin operators). *Let \mathbf{M}_1 and \mathbf{M}_2 be two models of margins, defined on the same problem description. We say that the demanded margin operators commute for $\mathbf{F} \subset \mathbf{E}$ when*

$$\forall (m_1, m_2) \in \mathbb{R}_+^{*2}, \quad \mathbf{dm}_{\mathbf{M}_1, m_1}(\mathbf{dm}_{\mathbf{M}_2, m_2}(\mathbf{F})) = \mathbf{dm}_{\mathbf{M}_2, m_2}(\mathbf{dm}_{\mathbf{M}_1, m_1}(\mathbf{F})).$$

In other terms, if we reduce the acceptable set by taking first the margin m_1 then the margin m_2 , it will results to the same set as if we took first the margin m_2 and then the margin m_1 , for any margin value.

We can easily exhibit a counterexample *e.g.* two demanded margin operators that does not commute, for instance when one margin is “additive” and the other one “multiplicative”. Let the problem description be $\mathbf{E} = \mathbb{R}$ and $\mathcal{C} = [1, +\infty)$ and let the first model of margin \mathbf{M}_1 be defined by

$$\begin{aligned} \mathcal{G}_{1, u} &= \mathcal{C} \\ \phi_{1, u}(v) &= v \end{aligned}$$

for $(u, v) \in \mathcal{C}^2$. The second model of margin \mathbf{M}_2 is defined by

$$\begin{aligned} \mathcal{G}_{2, u} &= \mathcal{C} \\ \phi_{2, u}(v) &= \frac{v}{u}. \end{aligned}$$

For a given failure set \mathbf{F} , if $\text{em}_{\mathbf{M}_1}(u) = m$, then u is at least at a distance m of any point in \mathbf{F} . On the other hand, if $\text{em}_{\mathbf{M}_2}(u) = m$, then u is at least at a distance mu from any point in \mathbf{F} . Let us take for instance $\mathbf{F} = (10, +\infty)$, and the demanded margins $m_1 = 3$ and $m_2 = 1$. We have

$$\begin{aligned}\mathbf{dm}_{\mathbf{M}_1, m_1}(\mathbf{dm}_{\mathbf{M}_2, m_2}(\mathbf{F})) &= \mathbf{dm}_{\mathbf{M}_1, m_1}((5, +\infty)) = (2, +\infty) \\ \mathbf{dm}_{\mathbf{M}_2, m_2}(\mathbf{dm}_{\mathbf{M}_1, m_1}(\mathbf{F})) &= \mathbf{dm}_{\mathbf{M}_2, m_2}((7, +\infty)) = (3.5, +\infty).\end{aligned}$$

Thus, even in one dimension, the demanded margin operator might not commute. There are some case in which it is possible to demonstrate the commutation.

Proposition 8.2.2 (Commutation of directional models of margins). *Let \mathbf{M}_1 and \mathbf{M}_2 be either directional or bidirectional models of margins, let $\mathbf{E} = \mathcal{C} = \mathbb{R}^n$ and let \mathbf{A} be a closed convex set. Then the demanded margins operators of \mathbf{M}_1 and \mathbf{M}_2 commute.*

Proof. Let us assume that \mathbf{M}_1 is an increasing unidirectional model of margin in the component i . Then, when \mathbf{A} is closed and convex, we can rewrite

$$\begin{aligned}\text{em}_{\mathbf{M}_1}(u) \geq m_1 &\Leftrightarrow \inf\{\lambda \geq 0 \mid u + \lambda e_i \in \mathbf{F}\} \geq m \\ &\Leftrightarrow \forall \lambda \in [0, m), u + \lambda e_i \in \mathbf{A} \\ &\Leftrightarrow u \in \mathbf{A} \text{ and } u + m_1 e_i \in \mathbf{A}.\end{aligned}$$

If \mathbf{M}_2 is also an increasing unidirectional model of margin in the component j , one can easily verify that

$$\begin{aligned}\mathbf{dm}_{\mathbf{M}_2, m_2}(\mathbf{dm}_{\mathbf{M}_1, m_1}) &= \mathbf{dm}_{\mathbf{M}_2, m_2}(\{v \in \mathcal{C} \mid v \in \mathbf{A} \text{ and } v + m_1 e_i \in \mathbf{A}\}) \\ &= \{v \in \mathcal{C} \mid v \in \mathbf{A}, v + m_1 e_i \in \mathbf{A}, v + m_2 e_j \in \mathbf{A} \text{ and } v + m_1 e_i + m_2 e_j \in \mathbf{A}\}.\end{aligned}$$

The last expression being symmetric in i and j , we conclude that it is also equals to $\mathbf{dm}_{\mathbf{M}_1, m_1}(\mathbf{dm}_{\mathbf{M}_2, m_2})$, proving the commutation of the operators.

This proof can be easily adapted to the negative directional model of margin replacing “ $u + m_1 e_i \in \mathbf{A}$ ” with “ $u - m_1 e_i \in \mathbf{A}$ ” and to the bidirectional model of margin replacing “ $u \in \mathbf{A}$ and $u + m_1 e_i \in \mathbf{A}$ ” with “ $u - m_1 e_i \in \mathbf{A}$ and $u + m_1 e_i \in \mathbf{A}$ ”. \square

However, when \mathcal{C} is not the full space \mathbb{R}^n , it is not clear when two directional models of margin commute, even if we assume that \mathbf{A} is closed and convex.

Part II

Uncertainty propagation in graphs of models

Chapter 9

Introduction and motivation

9.1 Industrial motivation

Industrial complex systems Industrial complex systems¹ are characterized by a large number of components that are assembled together to satisfy a huge number of requirements. Examples of such systems are cars, airplanes, space engines, nuclear reactors etc. One of the main sources of challenges comes from the fact that “satisfactory components do not necessarily combine to produce a satisfactory system” [102]. Thus, the behavior of the system as a whole must be assessed, instead of characterizing only each component separately. In terms of organization, it implies that a huge number of engineering disciplines must interact during the design process, to optimize the design and validate the requirements. These interactions can be naturally modeled with a graph $\mathcal{G} = (\mathcal{V}, \mathcal{E})$, where the nodes \mathcal{V} are the disciplines and the edges \mathcal{E} are the interactions (see Figure 9.1).

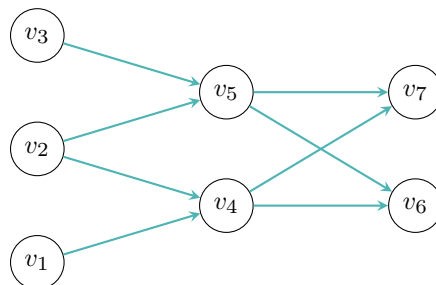


Figure 9.1: Graph of interactions between disciplines. A vertex v_i represents a discipline and an edge represents an interaction.

Uncertainty quantification and sensitivity analysis Uncertainties arise at all steps and at all scales during the design process of industrial complex systems. In this part, we assume that each discipline v models the part of the system they are in charge with a function

$$Y_v = f_v(X_v),$$

¹Industrial complex systems, are distinct from complex systems in physics, which have a different definition.

such that X_v is a vector of random variables that models probabilistically the uncertainties. They can then perform a *uncertainty quantification* and a *sensitivity analysis* phase, to characterize the uncertainties on the important variables of the system.

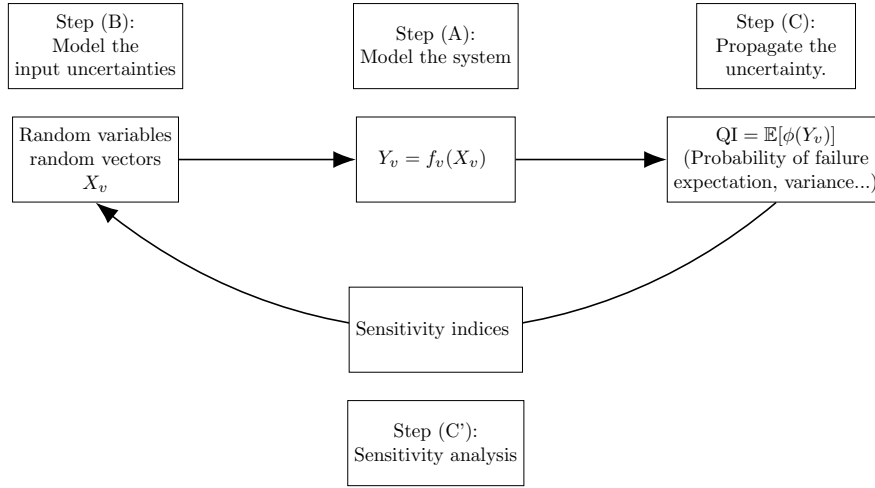


Figure 9.2: ABCC' methodology.

These practices are well identified in the industry [37] and are parts of the “ABCC” methodology (Figure 9.2).

- (A) Provide a model of the system, through the mathematical relationship $Y_v = f_v(X_v)$.
- (B) Provide a probabilistic model for the input variables X_v .
- (C) Propagate/quantify uncertainties (U.Q), *i.e.* compute either the law of the output or an associated quantity of interest.
- (C') Perform a sensitivity analysis (S.A) to characterize which components among $X_v = (X_{v,1}, \dots, X_{v,n})$ have the greatest influence on the variability of Y .

The same letter is used for (C) and (C') to signify that in some contexts, only one of these steps is performed. While Steps (A) and (B) depend inherently on the phenomenon modeled, Steps (C) and (C') are studied transversally and they are the source of a still growing academic literature [54, 66, 100]. In U.Q, some of the works consists in constructing metamodels/response surfaces/regression methods, with techniques such as Kriging, chaos polynomials, etc... In S.A, a part of the research focuses on defining and computing indices that can rank each input by its influence on the output.

Multidisciplinary interactions The industrial goal is to perform U.Q and S.A in a multidisciplinary context. The model of the phenomenon now writes

$$Y_v = f_v(X_v, \Theta_v).$$

We distinguish the input variables that

- comes from other disciplines, is denoted by X_v and is called *external variable*;

- is modeled by the discipline, is denoted by Θ_v and is called *internal variable*.

The variables X_v and Θ_v are assumed independent. In this part, we denote the space in which Y_v takes its values by F_v , the space in which X_v takes its values by E_v and the space in which Θ_v takes its values by Θ_v .

Let us denote the direct parents of v by $\mathcal{P}(v) = \{u \in \mathcal{V} | (u, v) \in \mathcal{E}\}$. The external input variable $X_v = (X_{u,v})_{u \in \mathcal{P}(v)}$ of v is composed by the output of the parents of v , up to a transformation $X_{u,v} = g_{u,v}(Y_u)$, where $g_{u,v}$ is typically easy to compute. In this context, the interactions between the disciplines are an exchange of variables and the graph from Figure 9.1, can be represented as a graph of computer codes in Figure 9.3. This graph shows that, for instance, Y_{v_5} is a function of Θ_{v_5} and the outputs of v_3 and v_2 , through the transformations $X_{v_3,v_5} = g_{v_3,v_5}(Y_{v_3})$ and $X_{v_2,v_5} = g_{v_2,v_5}(Y_{v_2})$.

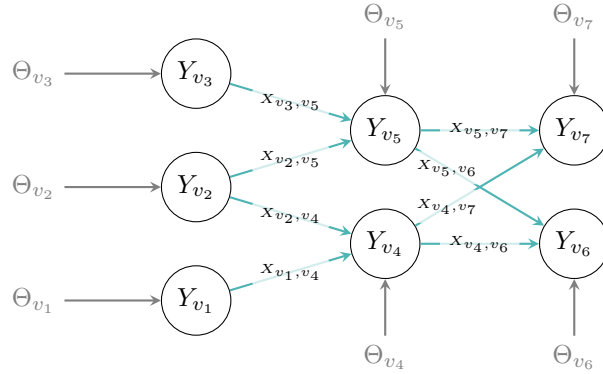


Figure 9.3: Graph of computer codes.

Disciplinary autonomy and decomposition-based approach for U.Q A natural way to perform uncertainty quantification in the graph of Figure 9.3 would be to use methods based on Monte Carlo sampling. In that case, each root v (*i.e.* the nodes with no parents), would generate n independent observations $(\Theta_{v,i})_{i \in \llbracket 1, n \rrbracket}$, compute $Y_{v,i} = f_v(\Theta_{v,i})$ and transmit the sample $(Y_{v,i})_{i \in \llbracket 1, n \rrbracket}$ to its children. Then the child w would use the sample $(g_{v,w}(Y_{v,i}))_{i \in \llbracket 1, n \rrbracket}$ along with n independent realizations of $(\Theta_{w,i})_{i \in \llbracket 1, n \rrbracket}$, to compute $Y_{w,i} = f_w(X_{w,i}, \Theta_{w,i})$, and then transmit the sample to its children and so on. Finally, a Monte Carlo estimator could be used to estimate any quantity of interest.

However, due to the complexity of the design process, the discipline might not have neither the same schedule nor the same geographical location. Exchanging samples in an online fashion would therefore be difficult in practice. For instance, the discipline v_3 could start performing its computation then stop, even before the discipline v_6 and v_7 are able to start their own computations. This problematic is described in the multidisciplinary optimization literature, under the name of “disciplinary autonomy” and a decomposition-based approach is required [3]. In Uncertainty Quantification, it means that it is not possible to perform a direct Monte Carlo approach. This part is dedicated to developing some decomposition-based approach for uncertainty quantification.

9.2 Sample reweighting

Our strategy to perform uncertainty quantification is based on a decomposition technique that was first proposed under this form in 2012 by S. Amaral, D. Allaire and K. Willcox [5, 6]. This algorithm has two steps.

Offline phase Each discipline v calls locally its own simulation code f_v . The roots generate a sample $(f_v(\Theta_v))_{j \in \llbracket 1, n_v \rrbracket}$ and non roots generate a sample $(Y'_{v,j})_{j \in \llbracket 1, n_v \rrbracket}$, with $Y'_{v,j} = f_v(X'_{v,j}, \Theta_{v,j})$ and the $X'_{v,j}$ being drawn independently according to a *chosen* law $\mu_{X'_v}$.

Online phase At each node v , the sample $(Y'_{v,j})_{j \in \llbracket 1, n_v \rrbracket}$ is reweighted according to a *weighting method* to approximate the true law of Y_v , using the the already weighted samples from its parents. No call of f_v is allowed in this phase.

One can remark that in the offline phase, the order in which the f_v are computed is not important, and the discipline v does not need to wait for its parents $\mathcal{S}(v)$ to obtain some external inputs samples. The law of $\mu_{X'_v}$ is chosen locally by each node v and is called the *proposal* or *synthetic* law. As it is very unlikely that the chosen law of $\mu_{X'_v}$ is exactly the true law of the input μ_{X_v} and that all the Y_v are independent, the online phase seeks to ponderate the synthetic outputs to approximate the theoretical joint law of $(Y_v)_{v \in \mathcal{V}}$. More precisely, for each multi-index

$$j_{\mathcal{V}} = (j_v)_{v \in \mathcal{V}}, \quad j_v \in \llbracket 1, n_v \rrbracket,$$

a weight $w_{j_{\mathcal{V}}}$ is computed, so that weighted probability measure approximates the joint law, *i.e.*

$$\sum_{j_{\mathcal{V}}} w_{j_{\mathcal{V}}} \delta_{(Y'_{v,j_v})_{v \in \mathcal{V}}} \simeq \mathcal{L}((Y_v)_{v \in \mathcal{V}}).$$

The seminal article [5] uses a weighting method based on a estimation of an importance ratio thanks to kernel density estimation. More generally, the field of density ratio estimation [109] proposes a variety of methods to compute such weights, as long as the law of X_v is absolutely continuous with respect to the law of X'_v .

In our context, however, $X_v = (X_{u,v})_{u \in \mathcal{S}(v)}$ is the output of the computer codes of the parents of v . The discipline v might know the extent of the support of X_v , but in a multidimensional case, this support might be a submanifold of the space. Knowing the shape of this submanifold would require a lot of information on the input random variable, that v might not have in practice. This entails the practical impossibility to construct X'_v to verify the absolute continuity. That is why, we are looking for weighting methods that are consistent without the absolute continuity assumption.

9.3 Outline of the part

Chapter 10 focuses on the theoretical study of a weighting method given by a Wasserstein distance minimization and quite interestingly, its weights are expressed in terms of Nearest-Neighbor. We obtain some consistency results in Section 10.3.1, along with some convergence rates in Section 10.3.2. These results are used to compute the convergence rates in the estimation of a quantity of interest in Section 10.4.

Chapter 11, is dedicated to the general weight propagation in graphs. In Section 11.2.1, we define the family of the Weighted Linear Approximation Methods (WLAMs), that are a specific family of weighting methods, for which we establish a local consistency criterion. Under the

assumption of local consistency at each node, we demonstrate the convergence to the theoretical law in the whole graph, in a certain sense, in Section 11.2.2.b. Finally, we define explicitly a discrete Bayesian network that simplify numerical computations in Section 11.3 and this method is applied to an industrial case in Section 11.4.

Chapter 10

Reweighting samples under covariate shift using a Wasserstein distance criterion

This chapter presents the works contained in the preprint [97], currently in revision, for publication in the Electronic Journal of Statistics (EJS).

10.1 Introduction

10.1.1 Covariate shift in U.Q

A common task in Uncertainty Quantification (U.Q) for Computer Experiments [37, 49] is the evaluation of a quantity of interest QI of the form

$$\text{QI} = \mathbb{E}[\phi(Y)],$$

where $Y \in \mathbb{F} = \mathbb{R}^e$ is a random vector which is typically the output of a numerical simulation with uncertain inputs and parameters, and $\phi : \mathbb{R}^e \rightarrow \mathbb{R}$ is the *observable*. Generically, the random vector Y writes

$$Y = f(X, \Theta),$$

where $X \in \mathbb{E} = \mathbb{R}^d$ represents the inputs of the numerical simulation, Θ is the set of parameters of this simulation (which takes its values in some measurable space Θ), and $f : \mathbb{R}^d \times \Theta \rightarrow \mathbb{R}^e$ is the *numerical model*, which is the function actually evaluated by the computer code. We denote by μ_X and μ_Θ the respective probability distributions of X and Θ and assume that these variables are independent. Virtually, if one is able to sample iid realizations $(X_1, \Theta_1), \dots, (X_n, \Theta_n)$ from $\mu_X \otimes \mu_\Theta$, then QI can be estimated by the direct Monte Carlo estimator

$$\widehat{\text{QI}}_n := \frac{1}{n} \sum_{i=1}^n f(X_i, \Theta_i).$$

The present work is motivated by the study of U.Q in complex engineering systems, where

- the input X can be itself the output of possibly several other “upstream” numerical simulations,

- each evaluation of the function f is costly.

When X is modeled by a deterministic variable, this problem can be treated by the so-called Collaborative Optimization methods [25, 125] in Multidisciplinary Analysis and Optimization. When X is a random variable, the implementation of the direct Monte Carlo method is impossible because, in practice, the law μ_X is unknown and one cannot wait for a sample X_1, \dots, X_n to be generated by the upstream numerical simulations before starting running one's own simulation. In contrast, we however assume that μ_Θ is known and that one is able to sample iid realizations $\Theta_1, \dots, \Theta_n$ from this distribution. This naturally leads one to generate a *synthetic* sample $X'_1, \dots, X'_{n_{\text{off}}}$ according to some user-chosen probability measure $\mu_{X'}$ on \mathbb{R}^d , and evaluate the numerical model f on the sample $(X'_1, \Theta_1), \dots, (X'_{n_{\text{off}}}, \Theta_{n_{\text{off}}})$ to obtain a corresponding set of realizations $Y'_1, \dots, Y'_{n_{\text{off}}}$ during some *offline* phase. Once actual realizations $X_1, \dots, X_{n_{\text{on}}}$ become available in a subsequent *online* phase, they have to be used in combination with the synthetic sample to construct an estimator of QI, but evaluations of the numerical model f are no longer allowed.

The assumption that the sequence $\Theta_1, \dots, \Theta_{n_{\text{off}}}$ be independent from $X'_1, \dots, X'_{n_{\text{off}}}$ then ensures that for all $x \in \mathbb{R}^d$,

$$\text{Law}(Y'|X' = x) = \text{Law}(f(x, \Theta)) = \text{Law}(Y|X = x).$$

This situation is known in the statistical learning literature as a *covariate shift* [25], [94, Section 1.4].

10.1.2 Density ratio estimation

Inspired by the *importance sampling* technique, an intuitive approach to estimate QI from the synthetic sample $\{(X'_j, \Theta_j; Y'_j), 1 \leq j \leq n_{\text{off}}\}$ consists in writing

$$\begin{aligned} \text{QI} &= \int_{\mathbb{R}^d \times \Theta} \phi(f(x, \theta)) d\mu_X(x) d\mu_\Theta(\theta) \\ &= \int_{\mathbb{R}^d \times \Theta} \phi(f(x', \theta)) \frac{d\mu_X}{d\mu_{X'}}(x') d\mu_{X'}(x') d\mu_\Theta(\theta), \end{aligned}$$

so that assuming that μ_X is absolutely continuous with respect to $\mu_{X'}$, an unbiased and consistent (in the $n_{\text{off}} \rightarrow +\infty$ limit) estimator of QI is given by

$$\frac{1}{n_{\text{off}}} \sum_{j=1}^{n_{\text{off}}} \rho_{X, X'}(X'_j) \phi(Y'_j), \quad \rho_{X, X'}(x') := \frac{d\mu_X}{d\mu_{X'}}(x').$$

Of course, the Radon–Nikodym derivative $\rho_{X, X'}$ is actually not known in this situation, and it has to be estimated in the online phase thanks to the sample $X_1, \dots, X_{n_{\text{on}}}$. Observe that this problem no longer involves neither $\Theta_1, \dots, \Theta_{n_{\text{off}}}$ nor $Y'_1, \dots, Y'_{n_{\text{off}}}$.

The theoretical issue of estimating the Radon–Nikodym derivative $\rho_{X, X'}$ from independent samples $\mathbf{X}_{n_{\text{on}}} := (X_1, \dots, X_{n_{\text{on}}})$ and $\mathbf{X}'_{n_{\text{off}}} := (X'_1, \dots, X'_{n_{\text{off}}})$ is known in the statistical learning literature as *density ratio estimation* [109]. A rather generic procedure consists in fixing some distance-like function d on the set of probability measures on \mathbb{R}^d , writing

$$\rho_{X, X'} = \arg \min_{\rho} d(\rho \mu_{X'}, \mu_X),$$

and estimating $\rho_{X, X'}$ by

$$\widehat{\rho}_{\mathbf{X}_{n_{\text{on}}}, \mathbf{X}'_{n_{\text{off}}}} := \arg \min_{\rho} d\left(\rho \widehat{\mu}_{\mathbf{X}'_{n_{\text{off}}}}, \widehat{\mu}_{\mathbf{X}_{n_{\text{on}}}}\right),$$

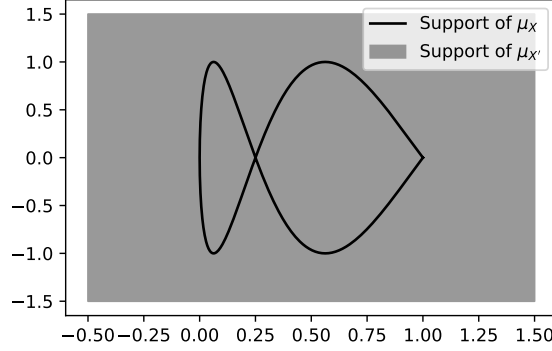


Figure 10.1: Example in which μ_X is not absolutely continuous with respect to $\mu_{X'}$, but its support is included in the support of $\mu_{X'}$.

with the empirical measures

$$\widehat{\mu}_{\mathbf{X}_{n_{\text{on}}}} := \frac{1}{n_{\text{on}}} \sum_{i=1}^{n_{\text{on}}} \delta_{X_i}, \quad \widehat{\mu}_{\mathbf{X}'_{n_{\text{off}}}} := \frac{1}{n_{\text{off}}} \sum_{j=1}^{n_{\text{off}}} \delta_{X'_j}.$$

Since the quantity which is minimized only depends on ρ through the measure $\rho \widehat{\mu}_{\mathbf{X}'_{n_{\text{off}}}}$, and thus through the values $\rho(X'_1), \dots, \rho(X'_{n_{\text{off}}})$, the actual output is a vector of *weights* $\widehat{w}_{n_{\text{off}}} := (\widehat{w}_1, \dots, \widehat{w}_{n_{\text{off}}})$ which approximate the values of $\rho_{X, X'}$ at the points $X'_1, \dots, X'_{n_{\text{off}}}$, and therefore yield the estimator

$$\widehat{\text{QI}}_{n_{\text{off}}, n_{\text{on}}} := \frac{1}{n_{\text{off}}} \sum_{j=1}^{n_{\text{off}}} \widehat{w}_j \phi(Y'_j) \quad (10.1)$$

of QI. This approach has been applied with several choices of distance-like functions \mathbf{d} , such as moment/kernel matching, L^2 distance, Kullback–Leibler divergences; we refer to [109] for an extensive review supplemented with a detailed list of references. Since the primary purpose of these methods is the approximation of the density ratio $\rho_{X, X'}$, the existence of this ratio (and often the existence of positive densities for μ_X and $\mu_{X'}$ with respect to the Lebesgue measure, at least on some bounded subset of \mathbb{R}^d) is almost always a necessary condition for their theoretical analysis.

However, in the Computer Experiment context in which we are interested, this ratio need not exist. Indeed, while some prior information on the law μ_X may be known, such as bounds on its support, mean or dispersion, it may happen for example that some components of the vector X be tied to each other by deterministic relations of the form $h(X) = 0$, so that the actual support of μ_X might be contained in a low-dimensional manifold and difficult to determine precisely, see Figure 10.1.

Therefore, designing a synthetic probability distribution $\mu_{X'}$ with respect to which μ_X is absolutely continuous may actually turn out to be impossible. Nevertheless, one may retain the idea to approximate QI by an estimator of the form (10.1), where the weights $(\widehat{w}_1, \dots, \widehat{w}_{n_{\text{off}}})$ only depend on the samples $\mathbf{X}_{n_{\text{on}}}$ and $\mathbf{X}'_{n_{\text{off}}}$, and are determined by minimizing some distance

between the empirical measure $\widehat{\mu}_{\mathbf{X}_{n_{\text{on}}}}$ and weighted empirical measures of the form

$$\widehat{\mu}_{\mathbf{X}'_{n_{\text{off}}}}^{\mathbf{w}_{n_{\text{off}}}} = \frac{1}{n_{\text{off}}} \sum_{j=1}^{n_{\text{off}}} w_j \delta_{X'_j}, \quad \mathbf{w}_{n_{\text{off}}} := (w_1, \dots, w_{n_{\text{off}}}).$$

This idea was for example applied in the U.Q context in [5–7]. Notice that for $\widehat{\mu}_{\mathbf{X}'_{n_{\text{off}}}}^{\mathbf{w}_{n_{\text{off}}}}$ to be a probability measure, the weights $(w_1, \dots, w_{n_{\text{off}}})$ must satisfy

$$\forall j \in \llbracket 1, n_{\text{off}} \rrbracket, \quad w_j \geq 0, \quad \text{and} \quad \sum_{j=1}^{n_{\text{off}}} w_j = n_{\text{off}}. \quad (10.2)$$

In this chapter, we follow this approach and study the estimator $\widehat{\text{QI}}_{n_{\text{off}}, n_{\text{on}}}$ of QI obtained by minimizing the *Wasserstein distance*, whose definition is recalled below, between $\widehat{\mu}_{\mathbf{X}_{n_{\text{on}}}}$ and $\widehat{\mu}_{\mathbf{X}'_{n_{\text{off}}}}^{\mathbf{w}_{n_{\text{off}}}}$. The main reason for this choice is that, unlike Kullback–Leibler or more general ϕ -divergences, or L^p distances, the Wasserstein distance between two probability measures on \mathbb{R}^d is not sensitive to whether these measures have densities with respect to the Lebesgue measure, or are absolutely continuous with respect to one another. The optimal weights can be expressed terms of *Nearest Neighbor* and our estimator can be interpreted as the Monte Carlo evaluation of a Nearest Neighbor Regression under covariate shift, for which we bound the error explicitly.

10.1.3 Organization of the chapter

The Wasserstein distance is introduced in Section 10.2, as well as the explicit form of the optimal weights and their reformulation in terms of Nearest Neighbor. Section 10.3 is devoted to the analysis of the convergence of the weighted empirical measure to μ_X , in terms of Wasserstein distance. The consistency is studied in Section 10.3.1 and we state our main result in Section 10.3.2, namely the asymptotic rates of convergence. The link between these results and the estimation of QI is discussed in Sections 10.4.1, 10.4.2 and 10.4.3, with the computation of rates of convergence for $\widehat{\text{QI}}_{n_{\text{off}}, n_{\text{on}}}$. Some links with the Nearest Neighbor literature are highlighted in Section 10.4.4. Numerical experiments are performed in Section 10.5, in which the impact of the difference between μ_X and $\mu_{X'}$ is investigated.

10.1.4 Notation

Throughout this chapter, we denote by \mathbb{N} the set of the natural integers including zero and by $\mathbb{N}^* = \mathbb{N} \setminus \{0\}$ the set of the positive integers. Given two integers $n_1 \leq n_2$, the set of the integers between n_1 and n_2 is written $\llbracket n_1, n_2 \rrbracket = \{n_1, \dots, n_2\}$. For $x \in \mathbb{R}$, $\lceil x \rceil$ (resp. $\lfloor x \rfloor$) is the unique integer verifying $x \leq \lceil x \rceil < x + 1$ (resp. $x - 1 < \lfloor x \rfloor \leq x$). For $(x, y) \in \mathbb{R}^2$, we use the join and meet notation $x \wedge y = \min(x, y)$ and $x \vee y = \max(x, y)$. The supremum norm of $\phi : \mathbb{R}^d \rightarrow \mathbb{R}$ is denoted by $\|\phi\|_\infty = \sup_{x \in \mathbb{R}^d} |\phi(x)|$.

10.2 Wasserstein distance minimization and Nearest Neighbor Regression

10.2.1 Optimal weights for Wasserstein distances

We begin by recalling the definition of the Wasserstein distance. Throughout this article, we fix a norm $|\cdot|$ on \mathbb{R}^d , which need not be the Euclidean norm.

Definition 10.2.1 (Wasserstein distance). Let $\mathcal{P}(\mathbb{R}^d)$ be the set of probability measures on \mathbb{R}^d and, for any $q \in [1, +\infty)$, let

$$\mathcal{P}_q(\mathbb{R}^d) = \left\{ \nu \in \mathcal{P}(\mathbb{R}^d) : \int_{\mathbb{R}^d} |x|^q d\nu(x) < +\infty \right\}.$$

The Wasserstein distance of order q between μ and $\nu \in \mathcal{P}_q(\mathbb{R}^d)$ is defined as

$$W_q(\mu, \nu) = \inf \left\{ \int_{\mathbb{R}^d \times \mathbb{R}^d} |x - x'|^q d\gamma(x, x') : \gamma \in \Pi(\mu, \nu) \right\}^{1/q},$$

where $\Pi(\mu, \nu)$ is the set of probability measures on $\mathbb{R}^d \times \mathbb{R}^d$ with marginals μ and ν .

We refer to [120, Section 6] for a general introduction to Wasserstein distances.

This definition allows for an explicit resolution of the minimization problem on $\mathbf{w}_{n_{\text{off}}}$, which relies on the notion of *Nearest Neighbor*. For $x \in \mathbb{R}^d$ and $k \in \llbracket 1, n_{\text{off}} \rrbracket$, we denote by $\text{NN}_{\mathbf{X}'_{n_{\text{off}}}}^{(k)}(x)$ the k -th *Nearest Neighbor* (k -NN) of x among the sample $\mathbf{X}'_{n_{\text{off}}}$, that is to say the k -th closest point to x among $X'_1, \dots, X'_{n_{\text{off}}}$ for the norm $|\cdot|$. If there are several such points, we define $\text{NN}_{\mathbf{X}'_{n_{\text{off}}}}^{(k)}(x)$ to be the point X'_j with lowest index j . We omit the superscript notation (k) when referring to the 1-NN, *i.e.*

$$\text{NN}_{\mathbf{X}'_{n_{\text{off}}}}(x) = \text{NN}_{\mathbf{X}'_{n_{\text{off}}}}^{(1)}(x).$$

In the next statement, for any $i \in \llbracket 1, n_{\text{on}} \rrbracket$ and $l \in \llbracket 1, n_{\text{off}} \rrbracket$, we denote by $j_i^{(l)}$ the (lowest) index j such that $X'_j = \text{NN}_{\mathbf{X}'_{n_{\text{off}}}}^{(l)}(X_i)$.

Proposition 10.2.2 (Optimal vector of weights). Let the k -NN vector of weights $\mathbf{w}_{n_{\text{off}}}^{(k)} = (w_1^{(k)}, \dots, w_{n_{\text{off}}}^{(k)})$ be defined by, for all $j, k \in \llbracket 1, n_{\text{off}} \rrbracket$,

$$w_j^{(k)} := \frac{n_{\text{off}}}{kn_{\text{on}}} \sum_{i=1}^{n_{\text{on}}} \sum_{l=1}^k \mathbb{1}_{\{j=j_i^{(l)}\}}. \quad (10.3)$$

The vector $\mathbf{w}_{n_{\text{off}}}^{(k)}$ satisfies (10.2) and verifies, for all $q \in [1, +\infty)$,

$$W_q^q \left(\widehat{\mu}_{\mathbf{X}_{n_{\text{on}}}}, \widehat{\mu}_{\mathbf{X}'_{n_{\text{off}}}}^{\mathbf{w}_{n_{\text{off}}}^{(k)}} \right) \leq \frac{1}{kn_{\text{on}}} \sum_{i=1}^{n_{\text{on}}} \sum_{l=1}^k \left| X_i - \text{NN}_{\mathbf{X}'_{n_{\text{off}}}}^{(l)}(X_i) \right|^q. \quad (10.4)$$

For $k = 1$, the equality is reached

$$W_q^q \left(\widehat{\mu}_{\mathbf{X}_{n_{\text{on}}}}, \widehat{\mu}_{\mathbf{X}'_{n_{\text{off}}}}^{\mathbf{w}_{n_{\text{off}}}^{(1)}} \right) = \frac{1}{n_{\text{on}}} \sum_{i=1}^{n_{\text{on}}} \left| X_i - \text{NN}_{\mathbf{X}'_{n_{\text{off}}}}(X_i) \right|^q, \quad (10.5)$$

and the vector is optimal in the sense that for any $\mathbf{w}_{n_{\text{off}}} = (w_1, \dots, w_{n_{\text{off}}})$ which also satisfies (10.2), we have

$$W_q \left(\widehat{\mu}_{\mathbf{X}_{n_{\text{on}}}}, \widehat{\mu}_{\mathbf{X}'_{n_{\text{off}}}}^{\mathbf{w}_{n_{\text{off}}}^{(1)}} \right) \leq W_q \left(\widehat{\mu}_{\mathbf{X}_{n_{\text{on}}}}, \widehat{\mu}_{\mathbf{X}'_{n_{\text{off}}}}^{\mathbf{w}_{n_{\text{off}}}} \right). \quad (10.6)$$

In other words, for a given $j \in \llbracket 1, n_{\text{off}} \rrbracket$, $w_j^{(k)}$ is proportional to the number of points X_i of which X'_j is one of the first k Nearest Neighbors. We refer to [79] for a numerical illustration of the use of the vector of weights $\mathbf{w}_{n_{\text{off}}}^{(1)}$ in the context of classification under covariate shift.

Proof. For a general vector of weights $\mathbf{w}_{n_{\text{off}}} = (w_1, \dots, w_{n_{\text{off}}})$ which satisfies (10.2), the Wasserstein distance $W_q^q(\hat{\mu}_{\mathbf{X}_{n_{\text{on}}}}, \hat{\mu}_{\mathbf{X}'_{n_{\text{off}}}}^{\mathbf{w}_{n_{\text{off}}}})$ is the solution of the following optimal transport problem

$$\begin{aligned} & \inf_{(\gamma_{i,j})_{(i,j) \in \llbracket 1, n_{\text{on}} \rrbracket \times \llbracket 1, n_{\text{off}} \rrbracket}} \sum_{i=1}^{n_{\text{on}}} \sum_{j=1}^{n_{\text{off}}} \gamma_{i,j} |X_i - X'_j|^q, \\ & \forall i \in \llbracket 1, n_{\text{on}} \rrbracket, \quad \sum_{j=1}^{n_{\text{off}}} \gamma_{i,j} = \frac{1}{n_{\text{on}}} \quad (\text{marginal condition on } \hat{\mu}_{\mathbf{X}_{n_{\text{on}}}}), \\ & \forall j \in \llbracket 1, n_{\text{off}} \rrbracket, \quad \sum_{i=1}^{n_{\text{on}}} \gamma_{i,j} = \frac{w_j}{n_{\text{off}}} \quad (\text{marginal condition on } \hat{\mu}_{\mathbf{X}'_{n_{\text{off}}}}^{\mathbf{w}_{n_{\text{off}}}}), \\ & \forall (i,j) \in \llbracket 1, n_{\text{on}} \rrbracket \times \llbracket 1, n_{\text{off}} \rrbracket, \quad \gamma_{i,j} \geq 0, \end{aligned} \tag{10.7}$$

where $\gamma_{i,j}$ is the coefficient of the discrete transport plan between δ_{X_i} and $\delta_{X'_j}$. For the k -NN vector of weights $\mathbf{w}_{n_{\text{off}}}^{(k)}$ defined by (10.3), the transport plan

$$\gamma_{i,j}^{(k)} = \frac{1}{kn_{\text{on}}} \sum_{l=1}^k \mathbb{1}_{\{j=j_i^{(l)}\}}$$

satisfies the two marginal conditions. Reordering the terms in the associated cost gives the upper bound of Equation (10.4).

We now prove the equality (10.5) and optimality (10.6) of $\mathbf{w}_{n_{\text{off}}}^{(1)}$ at the same time. For a given $\mathbf{w}_{n_{\text{off}}}$, if we drop the marginal condition on $\hat{\mu}_{\mathbf{X}'_{n_{\text{off}}}}^{\mathbf{w}_{n_{\text{off}}}}$, the values of $(\gamma_{i,j})_{j \in \llbracket 1, n_{\text{off}} \rrbracket}$ for a given i do not constrain the values of $(\gamma_{i',j})_{j \in \llbracket 1, n_{\text{off}} \rrbracket}$ for another $i' \neq i$. Thus, the optimal values can be found by minimizing separately the following subproblem for $i \in \llbracket 1, n_{\text{on}} \rrbracket$

$$\begin{aligned} & \inf_{(\gamma_{i,j})_{j \in \llbracket 1, n_{\text{off}} \rrbracket}} \sum_{j=1}^{n_{\text{off}}} \gamma_{i,j} |X_i - X'_j|^q, \\ & \sum_{j=1}^{n_{\text{off}}} \gamma_{i,j} = \frac{1}{n_{\text{on}}}, \\ & \forall j \in \llbracket 1, n_{\text{off}} \rrbracket, \quad \gamma_{i,j} \geq 0, \end{aligned}$$

the solution of which is trivially $\frac{1}{n_{\text{on}}} |X_i - \text{NN}_{\mathbf{X}'_{n_{\text{off}}}}(X_i)|^q$. As a consequence, we get the estimate

$$W_q^q(\hat{\mu}_{\mathbf{X}_{n_{\text{on}}}}, \hat{\mu}_{\mathbf{X}'_{n_{\text{off}}}}^{\mathbf{w}_{n_{\text{off}}}}) \geq \frac{1}{n_{\text{on}}} \sum_{i=1}^{n_{\text{on}}} |X_i - \text{NN}_{\mathbf{X}'_{n_{\text{off}}}}(X_i)|^q \tag{10.8}$$

for any $\mathbf{w}_{n_{\text{off}}}$ satisfying Equation (10.2). Taking $\mathbf{w}_{n_{\text{off}}} = \mathbf{w}_{n_{\text{off}}}^{(1)}$ in the left-hand side and combining this inequality with (10.4) for $k = 1$, we obtain both the equality (10.5) and optimality (10.6). \square

Remark 10.2.3. *In order to alleviate notation, from now on we shall write $\hat{\mu}_{\mathbf{X}'_{n_{\text{off}}}}^{(k)} = \hat{\mu}_{\mathbf{X}'_{n_{\text{off}}}}^{\mathbf{w}_{n_{\text{off}}}^{(k)}}$.*

10.2.2 NNR reformulation

With the choice of weights $\mathbf{w}_{n_{\text{off}}}^{(k)}$ introduced in Proposition 10.2.2, the resulting estimator of QI writes

$$\widehat{\text{QI}}_{n_{\text{off}}, n_{\text{on}}}^{(k)} = \frac{1}{n_{\text{on}}} \sum_{i=1}^{n_{\text{on}}} \frac{1}{k} \sum_{l=1}^k \phi \left(Y'_{j_i^{(l)}} \right),$$

which makes the method very close to Nearest Neighbor Regression (NNR) [18, Chapter 9], since it may be reformulated as the following two-step procedure:

1. define the *regression function* ψ of $\phi(Y)$ on X by, for any $x \in \mathbb{R}^d$,

$$\psi(x) := \mathbb{E}[\phi(Y)|X = x] = \mathbb{E}[\phi(f(x, \Theta))], \quad (10.9)$$

and let the k -NNR estimator of $\psi(x)$ be given by

$$\widehat{\psi}_{n_{\text{off}}}^{(k)}(x) := \frac{1}{k} \sum_{l=1}^k \phi \left(Y'_{j^{(l)}(x)} \right), \quad (10.10)$$

where $j^{(l)}(x)$ is the (lowest) index j such that $X'_j = \text{NN}_{\mathbf{X}'_{n_{\text{off}}}}^{(l)}(x)$;

2. approximate the expectation

$$\text{QI} = \mathbb{E}[\phi(Y)] = \mathbb{E}[\psi(X)]$$

by the empirical mean

$$\frac{1}{n_{\text{on}}} \sum_{i=1}^{n_{\text{on}}} \widehat{\psi}_{n_{\text{off}}}^{(k)}(X_i) = \widehat{\text{QI}}_{n_{\text{off}}, n_{\text{on}}}^{(k)}.$$

In this context, the peculiar fact that the law of the *evaluation* set $X_1, \dots, X_{n_{\text{on}}}$ differs from the law of the *training* set $X'_1, \dots, X'_{n_{\text{off}}}$ is referred to as *domain adaptation* [94]. From a U.Q point of view, the first step may be reinterpreted as the construction, based on the Nearest Neighbor approach, of a metamodel for the regression function ψ .

10.3 Convergence analysis

As is evidenced by its reformulation in terms of NNR, the method does not actually depend on the choice of the observable $\phi \circ f$, and its primary purpose is rather the direct estimation of the law μ_X by the weighted empirical measure $\widehat{\mu}_{\mathbf{X}'_{n_{\text{off}}}}^{(k)}$. Rewriting

$$\text{QI} = \mathbb{E}[\phi(Y)] = \int_{\mathbb{R}^d} \psi(x) d\mu_X(x),$$

we observe that estimates on the approximation of QI by $\widehat{\text{QI}}_{n_{\text{off}}, n_{\text{on}}}^{(k)}$ which are uniform in ϕ can be obtained from estimates on the approximation of μ_X by $\widehat{\mu}_{\mathbf{X}'_{n_{\text{off}}}}^{(k)}$. Therefore, we turn our attention to the convergence, when the sizes n_{off} and n_{on} of the two samples go to ∞ , of $\widehat{\mu}_{\mathbf{X}'_{n_{\text{off}}}}^{(k)}$ to μ_X . We naturally work with Wasserstein distances.

10.3.1 Consistency

Let us fix $q \in [1, +\infty)$ and use Jensen's inequality to write

$$\mathbb{E} \left[W_q^q \left(\mu_X, \hat{\mu}_{\mathbf{X}'_{n_{\text{off}}}}^{(k)} \right) \right] \leq 2^{q-1} \left(\mathbb{E} \left[W_q^q \left(\mu_X, \hat{\mu}_{\mathbf{X}_{n_{\text{on}}}} \right) \right] + \mathbb{E} \left[W_q^q \left(\hat{\mu}_{\mathbf{X}_{n_{\text{on}}}}, \hat{\mu}_{\mathbf{X}'_{n_{\text{off}}}}^{(k)} \right) \right] \right). \quad (10.11)$$

As soon as there exists $s > q$ such that $\mathbb{E}[|X|^s] < +\infty$, the first term $\mathbb{E}[W_q^q(\mu_X, \hat{\mu}_{\mathbf{X}_{n_{\text{on}}}})]$ is known to converge to 0 when $n_{\text{on}} \rightarrow +\infty$ and explicit rates are available [50], see also the discussion in Subsection 10.4.1 below. We therefore focus on the second term and first observe that, by Proposition 10.2.2, we have

$$\begin{aligned} \mathbb{E} \left[W_q^q \left(\hat{\mu}_{\mathbf{X}_{n_{\text{on}}}}, \hat{\mu}_{\mathbf{X}'_{n_{\text{off}}}}^{(1)} \right) \right] &= \mathbb{E} \left[\frac{1}{n_{\text{on}}} \sum_{i=1}^{n_{\text{on}}} \left| X_i - \text{NN}_{\mathbf{X}'_{n_{\text{off}}}}(X_i) \right|^q \right] \\ &= \mathbb{E} \left[\left| X - \text{NN}_{\mathbf{X}'_{n_{\text{off}}}}(X) \right|^q \right], \end{aligned} \quad (10.12)$$

for $k = 1$, and

$$\begin{aligned} \mathbb{E} \left[W_q^q \left(\hat{\mu}_{\mathbf{X}_{n_{\text{on}}}}, \hat{\mu}_{\mathbf{X}'_{n_{\text{off}}}}^{(k)} \right) \right] &\leq \mathbb{E} \left[\frac{1}{kn_{\text{on}}} \sum_{i=1}^{n_{\text{on}}} \sum_{l=1}^k \left| X_i - \text{NN}_{\mathbf{X}'_{n_{\text{off}}}}^{(l)}(X_i) \right|^q \right] \\ &= \frac{1}{k} \sum_{l=1}^k \mathbb{E} \left[\left| X - \text{NN}_{\mathbf{X}'_{n_{\text{off}}}}^{(l)}(X) \right|^q \right], \end{aligned} \quad (10.13)$$

for $k \geq 2$. Observe that the right-hand side of both (10.12) and (10.13) no longer depend on n_{on} .

We now formulate two crucial assumptions and then state our first main result. For all $x \in \mathbb{R}^d$ and $r \geq 0$, we denote $B(x, r) := \{x' \in \mathbb{R}^d : |x - x'| \leq r\}$, and recall that the *support* of a probability measure $\nu \in \mathcal{P}(\mathbb{R}^d)$ is defined by

$$\text{supp}(\nu) := \left\{ x \in \mathbb{R}^d : \forall r > 0, \nu(B(x, r)) > 0 \right\}.$$

Assumption 10.3.1 (Support condition). *We have $\text{supp}(\mu_X) \subset \text{supp}(\mu_{X'})$.*

Assumption 10.3.2 (Min-integrability). *There exists an integer $m_0 \geq 1$ such that*

$$\mathbb{E} \left[\min_{j \in \llbracket 1, m_0 \rrbracket} |X'_j| \right] < +\infty.$$

Theorem 10.3.3 (Consistency). *Let Assumptions 10.3.1 and 10.3.2 hold. For all $q \in [1, +\infty)$ such that $\mathbb{E}[|X|^q] < +\infty$, and any sequence of positive integers $(k_n)_{n \geq 1}$ such that $k_n/n \rightarrow 0$ when $n \rightarrow \infty$, we have*

$$\lim_{n_{\text{off}} \rightarrow +\infty} \mathbb{E} \left[W_q^q \left(\hat{\mu}_{\mathbf{X}_{n_{\text{on}}}}, \hat{\mu}_{\mathbf{X}'_{n_{\text{off}}}}^{(k_n)} \right) \right] = 0,$$

uniformly in n_{on} .

Remark 10.3.4 (On Assumption 10.3.2). *Assumption 10.3.2 is obviously satisfied if X' has a finite first order moment, but also for some heavy-tailed distributions. It writes under the equivalent form*

$$\int_0^\infty \mathbb{P}(|X'| > r)^{m_0} dr < +\infty,$$

which may be easier to check. An example of a random variable which does not satisfy this assumption, in dimension $d = 1$, is $X' = \exp(1/U)$ where U is a uniform random variable on $[0, 1]$.

Theorem 10.3.3 is proved in Subsection 10.3.3.

10.3.2 Rates of convergence

The next step of our study consists in complementing Theorem 10.3.3 with a rate of convergence. We first discuss the case $k = 1$. Following (10.12), we start by writing

$$\begin{aligned} \mathbb{E} \left[W_q^q \left(\widehat{\mu}_{\mathbf{X}_{n_{\text{on}}}}, \widehat{\mu}_{\mathbf{X}'_{n_{\text{off}}}}^{(1)} \right) \right] &= \mathbb{E} \left[\left| X - \text{NN}_{\mathbf{X}'_{n_{\text{off}}}}(X) \right|^q \right] \\ &= \mathbb{E} \left[\mathbb{E} \left[\left| X - \text{NN}_{\mathbf{X}'_{n_{\text{off}}}}(X) \right|^q \middle| X \right] \right], \end{aligned} \quad (10.14)$$

and observe that for any $x \in \text{supp}(\mu_X)$, $|x - \text{NN}_{\mathbf{X}'_{n_{\text{off}}}}(x)| = \min_{j \in \llbracket 1, n_{\text{off}} \rrbracket} |x - X'_j|$. If there is an open set U of \mathbb{R}^d containing x and such that $\mu_{X'}(\cdot \cap U)$ has a density $p_{X'}$ with respect to the Lebesgue measure which is continuous at x , then an elementary computation shows that, for all $r \geq 0$,

$$\lim_{n_{\text{off}} \rightarrow +\infty} \mathbb{P} \left(n_{\text{off}}^{1/d} \min_{j \in \llbracket 1, n_{\text{off}} \rrbracket} |x - X'_j| > r \right) = \exp \left(-r^d v_d p_{X'}(x) \right),$$

where v_d denotes the volume of the unit sphere of \mathbb{R}^d for the norm $|\cdot|$. If $p_{X'}(x) > 0$ then this indicates that the correct order of convergence in Theorem 10.3.3 should be $n_{\text{off}}^{-q/d}$. If $p_{X'}(x) = 0$, or if the measure $\mu_{X'}(\cdot \cap U)$ is not absolutely continuous with respect to the Lebesgue measure, it is easy to construct elementary examples yielding different rates of convergence; see also [18, Chapter 2] for the singular case. We leave these peculiarities apart and work under the following strengthening of the support condition of Assumption 10.3.1.

Assumption 10.3.5 (Strong support condition). *There exists an open set $U \subset \mathbb{R}^d$ which contains $\text{supp}(\mu_X)$ and such that:*

- (i) *the measure $\mu_{X'}(\cdot \cap U)$ has a density $p_{X'}$ with respect to the Lebesgue measure;*
- (ii) *the density $p_{X'}$ is continuous and positive on U ;*
- (iii) *there exist $\kappa \in (0, 1]$ and $r_\kappa > 0$ such that, for any $x \in U$, for any $r \in [0, r_\kappa]$,*

$$\mathbb{P} (X' \in B(x, r)) \geq \kappa p_{X'}(x) v_d r^d.$$

Obviously, Assumption 10.3.5 implies Assumption 10.3.1 because then $\text{supp}(\mu_X) \subset U \subset \text{supp}(\mu_{X'})$. Part (iii) of Assumption 10.3.5 was introduced in [52] in the context of Nearest Neighbor Classification, and called *Strong minimal mass assumption* there.

Under Assumption 10.3.5, for all $x \in \text{supp}(\mu_X)$, a positive random variable Z such that $\mathbb{P}(Z > r) = \exp(-r^d v_d p_{X'}(x))$ has moments

$$\mathbb{E} [Z^q] = \frac{\Gamma(1 + q/d)}{(v_d p_{X'}(x))^{q/d}},$$

where Γ denotes Euler's Gamma function. Therefore, as soon as the sequence

$$n_{\text{off}}^{q/d} \min_{j \in \llbracket 1, n_{\text{off}} \rrbracket} |X - X'_j|^q$$

is uniformly integrable, the normalized quantity

$$n_{\text{off}}^{q/d} \mathbb{E} \left[W_q^q \left(\widehat{\mu}_{\mathbf{X}_{n_{\text{on}}}}, \widehat{\mu}_{\mathbf{X}'_{n_{\text{off}}}}^{(1)} \right) \right]$$

converges to

$$\frac{\Gamma(1 + q/d)}{v_d^{q/d}} \mathbb{E} \left[\frac{1}{p_{X'}(X)^{q/d}} \right],$$

when n_{off} goes to infinity. This statement appears in the literature of stochastic quantization of probability distributions [55, Theorem 9.1]. Here, we provide an explicit moment condition ensuring uniform integrability.

Assumption 10.3.6 (Moments). *In addition to Assumption 10.3.5, the condition*

$$\mathbb{E} \left[\frac{1 + |X|^q}{p_{X'}(X)^{q/d}} \right] < +\infty$$

holds.

Assumptions 10.3.5 and 10.3.6 are discussed in more detail below. We now state our second main result.

Theorem 10.3.7 (Convergence rates for $k = 1$). *Let Assumptions 10.3.2 and 10.3.5 hold, and let $q \in [1, +\infty)$ be such that Assumption 10.3.6 holds. Then we have*

$$\lim_{n_{\text{off}} \rightarrow +\infty} n_{\text{off}}^{q/d} \mathbb{E} \left[W_q^q \left(\hat{\mu}_{\mathbf{X}_{n_{\text{on}}}}, \hat{\mu}_{\mathbf{X}'_{n_{\text{off}}}}^{(1)} \right) \right] = \frac{\Gamma(1 + q/d)}{v_d^{q/d}} \mathbb{E} \left[\frac{1}{p_{X'}(X)^{q/d}} \right].$$

Theorem 10.3.7 is proved in Subsection 10.3.3.

We now discuss the estimation of $\hat{\mu}_{\mathbf{X}_{n_{\text{on}}}}$ by the weighted empirical measure $\hat{\mu}_{\mathbf{X}'_{n_{\text{off}}}}^{(k)}$ for an arbitrary $k \in \llbracket 1, n_{\text{off}} \rrbracket$. By (10.8), we first observe that we always have

$$W_q \left(\hat{\mu}_{\mathbf{X}_{n_{\text{on}}}}, \hat{\mu}_{\mathbf{X}'_{n_{\text{off}}}}^{(k)} \right) \geq W_q \left(\hat{\mu}_{\mathbf{X}_{n_{\text{on}}}}, \hat{\mu}_{\mathbf{X}'_{n_{\text{off}}}}^{(1)} \right),$$

so that the estimation of $\hat{\mu}_{\mathbf{X}_{n_{\text{on}}}}$ is deteriorated by increasing the number of neighbors. Still, in the asymptotic regime of Theorem 10.3.3, a bound of the same order of magnitude as Theorem 10.3.7 may be obtained.

Corollary 10.3.8 (Convergence rates for k -NN). *Under the assumptions of Theorem 10.3.7, for any nondecreasing sequence of positive integers $(k_n)_{n \geq 1}$ such that $k_n/n \rightarrow 0$ when $n \rightarrow \infty$, we have*

$$\limsup_{n_{\text{off}} \rightarrow +\infty} \left(\frac{n_{\text{off}}}{k_{n_{\text{off}}}} \right)^{q/d} \mathbb{E} \left[W_q^q \left(\hat{\mu}_{\mathbf{X}_{n_{\text{on}}}}, \hat{\mu}_{\mathbf{X}'_{n_{\text{off}}}}^{(k_{n_{\text{off}}})} \right) \right] \leq c_{d,q} \frac{\Gamma(1 + q/d)}{v_d^{q/d}} \mathbb{E} \left[\frac{1}{p_{X'}(X)^{q/d}} \right],$$

with some constant $c_{d,q} > 1$.

Corollary 10.3.8 is proved in Subsection 10.3.3, where the explicit expression of the constant $c_{d,q}$ is also given.

Remark 10.3.9 (Optimal synthetic distribution). *When X also has a density p_X with respect to the Lebesgue measure, an interesting fact is that the minimum of $\mathbb{E} \left[1/p_{X'}(X)^{q/d} \right]$ over the probability measure $p_{X'}$ is not reached when $p_{X'} = p_X$. Instead, according to [126], the minimum is attained when $p_{X'}(x) \propto p_X(x)^{d/(q+d)}$.*

Let us conclude this subsection with some comments on Assumptions 10.3.5 and 10.3.6. When X has a compact support, Assumptions 10.3.5 and 10.3.6 are verified as soon as $\mu_{X'}$ has a continuous density $p_{X'}$ which is bounded from below and above on an open set containing the support of μ_X . Indeed, in that case this open set can be taken as U and contains an ϵ -neighborhood of $\text{supp}(\mu_X)$ for some $\epsilon > 0$. Then, Assumption 10.3.5(iii) is verified with $r_\kappa = \epsilon$ and $\kappa = \inf_{x \in U} p_{X'}(x) / \sup_{x \in U} p_{X'}(x)$.

Assumptions 10.3.5 and 10.3.6 also hold in some nontrivial noncompact cases. An example of a sufficient condition for Assumption 10.3.5, which does not depend on μ_X , is given in the next statement and is proved in Subsection 10.3.3.

Lemma 10.3.10 (Radial density - Sufficient condition for Assumption 10.3.5). *Let $\|\cdot\|$ be a norm on \mathbb{R}^d , induced by an inner product and not necessarily identical to $|\cdot|$. If $\mu_{X'}$ has a density $p_{X'}$ with respect to the Lebesgue measure on \mathbb{R}^d , which writes $p_{X'}(x) = h(\|x - x_0\|)$ for some $x_0 \in \mathbb{R}^d$ and $h : [0, +\infty) \rightarrow \mathbb{R}$ continuous, positive and nonincreasing, then Assumption 10.3.5 holds with $U = \mathbb{R}^d$.*

We also refer to [52, Section 2.4] for a discussion of this assumption.

Assumption 10.3.6 gives a relationship between μ_X and $p_{X'}$ to ensure the convergence. In essence, it asserts that the tail of μ_X must be quite lightweight compared to the tail of $p_{X'}$. For instance, if X and X' are centered Gaussian vectors with respective covariance $\sigma^2 I_d$ and $\sigma'^2 I_d$, then by Lemma 10.3.10, Assumption 10.3.5 is satisfied with $U = \mathbb{R}^d$, and it is easy to check that for $q \in [1, +\infty)$, Assumption 10.3.6 holds if and only if $\sigma'^2 > \sigma^2 q/d$.

10.3.3 Proofs

In this subsection, we present the proofs of Theorems 10.3.3 and 10.3.7, Corollary 10.3.8 and Lemma 10.3.10.

Proof of Theorem 10.3.3. We begin our proof with the constant case $k_n = 1$ for all n and then extend it to the general case. We recall that by (10.12),

$$\mathbb{E} \left[W_q^q \left(\widehat{\mu}_{\mathbf{X}_{n_{\text{on}}}}, \widehat{\mu}_{\mathbf{X}'_{n_{\text{off}}}}^{(1)} \right) \right] = \mathbb{E} \left[\left| X - \text{NN}_{\mathbf{X}'_{n_{\text{off}}}}(X) \right|^q \right] = \mathbb{E} \left[\min_{j \in \llbracket 1, n_{\text{off}} \rrbracket} |X - X'_j|^q \right].$$

By Assumption 10.3.1, $X \in \text{supp}(\mu_{X'})$ almost surely, so that we deduce from Lemma 2.2 in [18, Chapter 2] that

$$\min_{j \in \llbracket 1, n_{\text{off}} \rrbracket} |X - X'_j|^q \xrightarrow[n_{\text{off}} \rightarrow +\infty]{a.s.} 0.$$

Let m_0 be the integer given by Assumption 10.3.2, we have

$$\min_{j \in \llbracket 1, n_{\text{off}} \rrbracket} |X - X'_j|^q \leq 2^{q-1} \left(|X|^q + \min_{j \in \llbracket 1, n_{\text{off}} \rrbracket} |X'_j|^q \right).$$

The random variable $|X|^q$ is integrable by assumption and for $n_{\text{off}} \geq \lceil q \rceil m_0$, the inequality

$$\begin{aligned} \mathbb{E} \left[\min_{j \in \llbracket 1, n_{\text{off}} \rrbracket} |X'_j|^q \right] &\leq \mathbb{E} \left[\min_{j \in \llbracket 1, n_{\text{off}} \rrbracket} |X'_j|^{\lceil q \rceil} \right]^{q/\lceil q \rceil} \\ &\leq \mathbb{E} \left[\min_{j \in \llbracket 1, m_0 \rrbracket} |X'_j| \min_{j \in \llbracket m_0+1, 2m_0 \rrbracket} |X'_j| \cdots \min_{j \in \llbracket (\lceil q \rceil - 1)m_0+1, \lceil q \rceil m_0 \rrbracket} |X'_j| \right]^{q/\lceil q \rceil} \\ &\leq \mathbb{E} \left[\min_{j \in \llbracket 1, m_0 \rrbracket} |X'_j| \right]^q < +\infty \end{aligned}$$

holds. Then by the dominated convergence theorem,

$$\mathbb{E} \left[\min_{j \in \llbracket 1, n_{\text{off}} \rrbracket} |X - X'_j|^q \right] \xrightarrow{n_{\text{off}} \rightarrow +\infty} 0.$$

For the general case $k_n/n \rightarrow 0$, we adapt directly the proof of [18, Theorem 2.4] to the context $\mu_X \neq \mu_{X'}$. Let us fix $l \in \llbracket 1, n_{\text{off}}/2 \rrbracket$ and partition the set $\{X'_1, \dots, X'_{n_{\text{off}}}\}$ into $2l$ sets of size n_1, \dots, n_{2l} with, for all $j \in \llbracket 1, 2l \rrbracket$,

$$\lfloor n_{\text{off}}/2l \rfloor \leq n_j \leq \lfloor n_{\text{off}}/2l \rfloor + 1.$$

We denote by $\text{NN}_{\mathbf{X}'_{n_{\text{off}}}}(1,j)$ the 1-NN among the subset j . By the definition of $\text{NN}_{\mathbf{X}'_{n_{\text{off}}}}^{(l)}$, there are at least l subsets j for which

$$|X - \text{NN}_{\mathbf{X}'_{n_{\text{off}}}}^{(l)}(X)| \leq |X - \text{NN}_{\mathbf{X}'_{n_{\text{off}}}}(1,j)(X)|,$$

therefore

$$|X - \text{NN}_{\mathbf{X}'_{n_{\text{off}}}}^{(l)}(X)|^q \leq \frac{1}{l} \sum_{j=1}^{2l} |X - \text{NN}_{\mathbf{X}'_{n_{\text{off}}}}(1,j)(X)|^q,$$

and consequently

$$\mathbb{E} \left[|X - \text{NN}_{\mathbf{X}'_{n_{\text{off}}}}^{(l)}(X)|^q \right] \leq 2 \mathbb{E} \left[|X - \text{NN}_{\mathbf{X}'_{\lfloor n_{\text{off}}/2l \rfloor}}(X)|^q \right].$$

Finally, we deduce from (10.13) that, as soon as $k_{n_{\text{off}}} \leq n_{\text{off}}/2$,

$$\begin{aligned} \mathbb{E} \left[W_q^q \left(\widehat{\mu}_{\mathbf{X}_{n_{\text{on}}}}, \widehat{\mu}_{\mathbf{X}'_{n_{\text{off}}}}^{(k_{n_{\text{off}}})} \right) \right] &\leq \frac{1}{k_{n_{\text{off}}}} \sum_{l=1}^{k_{n_{\text{off}}}} \mathbb{E} \left[|X - \text{NN}_{\mathbf{X}'_{n_{\text{off}}}}^{(l)}(X)|^q \right] \\ &\leq \frac{2}{k_{n_{\text{off}}}} \sum_{l=1}^{k_{n_{\text{off}}}} \mathbb{E} \left[|X - \text{NN}_{\mathbf{X}'_{\lfloor n_{\text{off}}/2l \rfloor}}(X)|^q \right] \\ &\leq 2 \mathbb{E} \left[|X - \text{NN}_{\mathbf{X}'_{\lfloor n_{\text{off}}/2k_{n_{\text{off}}} \rfloor}}(X)|^q \right], \end{aligned} \quad (10.15)$$

which goes to 0 as a consequence of the first part of the proof when $n_{\text{off}}/2k_{n_{\text{off}}}$ goes to infinity. \square

Proof of Theorem 10.3.7. By (10.12), we have

$$\begin{aligned} \mathbb{E} \left[n_{\text{off}}^{q/d} W_q^q \left(\widehat{\mu}_{\mathbf{X}_{n_{\text{on}}}}, \widehat{\mu}_{\mathbf{X}'_{n_{\text{off}}}}^{(1)} \right) \right] &= \mathbb{E} \left[\mathbb{E} \left[n_{\text{off}}^{q/d} \min_{j \in \llbracket 1, n_{\text{off}} \rrbracket} |X - X'_j|^q \middle| X \right] \right] \\ &= \int_{\mathbb{R}^d} \int_0^{+\infty} \mathbb{P} \left(n_{\text{off}}^{q/d} \min_{j \in \llbracket 1, n_{\text{off}} \rrbracket} |x - X'_j|^q > t \right) dt d\mu_X(x) \\ &= \int_{\mathbb{R}^d} \int_0^{+\infty} \mathbb{P} \left(n_{\text{off}}^{q/d} |x - X'|^q > t \right)^{n_{\text{off}}} dt d\mu_X(x), \end{aligned} \quad (10.16)$$

by independence of the X'_j . The proof consists in computing the pointwise limit of $\mathbb{P}(n_{\text{off}}^{p/d} |x - Y|^p > t)^{n_{\text{off}}}$ for $(x, t) \in \text{supp}(\mu_X) \times \mathbb{R}^+$ and then establishing the convergence of the integral via the dominated convergence theorem.

Pointwise convergence. We have

$$\begin{aligned} \mathbb{P}(n_{\text{off}}^{q/d}|x - X'|^q > t)^{n_{\text{off}}} &= \left(1 - \mathbb{P}(|x - X'| \leq t^{1/q}/n_{\text{off}}^{1/d})\right)^{n_{\text{off}}} \\ &= \exp\left(n_{\text{off}} \log\left(1 - \mathbb{P}(|x - X'| \leq t^{1/q}/n_{\text{off}}^{1/d})\right)\right). \end{aligned}$$

By Assumption 10.3.5, we have

$$\mathbb{P}(|x - X'| \leq t^{1/q}/n_{\text{off}}^{1/d}) = p_{X'}(x)v_d t^{d/q}/n_{\text{off}} + o(1/n_{\text{off}}),$$

with v_d the volume of the unit sphere. Thus

$$n_{\text{off}} \log\left(1 - \mathbb{P}(|x - X'| \leq t^{1/q}/n_{\text{off}}^{1/d})\right) = -p_{X'}(x)v_d t^{d/q} + o(1),$$

and we conclude that

$$\mathbb{P}(n_{\text{off}}^{q/d}|x - X'|^q > t)^{n_{\text{off}}} \xrightarrow[n_{\text{off}} \rightarrow +\infty]{} \exp\left(-p_{X'}(x)v_d t^{d/q}\right).$$

Dominated convergence. Let $r_\kappa > 0$ be given by Assumption 10.3.5. We split the integral in the right-hand side of (10.16) and study each term separately

$$\int_{\mathbb{R}^d} \int_0^{+\infty} \mathbb{P}(n_{\text{off}}^{q/d}|x - X'|^q > t)^{n_{\text{off}}} dt d\mu_X(x) = \text{I} + \text{II}$$

with

$$\begin{aligned} \text{I} &:= \int_{\mathbb{R}^d} \int_0^{r_\kappa^q n_{\text{off}}^{q/d}} \mathbb{P}(|x - X'| > t^{1/q}/n_{\text{off}}^{1/d})^{n_{\text{off}}} dt d\mu_X(x), \\ \text{II} &:= \int_{\mathbb{R}^d} \int_{r_\kappa^q n_{\text{off}}^{q/d}}^{+\infty} \mathbb{P}(|x - X'| > t^{1/q}/n_{\text{off}}^{1/d})^{n_{\text{off}}} dt d\mu_X(x). \end{aligned}$$

Convergence of I. For $t \in [0, r_\kappa^q n_{\text{off}}^{q/d}]$, we have $t^{1/q}/n_{\text{off}}^{1/d} \leq r_\kappa$ and thus

$$\begin{aligned} \mathbb{P}(|x - X'| > t^{1/q}/n_{\text{off}}^{1/d})^{n_{\text{off}}} &= \left(1 - \mathbb{P}(|x - X'| \leq t^{1/q}/n_{\text{off}}^{1/d})\right)^{n_{\text{off}}} \\ &\leq \left(1 - \frac{p_{X'}(x)v_d \kappa t^{d/q}}{n_{\text{off}}}\right)^{n_{\text{off}}} \end{aligned}$$

by Assumption 10.3.5.

Using the elementary inequality $(1 - a/n)^n \leq \exp(-a)$ for $a \leq n$, we can write

$$\mathbb{P}(|x - X'| > t^{1/q}/n_{\text{off}}^{1/d})^{n_{\text{off}}} \leq \exp(-\kappa v_d p_{X'}(x) t^{d/q}).$$

This bound does not depend on n_{off} and the integral

$$\begin{aligned} \int_{\mathbb{R}^d} \int_0^{+\infty} \exp\left(-\kappa v_d p_{X'}(x) t^{d/q}\right) dt d\mu_X(x) &= \int_{\mathbb{R}^d} \frac{\Gamma(1 + q/d)}{(\kappa v_d p_{X'}(x))^{q/d}} d\mu_X(x) \\ &= \frac{\Gamma(1 + q/d)}{(\kappa v_d)^{q/d}} \mathbb{E}\left[\frac{1}{p_{X'}(X)^{q/d}}\right], \end{aligned}$$

is finite by Assumption 10.3.6. We therefore deduce from the dominated convergence theorem that

$$I \xrightarrow{n_{\text{off}} \rightarrow +\infty} \int_{\mathbb{R}^d} \int_0^{+\infty} \exp\left(-p_{X'}(x)v_d t^{d/q}\right) dt \mu_X(dx) = \frac{\Gamma(1+q/d)}{v_d^{q/d}} \mathbb{E}\left[\frac{1}{p_{X'}(X)^{q/d}}\right].$$

Convergence of II. Let $n_{\text{off}} \geq 2(q+1)m_0$. Using the change of variable $r^q = t/n_{\text{off}}^{q/d}$, we have

$$\begin{aligned} \text{II} &= q \int_{\mathbb{R}^d} \int_{r_\kappa}^{+\infty} n_{\text{off}}^{q/d} r^{q-1} \mathbb{P}(|x - X'| > r)^{n_{\text{off}}} dr d\mu_X(x) \\ &\leq q \int_{\mathbb{R}^d} \int_{r_\kappa}^{+\infty} V_{n_{\text{off}}}(x, r) dr d\mu_X(x), \end{aligned}$$

with

$$V_{n_{\text{off}}}(x, r) := n_{\text{off}}^{q/d} \mathbb{P}(|x - X'| > r_\kappa)^{n_{\text{off}} - (q+1)m_0} r^{q-1} \mathbb{P}(|x - X'| > r)^{(q+1)m_0}.$$

As $\mathbb{P}(|x - X'| > r_\kappa) < 1$ for all x in U , by Assumption 10.3.5, $V_{n_{\text{off}}}(x, r)$ is pointwise convergent to 0 on the support of μ_X . We check that $V_{n_{\text{off}}}(x, r)$ is bounded from above by an integrable function which does not depend on n_{off} . Let us denote $n_{\text{off}}' = n_{\text{off}} - (q+1)m_0 \geq n_{\text{off}}/2$ and rewrite

$$\begin{aligned} n_{\text{off}}^{q/d} \mathbb{P}(|x - X'| > r_\kappa)^{n_{\text{off}} - (q+1)m_0} &= \left(\frac{n_{\text{off}}}{n_{\text{off}}'}\right)^{q/d} n_{\text{off}}'^{q/d} \mathbb{P}(|x - X'| > r_\kappa)^{n_{\text{off}}'} \\ &\leq 2^{q/d} n_{\text{off}}'^{q/d} (1 - \mathbb{P}(|x - X'| \leq r_\kappa))^{n_{\text{off}}'} \\ &\leq 2^{q/d} n_{\text{off}}'^{q/d} \exp\left(-n_{\text{off}}' \kappa p_{X'}(x) v_d r_\kappa^d\right), \end{aligned}$$

where we have used Assumption 10.3.5 and the elementary above inequality at the third line. We deduce that

$$n_{\text{off}}^{q/d} \mathbb{P}(|x - X'| > r_\kappa)^{n_{\text{off}} - (q+1)m_0} \leq \frac{C_1}{p_{X'}(x)^{q/d}}, \quad C_1 := \frac{2^{q/d}}{(\kappa v_d r_\kappa^d)^{q/d}} \sup_{u \geq 0} (u^{q/d} e^{-u}),$$

so that

$$V_{n_{\text{off}}}(x, r) \leq \tilde{V}(x, r) := \frac{C_1}{p_{X'}(x)^{q/d}} r^{q-1} \mathbb{P}(|x - X'| > r)^{(q+1)m_0}. \quad (10.17)$$

To complete the proof, we verify that $\tilde{V}(x, r)$ is integrable on $U \times [r_\kappa, +\infty)$. We first fix $x \in \mathbb{R}^d$ and estimate the integral of $\tilde{V}(x, r)$ in r . Using the fact that if $|x - X'| > r$ then $|X'| > r - |x|$, we first write

$$\begin{aligned} \int_{r_\kappa}^{+\infty} r^{q-1} \mathbb{P}(|x - X'| > r)^{(q+1)m_0} dr &\leq \int_0^{+\infty} r^{q-1} \mathbb{P}(|X'| > r - |x|)^{(q+1)m_0} dr \\ &= \int_{-|x|}^{+\infty} (r + |x|)^{q-1} \mathbb{P}(|X'| > r)^{(q+1)m_0} dr. \end{aligned}$$

On the interval $[-|x|, 0]$, we have

$$\int_{-|x|}^0 (r + |x|)^{q-1} \mathbb{P}(|X'| > r)^{(q+1)m_0} dr = \int_{-|x|}^0 (r + |x|)^{q-1} dr = \frac{|x|^q}{q}.$$

On the interval $[0, +\infty)$, we first rewrite

$$\int_0^{+\infty} (r + |x|)^{q-1} \mathbb{P}(|X'| > r)^{(q+1)m_0} dr = \int_0^{+\infty} (r + |x|)^{q-1} \mathbb{P}\left(\min_{j \in \llbracket 1, m_0 \rrbracket} |X'_j| > r\right)^{q+1} dr,$$

and recall from Assumption 10.3.2 that $C_2 := \mathbb{E}[\min_{j \in \llbracket 1, m_0 \rrbracket} |X'_j|] < \infty$. As a consequence, we deduce from Markov's inequality that the right-hand side in the previous equality is bounded from above by

$$\int_0^{|x| \vee 1} (r + |x|)^{q-1} dr + C_2^{q+1} \int_{|x| \vee 1}^{+\infty} \frac{(r + |x|)^{q-1}}{r^{q+1}} dr.$$

If $|x| \leq 1$ then this expression is bounded from above. If $|x| > 1$, then we have

$$\int_0^{|x|} (r + |x|)^{q-1} dr \leq 2^{q-1} |x|^q$$

on the one hand, and

$$\int_{|x|}^{+\infty} \frac{(r + |x|)^{q-1}}{r^{q+1}} dr = \frac{1}{|x|} \int_1^{+\infty} \frac{(u + 1)^{q-1}}{u^{q+1}} du,$$

which is bounded from above, on the other hand. Overall, we conclude that there exists a constant C_3 such that

$$\int_{r_\kappa}^{+\infty} r^{q-1} \mathbb{P}(|x - X'| > r)^{(q+1)m_0} dr \leq C_3(1 + |x|^q). \quad (10.18)$$

As a consequence, the combination of (10.17) and (10.18) yields

$$\int_{\mathbb{R}^d} \int_{r_\kappa}^{+\infty} \tilde{V}(x, r) dr d\mu_X(x) \leq C_1 C_3 \mathbb{E} \left[\frac{1 + |X|^q}{p_{X'}(X)^{q/d}} \right],$$

which by Assumption 10.3.6 allows to apply the dominated convergence theorem to show that Π goes to 0, and thereby completes the proof. \square

Proof of Corollary 10.3.8. We start from the second line of Equation (10.15) and estimate its right-hand side

$$\begin{aligned} \mathbb{E} \left[W_q^q(\hat{\mu}_{\mathbf{X}_{n_{\text{on}}}}, \hat{\mu}_{\mathbf{X}'_{n_{\text{off}}}}^{(k_{n_{\text{off}}})}) \right] &\leq \frac{2}{k_{n_{\text{off}}}} \sum_{l=1}^{k_{n_{\text{off}}}} \mathbb{E} \left[|X - \text{NN}_{\mathbf{X}'_{\lfloor n_{\text{off}}/2l \rfloor}}(X)|^q \right] \\ &= \frac{2}{k_{n_{\text{off}}}} \sum_{l=1}^{k_{n_{\text{off}}}} \left(\frac{2k_{n_{\text{off}}}}{n_{\text{off}}} \frac{l}{k_{n_{\text{off}}}} \frac{n_{\text{off}}}{2l} \right)^{q/d} \mathbb{E} \left[|X - \text{NN}_{\mathbf{X}'_{\lfloor n_{\text{off}}/2l \rfloor}}(X)|^q \right] \\ &= \left(\frac{k_{n_{\text{off}}}}{n_{\text{off}}} \right)^{q/d} \frac{2^{q/d+1}}{k_{n_{\text{off}}}} \sum_{l=1}^{k_{n_{\text{off}}}} \left(\frac{l}{k_{n_{\text{off}}}} \right)^{q/d} F \left(\frac{n_{\text{off}}}{2l} \right) \end{aligned}$$

with $F(u) = u^{q/d} \mathbb{E}[|X - \text{NN}_{\mathbf{X}'_{\lfloor u \rfloor}}(X)|^q]$. Let $\epsilon > 0$. By Theorem 10.3.7, there exists $u_\epsilon \geq 0$ such that, for all $u \geq u_\epsilon$,

$$\left| F(u) - \frac{\Gamma(1 + q/d)}{v_d^{q/d}} \mathbb{E} \left[\frac{1}{p_{X'}(X)^{q/d}} \right] \right| \leq \epsilon.$$

We can remark that for $n_{\text{off}} \in \mathbb{N}^*$ and $l \in \llbracket 1, k_{n_{\text{off}}} \rrbracket$,

$$\frac{n_{\text{off}}}{2l} \geq \frac{n_{\text{off}}}{2k_{n_{\text{off}}}} \xrightarrow{n_{\text{off}} \rightarrow +\infty} +\infty.$$

Thus, if we take n_ϵ such that for all $n \geq n_\epsilon$, $\lfloor \frac{n}{2k_n} \rfloor \geq u_\epsilon$, we have

$$\left| F\left(\frac{n_{\text{off}}}{2l}\right) - \frac{\Gamma(1+q/d)}{v_d^{q/d}} \mathbb{E}\left[\frac{1}{p_{X'}(X)^{q/d}}\right] \right| \leq \epsilon$$

for any $n_{\text{off}} \geq n_\epsilon$ and $l \leq k_{n_{\text{off}}}$. Consequently,

$$\begin{aligned} & \left| \frac{1}{k_{n_{\text{off}}}} \sum_{l=1}^{k_{n_{\text{off}}}} \left(\frac{l}{k_{n_{\text{off}}}}\right)^{q/d} \left(F\left(\frac{n_{\text{off}}}{2l}\right) - \frac{\Gamma(1+q/d)}{v_d^{q/d}} \mathbb{E}\left[\frac{1}{p_{X'}(X)^{q/d}}\right] \right) \right| \\ & \leq \epsilon \left| \frac{1}{k_{n_{\text{off}}}} \sum_{l=1}^{k_{n_{\text{off}}}} \left(\frac{l}{k_{n_{\text{off}}}}\right)^{q/d} \right| \\ & \leq \epsilon, \\ & \lim_{n_{\text{off}} \rightarrow +\infty} \frac{2^{q/d+1}}{k_{n_{\text{off}}}} \sum_{l=1}^{k_{n_{\text{off}}}} \left(\frac{l}{k_{n_{\text{off}}}}\right)^{q/d} F\left(\frac{n_{\text{off}}}{2l}\right) = c_{d,q} \frac{\Gamma(1+q/d)}{v_d^{q/d}} \mathbb{E}\left[\frac{1}{p_{X'}(X)^{q/d}}\right], \end{aligned}$$

where

$$\begin{aligned} c_{d,q} & := \lim_{n \rightarrow +\infty} \frac{2^{q/d+1}}{k_n} \sum_{l=1}^{k_n} \left(\frac{l}{k_n}\right)^{q/d} \\ & = \begin{cases} \frac{2^{q/d+1}}{k} \sum_{l=1}^k \left(\frac{l}{k}\right)^{q/d} & \text{if } \sup_{n \geq 1} k_n = k < +\infty, \\ 2^{q/d+1} \int_0^1 u^{q/d} du = \frac{2^{q/d+1}}{q/d+1} & \text{if } \sup_{n \geq 1} k_n = +\infty, \end{cases} \end{aligned}$$

because $k_{n_{\text{off}}}$ is nondecreasing. This concludes the proof. \square

Proof of Lemma 10.3.10. Obviously, it suffices to check that $p_{X'}$ satisfies the point (iii) of Assumption 10.3.5. Let us denote by $\langle \cdot, \cdot \rangle$ and $\mathcal{B}(x, r)$ respectively the inner product and the ball of center x and radius r associated to $\|\cdot\|$. We set $x_0 = 0$ without loss of generality. As h is positive and nonincreasing, we may fix $r_0 > 0$ and define

$$\bar{\kappa} := \frac{h(r_0)}{h(0)} \in (0, 1].$$

If $\|x\| \leq r_0/2$, then for all $y \in \mathcal{B}(0, r_0/2)$, the monotonicity of h ensures that $p_{X'}(x+y) \geq \bar{\kappa} p_{X'}(x)$. By the equivalence of the norms, there exist $C \geq c > 0$ such that for any $x \in \mathbb{R}^d$ and any $r \geq 0$, $\mathcal{B}(x, cr) \subset B(x, r) \subset \mathcal{B}(x, Cr)$. Thus

$$\forall r \leq r_0/2c, \quad \mathbb{P}(X' \in B(x, r)) \geq \mathbb{P}(X' \in \mathcal{B}(x, cr)) \geq (c/C)^d v_d \bar{\kappa} p_{X'}(x) r^d.$$

If $\|x\| > r_0/2$, let us introduce the half-cone

$$\mathcal{C}_x = \left\{ x' \in \mathbb{R}^d : \langle x' - x, -x \rangle \geq \frac{\|x' - x\| \|x\|}{2} \right\},$$

and notice that for all $r \leq r_0/2$ and $x' \in \mathcal{C}_x \cap \mathcal{B}(x, r)$,

$$\begin{aligned} \|x'\|^2 &= \|x\|^2 + \|x' - x\|^2 + 2\langle x' - x, x \rangle \\ &\leq \|x\|^2 + \|x' - x\|^2 - \|x' - x\| \|x\| \\ &\leq \|x\|^2 + \|x' - x\|^2 - \|x' - x\|^2 \\ &= \|x\|^2. \end{aligned}$$

Thus, for all $x' \in \mathcal{C}_x \cap \mathcal{B}(x, r)$, $p_{X'}(x') \geq p_{X'}(x)$. For a given r , the sets $\mathcal{C}_x \cap \mathcal{B}(x, r)$ have the same volume for all x , which we denote by $\alpha v_d r^d$ for some $\alpha \in (0, 1/C^d)$. Finally, we have

$$\forall r \leq r_0/2c, \quad \mathbb{P}(X' \in B(x, r)) \geq \mathbb{P}(X' \in \mathcal{B}(x, cr) \cap \mathcal{C}_x) \geq \alpha c^d v_d p_{X'}(x) r^d.$$

If we take $\kappa = (c/C)^d \min(\alpha C^d, \bar{\kappa})$ and $r_\kappa = r_0/2c$, we obtain the point (iii) of Assumption 10.3.5. \square

10.4 Discussion

Going back to our initial problem, we are now able to compute L^q rates of convergence of the weighted estimator

$$\widehat{\text{QI}}_{n_{\text{off}}, n_{\text{on}}}^{(k_{n_{\text{off}}})} = \frac{1}{n_{\text{off}}} \sum_{j=1}^{n_{\text{off}}} w_j^{(k_{n_{\text{off}}})} \phi(Y_j')$$

to $\text{QI} = \mathbb{E}[\phi(Y)]$. First, in Section 10.4.1, we derive the convergence rates of $\widehat{\mu}_{\mathbf{X}'_{n_{\text{off}}}}^{(k_{n_{\text{off}}})}$ to μ_X in terms of Wasserstein distance. Then in Section 10.4.2, we study the case in which $Y = f(X)$ and there is no external source of uncertainty, that we call the noiseless case, using the terminology from statistical Machine Learning regression. The noisy case $Y = f(X, \Theta)$ is treated in Section 10.4.3.

Finally, in Section 10.4.4, we reinterpret Theorem 10.3.7 under the prism of the Nearest Neighbor literature.

10.4.1 Convergence to μ_X

Let us focus on the speed of convergence of $\widehat{\mu}_{\mathbf{X}'_{n_{\text{off}}}}^{(k_{n_{\text{off}}})}$ to μ_X . Provided that X has enough moments, namely that there exists $s > 2q$ such that $\mathbb{E}[|X|^s] < +\infty$, we have from [50, Theorem 1]

$$\mathbb{E} [W_q^q(\mu_X, \widehat{\mu}_{\mathbf{X}'_{n_{\text{on}}}})] = \begin{cases} O(n_{\text{on}}^{-1/2}) & \text{if } q > d/2, \\ O(n_{\text{on}}^{-1/2} \log(1 + n_{\text{on}})) & \text{if } q = d/2, \\ O(n_{\text{on}}^{-q/d}) & \text{if } q < d/2. \end{cases}$$

In dimension $d = 1$, we deduce from (10.11) that

$$\mathbb{E} [W_q^q(\mu_X, \widehat{\mu}_{\mathbf{X}'_{n_{\text{off}}}}^{(k_{n_{\text{off}}})})]^{1/q} = O\left(\left(\frac{1}{n_{\text{on}}}\right)^{1/2q} + \frac{k_{n_{\text{off}}}}{n_{\text{off}}}\right)$$

for any value of $q \geq 1$. For the choice $q = 1$, both error terms have the same order of magnitude if the sizes of the offline and online samples satisfy

$$n_{\text{on}} \propto \left(\frac{n_{\text{off}}}{k_{n_{\text{off}}}} \right)^2.$$

In dimension $d \geq 2$, the minimal upper bound for $\mathbb{E}[W_q^q(\mu_X, \widehat{\mu}_{\mathbf{X}_{n_{\text{on}}}})]^{1/q}$ is achieved as soon as $q \leq d/2$, in which case, up to the logarithmic correction,

$$\mathbb{E} \left[W_q^q \left(\mu_X, \widehat{\mu}_{\mathbf{X}'_{n_{\text{off}}}} \right) \right]^{1/q} = O \left(\left(\frac{1}{n_{\text{on}}} \right)^{1/d} + \left(\frac{k_{n_{\text{off}}}}{n_{\text{off}}} \right)^{1/d} \right),$$

and both error terms have the same order of magnitude if the sizes of the offline and online samples satisfy

$$n_{\text{on}} \propto \frac{n_{\text{off}}}{k_{n_{\text{off}}}}.$$

10.4.2 Rate of convergence of $\widehat{\text{QI}}_{n_{\text{off}}, n_{\text{on}}}^{(k_{n_{\text{off}}})}$ in the noiseless case

We assume that $Y = f(X)$ and study the rate of convergence of $\widehat{\text{QI}}_{n_{\text{off}}, n_{\text{on}}}^{(k_{n_{\text{off}}})}$ to QI. When $\phi \circ f$ is L -Lipschitz continuous, we can derive the result using the duality formula of the W_1 Wasserstein distance [120, Remark 6.5]

$$W_1 \left(\mu_X, \widehat{\mu}_{\mathbf{X}'_{n_{\text{off}}}} \right) = \sup_{|\varphi|_{\text{Lip}} \leq 1} \left\{ \int_{\mathbb{R}^d} \varphi(x) d\mu_X(x) - \int_{\mathbb{R}^d} \varphi(x) d\widehat{\mu}_{\mathbf{X}'_{n_{\text{off}}}} \right\} \quad (10.19)$$

and bound

$$\begin{aligned} \left| \text{QI} - \widehat{\text{QI}}_{n_{\text{off}}, n_{\text{on}}}^{(k_{n_{\text{off}}})} \right|^q &= \left| \int_{\mathbb{R}^d} \phi \circ f(x) d\mu_X(x) - \int_{\mathbb{R}^d} \phi \circ f(x) d\widehat{\mu}_{\mathbf{X}'_{n_{\text{off}}}} \right|^q \\ &\leq L^q W_1^q \left(\mu_X, \widehat{\mu}_{\mathbf{X}'_{n_{\text{off}}}} \right) \\ &\leq L^q W_q^q \left(\mu_X, \widehat{\mu}_{\mathbf{X}'_{n_{\text{off}}}} \right). \end{aligned}$$

We can conclude from Section 10.4.1.

Proposition 10.4.1 (Rates of convergence in the noiseless case). *Assume that:*

- (i) the function f does not depend on Θ ,
- (ii) the function $\phi \circ f$ is globally Lipschitz continuous,

and let the assumptions of Corollary 10.3.8 hold. We have, as soon as $q \neq d/2$ and there exists $s > 2q$ such that $\mathbb{E}[|X|^s] < +\infty$,

$$\mathbb{E} \left[\left| \text{QI} - \widehat{\text{QI}}_{n_{\text{off}}, n_{\text{on}}}^{(k_{n_{\text{off}}})} \right|^q \right]^{1/q} = O \left(n_{\text{on}}^{-\min(1/2q, 1/d)} \right) + O \left(\left(\frac{k_{n_{\text{off}}}}{n_{\text{off}}} \right)^{1/d} \right). \quad (10.20)$$

There is no need for $k_{n_{\text{off}}}$ to go to infinity and thus $k_{n_{\text{off}}} = 1$ seems a reasonable choice.

These computations can be adapted to cases other than $\phi \circ f$ Lipschitz continuous. For instance, if $A \subset \mathbb{R}^e$, $\phi(y) = \mathbb{1}_{\{y \in A\}}$ and f is globally Lipschitz continuous, it is possible to use the margin assumption of [116] to deduce theoretical rates of convergence in the estimation of $\text{QI} = \mathbb{P}(Y \in A)$.

10.4.3 Noisy case

We now study the convergence of $\widehat{\text{QI}}_{n_{\text{off}}, n_{\text{on}}}^{(k_{n_{\text{off}}})}$ to QI when $Y = f(X, \Theta)$. A first striking result is then that even under the assumptions of Theorem 10.3.3, the estimator $\widehat{\text{QI}}_{n_{\text{off}}, n_{\text{on}}}^{(1)}$ need not be consistent. Indeed, consider the case where X is actually deterministic and always equal to some $x_0 \in \mathbb{R}^d$. Then we have

$$\widehat{\text{QI}}_{n_{\text{off}}, n_{\text{on}}}^{(1)} = \frac{1}{n_{\text{on}}} \sum_{i=1}^{n_{\text{on}}} \phi(Y'_{j_i^{(1)}}),$$

where $j_i^{(1)}$ is the index of the closest X'_j to X_i . But since $X_i = x_0$ for all i , all indices $j_i^{(1)}$ are equal to some $j^{(1)}$ and the estimator rewrites

$$\widehat{\text{QI}}_{n_{\text{off}}, n_{\text{on}}}^{(1)} = \phi(Y'_{j^{(1)}}) = \phi(f(X'_{j^{(1)}}, \Theta_{j^{(1)}})).$$

While Assumption 10.3.1 ensures that $X'_{j^{(1)}}$ converges to x_0 when $n_{\text{off}} \rightarrow +\infty$, in general the corresponding sequence of $\Theta_{j^{(1)}}$ does not converge.

As is evidenced on this example, the presence of an atom in the law of X makes the estimator $\widehat{\text{QI}}_{n_{\text{off}}, n_{\text{on}}}^{(1)}$ depend on a single realization of Θ and therefore prevents this estimator to display an averaging behavior with respect to the law of Θ . In Proposition 10.4.2, we clarify this point by exhibiting a necessary and sufficient condition for the estimator $\widehat{\text{QI}}_{n_{\text{off}}, n_{\text{on}}}^{(1)}$ to be consistent, while in Proposition 10.4.4, we show that replacing $\widehat{\text{QI}}_{n_{\text{off}}, n_{\text{on}}}^{(1)}$ with $\widehat{\text{QI}}_{n_{\text{off}}, n_{\text{on}}}^{(k_{n_{\text{off}}})}$ with $k_{n_{\text{off}}} \rightarrow +\infty$ allows to recover such an averaging behavior and make the estimator consistent, even when μ_X has atoms. In the latter case, we also provide rates of convergence.

We recall that $\psi(x) = \mathbb{E}[\phi(f(x, \Theta))]$ is defined in Equation (10.9). In the next statement, we denote by \mathcal{A}_X the set of atoms of μ_X , that is to say the set of $x \in \mathbb{R}^d$ such that $\mathbb{P}(X = x) > 0$, and introduce the notation $\vartheta(x) := \text{Var}(\phi(f(x, \Theta)))$.

Proposition 10.4.2 (Consistency of the 1-NN in the noisy case). *Assume that:*

- (i) *the function ϕ is bounded,*
- (ii) *the function ψ is globally Lipschitz continuous,*
- (iii) *the function ϑ is continuous,*

and let the assumptions of Theorem 10.3.3 hold. We have

$$\mathbb{E} \left[\left| \widehat{\text{QI}}_{n_{\text{off}}, n_{\text{on}}}^{(1)} - \text{QI} \right| \right] \xrightarrow{n_{\text{off}}, n_{\text{on}} \rightarrow +\infty} 0$$

if and only if,

$$\forall x \in \mathcal{A}_X, \quad \text{Var}(\phi(f(x, \Theta))) = 0.$$

In particular, under the above assumptions, if the law of X has no atom, *i.e.* $\mathcal{A}_X = \emptyset$, then $\widehat{\text{QI}}_{n_{\text{off}}, n_{\text{on}}}^{(1)}$ converges to QI.

Proof. Let us write

$$\widehat{\text{QI}}_{n_{\text{off}}, n_{\text{on}}}^{(1)} - \text{QI} = \left(\widehat{\text{QI}}_{n_{\text{off}}, n_{\text{on}}}^{(1)} - \widetilde{\text{QI}}_{n_{\text{off}}, n_{\text{on}}}^{(1)} \right) + \left(\widetilde{\text{QI}}_{n_{\text{off}}, n_{\text{on}}}^{(1)} - \text{QI} \right),$$

with

$$\widetilde{\mathbb{Q}}_{n_{\text{off}}, n_{\text{on}}}^{(1)} = \frac{1}{n_{\text{off}}} \sum_{j=1}^{n_{\text{off}}} w_j^{(1)} \psi(X'_j).$$

Using the Lipschitz continuity of ψ , the duality formula (10.19) and Theorem 10.3.3, we get that $\widetilde{\mathbb{Q}}_{n_{\text{off}}, n_{\text{on}}}^{(1)} - \text{QI}$ converges to 0 when $n_{\text{off}}, n_{\text{on}} \rightarrow +\infty$, in L^1 . Therefore, $\widehat{\mathbb{Q}}_{n_{\text{off}}, n_{\text{on}}}^{(1)} - \text{QI}$ converges to 0 if and only if $\widehat{\mathbb{Q}}_{n_{\text{off}}, n_{\text{on}}}^{(1)} - \widetilde{\mathbb{Q}}_{n_{\text{off}}, n_{\text{on}}}^{(1)}$ converges to 0.

Let us rewrite

$$\begin{aligned} \widehat{\mathbb{Q}}_{n_{\text{off}}, n_{\text{on}}}^{(1)} - \widetilde{\mathbb{Q}}_{n_{\text{off}}, n_{\text{on}}}^{(1)} &= \frac{1}{n_{\text{off}}} \sum_{j=1}^{n_{\text{off}}} w_j^{(1)} (\phi((X'_j, \Theta_j)) - \psi(X'_j)) \\ &= \frac{1}{n_{\text{on}}} \sum_{i=1}^{n_{\text{on}}} \left(\phi\left(f\left(X'_{j_i^{(1)}}, \Theta_{j_i^{(1)}}\right)\right) - \psi\left(X'_{j_i^{(1)}}\right) \right), \end{aligned}$$

introduce the notation

$$\mathcal{A}_X^+ := \{x \in \mathcal{A}_X : \vartheta(X) > 0\},$$

and denote

$$\begin{aligned} e_1 &:= \frac{1}{n_{\text{on}}} \sum_{i=1}^{n_{\text{on}}} \left(\phi\left(f\left(X'_{j_i^{(1)}}, \Theta_{j_i^{(1)}}\right)\right) - \psi\left(X'_{j_i^{(1)}}\right) \right) \mathbb{1}_{\{X_i \notin \mathcal{A}_X^+\}}, \\ e_2 &:= \frac{1}{n_{\text{on}}} \sum_{i=1}^{n_{\text{on}}} \left(\phi\left(f\left(X'_{j_i^{(1)}}, \Theta_{j_i^{(1)}}\right)\right) - \psi\left(X'_{j_i^{(1)}}\right) \right) \mathbb{1}_{\{X_i \in \mathcal{A}_X^+\}}. \end{aligned}$$

In Step 1 below, we prove that

$$\mathbb{E}[|e_1|] \xrightarrow[n_{\text{on}}, n_{\text{off}} \rightarrow +\infty]{} 0,$$

demonstrating at the same time the direct implication of the convergence when $\mathcal{A}_X^+ = \emptyset$. In Step 2, we show that if $\mathcal{A}_X^+ \neq \emptyset$ then $\mathbb{E}[|e_2|]$ does not converge to 0, which implies that in this case, $\widehat{\mathbb{Q}}_{n_{\text{off}}, n_{\text{on}}}^{(1)} - \widetilde{\mathbb{Q}}_{n_{\text{off}}, n_{\text{on}}}^{(1)}$ does not converge to 0 in L^1 .

In both steps, we shall use the following preliminary remark: given a measurable subset \mathcal{A} of \mathbb{R}^d , taking the conditional expectation with respect to $(\mathbf{X}_{n_{\text{on}}}, \mathbf{X}'_{n_{\text{off}}})$ it is easy to see that for $i \in \llbracket 1, n_{\text{on}} \rrbracket$,

$$\mathbb{E} \left[(\phi(f(X'_{j_i^{(1)}}), \Theta_{j_i^{(1)}})) - \psi(X'_{j_i^{(1)}}) \mathbb{1}_{\{X_i \in \mathcal{A}\}} \right] = 0,$$

and for $(i_1, i_2) \in \llbracket 1, n_{\text{on}} \rrbracket^2$,

$$\begin{aligned} &\mathbb{E} \left[(\phi(f(X'_{j_{i_1}^{(1)}}), \Theta_{j_{i_1}^{(1)}})) - \psi(X'_{j_{i_1}^{(1)}}) \mathbb{1}_{\{X_{i_1} \in \mathcal{A}\}} \right) (\phi(f(X'_{j_{i_2}^{(1)}}), \Theta_{j_{i_2}^{(1)}})) - \psi(X'_{j_{i_2}^{(1)}}) \mathbb{1}_{\{X_{i_2} \in \mathcal{A}\}} \right] \\ &= \mathbb{E} \left[\mathbb{1}_{\{j_{i_1}^{(1)} = j_{i_2}^{(1)}\}} \vartheta(X'_{j_{i_1}^{(1)}}) \mathbb{1}_{\{X_{i_1} \in \mathcal{A}, X_{i_2} \in \mathcal{A}\}} \right]. \end{aligned}$$

Therefore,

$$\begin{aligned} \mathbb{E}[|e_1|^2] &= \frac{1}{n_{\text{on}}^2} \left(\sum_{i=1}^{n_{\text{on}}} \mathbb{E} \left[\vartheta(X'_{j_i^{(1)}}) \mathbb{1}_{\{X_i \notin \mathcal{A}_X^+\}} \right] + \sum_{i_1 \neq i_2} \mathbb{E} \left[\mathbb{1}_{\{j_{i_1}^{(1)} = j_{i_2}^{(1)}\}} \vartheta(X'_{j_{i_1}^{(1)}}) \mathbb{1}_{\{X_{i_1} \notin \mathcal{A}_X^+, X_{i_2} \notin \mathcal{A}_X^+\}} \right] \right) \\ &= \frac{1}{n_{\text{on}}} \mathbb{E} \left[\vartheta(X'_{j_1^{(1)}}) \mathbb{1}_{\{X_1 \notin \mathcal{A}_X^+\}} \right] + \frac{n_{\text{on}} - 1}{n_{\text{on}}} \mathbb{E} \left[\mathbb{1}_{\{j_1^{(1)} = j_2^{(1)}\}} \vartheta(X'_{j_1^{(1)}}) \mathbb{1}_{\{X_1 \notin \mathcal{A}_X^+, X_2 \notin \mathcal{A}_X^+\}} \right], \end{aligned}$$

and a similar expression holds for $\mathbb{E}[|e_2|^2]$.

Step 1. Thanks to the boundedness of ϕ , and thus of ϑ , it is immediate that $\frac{1}{n_{\text{on}}}\mathbb{E}[\vartheta(X'_{j_1^{(1)}})\mathbb{1}_{\{X_1 \notin \mathcal{A}_X^+\}}]$ converges to 0 when $n_{\text{on}} \rightarrow +\infty$, uniformly in n_{off} . Therefore, to show that $\mathbb{E}[|e_1|^2]$ converges to 0, it suffices to prove that

$$\mathbb{E}\left[\mathbb{1}_{\{j_1^{(1)}=j_2^{(1)}\}}\vartheta(X'_{j_1^{(1)}})\mathbb{1}_{\{X_1 \notin \mathcal{A}_X^+, X_2 \notin \mathcal{A}_X^+\}}\right] \xrightarrow{n_{\text{off}} \rightarrow +\infty} 0.$$

In this purpose, let us first write

$$\mathbb{E}\left[\mathbb{1}_{\{j_1^{(1)}=j_2^{(1)}\}}\vartheta(X'_{j_1^{(1)}})\mathbb{1}_{\{X_1 \notin \mathcal{A}_X^+, X_2 \notin \mathcal{A}_X^+\}}\right] \leq \mathbb{E}\left[\mathbb{1}_{\{\text{NN}_{\mathbf{X}'_{n_{\text{off}}}}(X_1)=\text{NN}_{\mathbf{X}'_{n_{\text{off}}}}(X_2)\}}\vartheta(\text{NN}_{\mathbf{X}'_{n_{\text{off}}}}(X_1))\mathbb{1}_{\{X_1 \notin \mathcal{A}_X^+\}}\right],$$

and recall that, by Assumption 10.3.1 and Lemma 2.2 in [18, Chapter 2], $\text{NN}_{\mathbf{X}'_{n_{\text{off}}}}(X_1)$ converges to X_1 and $\text{NN}_{\mathbf{X}'_{n_{\text{off}}}}(X_2)$ converges to X_2 , almost surely. As a consequence, if $X_1 \in \mathcal{A}_X \setminus \mathcal{A}_X^+$ then $\vartheta(X_1) = 0$ and by the continuity of ϑ and the boundedness of ϕ , the dominated convergence theorem shows that

$$\mathbb{E}\left[\mathbb{1}_{\{X_1 \in \mathcal{A}_X \setminus \mathcal{A}_X^+\}}\mathbb{1}_{\{\text{NN}_{\mathbf{X}'_{n_{\text{off}}}}(X_1)=\text{NN}_{\mathbf{X}'_{n_{\text{off}}}}(X_2)\}}\vartheta(\text{NN}_{\mathbf{X}'_{n_{\text{off}}}}(X_1))\right] \xrightarrow{n_{\text{off}} \rightarrow +\infty} 0.$$

On the other hand, if $X_1 \notin \mathcal{A}_X$, then almost surely $X_1 \neq X_2$, and therefore $\mathbb{1}_{\{\text{NN}_{\mathbf{X}'_{n_{\text{off}}}}(X_1)=\text{NN}_{\mathbf{X}'_{n_{\text{off}}}}(X_2)\}}$ converges to 0 almost surely. Using the boundedness of ϕ and the dominated convergence theorem again, we deduce that

$$\mathbb{E}\left[\mathbb{1}_{\{X_1 \notin \mathcal{A}_X\}}\mathbb{1}_{\{\text{NN}_{\mathbf{X}'_{n_{\text{off}}}}(X_1)=\text{NN}_{\mathbf{X}'_{n_{\text{off}}}}(X_2)\}}\vartheta(\text{NN}_{\mathbf{X}'_{n_{\text{off}}}}(X_1))\right] \xrightarrow{n_{\text{off}} \rightarrow +\infty} 0,$$

which completes the proof of the fact that $\mathbb{E}[|e_1|^2]$, and thus $\mathbb{E}[|e_1|]$, converge to 0.

Step 2. Let us now assume that \mathcal{A}_X^+ is nonempty and show that e_2 does not converge to 0 in L^1 . We shall actually prove that e_2 does not converge to 0 in L^2 : since e_2 is bounded then this prevents the convergence from occurring in L^1 . From the preliminary remark, we write

$$\mathbb{E}[|e_2|^2] = \frac{1}{n_{\text{on}}}\mathbb{E}\left[\vartheta(X'_{j_1^{(1)}})\mathbb{1}_{\{X_1 \in \mathcal{A}_X^+\}}\right] + \frac{n_{\text{on}} - 1}{n_{\text{on}}}\mathbb{E}\left[\mathbb{1}_{\{j_1^{(1)}=j_2^{(1)}\}}\vartheta(X'_{j_1^{(1)}})\mathbb{1}_{\{X_1 \in \mathcal{A}_X^+, X_2 \in \mathcal{A}_X^+\}}\right],$$

and we prove that

$$\liminf_{n_{\text{off}} \rightarrow +\infty} \mathbb{E}\left[\mathbb{1}_{\{j_1^{(1)}=j_2^{(1)}\}}\vartheta(X'_{j_1^{(1)}})\mathbb{1}_{\{X_1 \in \mathcal{A}_X^+, X_2 \in \mathcal{A}_X^+\}}\right] > 0.$$

Let $x \in \mathcal{A}_X^+$. Obviously,

$$\begin{aligned} \mathbb{E}\left[\mathbb{1}_{\{j_1^{(1)}=j_2^{(1)}\}}\vartheta(X'_{j_1^{(1)}})\mathbb{1}_{\{X_1 \in \mathcal{A}_X^+, X_2 \in \mathcal{A}_X^+\}}\right] &\geq \mathbb{E}\left[\mathbb{1}_{\{j_1^{(1)}=j_2^{(1)}\}}\vartheta(X'_{j_1^{(1)}})\mathbb{1}_{\{X_1=X_2=x\}}\right] \\ &= \mathbb{E}\left[\vartheta(\text{NN}_{\mathbf{X}'_{n_{\text{off}}}}(x))\mathbb{1}_{\{X_1=X_2=x\}}\right]. \end{aligned}$$

By Assumption 10.3.1 and Lemma 2.2 in [18, Chapter 2] again, $\text{NN}_{\mathbf{X}'_{n_{\text{off}}}}(x)$ converges to x almost surely, therefore using the continuity and boundedness assumptions on ϑ , the dominated convergence theorem shows that

$$\mathbb{E}\left[\vartheta(\text{NN}_{\mathbf{X}'_{n_{\text{off}}}}(x))\mathbb{1}_{\{X_1=X_2=x\}}\right] \xrightarrow{n_{\text{off}} \rightarrow +\infty} \vartheta(x)\mu_X(\{x\})^2 > 0,$$

which completes the proof. \square

We now study the estimator $\widehat{\mathbf{QI}}_{n_{\text{off}}, n_{\text{on}}}^{(k_{n_{\text{off}}})}$ and show that it is unconditionally consistent as soon as $k_{n_{\text{off}}} \rightarrow +\infty$. We provide L^2 convergence rates in Proposition 10.4.4.

Proposition 10.4.3 (Consistency in the noisy case). *Assume that*

- (i) *the function ϕ is bounded,*
- (ii) *the function ψ is globally Lipschitz continuous,*
- (iii) *there exists $\epsilon > 0$ such that $\mathbb{E} [|X|^{2+\epsilon}] < +\infty$,*

then, as soon as $k_{n_{\text{off}}}$ goes to infinity with n_{off} , we have

$$\mathbb{E} \left[\left| \widehat{\mathbf{QI}}_{n_{\text{off}}, n_{\text{on}}}^{(k_{n_{\text{off}}})} - \mathbf{QI} \right|^2 \right]^{1/2} \xrightarrow{n_{\text{on}}, n_{\text{off}} \rightarrow +\infty} 0.$$

Proof. We decompose the error as

$$\widehat{\mathbf{QI}}_{n_{\text{off}}, n_{\text{on}}}^{(k_{n_{\text{off}}})} - \mathbf{QI} = \left(\widehat{\mathbf{QI}}_{n_{\text{off}}, n_{\text{on}}}^{(k_{n_{\text{off}}})} - \widetilde{\mathbf{QI}}_{n_{\text{off}}, n_{\text{on}}}^{(k_{n_{\text{off}}})} \right) + \left(\widetilde{\mathbf{QI}}_{n_{\text{off}}, n_{\text{on}}}^{(k_{n_{\text{off}}})} - \mathbf{QI} \right),$$

with

$$\widetilde{\mathbf{QI}}_{n_{\text{off}}, n_{\text{on}}}^{(k_{n_{\text{off}}})} = \frac{1}{n_{\text{off}}} \sum_{j=1}^{n_{\text{off}}} w_j^{(k_{n_{\text{off}}})} \psi(X'_j).$$

As ψ is globally Lipschitz continuous and does not depend on Θ , we have

$$\begin{aligned} \mathbb{E} \left[\left(\widetilde{\mathbf{QI}}_{n_{\text{off}}, n_{\text{on}}}^{(k_{n_{\text{off}}})} - \mathbf{QI} \right)^2 \right]^{1/2} &\leq L \mathbb{E} \left[W_2^2 \left(\mu_X, \widehat{\mu}_{\mathbf{X}'_{n_{\text{off}}}}^{(k_{n_{\text{off}}})} \right) \right]^{1/2} \\ &\leq L \left(2^{q-1} \mathbb{E} \left[W_2^2 \left(\mu_X, \widehat{\mu}_{\mathbf{X}_{n_{\text{on}}}} \right) \right] + 2^{q-1} \mathbb{E} \left[W_2^2 \left(\widehat{\mu}_{\mathbf{X}_{n_{\text{on}}}}, \widehat{\mu}_{\mathbf{X}'_{n_{\text{off}}}}^{(k_{n_{\text{off}}})} \right) \right] \right)^{1/2} \end{aligned}$$

by Jensen's inequality, with L the Lipschitz constant of ψ . The second term $\mathbb{E} \left[W_2^2 \left(\widehat{\mu}_{\mathbf{X}_{n_{\text{on}}}}, \widehat{\mu}_{\mathbf{X}'_{n_{\text{off}}}}^{(k_{n_{\text{off}}})} \right) \right]$ goes to 0 by theorem Theorem 10.3.3. For the first term, let us remark that

$$\begin{aligned} \left(W_2^2 \left(\mu_X, \widehat{\mu}_{\mathbf{X}_{n_{\text{on}}}} \right) \right)^{1+\epsilon/2} &= W_2^{2+\epsilon} \left(\mu_X, \widehat{\mu}_{\mathbf{X}_{n_{\text{on}}}} \right) \\ &\leq W_{2+\epsilon}^{2+\epsilon} \left(\mu_X, \widehat{\mu}_{\mathbf{X}_{n_{\text{on}}}} \right) \\ &\leq 2^{2+\epsilon-1} \left(\frac{1}{n_{\text{on}}} \sum_{i=1}^{n_{\text{on}}} |X_i|^{2+\epsilon} + \mathbb{E} [|X|^{2+\epsilon}] \right). \end{aligned}$$

Thus, for any $n_{\text{on}} \in \mathbb{N}^*$, we have

$$\mathbb{E} \left[\left(W_2^2 \left(\mu_X, \widehat{\mu}_{\mathbf{X}_{n_{\text{on}}}} \right) \right)^{1+\epsilon/2} \right] \leq 2^{2+\epsilon} \mathbb{E} [|X|^{2+\epsilon}] < +\infty$$

and the sequence $W_2^2 \left(\mu_X, \widehat{\mu}_{\mathbf{X}_{n_{\text{on}}}} \right)$ is uniformly integrable [20, Section 5]. Therefore, since $W_2^2 \left(\mu_X, \widehat{\mu}_{\mathbf{X}_{n_{\text{on}}}} \right)$ converges in probability to 0 [90], its expectation $\mathbb{E} \left[W_2^2 \left(\mu_X, \widehat{\mu}_{\mathbf{X}_{n_{\text{on}}}} \right) \right]$ also converges to 0. Let us

consider the other part of the decomposition. We write the quadratic error

$$\begin{aligned}
& \mathbb{E} \left[\left| \widehat{\mathbb{Q}}_{n_{\text{off}}, n_{\text{on}}}^{(k_{n_{\text{off}}})} - \widetilde{\mathbb{Q}}_{n_{\text{off}}, n_{\text{on}}}^{(k_{n_{\text{off}}})} \right|^2 \right] \\
&= \mathbb{E} \left[\left(\frac{1}{n_{\text{off}}} \sum_{j=1}^{n_{\text{off}}} w_j^{(k_{n_{\text{off}}})} (\psi(X'_j) - \phi(f(X'_j, \Theta_j))) \right)^2 \right] \\
&= \mathbb{E} \left[\frac{1}{n_{\text{off}}^2} \sum_{j=1}^{n_{\text{off}}} w_j^{(k_{n_{\text{off}}})2} (\psi(X'_j) - \phi(f(X'_j, \Theta_j)))^2 \right] \\
&\quad + \mathbb{E} \left[\frac{n_{\text{off}} - 1}{n_{\text{off}}^2} \sum_{j,l=1, j \neq l}^{n_{\text{off}}} w_j^{(k_{n_{\text{off}}})} w_l^{(k_{n_{\text{off}}})} (\psi(X'_j) - \phi(f(X'_j, \Theta_j))) (\psi(X'_l) - \phi(f(X'_l, \Theta_l))) \right].
\end{aligned}$$

Using the fact that $\mathbb{E}[w_j^{(k_{n_{\text{off}}})} f(X'_j, \Theta_j) | \mathbf{X}_{n_{\text{on}}}, \mathbf{X}'_{n_{\text{off}}}] = w_j^{(k_{n_{\text{off}}})} \psi(X'_j)$ by definition and the independence of the Θ_j , the cross terms vanish. The remaining quadratic term is

$$\begin{aligned}
\mathbb{E} \left[\frac{1}{n_{\text{off}}^2} \sum_{j=1}^{n_{\text{off}}} w_j^{(k_{n_{\text{off}}})2} (\psi(X'_j) - \phi(f(X'_j, \Theta_j)))^2 \right] &= \frac{1}{n_{\text{off}}^2} \sum_{j=1}^{n_{\text{off}}} \mathbb{E} \left[w_j^{(k_{n_{\text{off}}})2} (\psi(X'_j) - \phi(f(X'_j, \Theta)))^2 \right] \\
&\leq \frac{4}{n_{\text{off}}^2} \sum_{j=1}^{n_{\text{off}}} \mathbb{E} \left[\left(w_j^{(k_{n_{\text{off}}})} \right)^2 \right] \|\phi\|_{L^\infty}^2.
\end{aligned} \tag{10.21}$$

We remark that

$$\sum_{j=1}^{n_{\text{off}}} \left(w_j^{(k_{n_{\text{off}}})} \right)^2 = \frac{n_{\text{off}}^2}{n_{\text{on}}^2 k_{n_{\text{off}}}^2} \sum_{i_1, i_2=1}^{n_{\text{on}}} \sum_{l_1, l_2=1}^{k_{n_{\text{off}}}} \mathbb{1}_{\{j_{i_1}^{(l_1)} = j_{i_2}^{(l_2)}\}}$$

and that for some fixed i_1, i_2 and l_1 , there exists exactly one $l_2 \in \llbracket 1, n_{\text{off}} \rrbracket$ such that $j_{i_1}^{(l_1)} = j_{i_2}^{(l_2)}$ as $(j_{i_2}^{(l)})_{1 \leq l \leq n_{\text{off}}}$ is a permutation of $\llbracket 1, n_{\text{off}} \rrbracket$. Therefore, there exists at most one $l_2 \in \llbracket 1, k_{n_{\text{off}}} \rrbracket$ verifying this property and, consequently,

$$\sum_{j=1}^{n_{\text{off}}} \left(w_j^{(k_{n_{\text{off}}})} \right)^2 \leq \frac{n_{\text{off}}^2}{n_{\text{on}}^2 k_{n_{\text{off}}}^2} \sum_{i_1, i_2=1}^{n_{\text{on}}} \sum_{l_1=1}^{k_{n_{\text{off}}}} 1 = \frac{n_{\text{off}}^2}{k_{n_{\text{off}}}}.$$

We can then bound the second term

$$\mathbb{E} \left[\left(\frac{1}{n_{\text{off}}} \sum_{j=1}^{n_{\text{off}}} w_j^{(k_{n_{\text{off}}})} (\psi(X'_j) - \phi(f(X'_j, \Theta_j))) \right)^2 \right]^{1/2} \leq \frac{2}{k_{n_{\text{off}}}^{1/2}} \|\phi\|_{L^\infty}$$

that converges to 0 when $k_{n_{\text{off}}}$ goes to infinity. \square

We now proceed to the derivation of the convergence rates.

Proposition 10.4.4 (Rates of convergence in the noisy case). *Assume that there exists $s > 4$ such that $\mathbb{E}[|X|^s] < +\infty$ and the assumptions of Corollary 10.3.8 and Proposition 10.4.3 hold. Then, the L^2 rate of convergence is optimal when $k_{n_{\text{off}}} \sim n_{\text{off}}^{2/(d+2)}$ and is, when $d \neq 4$,*

$$\mathbb{E} \left[\left| \widehat{\text{QI}}_{n_{\text{off}}, n_{\text{on}}}^{(k_{n_{\text{off}}})} - \text{QI} \right|^2 \right]^{1/2} = O \left(n_{\text{on}}^{-\min(1/4, 1/d)} \right) + O \left(n_{\text{off}}^{-1/(d+2)} \right).$$

When $d = 4$, the first term is replaced with $n_{\text{on}}^{-1/4} \log(1 + n_{\text{on}})^{1/2}$.

The loss of convergence order with respect to Proposition 10.4.1 is similar to the NNR context, in which it deteriorates from the rate $1/d$ in the noiseless case to the rate of $1/(d+2)$ in the noisy case [18, Section 14.6 and Section 15.3].

Proof. With the additional assumption of Corollary 10.3.8, the proof of Proposition 10.4.3 can be adapted by remarking that

$$\mathbb{E} \left[\left(\widetilde{\text{QI}}_{n_{\text{off}}, n_{\text{on}}}^{(k_{n_{\text{off}}})} - \text{QI} \right)^2 \right]^{1/2} = O \left(n_{\text{on}}^{-\min(1/4, 1/d)} \right) + O \left(\left(\frac{k_{n_{\text{off}}}}{n_{\text{off}}} \right)^{1/d} \right),$$

as a direct application of Proposition 10.4.1. Finally, the triangle inequality gives

$$\mathbb{E} \left[\left| \text{QI} - \widehat{\text{QI}}_{n_{\text{off}}, n_{\text{on}}}^{(k_{n_{\text{off}}})} \right|^2 \right]^{1/2} = O \left(\left(\frac{1}{n_{\text{on}}} \right)^{\min(1/4, 1/d)} + \left(\frac{k_{n_{\text{off}}}}{n_{\text{off}}} \right)^{1/d} + \frac{1}{k_{n_{\text{off}}}^{1/2}} \right),$$

and the optimal rate of growth is reached at $k_{n_{\text{off}}} \sim n_{\text{off}}^{2/(d+2)}$, leading to

$$\mathbb{E} \left[\left| \text{QI} - \widehat{\text{QI}}_{n_{\text{off}}, n_{\text{on}}}^{(k_{n_{\text{off}}})} \right|^2 \right]^{1/2} \leq O \left(n_{\text{on}}^{-\min(1/4, 1/d)} + n_{\text{off}}^{-1/(d+2)} \right). \quad \square$$

10.4.4 Reformulation of our results in terms of Nearest Neighbors

In this section, we do not refer to an offline and an online phase. Instead, we consider a sample $(X'_j)_{j \in [1, n]}$ of n iid observation of law $\mu_{X'}$ and a random variable $X \sim \mu_X$ independent of the sample. We do not distinguish anymore $\phi \circ f$ from f in the regression function defined in Equation (10.9), that now writes

$$\psi(X) = \mathbb{E}[f(X, \Theta)|X]$$

and its Nearest Neighbor approximation of Equation (10.10) is

$$\widehat{\psi}_n^{(k)}(x) = \frac{1}{k} \sum_{l=1}^k f(X_{j^{(l)}(x)}, \Theta_{j^{(l)}(x)}).$$

In Section 10.4.4.a, we study the case $\mu_X = \mu_{X'}$ and in Section 10.4.4.b the case $\mu_X \neq \mu_{X'}$.

10.4.4.a Convergence of the Nearest Neighbor distance for non compact support

By rewriting

$$\mathbb{E}[W_q^q(\widehat{\mu}_{\mathbf{X}_{n_{\text{on}}}}, \widehat{\mu}_{\mathbf{X}'_{n_{\text{off}}}}^{(1)})] = \mathbb{E}[|X - \text{NN}_{\mathbf{X}'_{n_{\text{off}}}}(X)|^q]$$

in Theorem 10.3.7, and choosing $\mu_{X'} = \mu_X$, we get some asymptotic properties on the Nearest Neighbor distance

$$\mathbb{E}[|X - \text{NN}_{\mathbf{X}_n}(X)|^q], \quad (10.22)$$

which has some application in the theoretical study of the Nearest Neighbor regressors and classifiers [18, Chapter 2]. The previous works on the topic focus mainly on the convergence when $q = 2$ and assume that X has a bounded support [18, 48, 78, 91].

Some works [26, 70] consider some random variables X with unbounded support in the context of the k -NN regression, *i.e.* they study the convergence of

$$\mathbb{E}\left[\left|\psi(X) - \widehat{\psi}_n^{(k)}(X)\right|\right].$$

However, they make the assumption of a bounded regression function ψ whereas, in Equation (10.22), we would like to take $\psi(X) = X$ and thus these results do not apply. A direct corollary from Theorem 10.3.7 is

Corollary 10.4.5. *Let X has a density p_X for which the strong minimal mass assumption 10.3.5 (iii) holds with $U = \mathbb{R}^d$ and*

$$\int_{\mathbb{R}^d} (1 + x^q) p_X(x)^{1-q/d} dx < +\infty.$$

We have

$$\mathbb{E}[|X - \text{NN}_{\mathbf{X}_n}(X)|^q] \underset{n \rightarrow +\infty}{\sim} \frac{\Gamma(1 + q/d)}{v_d^{q/d} n^{q/d}} \int_{\mathbb{R}^d} p_X(x)^{1-q/d} dx.$$

This extends the results of the literature by ensuring the asymptotic equivalence for some random variables with unbounded support.

10.4.4.b L^2 convergence rates of the generalization error under covariate shift

The case $\mu_X \neq \mu_{X'}$ is also of interest in the framework of the Nearest Neighbor regression. The law of the training sample is $\mu_{X'}$ and is different from the law of the test sample μ_X , leading to the so-called covariate shift.

Theorem 10.4.6 (L^2 generalization error of the k -NN regression under covariate shift). *Let μ_X (the law of the test sample) and $\mu_{X'}$ (the law of the training sample) verify the assumptions of Theorem 10.3.7, f be Lipschitz continuous in x of constant $L > 0$ uniform in Θ , and $\text{Var}(f(x, \Theta)) = \mathbb{E}[|f(x, \Theta) - \mathbb{E}[f(x, \Theta)]|^2] \leq \sigma^2 < +\infty$ for all x in the support of $\mu_{X'}$. When $k_n \sim n^{2/(d+2)}$, we have*

$$\limsup_{n \rightarrow +\infty} n^{1/(2+d)} \mathbb{E}\left[\left|\psi(X) - \widehat{\psi}_n^{(k_n)}(X)\right|^2\right]^{1/2} \leq \sigma + C \mathbb{E}\left[\frac{1}{p_{X'}(X)^{2/d}}\right]^{1/2}$$

with C a positive constant.

We retrieve essentially the same orders of convergence as in the case without covariate shift. The quantity $\mathbb{E}\left[1/p_{X'}(X)^{2/d}\right]^{1/2}$ seems to be the relevant bound of the loss due to the use of $\mu_{X'}$ instead of μ_X and we expect that the greater this quantity is, the slower the convergence will be.

Proof. The proof is an adaptation of [18, Theorem 14.5], using elements of the proof the Theorem 10.3.7 and Corollary 10.3.8. We can decompose the L^2 error

$$\mathbb{E} \left[\left| \psi(X) - \widehat{\psi}_n^{(k)}(X) \right|^2 \right]^{1/2} \leq \mathbb{E} \left[\left| \psi(X) - \widetilde{\psi}_n^{(k_n)}(X) \right|^2 \right]^{1/2} + \mathbb{E} \left[\left| \widetilde{\psi}_n^{(k_n)}(X) - \widehat{\psi}_n^{(k_n)}(X) \right|^2 \right]^{1/2}$$

with $\widetilde{\psi}_n^{(k_n)}(x) = \frac{1}{k_n} \sum_{i=1}^{k_n} \mathbb{E}[f(\text{NN}_{\mathbf{X}_n}^{(i)}(x), \Theta)]$. The first term can be bounded by

$$\mathbb{E} \left[\left| \psi(X) - \widetilde{\psi}_n^{(k_n)}(X) \right|^2 \right]^{1/2} \leq L \mathbb{E} \left[\left| X - \text{NN}_{\mathbf{X}'_n}^{(k_n)}(X) \right|^2 \right]^{1/2}$$

and then

$$\limsup_{n \rightarrow +\infty} \left(\frac{n}{k_n} \right)^{1/d} \mathbb{E} \left[\left| \psi(X) - \widetilde{\psi}_n^{(k_n)}(X) \right|^2 \right]^{1/2} \leq L c_{d,2} \mathbb{E} \left[\frac{1}{p_{X'}(X)^{2/d}} \right]^{1/2}$$

by Corollary 10.3.8. The second term is bounded by

$$\begin{aligned} \mathbb{E} \left[\left| \widetilde{\psi}_n^{(k_n)}(X) - \widehat{\psi}_n^{(k_n)}(X) \right|^2 \right]^{1/2} &= \frac{1}{k_n} \mathbb{E} \left[\sum_{i=1}^{k_n} \left(f(\text{NN}_{\mathbf{X}'_n}^{(i)}(X), \Theta_{l_i}) - \mathbb{E}[f(\text{NN}_{\mathbf{X}'_n}^{(i)}(X), \Theta) | X] \right)^2 \right]^{1/2} \\ &\leq \frac{1}{k_n^{1/2}} \sigma \end{aligned}$$

The optimal rate is $k_n \sim n^{2/(2+d)}$, leading to

$$\limsup_{n \rightarrow +\infty} n^{1/(2+d)} \mathbb{E} \left[\left| \psi(X) - \widehat{\psi}_n^{(k_n)}(X) \right|^2 \right]^{1/2} \leq \sigma + C \mathbb{E} \left[\frac{1}{p_{X'}(X)^{2/d}} \right]^{1/2},$$

with $C = L c_{d,2}$ □

10.5 Numerical illustration

10.5.1 Influence of $\mu_{X'}$ on the convergence of $\widehat{\mu}_X^{(1)}$

We investigate how the relationship between μ_X and $\mu_{X'}$ impacts the convergence of $\widehat{\mu}_{\mathbf{X}'_{n_{\text{off}}}}^{(1)}$ presented Section 10.4.1 . In this numerical experiment, we set the dimension $d = 2$, choose

$$X = (U, U), \quad U \sim \mathcal{U}([0, 1]),$$

and

$$X' \sim \mathcal{N} \left(\begin{pmatrix} \mu \\ \mu \end{pmatrix}, \sigma^2 \begin{pmatrix} 1 & s_{\text{corr}} \\ s_{\text{corr}} & 1 \end{pmatrix} \right),$$

with $\mu = 0.5$, $\sigma = 0.3$ and various s_{corr} in $(-1, 1)$. Intuitively, the closer s_{corr} is to 1, the closer $\mu_{X'}$ is to μ_X , as illustrated in Figure 10.2.

In order to quantify the quality of the reconstruction, we estimate the measure $\widehat{\mu}_{\mathbf{X}'_{n_{\text{off}}}}^{(1)}$ by Gaussian kernel density estimation [119], *i.e.*

$$\widehat{\rho}(x_1, x_2) = K_h * \widehat{\mu}_{\mathbf{X}'_{n_{\text{off}}}}^{(1)}(x_1, x_2) = \frac{1}{n_{\text{off}}} \sum_{j=1}^{n_{\text{off}}} w_j^{(1)} K_h((x_1, x_2) - X'_j)$$

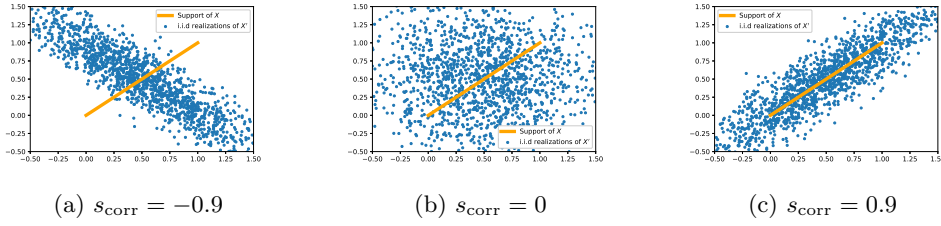


Figure 10.2: Plot of the support of X and 1500 iid realizations of X' for different values of s_{corr} .

with $K_h(x_1, x_2) = \frac{1}{2\pi h^2} \exp(-(x_1^2 + x_2^2)/2h^2)$. Then, we estimate the density of the first marginal of the conditional distribution of $\hat{\rho}$ on the support of X

$$\hat{\rho}_{[0,1]}(x) = \frac{\hat{\rho}(x, x)}{\int_0^1 \hat{\rho}(u, u) du}, \quad x \in [0, 1]$$

and we compute the integrated L^2 error of this estimation with respect to the theoretical measure $\rho_{[0,1]}(x) = 1, x \in [0, 1]$

$$e_2 = \left(\int_0^1 (\hat{\rho}_{[0,1]}(x) - \rho_{[0,1]}(x))^2 dx \right)^{1/2} = \left(\int_0^1 (\hat{\rho}_{[0,1]}(x) - 1)^2 dx \right)^{1/2}.$$

As this quantity depends on $\mathbf{X}_{n_{\text{on}}}$ and $\mathbf{X}'_{n_{\text{off}}}$, we estimate its expectation $\mathbb{E}[e_2]$.

We can see in Figure 10.3 that the greater s_{corr} is, the better the reconstruction looks like. This observation is confirmed in Figure 10.4, illustrating that $\mathbb{E}[e_2]$ decreases when s_{corr} increases, *i.e.* when the $\mu_{X'}$ gets closer to μ_X . The important amount error that is done for negative values of s_{corr} can be explained by Figures 10.2a and 10.3. Indeed, when s_{corr} is low, an observation of X' has a low probability to be drawn close to the segments $[(0, 0), (0.25, 0.25)]$ and $[(0.75, 0.75), (1, 1)]$, and thus, some values are “missed”. This effect is mitigated for greater values of s_{corr} in which some observations are closer to the segments.

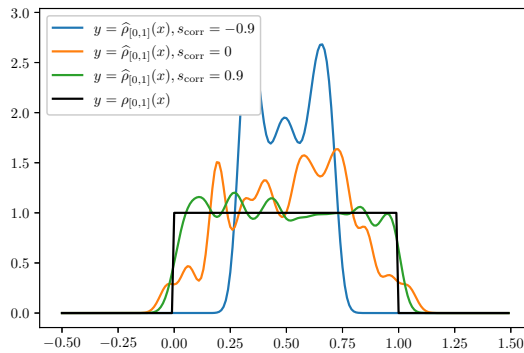


Figure 10.3: Kernel density estimation $\hat{\rho}_{[0,1]}(x)$ for different values of s_{corr} .

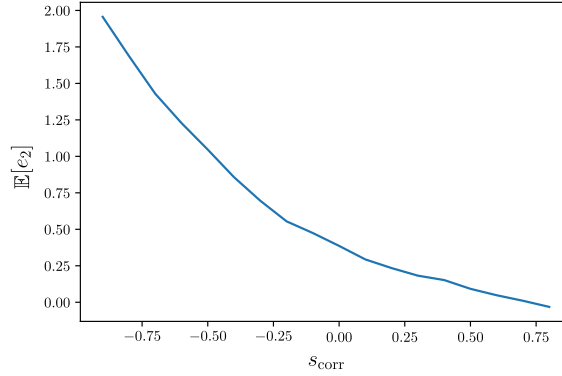


Figure 10.4: Estimation of $\mathbb{E}[e_2]$ with respect to s_{corr} by a Monte Carlo estimation of size 500 with $n_{\text{off}} = n_{\text{on}} = 600$.

10.5.2 Influence of $\mu_{X'}$ on the convergence of $\widehat{\text{QI}}_{n_{\text{off}}, n_{\text{on}}}^{(k_{n_{\text{off}}})}$

We now concentrate on the impact on the efficiency $\widehat{\text{QI}}_{n_{\text{off}}, n_{\text{on}}}^{(k_{n_{\text{off}}})}$. We keep the framework of Section 10.5.1, and we try to estimate the quantity of interest

$$\text{QI} = \mathbb{E}[\phi(f(X, \Theta))], \quad f((x_1, x_2), \theta) = \sin(2\pi x_1) \sin(2\pi x_2)(1 + \theta)$$

with $\Theta \sim \mathcal{U}([-1, 1])$ and $\phi(y) = y$. The L^2 error

$$\mathbb{E} \left[\left| \widehat{\text{QI}}_{n_{\text{off}}, n_{\text{on}}}^{(k_{n_{\text{off}}})} - \text{QI} \right|^2 \right]^{1/2} = \mathbb{E} \left[\left| \widehat{\text{QI}}_{n_{\text{off}}, n_{\text{on}}}^{(k_{n_{\text{off}}})} - 0.5 \right|^2 \right]^{1/2}$$

is computed by Monte Carlo estimation. As highlighted in Figure 10.5, the closeness of μ_X to $\mu_{X'}$ is an important factor for the efficiency of the estimator.

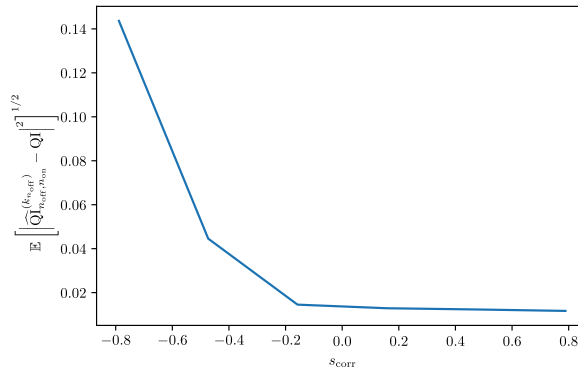


Figure 10.5: Estimation of the L^2 error with respect to s_{corr} for $n_{\text{on}} = n_{\text{off}} = 900$ and $k_{n_{\text{off}}} = 4$, averaged on 2000 replications.

Chapter 11

Uncertainty quantification in graphs of functions using reweighting methods

11.1 Introduction

This chapter is dedicated to the study of a method to propagate uncertainties in graphs of functions/computer codes. This problematic, originally motivated by the need for simulation in complex systems, has been the main focus of recent research works [4, 6, 57, 82, 84, 101].

Our approach is based more specifically on sample reweighting and propagation of the weights in a graph. It can be seen as a generalization of the method exposed in [6] and it keeps the benefit of being compatible with a “disciplinary autonomy”, as exposed in Section 9.1.

From a technical point of view, we can summarize the approach with three “key ideas”.

1. A graph of composition of computer codes is in general a *continuous Bayesian network*, provided that the graph is directed and acyclic. It can then be described only by the local conditional dependencies given between the random variables at each nodes. These dependencies are given by the equation $Y_v = f(X_v, \Theta_v)$.
2. Nonparametric linear regressions and some supervised machine learning methods gives naturally a weighting procedure, that we call WLAM. They can provide some approximate conditional laws of Y_v given X_v under the form of *discrete conditional probability tables*.
3. When we replace the true laws by the approximate laws at each node, the resulting Bayesian network is now *discrete*. It is possible to compute the approximate full law of any subset of variables using the already existing algorithms for discrete Bayesian network.

The steps 1 and 3 are relatively straightforward, once stated rigorously. One remaining fundamental challenge is to know when the WLAMs can approximate the true law and how good they are at doing it, as this directly drives the performances of the algorithm.

Our works focus on providing a rigorous definition of a WLAM and a “local” consistency criterion at a node that ensure the consistency of the “global” propagation in the graph, in a weak sense. We also exhibit the general expression of the weights, along with a way to construct explicitly the discrete Bayesian network of step 3.

11.1.1 Graph of computer codes

In this section, we recall the definitions introduced in Chapter 9 for a graph of computer codes and we introduce the required probabilistic framework. In our context, the design process of complex industrial systems is naturally modeled by a directed graph structure $\mathcal{G} = (\mathcal{V}, \mathcal{E})$. More precisely, each vertex $v \in \mathcal{V}$ is associated with a function

$$f_v : \begin{cases} \mathbf{E}_v \times \Theta_v & \rightarrow \mathbf{F}_v \\ (x_v, \theta_v) & \mapsto y_v \end{cases}$$

and a pair of vertices (u, v) belongs to the set of edges \mathcal{E} if the output y_u is an input of v . Thus, each edge $(u, v) \in \mathcal{E}$ is associated with a function

$$g_{u,v} : \begin{cases} \mathbf{F}_u & \rightarrow \mathbf{E}_{u,v} \\ y_u & \mapsto x_{u,v} \end{cases}$$

which represents the actual information contained in y_u which is taken as an input for v , and the vertices satisfy the compatibility condition

$$\forall v \in \mathcal{V}, \quad \mathbf{E}_v = \prod_{u \in \mathcal{J}(v)} \mathbf{E}_{u,v},$$

where $\mathcal{J}(v) := \{u \in \mathcal{V} : (u, v) \in \mathcal{E}\}$ denotes the set of *parents* of v in \mathcal{G} . When $\mathcal{J}(v) = \emptyset$, we call v a *root* of \mathcal{G} .

In the sequel, we shall work under the crucial assumption that \mathcal{G} is a *Directed Acyclic Graph* (DAG), that is to say that it does not contain oriented cycles. This excludes the situation, called *strong coupling* in the industrial context, where two numerical models take as input the output of each other. This structural assumption induces a partial order on \mathcal{V} which then allows to define inductively, given $(\theta_v)_{v \in \mathcal{V}}$:

- for any root v , the variable $y_v = f_v(\theta_v)$;
- for any edge (u, v) for which y_u is defined, $x_{u,v} = g_{u,v}(y_u)$;
- for any vertex v such that the variables $x_{u,v}$, $u \in \mathcal{J}(v)$ are defined, the variable $y_v = f_v(x_v, \theta_v)$, with $x_v = (x_{u,v})_{u \in \mathcal{J}(v)}$.

Thus, the vector $y_{\mathcal{V}} := (y_v)_{v \in \mathcal{V}}$ is well-defined as a (composite) function of $\theta_{\mathcal{V}} := (\theta_v)_{v \in \mathcal{V}}$, which we denote by

$$F_{\mathcal{V}} : \begin{cases} \prod_{v \in \mathcal{V}} \Theta_v & \rightarrow \prod_{v \in \mathcal{V}} \mathbf{F}_v, \\ \theta_{\mathcal{V}} & \mapsto y_{\mathcal{V}}. \end{cases}$$

These definitions are illustrated on Figure 11.1. We shall from now on assume that all sets \mathbf{E}_v , Θ_v and \mathbf{F}_v are endowed with a σ -field (and in particular that the σ -field over \mathbf{E}_v is the product of the σ -fields over $\mathbf{E}_{u,v}$, $u \in \mathcal{J}(v)$), and that all functions f_v , $g_{u,v}$ are measurable. We define the *canonical probability space* $(\Omega, \mathcal{F}, \mathbb{P})$ by $\Omega = \prod_{v \in \mathcal{V}} \Theta_v$, \mathcal{F} the associated product σ -field, and $\mathbb{P} = \otimes_{v \in \mathcal{V}} \mu_{\Theta_v}$. On this canonical space, elements of Ω are generically denoted by $\Theta_{\mathcal{V}} := (\Theta_v)_{v \in \mathcal{V}}$ and, for any $v \in \mathcal{V}$ and $(u, v) \in \mathcal{E}$, the random variables $X_{u,v}$, X_v , Y_v are defined according to the procedure above. Our purpose is then to estimate quantities of interest related with the joint law of $Y_{\mathcal{V}} := (Y_v)_{v \in \mathcal{V}}$. Notice that for sensitivity analysis, quantities of interest related with the joint law of $\{\Theta_{\mathcal{V}}, Y_{\mathcal{V}}\}$ are also relevant.

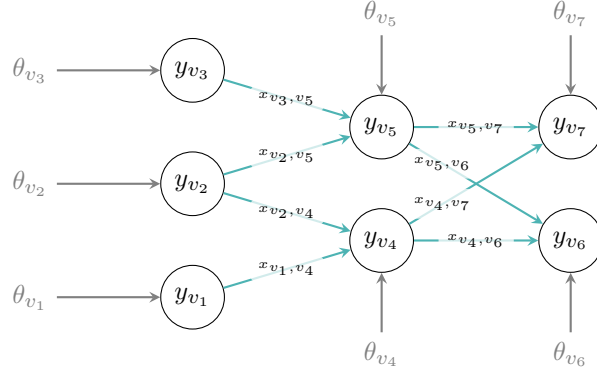


Figure 11.1: An example of a graph of numerical models with 7 vertices. The vertices v_3, v_2, v_1 are roots, and the vertices v_7, v_6 are leaves.

11.1.2 Reweighting methods

Let $\Phi : \prod_{v \in \mathcal{V}} F_v \rightarrow \mathbb{R}$ be a measurable (and, say, bounded) function. In order to estimate the quantity of interest

$$\text{QI} := \mathbb{E} [\Phi (Y_{\mathcal{V}})],$$

an obvious direct Monte Carlo procedure consists in fixing $n \geq 1$ and proceeding sequentially, following the DAG structure of \mathcal{G} , as follows:

- each root v generates n independent realisations $\Theta_{v,1}, \dots, \Theta_{v,n}$ according to μ_{Θ_v} and computes a sample $Y_{v,1} = f_v(\Theta_{v,1}), \dots, Y_{v,n} = f_v(\Theta_{v,n})$ which we denote by $\mathbf{Y}_{v,n}$;
- for each $v \in \mathcal{V}$ such that the samples $\mathbf{Y}_{u,n}, u \in \mathcal{J}(v)$ have been computed, the vertex v generates n independent realisations $\Theta_{v,1}, \dots, \Theta_{v,n}$ according to μ_{Θ_v} and computes a sample $Y_{v,1} = f_v(X_{v,1}, \Theta_{v,1}), \dots, Y_{v,n} = f_v(X_{v,n}, \Theta_{v,n})$ which we denote by $\mathbf{Y}_{v,n}$, with $X_{v,j} = (g_{u,v}(Y_{u,j}))_{u \in \mathcal{J}(v)}$ for any $j \in \{1, \dots, n\}$;

and QI is estimated by

$$\widehat{\text{QI}}_n^{\text{MC}} := \frac{1}{n} \sum_{j=1}^n \Phi (Y_{\mathcal{V},j}), \quad Y_{\mathcal{V},j} := (Y_{v,j})_{v \in \mathcal{V}}.$$

Since this estimator directly rewrites

$$\widehat{\text{QI}}_n^{\text{MC}} = \frac{1}{n} \sum_{j=1}^n \Phi (F_{\mathcal{V}}(\Theta_{\mathcal{V},j})), \quad \Theta_{\mathcal{V},j} := (\Theta_{v,j})_{v \in \mathcal{V}},$$

and the vectors $\Theta_{\mathcal{V},j}, j \in \{1, \dots, n\}$ are iid according to \mathbb{P} , it is clear that it is (strongly) consistent, in the sense that when $n \rightarrow +\infty$, it converges almost surely to QI. Notice that all random variables involved in this procedure need not be defined on the canonical probability space, but on the contrary it is more natural to define them on some *experimental* probability space on which each vertex $v \in \mathcal{V}$ is assumed to be able to generate a sequence $(\Theta_{v,j})_{j \geq 1}$ of independent realisations of μ_{Θ_v} .

This direct Monte Carlo procedure is generally difficult to implement in practice for large networks because it requires each vertex v to wait for the results of all upstream codes before

running its own code, and if the evaluation of f_v is time consuming then the whole process becomes intractable. In this chapter, we study a decomposition method, partially inspired by [4, 6], in which all vertices work in parallel with a *synthetic sample* $X'_{v,1}, \dots, X'_{v,n_v}$ which is generated locally, independently from the results of other codes, during some *offline* phase. We however assume that during this offline phase, each vertex remains able to sample independent realisations $\Theta_{v,1}, \dots, \Theta_{v,n_v}$ from the ‘true’ distribution μ_{Θ_v} . The offline phase results in a family of samples $\mathbf{S}_{v,n_v} = (X'_{v,j}, Y'_{v,j})_{1 \leq j \leq n_v}$, with $Y'_{v,j} = f_v(X'_{j,v}, \Theta_{j,v})$, which are sent to a *simulation architect*. In an *online* phase, the simulation architect then has to construct an estimator of QI based only on the collection of samples $\mathbf{S}_{\mathcal{V}} := (\mathbf{S}_{v,n_v})_{v \in \mathcal{V}}$.

11.1.3 Outline and main results

We address the estimation of QI in this offline/online context by looking for estimators of the form

$$\widehat{\text{QI}}_{n_{\mathcal{V}}} = \sum_{j_{\mathcal{V}} \in \mathcal{N}_{\mathcal{V}}} w_{j_{\mathcal{V}}}(\mathbf{S}_{\mathcal{V}}) \Phi(Y'_{j_{\mathcal{V}}}), \quad (11.1)$$

with

$$n_{\mathcal{V}} := (n_v)_{v \in \mathcal{V}}, \quad j_{\mathcal{V}} := (j_v)_{v \in \mathcal{V}}, \quad \mathcal{N}_{\mathcal{V}} := \prod_{v \in \mathcal{V}} \{1, \dots, n_v\}, \quad Y'_{j_{\mathcal{V}}} := (Y'_{v,j_v})_{v \in \mathcal{V}}. \quad (11.2)$$

In this formula, $(w_{j_{\mathcal{V}}}(\mathbf{S}_{\mathcal{V}}))_{j_{\mathcal{V}} \in \mathcal{N}_{\mathcal{V}}}$ is some family of *weights* which somehow represent how likely each observation $Y'_{j_{\mathcal{V}}}$ should be under \mathbb{P} . We shall proceed in two steps.

In Section 11.2, we assume that for each vertex v and any $x_v \in \mathbf{E}_v$, we are given a method to compute an estimator of

$$\ell_v(x_v, dy_v) := \mathbb{P}(Y_v \in dy_v | X_v = x_v) = \mu_{\Theta_v} \circ f_v(x_v, \cdot)^{-1}(dy_v)$$

of the form

$$\sum_{j=1}^{n_v} W_{v,j}(\mathbf{S}_{v,n_v}, x_v) \delta_{Y'_{v,j}}(dy_v).$$

When v is a root, that is to say $\mathbf{E}_v = \emptyset$, we adapt the notation above and assume that we are given estimators of

$$\ell_v(dy_v) := \mathbb{P}(Y_v \in dy_v) = \mu_{\Theta_v} \circ f_v^{-1}(dy_v)$$

of the form

$$\sum_{j=1}^{n_v} W_{v,j} \delta_{Y'_{v,j}}(dy_v).$$

We call such a method a *Weighted Linear Approximation Method* (WLAM). The main results of Section 11.2 are the formula (11.9), which defines the global weight $w_{j_{\mathcal{V}}}(\mathbf{S}_{\mathcal{V}})$ as a function of the local weights $W_{v,j}(\mathbf{S}_{v,n_v}, x_v)$ and Theorem 11.2.9 which shows the consistency of this formula.

In Section 11.2.1.c, we then construct a particular instance of a WLAM, based on the Nearest Neighbor regression method studied in Chapter 10. Combining this construction with the results from Theorem 11.2.9 finally yields a consistent estimator of QI.

Section 11.3 is dedicated to some numerical considerations. We construct an intermediary discrete Bayesian network, that permits to simplify the computations of the weights $w_{j_{\mathcal{V}}}(\mathbf{S}_{\mathcal{V}})$ using classic results from the Bayesian network literature. Finally, this procedure is applied in Section 11.4 on an industrial multidisciplinary use case.

11.2 Reweighting procedure

In this section, we provide a practical algorithm to compute a family of weights $(w_{j_{\mathcal{V}}}(\mathbf{S}_{\mathcal{V}}))_{j_{\mathcal{V}} \in \mathcal{N}_{\mathcal{V}}}$ which makes the estimator $\widehat{\mathbb{Q}}_{n_{\mathcal{V}}}$ defined in (11.1) consistent, in a certain sense, when the sizes n_v , $v \in \mathcal{V}$ of all samples go to $+\infty$. The building brick of our method is the notion of WLAM introduced in Subsection 11.2.1 on a single vertex, and then applied to the graph in Subsection 11.2.2.

11.2.1 Weighted Linear Approximation Method

In this subsection we work at the level of a single vertex and therefore remove the subscript v from our notation. We thus let \mathbf{E} , \mathbf{T} and \mathbf{F} be three measurable spaces, $f : \mathbf{E} \times \mathbf{T} \rightarrow \mathbf{F}$ be a measurable function, and μ_{Θ} be a probability measure on \mathbf{T} .

We assume that, on some *canonical* probability space $(\Omega, \mathcal{F}, \mathbb{P})$, two independent random variables X and Θ are defined, with respective distribution μ_X and μ_{Θ} , and let $Y = f(X, \Theta)$. For any $x \in \mathbf{E}$, the conditional distribution of Y given $X = x$, which is the pushforward measure of μ_{Θ} by the function $f(x, \cdot)$, is then denoted by $\ell(x, dy)$ (and simply $\ell(dy)$ if $\mathbf{E} = \emptyset$).

We also assume that, on some *experimental* probability space $(\Omega^*, \mathcal{F}^*, \mathbb{P}^*)$, a sequence of independent random variables $(\Theta_j)_{j \geq 1}$ distributed according to μ_{Θ} is defined.

Last, we denote by $\mathfrak{B}_{\mathbf{F}}$ the space of real-valued, bounded and measurable functions on \mathbf{F} .

11.2.1.a Definition and consistency

Definition 11.2.1 (WLAM). *In the setting described above, an n -Weighted Linear Approximation Method (n -WLAM) is a pair $(\mathbf{W}_n, \mathbf{X}'_n)$ such that:*

- $\mathbf{X}'_n = (X'_j)_{1 \leq j \leq n}$ is a collection of \mathbf{E} -valued random variables, defined on the probability space $(\Omega^*, \mathcal{F}^*, \mathbb{P}^*)$, and independent from the sequence $(\Theta_j)_{j \geq 1}$;
- $\mathbf{W}_n = (W_j)_{1 \leq j \leq n} : (\mathbf{E} \times \mathbf{F})^n \times \mathbf{E} \rightarrow [0, +\infty)^n$ is a function such that, for any $\mathbf{s}_n \in (\mathbf{E} \times \mathbf{F})^n$ and $x \in \mathbf{E}$,

$$\sum_{j=1}^n W_j(\mathbf{s}_n, x) = 1.$$

In the particular case where $\mathbf{E} = \emptyset$, an n -WLAM is simply a vector $\mathbf{W}_n = (W_j)_{1 \leq j \leq n}$ of nonnegative numbers whose sum equals to 1.

An n -WLAM naturally induces a random Markov kernel $\widehat{\ell}_n(x, dy)$ from \mathbf{E} to \mathbf{F} , defined by

$$\forall x \in \mathbf{E}, \quad \widehat{\ell}_n(x, dy) = \sum_{j=1}^n W_j(\mathbf{S}_n, x) \delta_{Y'_j}(dy),$$

where the sample \mathbf{S}_n is defined on the experimental probability space by $\mathbf{S}_n = (X'_j, Y'_j)_{1 \leq j \leq n}$, with $Y'_j = f(X'_j, \Theta_j)$.

Definition 11.2.2 (Consistency). *Let \mathfrak{B} be a linear subspace of $\mathfrak{B}_{\mathbf{F}}$. A sequence of n -WLAMs, $n \geq 1$, is called \mathfrak{B} -consistent if, for any $x \in \mathbf{E}$ and $\phi \in \mathfrak{B}$,*

$$\lim_{n \rightarrow +\infty} \int_{y \in \mathbf{F}} \phi(y) \widehat{\ell}_n(x, dy) = \int_{y \in \mathbf{F}} \phi(y) \ell(x, dy), \quad \text{in probability on } (\Omega^*, \mathcal{F}^*, \mathbb{P}^*).$$

In the sequel we shall always implicitly consider sequences of n -WLAMs, to which we shall simply refer as ‘WLAM’.

Definition 11.2.2 rewrites, for any $\phi \in \mathfrak{B}$, for any $x \in \mathbf{E}$,

$$\lim_{n \rightarrow +\infty} \sum_{j=1}^n W_j(\mathbf{S}_n, x) \phi(Y_j) = \mathbb{E}[\phi(Y)|X = x],$$

in probability. In other words, a WLAM can be reinterpreted as a linear nonparametric regression estimator for $\mathbb{E}[\phi(Y)|X = x] = \mathbb{E}[\phi(f(x, \Theta))]$ [117, Section 1.5], which is consistent for any function ϕ in the class \mathfrak{B} .

11.2.1.b Examples and comments

Example 11.2.3 (Case $\mathbf{E} = \emptyset$). If $\mathbf{E} = \emptyset$, the WLAM \mathbf{W}_n defined by $W_j = 1/n$ for any $j \in \{1, \dots, n\}$ is \mathfrak{B}_F -consistent.

Example 11.2.4 (Discrete case). Assume that \mathbf{E} is a discrete space and let $\mu_{X'}$ be a probability measure on \mathbf{E} such that $\mu_{X'}(x) > 0$ for any $x \in \mathbf{E}$. Consider the WLAM composed by a sample \mathbf{X}'_n of independent random variables X'_1, \dots, X'_n distributed according to $\mu_{X'}$, and the function \mathbf{W}_n defined by

$$W_j(\mathbf{S}_n, x) = \begin{cases} \frac{1}{n} & \text{if } \Sigma(x) = 0, \\ \frac{\mathbb{1}_{\{x=X'_j\}}}{\Sigma(x)} & \text{if } \Sigma(x) > 0, \end{cases}$$

where $\Sigma(x) := \sum_{j=1}^n \mathbb{1}_{\{x=X'_j\}}$. This WLAM is \mathfrak{B}_F -consistent.

Example 11.2.5 (Nadaraya–Watson WLAM). If $\mathbf{E} = \mathbb{R}^d$, a natural generalisation of Example 11.2.4 would be to draw an iid synthetic sample X'_1, \dots, X'_n according to some probability measure $\mu_{X'}$, and set

$$W_j(\mathbf{S}_n, x) = \frac{\delta_{X'_j}(dx)}{\Sigma(x)}, \quad \Sigma(x) := \sum_{j=1}^n \delta_{X'_j}(dx),$$

but of course this expression does not make sense. Smoothing the Dirac masses by convolution with a kernel $K > 0$ and a bandwidth $h > 0$, we get

$$W_j(\mathbf{S}_n, x) = \frac{K(h^{-1}(x - X'_j))}{\Sigma_h(x)}, \quad \Sigma_h(x) := \sum_{j=1}^n K(h^{-1}(x - X'_j)).$$

For any $\phi \in \mathfrak{B}_F$, the quantity

$$\int_{y \in \mathbf{F}} \phi(y) \widehat{\ell}_n(x, dy) = \sum_{j=1}^n W_j(\mathbf{S}_n, x) \phi(Y'_j)$$

then turns out to be the Nadaraya–Watson estimator of the regression function $\mathbb{E}[\phi(Y)|X = x]$ [117, Section 1.5]. From standard results in kernel density estimation, it can be checked that if $\mu_{X'}$ has a positive and continuous density with respect to the Lebesgue measure on \mathbb{R}^d , and the bandwidth $h = h_n$ is chosen so that $h_n \rightarrow 0$, $nh_n \rightarrow +\infty$, then this WLAM is \mathfrak{B} -consistent, for any class \mathfrak{B} of measurable and bounded functions ϕ for which the mapping $x \mapsto \mathbb{E}[\phi(f(x, \Theta))]$ is continuous.

A WLAM based on another popular nonparametric regression method, the Nearest Neighbor method, will be discussed in detail in Section 11.2.1.c. In contrast, parametric regression methods, such as linear or logistic, may only be expected to yield consistent WLAMs for drastically restricted classes of functions ϕ and f .

In the previous examples, the weights $W_j(\mathbf{S}_n, x)$ only depend on the sample \mathbf{S}_n through \mathbf{X}'_n , but there are nonparametric regression methods, such as regression trees [59], for which weights also depend on (Y'_1, \dots, Y'_n) . Last, let us also emphasise the fact that while in the examples above, the design \mathbf{X}'_n is iid, our framework also allows to work with deterministic, user-chosen designs, as long as they fulfill the consistency property of Definition 11.2.2.

11.2.1.c The Nearest Neighbor WLAM

From the results of Chapter 10, we naturally infer the construction of the following WLAM: \mathbf{X}'_n is the synthetic sample X'_1, \dots, X'_n , taken iid according to $\mu_{X'}$, and for any $\mathbf{s}_n = (\mathbf{x}'_n, \mathbf{y}_n)$ and $x \in \mathbb{R}^d$, we let $\mathbf{W}_n^{(k)} = (W_j^{(k)})_{1 \leq j \leq n}$ be defined by

$$W_j^{(k)}(\mathbf{s}_n, x) = \frac{1}{k} \sum_{l=1}^k \mathbb{1}_{\{j=j^{(l)}(x)\}},$$

with $j^{(l)}(x)$ the (lowest) index j such that x'_j is the l -th closest point to x , among the sample \mathbf{x}'_n . The consistency of this WLAM follows from Proposition 10.4.3 with $\mu_X = \delta_x$.

Proposition 11.2.6 (Consistency of the Nearest Neighbor WLAM). *Assume that the synthetic sample \mathbf{X}'_n is drawn according to a probability measure $\mu_{X'}$ with support \mathbb{R}^d and such that there exists $m_0 \geq 1$ for which $\mathbb{E}[\min_{1 \leq j \leq m_0} |X'_j|] < +\infty$. Then for any sequence of positive integers $(k_n)_{n \geq 1}$ such that $k_n \rightarrow +\infty$ and $k_n/n \rightarrow 0$, the WLAM $(\mathbf{X}'_n, \mathbf{W}_n^{(k_n)})$ is \mathfrak{B} -consistent, for any class \mathfrak{B} of measurable and bounded functions ϕ for which the mapping $x \mapsto \mathbb{E}[\phi(f(x, \Theta))]$ is Lipschitz continuous.*

More explicitly, if the mapping $x \mapsto f(x, \theta)$ is assumed to be Lipschitz continuous, uniformly in θ , then under the assumptions of Proposition 11.2.6, the WLAM $(\mathbf{X}'_n, \mathbf{W}_n^{(k_n)})$ is \mathfrak{B} -consistent with \mathfrak{B} the class of bounded and Lipschitz continuous functions.

11.2.1.d Toward WLAM composition

As a consequence of Definition 11.2.2, if a WLAM $(\mathbf{W}_n, \mathbf{X}'_n)_{n \geq 1}$ is \mathfrak{B} -consistent, then for any measurable and bounded function $\Phi : \mathbb{E} \times \mathbb{F} \rightarrow \mathbb{R}$ such that $\Phi(x, \cdot) \in \mathfrak{B}$ for all $x \in \mathbb{E}$, we have

$$\lim_{n \rightarrow +\infty} \int_{\mathbb{E}} \sum_{j=1}^n W_j(\mathbf{S}_n, x) \Phi(x, Y'_j) \mu_X(dx) = \mathbb{E}[\Phi(X, Y)], \quad (11.3)$$

in probability. This suggests that if the probability measure μ_X is approximated by a finite sum of Dirac masses

$$\hat{\mu}_{X,m} = \sum_{i=1}^m w_i \delta_{X'_i},$$

then the joint law of (X, Y) should be approximated by the probability measure

$$\sum_{i=1}^m \sum_{j=1}^n w_i W_j(\mathbf{S}_n, X'_i) \delta_{(X'_i, Y'_j)}. \quad (11.4)$$

This remark will be generalised in the next subsection.

Remark 11.2.7 (Linearity of a WLAM). *The linear nature of the WLAM is exhibited in Equation (11.3). Indeed, even though the mapping $x \mapsto W_j(\mathbf{S}_n, x)$ is far from linear in general, we can define the image operator G of a WLAM so that, for each measure ρ ,*

$$G(\rho) = \sum_{i=1}^n \left(\int_E W_j(\mathbf{S}_n, x) \rho(dx) \right) \delta_{Y_j'}.$$

This operator is linear on the vector space of the finite measures on E and verifies $G(\rho)(F) = \rho(E)$. In particular a probability measure on E is mapped to a probability measure on F .

11.2.2 Computing weights on the graph

In this subsection, we come back to the study of the graph of numerical models \mathcal{G} and assume that each vertex $v \in \mathcal{V}$ is provided with a consistent WLAM $(\mathbf{W}_{v, n_v}, \mathbf{X}'_{v, n_v})$ defined on some experimental probability space $(\Omega_v^*, \mathcal{F}_v^*, \mathbb{P}_v^*)$. We denote by $\mathbf{S}_{v, n_v} = (X'_{v, j}, Y_{v, j})_{1 \leq j \leq n_v}$ the associated sample, defined on the product $(\Omega_{\mathcal{V}}^*, \mathcal{F}_{\mathcal{V}}^*, \mathbb{P}_{\mathcal{V}}^*)$ of all the experimental spaces.

Our purpose is now to describe an ‘online’ algorithm taking as an input the WLAMs of all vertices and returning a family of weights $(w_{j_{\mathcal{V}}}(\mathbf{S}_{\mathcal{V}}))_{j_{\mathcal{V}} \in \mathcal{N}_{\mathcal{V}}}$ making the estimator $\widehat{\text{QI}}_{n_{\mathcal{V}}}$ of QI defined in (11.1) consistent.

11.2.2.a Markov property and factorisation formula

A *leaf* is a vertex $v \in \mathcal{V}$ which has no descendent, that is to say that there is no edge in \mathcal{G} of the form (v, w) . Let us denote by $\mathcal{L} \subset \mathcal{V}$ the set of leaves, and introduce the sub- σ -field of the canonical probability space

$$\mathcal{F}_- := \sigma((\Theta_v)_{v \in \mathcal{V} \setminus \mathcal{L}}),$$

which is generated by the family of random variables Θ_v which are not located on leaves. Clearly, for any $v \in \mathcal{L}$, the random variable X_v is \mathcal{F}_- -measurable, while Θ_v is independent from \mathcal{F}_- . Therefore, since the random variables $(\Theta_v)_{v \in \mathcal{L}}$ are independent, the conditional distribution of $(Y_v)_{v \in \mathcal{L}}$ given \mathcal{F}_- is the product measure¹

$$\prod_{v \in \mathcal{L}} \ell_v(X_v, dy_v),$$

where we recall that, for each $v \in \mathcal{L}$, $X_v = (g_{u, v}(Y_u))_{u \in \mathcal{J}(v)}$. This fact can be seen as a Markov property for the graph structure of \mathcal{G} .

We deduce that the joint law $\mu_{Y_{\mathcal{V}}}(dy_{\mathcal{V}})$ of the complete vector $Y_{\mathcal{V}} = (Y_v)_{v \in \mathcal{V}}$ satisfies the disintegration formula

$$\mu_{Y_{\mathcal{V}}}(dy_{\mathcal{V}}) = \mu_{Y_{\mathcal{V} \setminus \mathcal{L}}}(dy_{\mathcal{V} \setminus \mathcal{L}}) \prod_{v \in \mathcal{L}} \ell_v(x_v, dy_v), \quad x_v = (g_{u, v}(y_u))_{u \in \mathcal{J}(v)},$$

where $\mu_{Y_{\mathcal{V} \setminus \mathcal{L}}}(dy_{\mathcal{V} \setminus \mathcal{L}})$ refers to the law of the vector $Y_{\mathcal{V} \setminus \mathcal{L}} = (Y_v)_{v \in \mathcal{V} \setminus \mathcal{L}}$. Since \mathcal{G} is a DAG with a finite number of vertices, it is easily seen that $\mathcal{L} \neq \emptyset$. Therefore, the disintegration formula may be iterated to yield inductively

$$\mu_{Y_{\mathcal{V}}}(dy_{\mathcal{V}}) = \prod_{v \in \mathcal{R}} \ell_v(dy_v) \prod_{v \in \mathcal{V} \setminus \mathcal{R}} \ell_v(x_v, dy_v), \quad x_v = (g_{u, v}(y_u))_{u \in \mathcal{J}(v)}, \quad (11.5)$$

where \mathcal{R} denotes the set of roots of \mathcal{V} .

¹In this expression, the terms corresponding to vertices v which are roots should write $\ell_v(dy_v)$ rather than $\ell_v(X_v, dy_v)$. In order not to overload the presentation, we shall often keep this distinction implicit in the sequel.

11.2.2.b Definition of weights and consistency theorem

We recall that, for each root $v \in \mathcal{R}$, the law $\ell_v(dy_v)$ of Y_v is approximated by

$$\widehat{\ell}_{v,n_v}(dy_v) = \sum_{j=1}^{n_v} W_{v,j} \delta_{Y'_{v,j}}(dy_v),$$

and for any $v \in \mathcal{V} \setminus \mathcal{R}$ and $x \in E_v$, the conditional distribution $\ell_v(x_v, dy_v)$ of Y_v given $X_v = x$ is approximated by

$$\widehat{\ell}_{v,n_v}(x, dy_v) = \sum_{j=1}^{n_v} W_{v,j}(\mathbf{S}_{v,n_v}, x) \delta_{Y'_{v,j}}(dy_v). \quad (11.6)$$

It is therefore natural to approximate the joint law $\mu_{Y_{\mathcal{V}}}(dy_{\mathcal{V}})$, which satisfies the factorisation formula (11.5), by the measure

$$\widehat{\mu}_{Y_{\mathcal{V}},n_{\mathcal{V}}}(dy_{\mathcal{V}}) := \prod_{v \in \mathcal{R}} \widehat{\ell}_{v,n_v}(dy_v) \prod_{v \in \mathcal{V} \setminus \mathcal{R}} \widehat{\ell}_{v,n_v}(x_v, dy_v), \quad x_v = (g_{u,v}(y_u))_{u \in \mathcal{F}(v)}. \quad (11.7)$$

The latter rewrites

$$\widehat{\mu}_{Y_{\mathcal{V}},n_{\mathcal{V}}}(dy_{\mathcal{V}}) = \sum_{j_{\mathcal{V}} \in \mathcal{N}_{\mathcal{V}}} w_{j_{\mathcal{V}}}(\mathbf{S}_{\mathcal{V}}) \delta_{Y'_{j_{\mathcal{V}}}}(dy_{\mathcal{V}}), \quad (11.8)$$

where we recall the notation from (11.2) and, for any $j_{\mathcal{V}} \in \mathcal{N}_{\mathcal{V}}$, we set

$$w_{j_{\mathcal{V}}}(\mathbf{S}_{\mathcal{V}}) := \prod_{v \in \mathcal{R}} W_{v,j_v} \prod_{v \in \mathcal{V} \setminus \mathcal{R}} W_{v,j_v}(\mathbf{S}_{v,n_v}, (g_{u,v}(Y'_{u,j_u}))_{u \in \mathcal{F}(v)}). \quad (11.9)$$

This definition generalises the derivation of (11.4).

We now study the consistency of the estimator $\widehat{\mathbf{Q}}\mathbf{I}_{n_{\mathcal{V}}}$, defined in (11.1), with weights $w_{j_{\mathcal{V}}}(\mathbf{S}_{\mathcal{V}})$ given by (11.9). We shall state a weak form of consistency, in which the limits $n_v \rightarrow +\infty$, $v \in \mathcal{V}$ must be taken in the reverse order induced by \mathcal{G} , see Theorem 11.2.9 below. We believe that stronger conditions on the model and the WLAMs may be imposed in order to make the consistency hold in the joint limit $(n_v)_{v \in \mathcal{V}} \rightarrow +\infty$, but stick to this simple statement as a ‘proof-of-concept’ theoretical justification of the approximation of QI by $\widehat{\mathbf{Q}}\mathbf{I}_{n_{\mathcal{V}}}$.

From now on, we denote by N the cardinality of \mathcal{V} .

Definition 11.2.8 (\mathcal{G} -coherent enumeration of \mathcal{V}). *An enumeration v_1, \dots, v_N of \mathcal{V} is \mathcal{G} -coherent if, for any pair of indices (k, l) such that $k < l$, there is no oriented path from v_l to v_k in \mathcal{G} .*

Given such an enumeration, to any measurable and bounded function $\Phi : \prod_{v \in \mathcal{V}} F_v \rightarrow \mathbb{R}$ we associate the family of measurable and bounded functions $\Phi_l : \prod_{k=1}^l F_{v_k} \rightarrow \mathbb{R}$, $l \in \{0, \dots, N\}$, defined by $\Phi_N := \Phi$ and, for $l \in \{0, \dots, N-1\}$,

$$\Phi_l((y_{v_k})_{1 \leq k \leq l}) := \int_{y_{v_{l+1}} \in F_{v_{l+1}}} \Phi_{l+1}(y_{v_1}, \dots, y_{v_l}, y_{v_{l+1}}) \ell_{v_{l+1}}(x_{v_{l+1}}, dy_{v_{l+1}}),$$

with $x_{v_{l+1}} = (g_{u,v_{l+1}}(y_u))_{u \in \mathcal{F}(v_{l+1})}$, and $\ell_{v_{l+1}}(x_{v_{l+1}}, dy_{v_{l+1}})$ replaced with $\ell_{v_{l+1}}(dy_{v_{l+1}})$ if $v_{l+1} \in \mathcal{R}$. This expression is well defined because $x_{v_{l+1}}$ can only depend on the values of y_{v_1}, \dots, y_{v_l} ; besides, $\Phi_0 = \mathbf{Q}\mathbf{I}$.

Theorem 11.2.9 (\mathcal{G} -consistency of $\widehat{\text{QI}}_{n_{\mathcal{V}}}$). *Assume that for each $v \in \mathcal{V}$, the WLAM $(\mathbf{W}_{v,n_v}, \mathbf{X}'_{v,n_v})$ is \mathfrak{B}_v -consistent, for some linear subspace \mathfrak{B}_v of the space of bounded and measurable functions \mathfrak{B}_{F_v} on F_v . Let v_1, \dots, v_N be a \mathcal{G} -coherent enumeration of \mathcal{V} . Let $\Phi : \prod_{v \in \mathcal{V}} F_v \rightarrow \mathbb{R}$ be a measurable and bounded function, and assume that for any $l \in \{1, \dots, N\}$, for all $(y_{v_k})_{1 \leq k \leq l-1}$, the function $y_{v_l} \mapsto \Phi_l(y_{v_1}, \dots, y_{v_{l-1}}, y_{v_l})$ belongs to \mathfrak{B}_{v_l} . Then we have*

$$\lim_{n_{v_1} \rightarrow +\infty} \cdots \lim_{n_{v_N} \rightarrow +\infty} \widehat{\text{QI}}_{n_{\mathcal{V}}} = \text{QI},$$

in probability on $(\Omega^*, \mathcal{F}^*, \mathbb{P}^*)$.

Proof. Let us define the family of functions $\widehat{\Phi}_l$, $l \in \{0, \dots, N\}$ by the same formulas as Φ_l but replacing each ℓ_v with $\widehat{\ell}_{v,n_v}$, so that in particular $\widehat{\Phi}_0 = \widehat{\text{QI}}_{n_{\mathcal{V}}}$. It follows from a backward inductive argument over $l \in \{0, \dots, N\}$, the consistency of each WLAM and the dominated convergence theorem that for any $(y_{v_k})_{1 \leq k \leq l}$,

$$\lim_{n_{v_{l+1}} \rightarrow +\infty} \cdots \lim_{n_{v_N} \rightarrow +\infty} \widehat{\Phi}_l((y_{v_k})_{1 \leq k \leq l}) = \Phi_l((y_{v_k})_{1 \leq k \leq l}),$$

in probability. For $l = 0$, this yields the claimed identity. \square

Let us assume that all roots $v \in \mathcal{R}$ are provided with the WLAM described in Example 11.2.3. On the one hand, if all spaces E_v , $v \in \mathcal{V} \setminus \mathcal{R}$ are discrete, and provided with a WLAM as described in Example 11.2.4, then the assumptions of Theorem 11.2.9 hold for any measurable and bounded function $\Phi : \prod_{v \in \mathcal{V}} F_v \rightarrow \mathbb{R}$, without any more condition over the functions f_v and $g_{u,v}$ than mere measurability. On the other hand, if some spaces E_v , $v \in \mathcal{V} \setminus \mathcal{R}$ are continuous and provided with the Nadaraya–Watson WLAM from Example 11.2.5, then more intricate uniform continuity conditions must be imposed over Φ and the functions f_v and $g_{u,v}$ for the assumptions of Theorem 11.2.9 to hold.

11.3 Algorithms for the numerical computation of the weights

So far, Theorem 11.2.9 has confirmed that the approximate law $\widehat{\mu}_{Y_{\mathcal{V}}, n_{\mathcal{V}}}(dy_{\mathcal{V}})$ converges towards the true law $\mu_{Y_{\mathcal{V}}}(dy_{\mathcal{V}})$, at least in a weak sense. However, from a computational point of view, the formulæ (11.1) and (11.9) defining $\widehat{\text{QI}}_{n_{\mathcal{V}}}$ are severely demanding, since in order to evaluate the latter quantity, the simulation architect has to compute the $\prod_{v \in \mathcal{V}} n_v$ weights $w_{j_{\mathcal{V}}}(\mathbf{S}_{\mathcal{V}})$. It is therefore likely that the combinatorics of the problem become prohibitive quickly.

Nonetheless, thanks to the factorization of $\widehat{\mu}_{Y_{\mathcal{V}}, n_{\mathcal{V}}}(dy_{\mathcal{V}})$ in Equation (11.7), the computation of the weights can be drastically reduced by the topology of \mathcal{G} and the number of variables on which Φ actually depends on. We illustrate this point in the extreme case where \mathcal{G} is a line graph in Section 11.3.1. We generalize this approach in Section 11.3.2 by introducing an intermediate Bayesian network for the needs of the computations.

11.3.1 Line graphs

When \mathcal{G} is a line graph (see Figure 11.2), each approximate Markov kernel $\widehat{\ell}_{v_i, n_{v_i}}$ can be represented by a matrix, and the computation of the weights is a succession of matrix products.

Let us consider the case of the line graph $\mathcal{V} = \{v_1, \dots, v_N\}$, $\mathcal{E} = \{(v_l, v_{l+1}), 1 \leq l \leq N-1\}$, and assume that the quantity of interest writes

$$\text{QI} = \mathbb{E}[\Phi(Y_{v_N})].$$

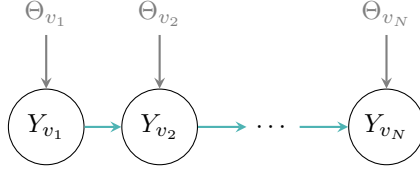


Figure 11.2: Line graph.

The estimator $\widehat{\mathbf{QI}}_{n_{\mathcal{Y}}}$ then writes

$$\widehat{\mathbf{QI}}_{n_{\mathcal{Y}}} = \sum_{j_{v_N}=1}^{n_{v_N}} w_{v_N, j_{v_N}} \Phi(Y'_{v_N, j_{v_N}}),$$

with weights given by

$$w_{v_N, j_{v_N}} = (W_{v_1} W_{v_2} \cdots W_{v_N})_{j_{v_N}}, \quad (11.10)$$

where W_{v_1} is the (row) vector with coordinates $(W_{v_1, j_{v_1}})_{1 \leq j_{v_1} \leq n_{v_1}}$ while, for $l \geq 2$, W_{v_l} is the $n_{v_{l-1}} \times n_{v_l}$ matrix with coordinates $(W_{v_l, j_{v_l}}(\mathbf{S}_{v_l, n_{v_l}}, g_{v_{l-1}, v_l}(Y'_{v_{l-1}, j_{v_{l-1}}}))_{1 \leq j_{v_{l-1}} \leq n_{v_{l-1}}, 1 \leq j_{v_l} \leq n_{v_l}}$. Computing the matrix product $W_{v_1} W_{v_2} \cdots W_{v_N}$ from the left to the right requires $n_{v_1} n_{v_2} + n_{v_2} n_{v_3} + \cdots + n_{v_{N-1}} n_{v_N}$ operations, which thus significantly reduces the computational cost of the method, in comparison with the $n_{v_1} n_{v_2} \cdots n_{v_N}$ weights to be computed in the formula (11.1).

11.3.2 General DAG with an intermediate Bayesian network

In the general case, such a marginalisation procedure can still be implemented, with the matrix product appearing in (11.10) replaced by some tensor operations, but the topology of the graph \mathcal{G} may make the whole operation tedious to track. Fortunately, we can construct a *discrete Bayesian network* whose law is exactly $\widehat{\mu}_{Y_{\mathcal{Y}}, n_{\mathcal{Y}}}(\mathrm{d}y_{\mathcal{Y}})$. Thus, we can readily employ the tools from this field for the numerical computation of $\widehat{\mathbf{QI}}_{n_{\mathcal{Y}}}$.

From now on, we consider that the experimental samples $Y'_{\mathcal{Y}, j_{\mathcal{Y}}}$ are fixed for all $j_{\mathcal{Y}} \in \mathcal{N}_{\mathcal{Y}}$ and we are looking to compute the weights associated to each realization, denoted by $w_{j_{\mathcal{Y}}}(\mathbf{S}_{\mathcal{Y}})$ in Equation (11.9).

11.3.2.a Definition of the intermediate random variables

In addition to the canonical and experimental probability spaces, we introduce a *computational probability space* $(\Omega^{\dagger}, \mathcal{F}^{\dagger}, \mathbb{P}^{\dagger})$, on which we define a family of discrete random variables $(Y_v^{\dagger})_{v \in \mathcal{V}}$ on the graph. For any $v \in \mathcal{V}$, the support of the associated random variable is given by

$$Y_v^{\dagger} \in \{Y'_{v,1}, \dots, Y'_{v, n_v}\},$$

with the $(Y_{v,j})_{j \in [1, n_v]}$ being part of the sample \mathbf{S}_{n_v} from Section 11.2.2. We define the conditional law of Y_v^{\dagger} with respect to its parents by

$$\mathbb{P}^{\dagger} \left(Y_v^{\dagger} = Y'_{v, j_v} \mid Y_u^{\dagger} = Y'_{u, j_u}, u \in \mathcal{P}(v) \right) = W_{v, j_v}(\mathbf{S}_{v, n_v}, (g_{u,v}(Y'_{u, j_u}))_{u \in \mathcal{P}(v)}) \quad (11.11)$$

with $j_w \in [1, n_w]$, for any $w \in \{v\} \cup \mathcal{P}(v)$. When v is a root, the formula naturally extends to

$$\mathbb{P}^{\dagger} \left(Y_v^{\dagger} = Y'_{v, j_v} \right) = W_{v, j_v} \quad (11.12)$$

by the definition of a WLAM in that case. When two collisions occur, *i.e.* if there exists two $j_1 \neq j_2$ such that $Y'_{v,j_1} = Y'_{v,j_2}$, we sum the weights so that $\mathbb{P}^\dagger \left(Y_v^\dagger = Y'_{v,j_1} \mid \dots \right) = W_{v,j_1}(\dots) + W_{v,j_2}(\dots)$, and we do the same for more than two collisions. Notice that it is the use of the probability measure \mathbb{P}^\dagger that permits to consider that the Y'_{v,j_v} are fixed.

In the Bayesian network language, we have defined the *conditional probability tables* in Equations (11.11) and (11.12). It is a standard result in this field that the joint law of $(Y_v^\dagger)_{v \in \mathcal{V}}$ is fully specified by these equations and that it writes

$$\mathbb{P}^\dagger \left(Y_{\mathcal{V}'}^\dagger = Y'_{\mathcal{V}',j_{\mathcal{V}'}} \right) = \prod_{v \in \mathcal{A}} \mathbb{P}^\dagger \left(Y_v^\dagger = Y'_{v,j_v} \right) \prod_{v \in \mathcal{V}' \setminus \mathcal{A}} \mathbb{P}^\dagger \left(Y_v^\dagger = Y'_{v,j_v} \mid Y_u^\dagger = Y'_{u,j_u}, u \in \mathcal{S}(v) \right), \quad (11.13)$$

with $j_{\mathcal{V}'} \in \mathcal{N}_{\mathcal{V}'}$. In other terms, the law of the $(Y_v^\dagger)_{v \in \mathcal{V}}$ factors over \mathcal{S} and $(\mathcal{S}, (Y_v^\dagger)_{v \in \mathcal{V}})$ is a discrete Bayesian network [71].

11.3.2.b Equality of the joint laws

As a consequence of Equations (11.8),(11.9) and (11.13), the law of $(Y_v^\dagger)_{v \in \mathcal{V}}$ under \mathbb{P}^\dagger is the probability measure $\widehat{\mu}_{Y_{\mathcal{V}'},n_{\mathcal{V}'}}$ on $\prod_{v \in \mathcal{V}'} F_v$. Thus, computing a quantity of interest with respect to the approximate law $\widehat{\mu}_{Y_{\mathcal{V}'},n_{\mathcal{V}'}}$ is actually equivalent to performing an *inference* [71] (with no *evidence*) in the Bayesian network $(\mathcal{S}, (Y_v^\dagger)_{v \in \mathcal{V}'})$. The numerical procedure can be decomposed in two steps.

1. For each node v , compute the conditional probability tables from the WLAMs using Equations (11.11) and (11.12).
2. Feed these tables to a Bayesian network inference algorithm (*e.g.* variable elimination, clique trees... [71, Chapter 10]) to propagate the law.

The inference algorithms from the literature typically take a subset of the nodes $\mathcal{V}' \subset \mathcal{V}$, called a request, as input and returns the joint probability table of the $(Y_v^\dagger)_{v \in \mathcal{V}'}$. This can be used for uncertainty propagation, by remarking that the approximate quantity of interest is computed by replacing $Y_{\mathcal{V}'}$ with $Y_{\mathcal{V}'}^\dagger$ in the real quantity of interest

$$\text{QI} = \mathbb{E} [\Phi(Y_{\mathcal{V}'})] \simeq \mathbb{E}^\dagger \left[\Phi \left(Y_{\mathcal{V}'}^\dagger \right) \right] = \widehat{\text{QI}}_{n_{\mathcal{V}'}}.$$

The joint probability table also permits to compute some variance-based sensitivity analysis indices. Indeed, given two nodes $u, v \in \mathcal{V}'$, we can approximate the quantity

$$\begin{aligned} \text{Var}(\mathbb{E}[Y_v | Y_u]) &= \mathbb{E}[\mathbb{E}[Y_v | Y_u]^2] - \mathbb{E}[Y_v]^2 \\ &\simeq \mathbb{E}^\dagger [\mathbb{E}^\dagger [Y_v^\dagger | Y_u^\dagger]^2] - \mathbb{E}^\dagger [Y_v^\dagger]^2. \end{aligned}$$

Using an inference algorithm, a request on $\mathcal{V}' = \{u, v\}$ would permit to obtain the joint tables

$$\left(\mathbb{P}^\dagger \left(Y_u^\dagger = Y'_{u,j_u}, Y_v^\dagger = Y'_{v,j_v} \right) \right)_{(j_u, j_v) \in \llbracket 1, n_u \rrbracket \times \llbracket 1, n_v \rrbracket}$$

so that we could compute the square of the expectation

$$\mathbb{E}^\dagger [Y_v^\dagger]^2 = \left(\sum_{j_v=1}^{n_v} Y'_{v,j_v} \mathbb{P}^\dagger \left(Y_v^\dagger = Y'_{v,j_v} \right) \right)^2$$

and the expectation of the square conditional expectation with the formula

$$\mathbb{E}^\dagger[\mathbb{E}^\dagger[Y_v^\dagger|Y_u^\dagger]^2] = \sum_{j_u=1}^{n_u} \left(\sum_{j_v=1}^{n_v} Y_{v,j_v}' \frac{\mathbb{P}^\dagger(Y_u^\dagger = Y_{u,j_u}', Y_v^\dagger = Y_{v,j_v}')}{\mathbb{P}^\dagger(Y_u^\dagger = Y_{u,j_u}')}\right)^2 \mathbb{P}^\dagger(Y_u^\dagger = Y_{u,j_u}').$$

The marginals are obtained by summing the joint law over one coordinate

$$\mathbb{P}^\dagger(Y_u^\dagger = Y_{u,j_u}') = \sum_{j=1}^{n_v} \mathbb{P}^\dagger(Y_u^\dagger = Y_{u,j_u}', Y_v^\dagger = Y_{v,j_v}').$$

The equivalence with the discrete Bayesian network also gives us information on the typical complexity for an algorithm that propagates the weights. For a general graph, the time complexity of the exact algorithms may be exponential in the number of nodes (they are NP-hard [31]) and polynomial with high degrees in the size of the sample n_v . However, this is greatly influenced by graphs topologies and computations are tractable for many of them, in practice. For instance, in Section 11.3.1, in the case of a line graph, the complexity is linear in the number of nodes and quadratic in the size of the sample n_v . For polytrees (*i.e.* DAG without undirected cycles), with a restricted number of parents at each nodes, these algorithms are also expected to behave well [71, 9.B].

11.3.2.c Extension to some nonlinear weighting methods

In [7], a weighting method is proposed that is not linear in the sense of Remark 11.2.7. More precisely, the weighting function does not depend only on the value of the parent variables but also on their probability of occurrence in a nonlinear way. The weighting function is now written in a more general form

$$W_{v,j_v}(\mathbf{S}_{v,n_v}, (g_{u,v}(Y_{u,j_u})), \mathbb{P}^\dagger(Y_u^\dagger = Y_{u,j_u}'))_{u \in \mathcal{P}(v)}.$$

Assuming that \mathcal{G} does not contain any directed cycle, the algorithms from Bayesian inference can be adapted to handle such a situation. For each node with a nonlinear weighting method, the full joint law of the parents must be computed before having to use the weight of the node in the inference. In a variable elimination algorithm, this would restrict the choice of the elimination ordering, for example.

11.4 Industrial application

The presented case is based on a model developed by the ROM team at IRT SystemX, as a part of the Airbus TOICA project (Thermal Overall Integrated Conception of Aircraft). The main motivation of the project is to validate the thermal constraints of an aircraft, coming from a system-level simulation down to the equipment behaviour (*i.e.* the component scale, see Figure 11.3). The purpose of these results is to be used in the design and certification phases.

In our application, we are interested in a simple model for a few components. The question is how to perform a multidisciplinary uncertainty quantification to account for the errors on various variables.

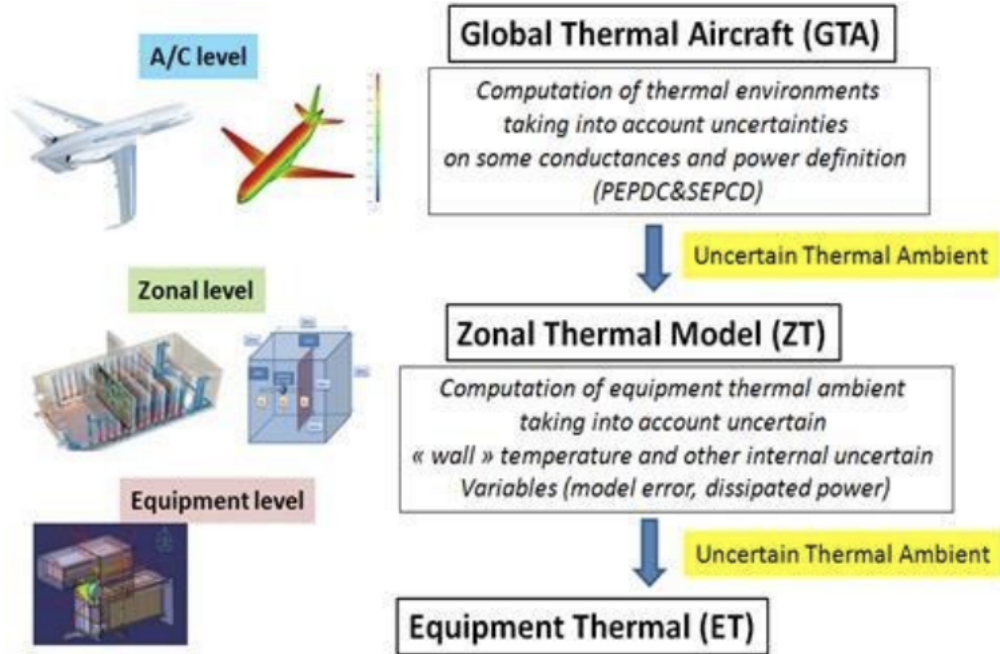


Figure 11.3: Outline of the thermal case objectives (figure provided by Airbus).

11.4.1 Description of the case

The thermal state of the components is modeled by eleven physical variables

$$(T_1, T_2, T_{i_1}, T_3, R_{12}, H_{23}, S_3, R_{23}, S_1, H_{12}, P_d)$$

and seven terms modeling the error

$$(\epsilon_1, \epsilon_{i_1}, \epsilon_2, \epsilon_3, \alpha_{i_1}, \alpha_1, \alpha_2),$$

that all are real-valued random variables. These variables are linked together by the following equations

$$R_{23} = f_{v_1}(S_3, H_{23}, \epsilon_3) = \frac{1 + \epsilon_3}{S_3 H_{23}}, \quad (11.14)$$

$$P_d = f_{v_2}(P_d) = P_d, \quad (11.15)$$

$$R_{12} = f_{v_3}(S_1, H_{12}, \epsilon_1) = \frac{1 + \epsilon_1}{S_1 H_{12}}, \quad (11.16)$$

$$T_2 = f_{v_4}(T_3, P_d, R_{23}, \alpha_2, \epsilon_2) = (1 + \epsilon_2)(T_3 + P_d R_{23}) + \alpha_2, \quad (11.17)$$

$$T_{i_1} = f_{v_5}(P_d, R_{12}, \epsilon_{i_1}, \alpha_{i_1}) = (1 + \epsilon_{i_1})P_d R_{12} + \alpha_{i_1}, \quad (11.18)$$

$$T_1 = f_{v_6}(T_2, T_{i_1}, \alpha_1) = T_2 + T_{i_1} + \alpha_1. \quad (11.19)$$

that are represented in the graph of the numerical models in Figure 11.4. The law of the internal variables is given in Table 11.1. In the context of this use case, the 10 disciplines have their own

timeline and the computations of the f_{v_i} cannot be done in an online Monte-Carlo fashion. The goal is to perform an uncertainty propagation to compute some quantity of interest on T_1 .

The disciplines v_4, v_5, v_6 have a Nearest-Neighbor WLAM, with the synthetic samples of law presented in Table 11.1. The disciplines v_1, v_2, v_3 are root nodes, and are equipped with a “Monte Carlo WLAM”, that assigns the weight $1/n_v$ to each (i.i.d) realization of their sample. Each v computes a sample of size $n_v = n$ and the law of T_1 is reconstructed with a variable elimination algorithm.

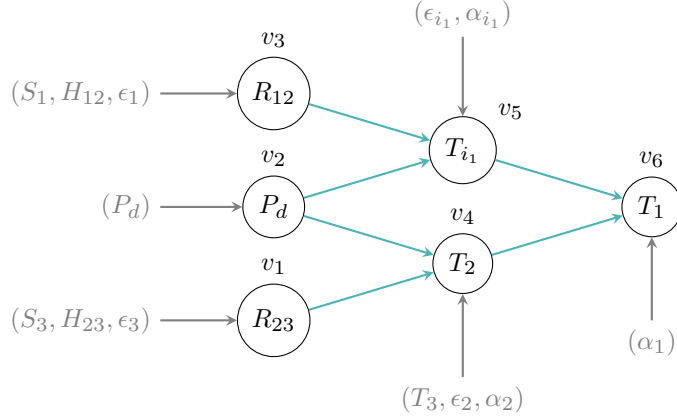


Figure 11.4: Graph of the numerical models in the use case. The internal parameters, which can be simulated locally by each nodes, are written in gray.

Symbol	Probability law
S_1	$\mathcal{U}(0.1, 0.2)$
H_{12}, H_{23}	$\mathcal{U}(4, 6)$
P_d	$\mathcal{U}(50, 70)$
S_3	$\mathcal{U}(1, 2)$
T_3	$\log -\mathcal{N}(20, 5, 0)$
$\alpha_1, \alpha_2, \alpha_{i1}$	$\mathcal{F}(-2.5, 0, 2.4)$
$\epsilon_1, \epsilon_2, \epsilon_3, \epsilon_{i1}$	$\mathcal{U}(0, 1)$

Table 11.1: True probability law of each internal variables (they are assumed independent).

Symbol	Probability law	Symbol	Probability law
v_4		v_5	
P'_d	$\mathcal{U}(40, 90)$	R'_{12}	$\mathcal{N}(1.55, 1)$
R'_{23}	$\mathcal{U}(0.05, 0.3)$	P'_d	$\mathcal{U}(30, 85)$
v_6			
T'_2	$\mathcal{N}(35, 20)$		
T'_{i1}	$\mathcal{U}(35, 180)$		

Table 11.2: Synthetic laws used by each nodes.

11.4.2 Results

The result of the sum-product algorithm is a weighting $(T'_{1,i}, w_i)_{i \in \llbracket 1, n_{v_1} \rrbracket}$ associated to each synthetic observation of T_1 . A first encouraging qualitative result is given in Figure 11.5. As expected, the synthetic samples drawn by v_1 are reweighted to approximate the theoretical law. We verify that, for various quantities of interest, the root of the mean squared error vanishes, as shown in Figure 11.6a, 11.6b and 11.6c. This gives some strong clues that these estimators are consistent. In Figure 11.6d, the convergence of the non normalized Kolmogorov-Smirnov statistic confirms that the approximation of the true law becomes more and more precise as the size of the sample increases. This algorithm can thus be used in a context that requires disciplinary autonomy.

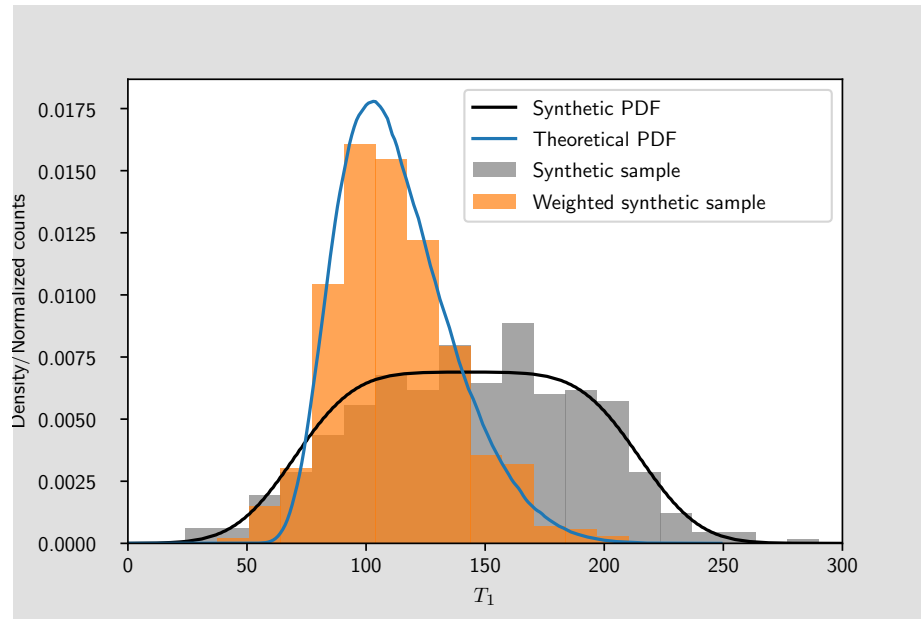


Figure 11.5: Comparison of the unweighted and weighted synthetic sample, to approximate the theoretical P.D.F ($n = 500$). The theoretical P.D.F is reconstructed by a kernel density estimation based on a huge number of samples from a direct Monte-Carlo procedures.

11.5 Conclusion and perspectives

The uncertainty propagation in graphs using weighting methods being a rather new technique, it carries a lot of open questions and interesting perspectives.

Measuring the efficiency of WLAMs Even though we have a pointwise criterion to ensure consistency, the rate of convergence depends on the weighting technique and Chapter 10 has shown that it also depends on how far the synthetic and the true samples are from each other. The numerical simulations show that this aspect is *critical* for the efficiency of the algorithm and controlling the error at each node seems to be one of the main criteria for success.

Studying the speed of convergence for some classic linear nonparametric regression methods to approximate the true law while learning on synthetic samples would be an interesting development. Ideally, it would give an *a posteriori* estimator of the error at each node, in order to identify if and where it is relevant to draw more samples. For instance, for a Nearest-Neighbor WLAM, Corollary 10.3.8 tells us that estimating the quantity

$$\left(\frac{k_{n_v}}{n_v}\right)^{1/d} c_{1,q} \frac{\Gamma(1+1/d)}{v_d^{1/d}} \mathbb{E} \left[1/p_{X'_v}(X_v)^{1/d} \right] \text{Lip}(f_v)$$

would give some estimate on the L_1 error due to the synthetic sample. The quantity $\text{Lip}(f_v)$ is the Lipschitz constant of f_v in X_v , uniformly in Θ_v .

Last, a very interesting theoretical work would be to derive some rates of convergence of the approximate law toward the theoretical law *in the whole graph*, with respect to the characteristics of each WLAM.

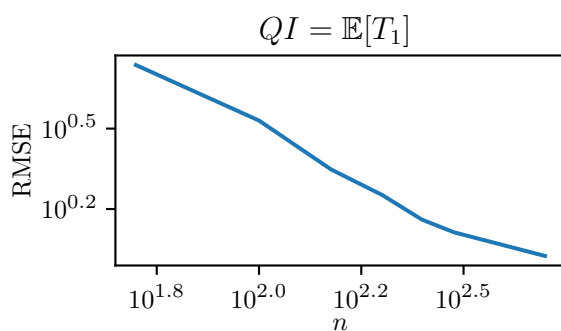
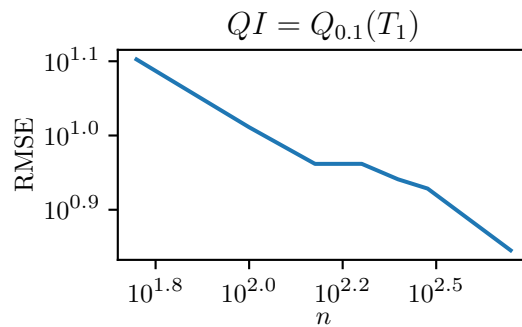
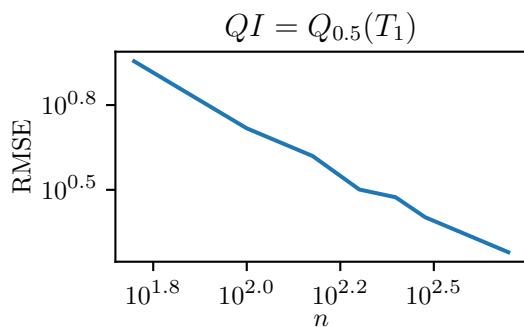
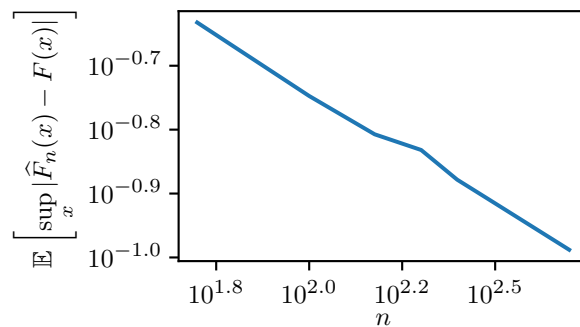
(a) Evolution of the RMSE for $QI = \mathbb{E}[T_1]$.(b) Evolution of the RMSE when QI is the quantile of level 0.1 of T_1 .(c) Evolution of the RMSE when QI is the median value of T_1 .(d) Evolution of the expected L_∞ difference between the weighted empirical CDF and the true CDF of T_1 .

Figure 11.6: Evolution of the expected error of various estimators, with respect to the number of samples. The experiment was replicated 200 times at each point to compute the mean error. The computations were done with a 4-core processor **i5-8250U CPU @ 3.40GHz** and **12GB** of RAM. For one experiment with $n = 200$, the time necessary to compute the Nearest-Neighbors at each node is approximately 6×10^{-1} s and the propagation phase using variable elimination takes approximately 1.7×10^{-4} s.

Change of function in one node In addition to allowing for disciplinary autonomy, this method can be seen as a way to change a function in a node, without having to compute the functions at the other node again. Assessing its performance in this context, in comparison with other techniques would be of practical interest.

Sparse conditional probability tables for numerical efficiency In polytrees (graph with no cycle), the only source of exponential complexity in the Bayesian network inference algorithms is when a node v as a huge number of parents u . Indeed, it is necessary to compute a conditional probability table

$$(W_{v,j_v}(\mathbf{S}_{v,n_v}, (g_{u,v}(Y_{u,j}))_{u \in \mathcal{P}(v)}))_{j_v \in \llbracket 1, n_v \rrbracket, j_u \in \llbracket 1, n_u \rrbracket, u \in \mathcal{P}(v)}$$

of size $n_v \prod_{u \in \mathcal{P}(v)} n_u$, leading to a complexity of $n^{\#\mathcal{P}(v)+1}$ when all the samples have a size n . However, assuming that we are not interested in the joint law of the parents of v , we could only consider the diagonal terms of the joint law,

$$(W_{v,j_v}(\mathbf{S}_{v,n_v}, (g_{u,v}(Y_{u,j}))_{u \in \mathcal{P}(v)}))_{j_v, j \in \llbracket 1, n \rrbracket^2}$$

reducing the table to a quadratic size n^2 , but loosing the information on the law the parents. We think that such a method cannot be performed in general Bayesian networks, because the cross terms are important in general. In our case however, the interpretation of the variable Y_v^\dagger in terms of bootstrap of a sample suggests that using only the diagonal terms would be close to a Monte-Carlo approach. Thus, any estimator based on this method would be consistent and the loss of variance due to leaving the cross terms out may be greatly compensated by the gain in computation speed.

For a given request $\mathcal{V}' \subset \mathcal{V}$, an algorithm could use only the diagonal terms in the part where the joint law are not required, while using the full cross-terms where it is necessary.

Algorithms for nonlinear weighting methods As shown in Section 11.3.2.c, some weighting methods that are nonlinear in the measure also exist. The propagation of the weights seems pretty clear in the case of polytrees, as one needs to compute the full law of the parents before computing the weights of a node. However, in the case of a DAG with an undirected cycle, it is less obvious how the dependency should be handled in the nonlinear case. Adapting the Bayesian network algorithms to this case would be an interesting development.

Estimating the law of the parameters This formalism does not include the internal variables Θ_v in the graph. It is thus not possible to make a request to perform a sensitivity analysis of an Y_u with respect to Θ_v . Including them in the analysis without having to consider them as external variables would be therefore of great interest.

Markov random fields for general graphs? So far, we concentrated on Directed Acyclic Graphs, as the law of $(Y_v)_{v \in \mathcal{V}}$ was straightforward to define in that case. A Bayesian network was therefore the natural related object to perform computations on. However, some industrial cases might include some directed loops also known as “strong coupling” (see *e.g.* [81]). Provided that the laws of the random variables are well defined in that case, the structure of $(\mathcal{G}, (Y_v)_{v \in \mathcal{V}})$ would be a Markov random field, generalizing the Bayesian network structure. A natural question is that if we construct the equivalent discrete Markov random field [71, Chapter 4] in a similar way as 11.3.2, would an inference algorithm approximate the true law of $(\mathcal{G}, (Y_v)_{v \in \mathcal{V}})$?

Bibliography

- [1] Indicating the safety factor. *Scientific American*, 125(16):277–277, 1921.
- [2] Jürgen Ackermann. *Robust control: Systems with uncertain physical parameters*. Springer Science & Business Media, 2012.
- [3] Natalia M Alexandrov and Robert Michael Lewis. Comparative properties of collaborative optimization and other approaches to MDO. 1999.
- [4] Douglas Allaire and Karen Willcox. Surrogate modeling for uncertainty assessment with application to aviation environmental system models. *AIAA journal*, 48(8):1791–1803, 2010.
- [5] Sergio Amaral, Douglas Allaire, and Karen Willcox. A decomposition approach to uncertainty analysis of multidisciplinary systems. In *12th AIAA Aviation Technology, Integration, and Operations (ATIO) Conference and 14th AIAA/ISSMO Multidisciplinary Analysis and Optimization Conference*, page 5563, 2012.
- [6] Sergio Amaral, Douglas Allaire, and Karen Willcox. A decomposition-based approach to uncertainty analysis of feed-forward multicomponent systems. *International Journal for Numerical Methods in Engineering*, 100(13):982–1005, 2014.
- [7] Sergio Amaral, Douglas Allaire, and Karen Willcox. Optimal L_2 -norm empirical importance weights for the change of probability measure. *Statistics and Computing*, 27(3):625–643, 2017.
- [8] Philippe Artzner, Freddy Delbaen, Jean-Marc Eber, and David Heath. Coherent measures of risk. *Mathematical finance*, 9(3):203–228, 1999.
- [9] Terje Aven. Risk assessment and risk management: Review of recent advances on their foundation. *European Journal of Operational Research*, 253(1):1–13, 2016.
- [10] Terje Aven, Piero Baraldi, Roger Flage, and Enrico Zio. *Uncertainty in risk assessment: the representation and treatment of uncertainties by probabilistic and non-probabilistic methods*. John Wiley & Sons, 2013.
- [11] Terje Aven and Enrico Zio. Foundational issues in risk assessment and risk management. *Risk analysis*, 34(7):1164–1172, 2014.
- [12] Yakov Ben-Haim. Set-models of information-gap uncertainty: Axioms and an inference scheme. *Journal of the Franklin Institute*, 336(7):1093–1117, 1999.
- [13] Yakov Ben-Haim. *Info-gap decision theory: decisions under severe uncertainty*. Elsevier, 2006.

- [14] Aharon Ben-Tal and Arkadi Nemirovski. Robust solutions of uncertain linear programs. *Operations research letters*, 25(1):1–13, 1999.
- [15] Allan Benjamin, Homayoon Dezfuli, and Chris Everett. Developing probabilistic safety performance margins for unknown and underappreciated risks. *Reliability Engineering & System Safety*, 145:329–340, 2016.
- [16] Dimitris Bertsimas, David B Brown, and Constantine Caramanis. Theory and applications of robust optimization. *SIAM review*, 53(3):464–501, 2011.
- [17] Dimitris Bertsimas, Vishal Gupta, and Nathan Kallus. Data-driven robust optimization. *Mathematical Programming*, 167(2):235–292, 2018.
- [18] Gérard Biau and Luc Devroye. *Lectures on the nearest neighbor method*. Springer, 2015.
- [19] Peter J Bickel and Kjell A Doksum. *Mathematical statistics: basic ideas and selected topics, volume I*, volume 117. CRC Press, 2015.
- [20] Patrick Billingsley. *Convergence of probability measures*. John Wiley & Sons, 2013.
- [21] Jérémy Bleyer and Patrick De Buhan. Lower bound static approach for the yield design of thick plates. *International Journal for Numerical Methods in Engineering*, 100(11):814–833, 2014.
- [22] Jérémy Bleyer and Patrick De Buhan. A numerical approach to the yield strength of shell structures. *European Journal of Mechanics - A/Solids*, 59:178–194, September 2016.
- [23] Arindam Brahma and David C Wynn. Margin value method for engineering design improvement. *Research in Engineering Design*, pages 1–29, 2020.
- [24] Arindam Brahma and DC Wynn. Calculating target thresholds for the margin value method using computational tools. In *Proceedings of the Design Society: DESIGN Conference*, volume 1, pages 111–120. Cambridge University Press, 2020.
- [25] Robert D Braun and Ilan M Kroo. Development and application of the collaborative optimization architecture in a multidisciplinary design environment. 1995.
- [26] George H Chen, Devavrat Shah, et al. Explaining the success of nearest neighbor methods in prediction. *Foundations and Trends® in Machine Learning*, 10(5-6):337–588, 2018.
- [27] Xin Chen. *Enablers for uncertainty quantification and management in early stage computational design. An aircraft perspective*. PhD thesis, 2017.
- [28] Mathilde Chevreuril, Régis Lebrun, Anthony Nouy, and Prashant Rai. A least-squares method for sparse low rank approximation of multivariate functions. *SIAM/ASA Journal on Uncertainty Quantification*, 3(1):897–921, 2015.
- [29] Pier Davide Ciampa and Björn Nagel. The agile paradigm: the next generation of collaborative mdo. In *18th AIAA/ISSMO multidisciplinary analysis and optimization conference*, page 4137, 2017.
- [30] John B Conway. *A course in functional analysis*, volume 96. Springer, 2019.
- [31] Gregory F Cooper. The computational complexity of probabilistic inference using bayesian belief networks. *Artificial intelligence*, 42(2-3):393–405, 1990.

- [32] David Roxbee Cox and David Victor Hinkley. *Theoretical statistics*. CRC Press, 1979.
- [33] Stephen Cranefield. Uml and the semantic web. In *Proceedings of the First International Conference on Semantic Web Working*, SWWS'01, page 113–130, Aachen, DEU, 2001. CEUR-WS.org.
- [34] Bernard Forest de Belidor. *La science des ingénieurs, dans la conduite des travaux de fortification et d'architecture civile*. Didot, 1729.
- [35] Comité Européen de Normalisation. Eurocode—basis of structural design. *EN1990, Comité Européen de Normalisation, Brussels*, 2002.
- [36] Etienne de Rocquigny. La maîtrise des incertitudes dans un contexte industriel. 1re partie: une approche methodologique globale basee sur des exemples. *Journal de la Societe francaise de statistique*, 147(3):33–71, 2006.
- [37] Etienne de Rocquigny, Nicolas Devictor, and Stefano Tarantola. *Uncertainty in industrial practice: a guide to quantitative uncertainty management*. John Wiley & Sons, 2008.
- [38] Homayoon Dezfuli, Allan Benjamin, Christopher Everett, Martin Feather, Peter Rutledge, Dev Sen, and Robert Youngblood. *NASA System Safety Handbook. Volume 2: System Safety Concepts, Guidelines, and Implementation Examples*. 2015.
- [39] Homayoon Dezfuli, Allan Benjamin, Christopher Everett, Gaspare Maggio, Michael Stamatelatos, Robert Youngblood, Sergio Guarro, Peter Rutledge, James Sherrard, Curtis Smith, et al. *NASA Risk Management Handbook. Version 1.0*. 2011.
- [40] Homayoon Dezfuli, Michael Stamatelatos, Gaspare Maggio, Christopher Everett, Robert Youngblood, Peter Rutledge, Allan Benjamin, Rodney Williams, Curtis Smith, and Sergio Guarro. *NASA Risk-Informed Decision Making Handbook*. 2010.
- [41] Francesco Di Maio, Claudia Picoco, Enrico Zio, and Valentin Rychkov. Safety margin sensitivity analysis for model selection in nuclear power plant probabilistic safety assessment. *Reliability Engineering & System Safety*, 162:122–138, 2017.
- [42] Francesco Di Maio, Ajit Rai, and Enrico Zio. A dynamic probabilistic safety margin characterization approach in support of integrated deterministic and probabilistic safety analysis. *Reliability Engineering & System Safety*, 145:9–18, 2016.
- [43] Claudia M Eckert, P John Clarkson, and Winfried Zanker. Change and customisation in complex engineering domains. *Research in engineering design*, 15(1):1–21, 2004.
- [44] Claudia M Eckert, Ola Isaksson, and Chris Earl. Design margins: a hidden issue in industry. *Design Science*, 5:e9, 2019.
- [45] Claudia M Eckert, Ola Isaksson, and Christopher Earl. Product property margins: An underlying critical problem of engineering design. 2012.
- [46] Claudia M Eckert, Ola Isaksson, Safaa Lebjioui, Christopher F Earl, and Stefan Edlund. Design margins in industrial practice. *Design Science*, 6, 2020.
- [47] Isaac Elishakoff. *Safety factors and reliability: friends or foes?* Springer Science & Business Media, 2012.

- [48] Dafydd Evans, Antonia J Jones, and Wolfgang M Schmidt. Asymptotic moments of near-neighbour distance distributions. *Proceedings of the Royal Society of London. Series A: Mathematical, Physical and Engineering Sciences*, 458(2028):2839–2849, 2002.
- [49] Kai-Tai Fang, Runze Li, and Agus Sudjianto. *Design and modeling for computer experiments*. CRC press, 2005.
- [50] Nicolas Fournier and Arnaud Guillin. On the rate of convergence in wasserstein distance of the empirical measure. *Probability Theory and Related Fields*, 162(3-4):707–738, 2015.
- [51] Gene F Franklin, J David Powell, and Abbas Emami-Naeini. *Feedback control of dynamic systems*. Addison-Wesley Reading, MA, sixth edition, 2010.
- [52] Sébastien Gadat, Thierry Klein, Clément Marteau, et al. Classification in general finite dimensional spaces with the k-nearest neighbor rule. *The Annals of Statistics*, 44(3):982–1009, 2016.
- [53] Nicolas Gayton, Alaa Mohamed, John Dalsgaard Sorensen, Maurice Pendola, and Maurice Lemaire. Calibration methods for reliability-based design codes. *Structural Safety*, 26(1):91–121, 2004.
- [54] Roger Ghanem, David Higdon, and Houman Owhadi. *Handbook of uncertainty quantification*, volume 6. Springer, 2017.
- [55] Siegfried Graf and Harald Luschgy. *Foundations of quantization for probability distributions*. Springer, 2007.
- [56] Marin D Guenov, Xin Chen, Arturo Molina-Cristóbal, Atif Riaz, Albert SJ van Heerden, and Mattia Padulo. Margin allocation and tradeoff in complex systems design and optimization. *AIAA Journal*, 56(7):2887–2902, 2018.
- [57] Sofia Guzzetti, LA Mansilla Alvarez, PJ Blanco, Kevin Thomas Carlberg, and A Veneziani. Propagating uncertainties in large-scale hemodynamics models via network uncertainty quantification and reduced-order modeling. *Computer Methods in Applied Mechanics and Engineering*, 358:112626, 2020.
- [58] Cecilia Haskins, Kevin Forsberg, Michael Krueger, D Walden, and D Hamelin. Systems engineering handbook. In *INCOSE*, volume 9, pages 13–16, 2006.
- [59] Trevor Hastie, Robert Tibshirani, and Jerome Friedman. *The elements of statistical learning: data mining, inference, and prediction*. Springer Science & Business Media, 2009.
- [60] Jon C Helton. Quantification of margins and uncertainties: Conceptual and computational basis. *Reliability Engineering & System Safety*, 96(9):976–1013, 2011.
- [61] Jon C Helton and Jay D Johnson. Quantification of margins and uncertainties: Alternative representations of epistemic uncertainty. *Reliability Engineering & System Safety*, 96(9):1034–1052, 2011.
- [62] Jon C Helton, Jay D Johnson, and Cedric J Sallaberry. Quantification of margins and uncertainties: example analyses from reactor safety and radioactive waste disposal involving the separation of aleatory and epistemic uncertainty. *Reliability Engineering & System Safety*, 96(9):1014–1033, 2011.

- [63] Steven R Hirshorn, Linda D Voss, and Linda K Bromley. *Nasa systems engineering handbook, Rev2*. 2017.
- [64] Miroslav Hrehor, Mirela Gavrilas, Josef Belac, Risto Sairanen, Giovanni Bruna, Michel Reocreux, Françoise Touboul, B Krzykacz-Hausmann, Jong Seuk Park, Andrej Prosek, et al. Task group on safety margins action plan (SMAP). safety margins action plan-final report. Technical report, Organisation for Economic Co-Operation and Development, 2007.
- [65] Sobol' Ilya M. Sensitivity estimates for nonlinear mathematical models. *Math. Model. Comput. Exp*, 1(4):407–414, 1993.
- [66] Bertrand Iooss and Paul Lemaître. A review on global sensitivity analysis methods. In *Uncertainty management in simulation-optimization of complex systems*, pages 101–122. Springer, 2015.
- [67] Ola Isaksson, Peter Lindroth, and Claudia M Eckert. Optimisation of products versus optimisation of product platforms: an engineering change margin perspective. In *DS 77: Proceedings of the DESIGN 2014 13th International Design Conference*, 2014.
- [68] Darren Anthony Jones, Claudia M Eckert, Kilian Gericke, et al. Margins leading to over-capacity. In *DS 92: Proceedings of the DESIGN 2018 15th International Design Conference*, pages 781–792, 2018.
- [69] Vladimir Leonidovich Kharitonov. The asymptotic stability of the equilibrium state of a family of systems of linear differential equations. *Differentsial'nye Uravneniya*, 14(11):2086–2088, 1978.
- [70] Michael Kohler, Adam Krzyżak, and Harro Walk. Rates of convergence for partitioning and nearest neighbor regression estimates with unbounded data. *Journal of Multivariate Analysis*, 97(2):311–323, 2006.
- [71] Daphne Koller and Nir Friedman. *Probabilistic graphical models: principles and techniques*. MIT press, 2009.
- [72] Alexander Kossiakoff, William N Sweet, Samuel J Seymour, and Steven M Biemer. *Systems engineering principles and practice*, volume 83. John Wiley & Sons, 2011.
- [73] S Kucherenko, Maria Rodriguez-Fernandez, C Pantelides, and Nilay Shah. Monte carlo evaluation of derivative-based global sensitivity measures. *Reliability Engineering & System Safety*, 94(7):1135–1148, 2009.
- [74] Idaho National Laboratory. Light water reactor sustainability research and development program plan – fiscal year 2009–2013. 12 2009.
- [75] Loic Le Gratiet and Josselin Garnier. Asymptotic analysis of the learning curve for gaussian process regression. *Machine Learning*, 98(3):407–433, 2015.
- [76] Maurice Lemaire, Alaa Chateauneuf, and Jean-Claude Mitteau. *Structural reliability*. Wiley Online Library, 2009.
- [77] William S Levine. *The Control Systems Handbook: Control System Fundamentals*. CRC press, second eddition edition, 2010.

- [78] Elia Liitiäinen, Amaury Lendasse, and Francesco Corona. Bounds on the mean power-weighted nearest neighbour distance. *Proceedings of the Royal Society A: Mathematical, Physical and Engineering Sciences*, 464(2097):2293–2301, 2008.
- [79] Marco Loog. Nearest neighbor-based importance weighting. In *2012 IEEE International Workshop on Machine Learning for Signal Processing*, pages 1–6. IEEE, 2012.
- [80] Henrik O Madsen, Steen Krenk, and Niels Christian Lind. *Methods of structural safety*. Courier Corporation, 2006.
- [81] Sankaran Mahadevan and Natasha Smith. Efficient first-order reliability analysis of multi-disciplinary systems. *International Journal of Reliability and Safety*, 1(1-2):137–154, 2006.
- [82] Sophie Marque-Pucheu, Guillaume Perrin, and Josselin Garnier. Efficient sequential experimental design for surrogate modeling of nested codes. *ESAIM: Probability and Statistics*, 23:245–270, 2019.
- [83] Sebastian Martorell, Yolanda Nebot, Jose F Villanueva, Sofia Carlos, Vincente Serradell, F Pelayo, and R Mendizàbal. Safety margins estimation method considering uncertainties within risk-informed decision making framework. In *Proceedings of the PHYSOR 2006 Conference”, Vancouver, Canada*, 2006.
- [84] Deyu Ming and Serge Guillas. Integrated emulators for systems of computer models. *arXiv preprint arXiv:1912.09468*, 2019.
- [85] Douglas C Montgomery. *Introduction to statistical quality control*. John Wiley & Sons, 2007.
- [86] Jerzy Neyman. Outline of a theory of statistical estimation based on the classical theory of probability. *Philosophical Transactions of the Royal Society of London. Series A, Mathematical and Physical Sciences*, 236(767):333–380, 1937.
- [87] Harry Nyquist. Regeneration theory. *Bell system technical journal*, 11(1):126–147, 1932.
- [88] Nicola E Owen, Peter Challenor, Prathyush P Menon, and Samir Bennani. Comparison of surrogate-based uncertainty quantification methods for computationally expensive simulators. *SIAM/ASA Journal on Uncertainty Quantification*, 5(1):403–435, 2017.
- [89] Houman Owhadi, Clint Scovel, Timothy John Sullivan, Mike McKerns, and Michael Ortiz. Optimal uncertainty quantification. *Siam Review*, 55(2):271–345, 2013.
- [90] Victor M Panaretos and Yoav Zemel. Statistical aspects of wasserstein distances. *Annual review of statistics and its application*, 6:405–431, 2019.
- [91] Mathew D Penrose and JE Yukich. Laws of large numbers and nearest neighbor distances. In *Advances in directional and linear statistics*, pages 189–199. Springer, 2011.
- [92] Martin Pilch, Timothy G Trucano, and Jon C Helton. Ideas underlying quantification of margins and uncertainties (QMU): a white paper. *Unlimited Release SAND2006-5001, Sandia National Laboratory, Albuquerque, New Mexico*, 87185(2), 2006.
- [93] Marcus Vitruvius Pollio. *De Architectura, Book II, Chapter VII, Methods of Building Walls*. 15 BC.

- [94] Joaquin Quionero-Candela, Masashi Sugiyama, Anton Schwaighofer, and Neil D Lawrence. *Dataset shift in machine learning*. The MIT Press, 2009.
- [95] Manny Rayner, Beth Ann Hockey, Nikos Chatzichrisafis, and Kim Farrell. Omg unified modeling language specification. In *Version 1.3, © 1999 Object Management Group, Inc.* Citeseer, 2005.
- [96] Louis M Rea and Richard A Parker. *Designing and conducting survey research: A comprehensive guide*. John Wiley & Sons, 2014.
- [97] Julien Reygner and Adrien Touboul. Reweighting samples under covariate shift using a wasserstein distance criterion. *arXiv preprint arXiv:2010.09267*, 2020.
- [98] Ralph Tyrrell Rockafellar. Coherent approaches to risk in optimization under uncertainty. In *OR Tools and Applications: Glimpses of Future Technologies*, pages 38–61. Informs, 2007.
- [99] Andrea Saltelli. Sensitivity analysis for importance assessment. *Risk analysis*, 22(3):579–590, 2002.
- [100] Andrea Saltelli, Marco Ratto, Terry Andres, Francesca Campolongo, Jessica Cariboni, Debora Gatelli, Michaela Saisana, and Stefano Tarantola. *Global sensitivity analysis: the primer*. John Wiley & Sons, 2008.
- [101] Francois Sanson, Olivier Le Maitre, and Pietro Marco Congedo. Systems of gaussian process models for directed chains of solvers. *Computer Methods in Applied Mechanics and Engineering*, 352:32–55, 2019.
- [102] Kenneth J Schlager. Systems engineering-key to modern development. *IRE Transactions on Engineering Management*, (3):64–66, 1956.
- [103] David H Sharp, Timothy C Wallstrom, and Merri M Wood-Schultz. Physics package confidence: “one” vs. “1.0” .”. *Rpt. LA-UR-04*, 496, 2004.
- [104] David H Sharp and Merri M Wood-Schultz. QMU and nuclear weapons certification-what’s under the hood? *Los Alamos Science*, 28:47–53, 2003.
- [105] John Dalsgaard Sørensen. Calibration of partial safety factors in danish structural codes. In *JCSS Workshop on Reliability Based Code Calibration*, volume 21, page 2002. Citeseer, 2002.
- [106] ISO Standard. 2394: 2. *General principles on reliability for structures*, 2015.
- [107] Bruno Sudret. Uncertainty propagation and sensitivity analysis in mechanical models – contributions to structural reliability and stochastic spectral methods. 01 2007.
- [108] Bruno Sudret. Meta-models for structural reliability and uncertainty quantification. *arXiv preprint arXiv:1203.2062*, 2012.
- [109] Masashi Sugiyama, Taiji Suzuki, and Takafumi Kanamori. *Density ratio estimation in machine learning*. Cambridge University Press, 2012.
- [110] Palle Thoft-Cristensen and Michael J Baker. *Structural reliability theory and its applications*. Springer Science & Business Media, 2012.

- [111] Daniel P Thunnissen. Method for determining margins in conceptual design. *Journal of spacecraft and rockets*, 41(1):85–92, 2004.
- [112] Daniel P Thunnissen. *Propagating and mitigating uncertainty in the design of complex multidisciplinary systems*. PhD thesis, California Institute of Technology, 2005.
- [113] Daniel P Thunnissen and Glenn T Tsuyuki. Margin determination in the design and development of a thermal control system. *SAE transactions*, pages 899–916, 2004.
- [114] Adrien Touboul, Romain Barbedienne, and Jean-Michel Edaliti. Models of margin: from the mathematical formulation to an operational implementation. In *2019 4th International Conference on System Reliability and Safety (ICSRS)*, pages 464–473. IEEE, 2019.
- [115] Adrien Touboul, Julien Reygner, Fabien Mangeant, and Pierre Benjamin. A formal framework to define margins in industrial processes. June 2019. working paper or preprint.
- [116] Alexander B Tsybakov. Optimal aggregation of classifiers in statistical learning. *The Annals of Statistics*, 32(1):135–166, 2004.
- [117] Alexandre B Tsybakov. *Introduction to nonparametric estimation*. Springer Science & Business Media, 2008.
- [118] Yakov Zalmanovich Tsytkin and Boris T Polyak. Frequency domain criteria for $l/\sup p$ -robust stability of continuous linear systems. *IEEE Transactions on Automatic Control*, 36(12):1464–1469, 1991.
- [119] Aad W Van der Vaart. *Asymptotic statistics*, volume 3. Cambridge university press, 2000.
- [120] Cédric Villani. *Optimal transport: old and new*, volume 338. Springer Science & Business Media, 2008.
- [121] Larry Wasserman. *All of statistics: a concise course in statistical inference*. Springer Science & Business Media, 2013.
- [122] Wolfram Wiesemann, Daniel Kuhn, and Melvyn Sim. Distributionally robust convex optimization. *Operations Research*, 62(6):1358–1376, 2014.
- [123] Samuel S Wilks. Statistical prediction with special reference to the problem of tolerance limits. *The annals of mathematical statistics*, 13(4):400–409, 1942.
- [124] Mingguan Yang. *Analyse de la stabilité au feu des murs en béton armé par l’approche calcul à la rupture*. Theses, Université Paris-Est, December 2018.
- [125] Wen Yao, Xiaoqian Chen, Wencai Luo, Michel van Tooren, and Jian Guo. Review of uncertainty-based multidisciplinary design optimization methods for aerospace vehicles. *Progress in Aerospace Sciences*, 47(6):450–479, 2011.
- [126] Paul Zador. Development and evaluation of procedures for quantizing multivariate distributions. Technical report, STANFORD UNIV CALIF, 1963.
- [127] Xujia Zhu and Bruno Sudret. Emulation of stochastic simulators using generalized lambda models. *arXiv preprint arXiv:2007.00996*, 2020.
- [128] Enrico Zio, Francesco Di Maio, and Jiejuan Tong. Safety margins confidence estimation for a passive residual heat removal system. *Reliability Engineering & System Safety*, 95(8):828 – 836, 2010.